PART I - PROPAGATION OF ACOUSTICAL GRAVITY WAVES FROM AN EXPLOSIVE SOURCE IN THE ATMOSPHERE

PART II - RAYLEIGH AND LOVE WAVES FROM SOURCES IN A MULTILAYERED ELASTIC HALF-SPACE

Thesis by

David Garrison Harkrider

In Partial Fulfillment of the Requirements

For the Degree of

Doctor of Philosophy

California Institute of Technology

Pasadena, California

1963

PART I

PROPAGATION OF ACOUSTICAL GRAVITY WAVES FROM AN EXPLOSIVE SOURCE IN THE ATMOSPHERE

ABSTRACT

A matrix formulation is used to derive the pressure variation for acoustic gravity waves from an explosive source in an atmosphere modelled by a large number of isothermal layers. Comparison of theoretical and experimental barograms from large thermonuclear explosions leads to the following conclusions: (1) The major features on the barogram can be explained by the super-position of four modes, (2) Different portions of the vertical temperature structure of the atmosphere control the relative excitation of these modes, (3) A normalized point source is sufficient to model thermonuclear explosions, (4) The observed shift in dominance of certain frequencies with yield and altitude can be explained using the empirical scaling laws derived from the direct wave near the explosion.

ACKNOWLEDGEMENTS

The author is grateful to Professor Frank Press for his support and encouragement throughout this study. Many valuable discussions were held with Dr. D. L. Anderson and Mr. C. B. Archambeau. Their cooperation and support is acknowledged with gratitude.

This research was supported by Grant No. AF-AFOSR-25-63 of the Air Force Office of Scientific Research as part of the Advanced Research Projects Agency Project VELA.

Mr. L. Lenches' help in preparation of the figures is acknowledged with special thanks.

TABLE OF CONTENTS

I. INTRODUCTION

Over the past few years, a large number of thermonuclear bombs have been exploded in the atmosphere. These events have given geophysicists a controlled experiment with which to test the theories of pulse propagation in a complex wave guide. The value of the experiment is enhanced by the fact that the "megaton"-class explosions were large enough to excite long atmospheric waves which were recorded by a world wide net of sensitive barographs. (Yamomoto, 1956, 1957; Hunt, Palmer and Penney, 1960; Oksman and Katajo, 1961; Carpenter, Harwood and Whiteside, 1961; Donn and Ewing 1961; Wexler and Haas, 1962.)

Interest in the propagation of a pulse in the atmosphere was initiated by the world wide pressure disturbances produced by the Krakatoa volcanic eruption of 1883. Additional data was obtained by the Siberian meteorite of 1908. The early studies of these events were primarily concerned with correlating the observed velocity and signature of the pulse with theories of pulse propagation. In addition the pulse was of interest to early investigators because it could provide information concerning the structure of the atmosphere. Today the structure of the atmosphere is not a significant variable of the problem since it is sufficiently well-known from rocket soundings and satellite observations. Therefore more recent studies

of pulses generated by nuclear explosions have placed major emphasis on using a reasonably well-known structure to explain the significant features observed on the barograms.

The first theoretical studies with this emphasis (Scorer, 1950; Pekeris, 1948; Yamomoto, 1957) provided much insight into the nature of pulse propagation, but their use in analyzing the barograms was limited since they were forced to assume oversimplified models of the atmosphere in order to obtain solutions.

With the advent of high speed computers it became possible to obtain numerical solution for more realistic atmospheric models. Numerical solutions of the problem have been formulated using two different approaches. The first study with a complex temperature model was given by Weston (1960, 1961a, 1961b, 1961c). He formulated the inhomogeneous problem of an explosive source in an atmosphere with a continuous vertical temperature distribution. The problem of determining the eigen frequencies and eigen functions was reduced to the evaluation of a second order differential equation with variable coefficients with respect to altitude. With the restraints of the boundary conditions at the earth's surface and at large altitude, the differential equation was solved numerically using the method of Runge-Kutta to obtain phase velocity and the vertical eigen function distribution as a function of frequency.

Papers by Press and Harkrider (1962) and Pfeffer and Zarichny (1962) used a matrix formulation suggested by Haskell (1953) in which the vertical temperature of the atmosphere was represented by a large number of isothermal layers. The equations of motion for each layer took on a particular simple form. Their solutions in matrix form yield a linear transformation of a pressure-displacement vector from the bottom to the top of each layer. Since this vector is continuous across each interface, it is possible to obtain a product matrix relation between the top and bottom of the multilayered array by successive matrix multiplication from layer to layer. With the matrix product relation and the boundary conditions at the earth's surface and at infinite altitudes they obtained a characteristic equation relating period and phase velocity. This matrix formulation is particularly suited for programing on a digital computer. In practice, 20 to 40 layers are sufficient to obtain an adequate approximation of the real atmosphere.

These papers presented results for the homogeneous problem of wave propagation in which the atmosphere is considered a two dimensional wave guide without a source. Phase and group velocity dispersion curves and vertical pressure distributions were numerically evaluated for a number of modes and discussed in terms of the different models of atmospheric structure. The results of Press and Harkrider (1962) and Pfeffer and Zarichny (1962) differed somewhat.

This was because the latter authors terminated their atmosphere model at a lower altitude. Later work with a more complete model gave results which agreed with the work of Press and Harkrider (1962).

This paper extends the homogeneous theory of Press and Harkrider (1962) to include the effect of an explosive source at various altitudes in the atmosphere. The strength of the source in the frequency domain is normalized so that the pressure variation with time of the direct wave near the source is in agreement with the observations near actual nuclear detonations. The inhomogeneous theory, i.e., source inclusion, then allows one to calculate the effect of source altitude and yield on the spectral amplitude of various modes. With the inhomogeneous theory and the known response of the observing barograph we are able to calculate theoretical barograms in the time domain. These theoretical barograms are compared to actual barograms recorded at Pasadena for the 1961 Russian nuclear atmospheric test series.

Earlier theoretical studies also included the effect of sources (Pekeris, 1948; Hunt, Palmer and Penny, 1960). These studies were restricted by the use of over simple atmosphere models. In addition the effect of source altitude was not investigated since they were concerned with surface explosions. The recent papers by Weston as mentioned earlier included the effect of source height. His

results are limited by the unrealistic nature of his assumed atmospheric temperature distribution and the approximations and assumptions used to normalize his source or Green's Function in order to represent an explosion in the frequency domain. The latter difficulty is overcome in this paper by obtaining a closed form expression for the source in an isothermal gravitating medium. The form of the source term is such that it may be readily normalized to represent the observed pressure-time variation of the direct wave at locations near the source.

II. THEORY

Introduction

In this chapter a theoretical model for the propagation of acoustic-gravity waves generated by an explosive source in the atmosphere is developed. We first represent the complex vertical temperature structure of the atmosphere by a large number of horizontally stratified isothermal layers. In one of the layers, we place a point source. The point source is then represented as a double integration over frequency and wave number of an integrand representing outgoing waves. The integrand is composed of terms which are the homogeneous solutions of the harmonic time equation of excess pressure for a layer without a source. To the integrand term we add the two homogeneous solutions for the source layer, one representing upgoing waves and the other downgoing, each with an arbitrary coefficient which is determined from the boundary condition at the layer interface. For the other isothermal layers, we use the two homogeneous solutions alone.

The solutions for the layers and the boundary conditions at each interface are then cast into a matrix formulation. The source is introduced into the formulation by a vector equation relating the source discontinuity across the horizontal source plane. Using the vector equation and the matrix formulation, we solve for the pressure

integrand at the surface. The actual pressure at the surface is then given by the double integral over frequency and wave number.

The far field term of the solution is obtained by evaluating the residue of the wave number integration. This solution is then approximately corrected for the curvature of a concentric layered atmosphere to obtain acoustic gravity waves traveling over a spherical earth.

Weston (1961) formulated a point source or Green's Function for a spherical atmosphere in terms of the homogeneous solutions. He then obtained a solution in terms of the Green's Function, the excess pressure, and normal velocity integrated over an area enclosing a general explosion. Since the needed observational data from a nuclear explosion, i.e., the actual excess pressure and normal velocity on a surface enclosing an explosion, were not available, he simplified the problem in the following manner. First, he let the surface be a small sphere about the source location. He then took the limit as the radius went to zero. Assuming an instantaneous velocity source, he obtained a solution for a point source located at the center of the explosion in terms of the homogeneous solutions and the total volume of gas introduced.

Since the total volume of gas introduced by a nuclear explosion is equally difficult to obtain from available data, we will take as our

source the Green's Function located at the explosion and then normalize the source so that the pressure variation with time for the direct wave is the same as actually measured near nuclear tests.

In order to retain continuity of presentation the following parts of this paper are given in the appendices:

Appendix A contains the derivation of the linearized equations of motion in terms of the perturbation pressure. The derivation has been obtained by many authors and is given only for reference.

Appendix B contains the derivation of a closed form expression for the Green's Function solution of the inhomogeneous equations of motion. When the gravity field is zero, the Green's Function reduces to the acoustic point source.

Appendix C develops the numerical technique used to evaluate the Fourier synthesis of barograms.

Explosive Source

As a source model for an atmospheric nuclear blast, we use an azimuthal symmetric simple point source located in layer s at an altitude D . We then normalize the source so that at a standard yield, W_o , and distance, $\hat{a}_o$, under the source, it will have the same pressure perturbation and time variation as measured in actual nuclear atmospheric tests. For bombs of different yields

and altitudes, we adjust this distance, $\hat{a}_s$, by means of empirically derived scaling laws.

Assume an $e^{i\omega t}$ time dependence. The point source is the Green's Function for the partial differential equation governing the excess pressure $\bar{p}$ in a gravitating isothermal space, or the solution of

$$\frac{1}{\pi}\frac{\partial}{\partial \pi}\left(\pi\frac{\partial \bar{p}}{\partial \pi}\right) + \frac{1}{h_s}\left(\frac{\partial^2 \bar{p}}{\partial z^2} + \gamma\frac{g_s}{\alpha_s^2}\frac{\partial \bar{p}}{\partial z} + \frac{\omega^2}{\alpha_s^2}\bar{p}\right) = \frac{\delta(\pi)}{\pi}\,\delta(z-0)e^{i\omega t} \qquad (1)$$

Quantities not defined in the text are given in Appendix D. The LHS of equation 1 equal to zero is the homogeneous equation for excess pressure in media without a source as shown in Appendix A, equation A15. The solution of equation 1 as derived in Appendix B, equation B19 is given by

$$\bar{p}_{so} = -\frac{h_s}{2}^{1/2}\, e^{-\lambda_s(z-0)}\,\frac{e^{-\kappa_s[\pi^2 + h_s(z-0)^2]^{1/2}}}{[\pi^2 + h_s(z-0)^2]^{1/2}}\, e^{i\omega t} \qquad (2)$$

where

$$\kappa_s^2 = \frac{1}{h_s\alpha_s^2}\left(\alpha_s^2\lambda_s^2 - \omega^2\right), \quad h_s = 1 - \frac{(\gamma-1)g_s^2}{\omega^2\alpha_s^2}, \text{ and } \lambda_s = \frac{\gamma g_s}{2\alpha_s^2} \qquad (3)$$

We now insert $f(\omega, \hat{a}_s$ in equation 2 so that after integrating equation 2 over ω we have at a distance, $\hat{a}_s$, directly below the source, the observed excess pressure-time variation (The Effects of

Nuclear Weapons, 1962).

$$[p_{so}(0, 0-\hat{a}_s; t)] = p_{as}\left(1 - \frac{\tau}{T_{+as}}\right) e^{-\tau/T_{+as}} \qquad \tau \geq 0$$
$$= 0 \qquad \tau < 0 \qquad (4)$$

where $\tau = t - t_{as}$

and where t_{as} is the arrival time of the peak pressure, p_{as} is the peak excess pressure, and T_{+as} is the duration of the positive phase measured at distance $\hat{a}_s$. Applying a Fourier transform to equation 4

$$\int_{-\infty}^{\infty} [p_{so}(0,0-\hat{a}_s; t)] e^{-i\omega t} dt = p_{as} e^{-i\omega t_{as}} \frac{i\omega}{\left(\frac{1}{T_{+as}} + i\omega\right)^2} \qquad (5)$$

and equating the result to equation 2 evaluated at $(0, 0-\hat{a}_s)$ with an $f(\omega, \hat{a}_s)$ inserted and the $e^{i\omega t}$ excluded, yields

$$f(\omega, \hat{a}_s) = -2 p_{as} e^{(x_s - \lambda_s)\hat{a}_s} e^{i\omega t_{as}} \hat{a}_s \frac{i\omega}{(b_s + i\omega)^2} \qquad (6)$$

where $b_s = \frac{1}{T_{+as}}$ and $x_s^2 = k_s^2 h_s$

Thus, for an explosive source, we have

$$\bar{p}_{so} = h_s^{1/2} p_{as} e^{(\chi_s - \lambda_s)\hat{a}_s} e^{-\lambda_s(z-D)} e^{-i\omega t_{as}} \frac{\hat{a}_s i\omega}{(b_s + i\omega)^2} \frac{e^{-\kappa_s[\pi^2 + h_s(z-D)^2]^{1/2}}}{[\pi^2 + h_s(z-D)^2]^{1/2}} e^{i\omega t} \qquad (7)$$

We note that χ_s has four branch points located at $\omega = \pm \tilde{a}_1, \pm \tilde{a}_2$ and $h_s^{1/2}$ has two branch points located at $\omega = \pm \tilde{a}_2$ where $\tilde{a}_1^2 = \frac{\gamma^2 g_s^2}{4\alpha_s^2}$ and $\tilde{a}_2^2 = \frac{(\gamma-1) g_s^2}{\alpha_s^2}$

In order that the integration of equation 7 over ω be convergent for all reasonable (π, z) outside of $\hat{a}_s$ we require that for

$$\tilde{a}_2 > \omega > -\tilde{a}_2$$

$$\kappa_s = i \frac{\omega}{\alpha_s} \frac{\sqrt{\tilde{a}_1^2 - \omega^2}}{\sqrt{\tilde{a}_2^2 - \omega^2}} \qquad \text{and} \qquad h_s^{1/2} = -\frac{i}{\omega} \sqrt{\tilde{a}_2^2 - \omega^2}$$

for $\tilde{a}_1 > \omega > \tilde{a}_2$ and $-\tilde{a}_1 < \omega < -\tilde{a}_2$

$$K_s = \frac{|\omega|}{\alpha_s} \frac{\sqrt{\tilde{a}_1^2 - \omega^2}}{\sqrt{\omega^2 - \tilde{a}_2^2}} \quad \text{and} \quad h_s^{1/2} = \frac{1}{|\omega|} \sqrt{\omega^2 - \tilde{a}_2^2} \qquad (9)$$

for $\omega > \tilde{a}_1$ and $-\tilde{a}_1 > \omega$

$$K_s = i \frac{\omega}{\alpha_s} \frac{\sqrt{\omega^2 - \tilde{a}_1^2}}{\sqrt{\omega^2 - \tilde{a}_2^2}} \quad \text{and} \quad h_s^{1/2} = \frac{1}{|\omega|} \sqrt{\omega^2 - \tilde{a}_2^2}$$

where $\tilde{a}_1^2 > \tilde{a}_2^2$ for $\gamma > 1$. Although not shown here, the above criteria can be obtained by shifting paths of integration in the complex ω plane arbitrarily close to the real axis under the condition that $\mathrm{Re}(K_s) > 0$ and $\mathrm{Re}(h_s^{1/2}) > 0$.

The condition that $\mathrm{Re}(K_s) > 0$ and $\mathrm{Re}(h_s^{1/2}) > 0$ enables us to write equation 7 as an integral expression from equation B18

$$\bar{p}_{so} = h_s p_{as} e^{(\chi_s - \lambda_s)\hat{a}_s} e^{-\lambda_s(z-D) - i\omega t_{as}} \hat{a}_s \, i\omega \int_0^\infty \frac{e^{-ik\eta_{as}|z-D|}}{ik\eta_{as}} J_0(kr) k \, dk \, e^{i\omega t} \quad (10)$$

This form will be used as our source term in the matrix formulation of the layered atmosphere because its integrand is ex pressed in the solutions of the homogeneous excess pressure equation.

Now instead of inserting a different p_{as}, $\hat{a}_s$, t_{as}, and T_{+as} for different yields and altitudes in order to synthesize a barogram, we use the measurements from a "standard" bomb size of one kiloton at a p_{ao} such that $\hat{a}_o$ is in the linear region, and then keeping p_{ao} fixed we scale the other quantities to explosives under different conditions by means of the empirical scale factors given in The Effects of Nuclear Weapons, 1962. For a given excess pressure, the distance at which it is found from the blast is given by the distance scale factor

$$\xi = \left(W_s \frac{p_a^\circ}{p_s^\circ} \right)^{1/3} \quad (11)$$

For the time measurements t_{as} and T_{+as} at this new distance, we use ξ and in addition a velocity ratio, since they are given at surface or sea level velocities. Using these scaling laws,

the appropriate bomb characteristics for yields and altitudes other than the reference or "standard" bomb are

$$\hat{a}_s = \xi\, \hat{a}_o \quad , \quad t_{as} = \xi \frac{\alpha_o}{\alpha_s}\, t_{ao} \qquad \text{and} \qquad T_{+os} = \xi \frac{\alpha_o}{\alpha_s}\, T_{+oo} \tag{12}$$

where

$$\xi = \left(W_s \frac{\rho_o^\circ}{\rho_s^\circ} \right)^{1/3} = \left(W_s \frac{\rho_o^\circ}{\rho_s^\circ} \frac{\alpha_o^2}{\alpha_s^2} \right)^{1/3} \tag{13}$$

since, by the equation of state

$$\rho^\circ = \frac{\alpha^2}{\gamma} \rho^\circ$$

Matrix Formulation and Solution for the Explosive Source in a Horizontally Stratified Atmosphere

For an isothermal or constant velocity layer m in a horizontally stratified atmosphere not containing the source, the equation for excess pressure is given from equation A15 by

$$\frac{1}{r} \frac{\partial}{\partial r} \left(r \frac{\partial p_m}{\partial r} \right) + \frac{1}{h_m} \left(\frac{\partial^2 p_m}{\partial z^2} + \frac{\gamma g_m}{\alpha_m^2} \frac{\partial p_m}{\partial z} + \frac{\omega^2}{\alpha_m^2} p_m \right) = 0$$

Assuming that the radial or r dependence of p_m is given by $J_0(kr)$, equation 14 reduces to

$$\frac{\partial^2 p_m}{\partial z^2} + \frac{\gamma g_m}{\alpha_m^2}\frac{\partial p_m}{\partial z} + \left(\frac{\omega^2}{\alpha_m^2} - h_m k^2\right) p_m = 0 \qquad (15)$$

and by equation A12, the vertical velocity perturbation is given as

$$w_m = \frac{i}{\omega \rho_m^\circ(z) h_m}\left(\frac{\partial p_m}{\partial z} + \frac{g_m}{\alpha_m^2} p_m\right) \qquad (16)$$

In addition, we have for the equilibrium state in each layer

$$\frac{\partial p^\circ}{\partial z} = -g\rho^\circ \quad , \quad p^\circ = RK^\circ \rho^\circ \quad , \quad \alpha^2 = \frac{\gamma p^\circ}{\rho^\circ} = \gamma R K^\circ \qquad (17)$$

From equation 17, we obtain for layer m

$$\rho_m^\circ(z) = \rho_m^\circ(z_{m-1}) e^{-2\lambda_m (z - z_{m-1})} = \rho_m^\circ e^{-2\lambda_m (z - z_{m-1/2})}$$

where $\lambda_m = \frac{\gamma g_m}{2\alpha_m^2}$, $\rho_m^\circ = \rho_m^\circ(z_{m-1/2})$,

and $z_{m-1/2}$ is the altitude of the m layer mid-point.

Since $\rho_m^0(z_{m-1}) = \rho_{m-1}^0(z_{m-1})$, we have

$$\frac{\rho_m^0(z_{m-1})}{\rho_{m-1}^0(z_{m-1})} = \frac{\alpha_{m-1}^2}{\alpha_m^2} \quad \frac{\rho_m^0(z_{m-1})}{\rho_{m-1}^0(z_{m-1})} = \frac{\alpha_{m-1}^2}{\alpha_m^2} \qquad (18)$$

We have assumed small motions and will impose the boundary conditions of continuity of vertical particle velocity and total pressure across the disturbed interfaces. Retaining only first order terms, we find that the change in total pressure of a small parcel which is displaced a vertical distance η from its static equilibrium position z is the pressure perturbation, $p(z)$, at the zero displacement position plus $\delta p = -g\rho^0(z)\eta$. Now defining

$$p_p(z) = p(z) + \delta p$$

using equation 16 and $W = i\omega\eta$ we obtain for layer m

$$p_{p_m} = p_m - \frac{g_m}{\omega^2 h_m}\left(\frac{\partial p_m}{\partial z} + \frac{g_m}{\alpha_m^2} p_m\right) \qquad (19)$$

At the layer interfaces we will now require

$$p_{p_{m-1}}(z_{m-1}) = p_{p_m}(z_{m-1})$$

in order to guarantee continuity of pressure. It is interesting to note that when there is no temperature or gravity discontinuity across an interface, one can use as a boundary condition continuity of $p(z)$ since for that particular case $p_{p_m}(z_{m-1}) = p_{p_{m-1}}(z_{m-1})$ is equivalent to $p_m(z_{m-1}) = p_{m-1}(z_{m-1})$ This relation was used by Pekeris (1948) in his model of the atmosphere.

The general solution of equation 14 is given by

$$p_m = e^{-\lambda_m z}\left[\underline{\underline{\Delta}}'_m e^{-ik/\alpha_m z} + \underline{\underline{\Delta}}''_m e^{ik/\alpha_m z}\right] J_0(kr)\, e^{i\omega t} \qquad (20)$$

where

$$(k/\alpha_m)^2 = \frac{\omega^2}{\alpha_m^2} - h_m k^2 - \frac{\gamma^2}{4}\frac{g_m^2}{\alpha_m^4} \qquad (21)$$

and using the definition of phase velocity

$$c = \frac{\omega}{k}$$

we can write equation 21 as

$$k\Lambda_{\alpha_m} = \left\{ k^2 \left(\frac{c^2}{\alpha_m^2} - 1 \right) - \frac{\sigma_{B_m}^2}{c^2} \left(\frac{c^2}{\beta_m^2} - 1 \right) \right\}^{1/2} \tag{22}$$

for (c, k) such that $(k\Lambda_{\alpha_m})^2 > 0$ and

$$k\Lambda_{\alpha_m} = -i \left\{ k^2 \left(1 - \frac{c^2}{\alpha_m^2} \right) - \frac{\sigma_{B_m}^2}{c^2} \left(1 - \frac{c^2}{\beta_m^2} \right) \right\}^{1/2}$$

for (c, k) such that $(k\Lambda_{\alpha_m})^2 < 0$. Here

$$\beta_m = 2\frac{(\gamma-1)}{\gamma}^{1/2} \alpha_m < \alpha_m$$

for all $\gamma \gg 1$ and σ_{B_m} is the Brunt resonant angular frequency for the constant velocity layer m, and is given by

$$\sigma_{Bm} = \frac{g_m (\gamma-1)^{1/2}}{\alpha_m} = \tilde{a}_2$$

In order to facilitate the evaluation of W_m and ρ_{pm} at the top, z_m, and bottom, z_{m-1}, of layer m, we define

$$\underline{\Delta}_m' = \underline{\underline{\Delta}}_m' \, e^{-ik\ell\alpha_m z_{m-1}}$$

and

$$\underline{\Delta}_m'' = \underline{\underline{\Delta}}_m'' \, e^{ik\ell\alpha_m z_{m-1}}$$

and equation 20 becomes

$$\rho_m(z) = e^{-\lambda_m z}\left[\underline{\Delta}_m' e^{-ik\ell\alpha_m (z-z_{m-1})} + \underline{\Delta}_m'' e^{ik\ell\alpha_m (z-z_{m-1})}\right] J_0(k\ell) e^{i\omega t} \qquad (24)$$

Substituting equation 24 in equation 16 and 19, evaluating at z_m and z_{m-1} and eliminating the constants $\underline{\Delta}_m'$ and $\underline{\Delta}_m''$ we obtain the following matrix relation

$$\begin{bmatrix} W_m(z_m) \\ p_{p_m}(z_m) \end{bmatrix} = \begin{bmatrix} (a_m)_{11} & (a_m)_{12} \\ (a_m)_{21} & (a_m)_{22} \end{bmatrix} \begin{bmatrix} W_m(z_{m-1}) \\ p_{p_m}(z_{m-1}) \end{bmatrix}$$

where

$$(a_m)_{11} = e^{\lambda_m d_m}\left\{\cos P_m + \frac{g_m}{\alpha_m^2}\left(\frac{\alpha_m^2}{c^2} - \frac{\gamma}{2}\right)\frac{\sin P_m}{(k\ell_{\alpha_m})}\right\}$$

$$(a_m)_{12} = i(kc)^3\frac{\left\{g_m^2\left(\frac{\alpha_m^2}{c^2} - \frac{\gamma}{2}\right)^2 + \alpha_m^2(k\ell_{\alpha_m})^2\right\}}{\rho_m^0\alpha_m^2\delta_m}\frac{\sin P_m}{(k\ell_{\alpha_m})}$$

(26)

$$(a_m)_{21} = i\frac{\rho_m^0\delta_m}{(kc)^3}\frac{\sin P_m}{(k\ell_{\alpha_m})}$$

$$(a_m)_{22} = e^{-\lambda_m d_m}\left\{\cos P_m - \frac{g_m}{\alpha_m^2}\left(\frac{\alpha_m^2}{c^2} - \frac{\gamma}{2}\right)\frac{\sin P_m}{(k\eta_{\alpha_m})}\right\}$$

$$P_m = (k\eta_{\alpha_m})\, d_m$$

$$d_m = z_m - z_{m-1}$$

and $\delta_m = g_m^2 k^2 - \omega^4$. In equations 26 we see that matrix elements $(a_m)_{jk}$ are pure real or pure imaginary for (c, k) real and j+k equal to even and odd integers respectively. Therefore the elements of a matrix resulting from the matrix multiplication of any number of layer matrices will be pure real or pure imaginary in the same sense as the individual matrices.

For $g_m = 0$ the a_m matrix reduces to a form equivalent to the non-gravitating liquid layer matrix given by Dorman (1962) in his discussion of elastic wave propagation in layered wave guides.

For layer s containing the source, we add a source term of the form

$$p_{s0}(z) = S_0 e^{-\lambda_s (z-D)} e^{-ik\eta\alpha_s |z-D|} J_0(k\eta) e^{i\omega t} \qquad (27)$$

where S_0 is not a function of z or η, so that we now have

$$p_s(z) = e^{-\lambda_s z}\left[\underline{\underline{\Delta}}_s' e^{-ik\eta\alpha_s z} + \underline{\underline{\Delta}}_s'' e^{ik\eta\alpha_s z} + S_0 e^{\lambda_s D} e^{-ik\eta\alpha_s |z-D|}\right] J_0(k\eta) e^{i\omega t} \qquad (28)$$

Decomposing layer s into two layers with the same temperature and g; layer $s2$ for $z_s \geq z \geq D$ and layer $s1$ for $D \geq z \geq z_{s-1}$, we can write equation 28 as

$$p_{s2}(z) = e^{-\lambda_s z}\left\{\left[\underline{\underline{\Delta}}_s' + S_0 e^{(\lambda_s + ik\eta\alpha_s)D}\right] e^{-ik\eta\alpha_s z} + \underline{\underline{\Delta}}_s'' e^{ik\eta\alpha_s z}\right\} J_0(k\eta) e^{i\omega t} \qquad (29)$$

and

$$p_{s1}(z) = e^{-\lambda_s z}\left\{\underline{\underline{\Delta}}_s' e^{-ik\Pi_{\alpha s} z} + \left[\underline{\underline{\Delta}}_s'' + S_0 e^{(\lambda_s - ik\Pi_{\alpha s})D}\right] e^{ik\Pi_{\alpha s} z}\right\} J_0(kr) e^{i\omega t} \quad (30)$$

Similar to our treatment of layer m , we define

$$\underline{\Delta}_{s2}' = \left[\underline{\underline{\Delta}}_s' + S_0 e^{(\lambda_s + ik\Pi_{\alpha s})D}\right] e^{-ik\Pi_{\alpha s} z_{s2-1}}$$

$$\underline{\Delta}_{s2}'' = \underline{\underline{\Delta}}_s'' e^{ik\Pi_{\alpha s} z_{s2-1}}$$

$$\underline{\Delta}_{s1}' = \underline{\underline{\Delta}}_s' e^{-ik\Pi_{\alpha s} z_{s1-1}} \quad (31)$$

and

$$\underline{\Delta}_{s1}'' = \left[\underline{\underline{\Delta}}_s'' + S_0 e^{(\lambda_s - ik\Pi_{\alpha s})D}\right] e^{ik\Pi_{\alpha s} z_{s1-1}}$$

where $z_{52} = z_5$, $z_{52-1} = D$, $z_{51} = D$

and $z_{51-1} = z_{5-1}$. Using relations 31, we can rewrite

equations 29 and 30 respectively as

$$p_{52}(z) = e^{-\lambda_5 z}\left[\underline{\Delta}'_{52}\, e^{-ik\beta_{\alpha 5}(z - z_{52-1})} + \underline{\Delta}''_{52}\, e^{ik\beta_{\alpha 5}(z - z_{52-1})}\right] J_0(kR)\, e^{i\omega t} \qquad (32)$$

$$p_{51}(z) = e^{-\lambda_5 z}\left[\underline{\Delta}'_{51}\, e^{-ik\beta_{\alpha 5}(z - z_{51-1})} + \underline{\Delta}''_{51}\, e^{ik\beta_{\alpha 5}(z - z_{51-1})}\right] J_0(kR)\, e^{i\omega t} \qquad (33)$$

Comparing equations 32 and 33 with equation 23, we see that for layers 52 and 51 we have the same matrix relations as given in equations 25 and 26 with the m subscripts replaced by 52 and 51 respectively, where

$d_{52} = z_5 - D$ and $d_{51} = D - z_{5-1}$

In addition, since temperature or velocity and g are the same for layers 52 and 51 , we have

$$\alpha_{s2} = \alpha_{s1} = \alpha_s \quad , \qquad g_{s2} = g_{s1} = g_s \quad ,$$

$$\mu_{\alpha s2} = \mu_{\alpha s1} = \mu_{\alpha s} \quad , \qquad \lambda_{s2} = \lambda_{s1} = \lambda_s \quad ,$$

$$\delta_{s2} = \delta_{s1} = \delta_s \quad , \qquad \rho^{\circ}_{s2} = \rho^{\circ}_s (z_{s2-1/2}) \tag{34}$$

$$\rho^{\circ}_{s1} = \rho^{\circ}_s (z_{s1-1/2}) \quad , \qquad z_{s2-1/2} = \frac{z_s + D}{2}$$

and $$z_{s1-1/2} = \frac{D + z_{s-1}}{2}$$

Also, it can be shown that the matrix product

$$a_{s2}\, a_{s1} = a_s \tag{35}$$

where a_s is the layer matrix for layer s if no source is present.

For all interfaces except the interface between layer

52 and 51, we have continuity of W and p_p. Using this continuity and the matrix relation 25, the following is obtained

$$\begin{bmatrix} W_{m-1}(z_{m-1}) \\ p_{m-1}(z_{m-1}) \end{bmatrix} = A^{52} \begin{bmatrix} W_{52}(0) \\ p_{p52}(0) \end{bmatrix}$$

and

$$\begin{bmatrix} W_{51}(0) \\ p_{p51}(0) \end{bmatrix} = A_{51} \begin{bmatrix} W_1(0) \\ p_{p1}(0) \end{bmatrix}$$

where $A^{52} = a_{m-1} \cdots a_{52}$ and $A_{51} = a_{51} \cdots a_1$.

At $z = 0$, layer 1 is in contact with a flat rigid boundary where we require $W_1(0) = 0$ and thus

$p_{P1}(0) = p_1(0) \equiv p_0$. Equation 37 then reduces to

$$\begin{bmatrix} \bar{W}_{S1}(0) \\ p_{PS1}(0) \end{bmatrix} = A_{S1} \begin{bmatrix} 0 \\ p_0 \end{bmatrix} \tag{38}$$

Since $\frac{\partial p_{S0}}{\partial z}$ is discontinuous across $z = D$,

we have, from equations 29 and 30 substituted in equations 16 and 19, the following relations

$$p_{S2}(0) - p_{S1}(0) = 0$$

$$\bar{W}_{S2}(0) - \bar{W}_{S1}(0) = \frac{i}{\omega \rho_s^\circ(0) h_s} \left[\frac{\partial p_{S2}}{\partial z}(0) - \frac{\partial p_{S1}}{\partial z}(0) \right]$$

(39)

$$p_{PS2}(0) - p_{PS1}(0) = -\frac{g_s}{\omega^2 h_s} \left[\frac{\partial p_{S2}}{\partial z}(0) - \frac{\partial p_{S1}}{\partial z}(0) \right]$$

and

$$\left[\frac{\partial p_{s2}(D)}{\partial z} - \frac{\partial p_{s1}(D)}{\partial z}\right] = -i2k\rho_{as} S_o J_o(kr) e^{i\omega t}$$

where the partial derivatives with respect to z are evaluated at D by letting z approach D from their respective layers. From equation 39 we obtain the vector relation

$$\begin{bmatrix} w_{s2}(D) \\ p_{ps2}(D) \end{bmatrix} = \begin{bmatrix} w_{s1}(D) \\ p_{ps1}(D) \end{bmatrix} + \begin{bmatrix} \delta w_s \\ \delta p_{ps} \end{bmatrix} \qquad (40)$$

where

$$\delta w_s = \frac{2k\rho_{as} S_o}{\omega h_s \rho_s^\circ(D)} J_o(kr) e^{i\omega t} \qquad (41)$$

and $$\delta p_{ps} = \frac{i g_s \rho_s^\circ(D)}{\omega} \delta w_s$$

We now define X and Y by the matrix operation

$$\begin{bmatrix} X \\ Y \end{bmatrix} = A_{S1}^{-1} \begin{bmatrix} W_{S2}(D) \\ p_{PS2}(D) \end{bmatrix} \qquad (42)$$

Multiplying equation 40 by A_{S1}^{-1}, and using equations 42 and 38, we have

$$\begin{bmatrix} X \\ Y \end{bmatrix} = \begin{bmatrix} 0 \\ p_0 \end{bmatrix} + A_{S1}^{-1} \begin{bmatrix} \delta W_S \\ \delta p_{PS} \end{bmatrix} \qquad (43)$$

or

$$X = (A_{S1}^{-1})_{11}\, \delta W_S + (A_{S1}^{-1})_{12}\, \delta p_{PS}$$

$$p_0 = Y - \left[(A_{S1}^{-1})_{21}\, \delta W_S + (A_{S1}^{-1})_{22}\, \delta p_{PS}\right] \qquad (44)$$

For the case of an atmosphere bounded by an isothermal half-space, we require that the n^{th} layer coefficient $\Delta_n'' = 0$.

For (c, k) such that $(k/\alpha_m)^2 > 0$ this is equivalent to requiring that there be no radiation from infinity into the wave guide. For (c, k) such that $(k/\alpha_m)^2 < 0$ this condition guarantees that the kinetic energy integrated over a column of atmosphere be finite.

Setting $\Delta_m'' = 0$ in equations for $W_m(z)$ and $\rho_{pm}(z)$ evaluated at z_{m-1} we find that

$$\begin{bmatrix} \Delta_m' \\ \Delta_m' \end{bmatrix} = E_m^{-1} \begin{bmatrix} W_{m-1}(z_{m-1}) \\ \rho_{pm-1}(z_{m-1}) \end{bmatrix} \tag{45}$$

and the matrix E_m^{-1} is given by

$$E_m^{-1} = \begin{bmatrix} (b_{1m})^{-1} & 0 \\ 0 & (b_{2m})^{-1} \end{bmatrix} \tag{46}$$

where

$$b_{1m} = \frac{e}{\delta_m} e^{\lambda_m z_{m-1}} e^{-ik\alpha_m z_{m-1}} (kc)^2 \left\{ q_m \left(\frac{\alpha_m^2}{c^2} - \frac{\gamma}{z} \right) - i\alpha_m^2 (k\alpha_m) \right\} J_0(kr) e^{i\omega t}$$

(47)

$$b_{2m} = i \frac{e}{\delta_m} e^{\lambda_m z_{m-1}} e^{-ik\alpha_m z_{m-1}} (kc)^2 \frac{\rho_m^0 (z_{m-1})}{(kc)^3} \alpha_m^2 \delta_m J_0(kr) e^{i\omega t}$$

Defining the matrix A by the matrix product

$$A = A^{s2} A_{s1} = a_{m-1} \cdots a_{s2} a_{s1} \cdots a_1 = a_{m-1} \cdots a_s \cdots a_1 ,$$

since by equations 35, $a_{s2} a_{s1} = a_s$, and in turn defining J by

$$J = E_m^{-1} A \tag{48}$$

we obtain from equations 45, 36, and 42

$$\begin{bmatrix} \Delta_m' \\ \Delta_m' \end{bmatrix} = J \begin{bmatrix} X \\ Y \end{bmatrix}$$

or

$$\Delta_m' = J_{11} X + J_{12} Y$$

$$\Delta_m' = J_{21} X + J_{22} Y \qquad (49)$$

Finally eliminating Δ_m' from equation 49, we have

$$Y = - \frac{(J_{11} - J_{21})}{(J_{12} - J_{22})} X \equiv i \frac{N_a^{(1)}}{F_a} X \qquad (50)$$

where

$$N_a^{(1)} = A_{11} - \frac{b_{1m}}{b_{2m}^*} A_{21}^*$$

$$F_a = A_{12}^* + \frac{b_{1m}}{b_{2m}^*} A_{22} \qquad (51)$$

$$i A_{jk}^* = A_{jk} \qquad \text{and} \qquad i b_{2m}^* = b_{2m} \; .$$

Substituting equation 50 in equation 44 yields

$$p_o = i \delta W_5 \frac{N_a^{(1)} N_a^{(2)}}{F_a} \qquad (52)$$

where

$$N_a^{(2)} = \left[(A_{S1}^{-1})_{11} + \frac{\delta p_{ps}}{\delta W_S}(A_{S1}^{-1})_{12}\right] - \frac{E_a}{N_a^{(1)}}\left[(A_{S1}^{-1})_{21} + \frac{\delta p_{ps}}{\delta W_S}(A_{S1}^{-1})_{22}\right] \quad (53)$$

From equation 26, we see that the determinant of the individual layer matrix is equal to unity or

$$|a_m| = 1 \quad (54)$$

and therefore, the determinant of any matrix product of these layer matrices is also equal to unity, and we have

$$|A_{S1}| = 1$$

Using equation 55, the inverse of A_{S1} is given by

$$A_{S1}^{-1} = \begin{bmatrix} (A_{S1})_{22} & -(A_{S1})_{12} \\ -(A_{S1})_{21} & (A_{S1})_{11} \end{bmatrix} \quad (56)$$

Substituting this result in equation 53 yields

$$N_a^{(2)} = \left[(A_{S1})_{22} - \frac{\delta p_{as}}{\delta W_s}(A_{S1})_{12}\right] + \frac{F_a}{N_a^{(1)}}\left[(A_{S1})_{21} - \frac{\delta p_{as}}{\delta W_s}(A_{S1})_{11}\right] \quad (57)$$

and using equation 41, the definition of p_p, and equation 38

$$N_a^{(2)} = \frac{p_{s1}(\cdot p)}{p_o} + i\frac{F_a}{N_a^{(1)}}\left[(A_{S1})_{21}^{*} - g_s\frac{\rho_s^{\circ}(0)}{\omega}(A_{S1})_{11}\right] \quad (58)$$

Now performing an integration over k where

$$\bar{p}_m = \int_0^\infty p_m\, dk \quad , \quad \bar{W}_m = \int_0^\infty W_m\, dk \quad , \quad \bar{p}_{pm} = \int_0^\infty p_{pm}\, dk \quad (59)$$

and letting

$$S_o = \rho_{as}\,\omega\,\hat{a}_s\, e^{(\chi_s - \lambda_s)\hat{a}_s}\,\frac{h_s}{(b_s + i\omega)^2}\,\frac{e^{-i\omega t_{as}}}{R_{as}} \quad (60)$$

in order that $\bar{\rho}_{so} = \int_0^\infty \rho_{so}\, dk$ be equal to equation 10 we have from equation 41

$$\delta W_s = \frac{2k}{\rho_s^\circ(D)}\, \hat{a}_s\, \rho_{as}\, \frac{e^{(x_s-\lambda_s)\hat{a}_s}}{(b_s+i\omega)^2}\, J_o(kr)\, e^{i\omega(t-t_{as})} \qquad (61)$$

and

$$\bar{\rho}_o = i\, \frac{\hat{a}_s \rho_{as}}{\rho_s^\circ(D)}\, \frac{e^{(x_s-\lambda_s)\hat{a}_s}}{(b_s+i\omega)^2}\, e^{i\omega(t-t_{as})}\, 2 \int_0^\infty \frac{N_o^{(1)} N_o^{(2)}}{F_a}\, J_o(kr)\, k\, dk \qquad (62)$$

In this paper we are interested only in the waves which are $O(r^{-1/2})$. These waves are given by the residue contribution of equation 62 due to the zero's of F_a. Evaluating equation 62 for the residue contribution, we obtain for each mode or k_j root, ω fixed, of $F_a = 0$.

$$\{\bar{p}_o\}_{a_j} = 2\pi \hat{a}_s \frac{\rho_{as}}{\rho_s(0)} \frac{e^{(\chi_s - \lambda_o)\hat{a}_s}}{(k_s + i\omega)^2} k_j \frac{N_{a_j}^{(1)} N_{a_j}^{(2)}}{\left(\frac{\partial F_a}{\partial k}\right)_{\omega,j}} H_0^{(2)}(k_j r) e^{i\omega(t - t_{as})} \qquad (63)$$

where $\left(\frac{\partial F_a}{\partial k}\right)_{\omega,j}$, $N_{a_j}^{(1)}$ and $N_{a_j}^{(2)}$ are evaluated at (ω, k_j) such that $F_a(\omega,k) = 0$.

$F_a(\omega, k_j) = 0$ is the period equation given in Press and Harkrider (1962). Roots, dispersion curves, and the homogeneous velocity and pressure ratios at altitude for various temperature models of the atmosphere, along with a discussion of the "cut-off" region can be found in this reference.

At $F_a(\omega, k_j) = 0$ by equation 58

$$N_{a_j}^{(2)} = \frac{p_{s1}(0)}{p_o} \qquad (64)$$

and since by equation 54

$$|A| \equiv A_{11} A_{22} + A_{12}^* A_{21}^* = 1$$

and

$$F_a \equiv A_{12}^{*} + \frac{b_{1m}}{b_{2m}^{*}} A_{22} = 0$$

we have

$$N_{a_j}^{(1)} = \frac{1}{A_{22}} \tag{65}$$

Evaluating the residue contributions of the integral representations for $\bar{W}_{s1}(0)$, $\bar{p}_{ps1}(0)$, $\bar{p}_{s1}(0)$, $\bar{W}_{s2}(0)$, $\bar{p}_{ps2}(0)$, and $\bar{p}_{s2}(0)$ by using equations 38 and 40, we find that

$$\{\bar{W}_{s1}(0)\}_{a_j} = (A_{s1})_{12} \{\bar{p}_o\}_{a_j}$$

$$\{\bar{p}_{ps1}(0)\}_{a_j} = (A_{s1})_{22} \{\bar{p}_o\}_{a_j}$$

$$\{\bar{p}_{s1}(0)\}_{a_j} = \left[(A_{s1})_{22} + \frac{\rho_s^{\circ}(0)}{\omega} g_s (A_{s1})_{12}^{*}\right] \{\bar{p}_o\}_{a_j} \tag{66}$$

$$\{\bar{W}_{s2}(0)\}_{a_j} = \{\bar{W}_{s1}(0)\}_{a_j}$$

$$\{\bar{p}_{PS2}(0)\}_{a_j} = \{\bar{p}_{PS1}(0)\}_{a_j}$$

$$\{\bar{p}_{S2}(0)\}_{a_j} = \{\bar{p}_{S1}(0)\}_{a_j} \qquad (67)$$

and thus there is no discontinuity across the source plane, $z = 0$ for the residue contributions. From equation 67 we have that

$$\{\bar{W}_m(z)\}^*_{a_j} = [A_m(z)]^*_{12}\ \{\bar{p}_o\}_{a_j} \equiv \left[\frac{\bar{W}^*_m(z)}{p_o}\right]_{H_j} \{\bar{p}_o\}_{a_j}$$

$$\{\bar{p}_{Pm}(z)\}_{a_j} = [A_m(z)]_{22}\ \{\bar{p}_o\}_{a_j} \equiv \left[\frac{p_{Pm}(z)}{p_o}\right]_{H_j} \{\bar{p}_o\}_{a_j} \qquad (68)$$

$$\{\bar{p}_m(z)\}_{a_j} = \left\{[A_m(z)]_{22} + \frac{\rho^o_m(z)}{\omega} g_m [A_m(z)]^*_{12}\right\} \{\bar{p}_o\}_{a_j}$$

$$\equiv \left[\frac{p_m(z)}{p_o}\right]_{H_j} \{\bar{p}_o\}_{a_j}$$

is true for all m above and below the source, and where

$$A_m(z) = a_m(z) a_{m-1} \cdots a_1$$

and $a_m(z)$ is the layer matrix for a sublayer in layer of thickness

$$d_m(z) = z - z_{m-1}$$

Rewriting equation 63 using equations 64, 65 and the definitions in equations 68, we obtain for the residue contribution for excess pressure at the surface of a horizontally stratified atmosphere

$$\{\bar{p}_0\}_{a_j} = 2\pi \frac{\hat{a}_s \rho_{as}}{\rho_s^\circ(0)} \frac{e^{(\chi_s - \lambda_s)\hat{a}_s}}{(b_s + i\omega)^2} k_j \frac{\left[\frac{p_s(0)}{p_0}\right]_{H_j}}{\left[\frac{p_{m-1}}{p_0}\right]_{H_j} \left(\frac{\partial F_a}{\partial k}\right)_{\omega, j}} H_0^{(2)}(k_j R) e^{i\omega(t - t_{as})} \tag{69}$$

where

$$\left[\frac{p_{m-1}}{p_0}\right]_{H_j} \equiv \left[\frac{p_{m-1}(z_{m-1})}{p_0}\right]_{H_j}$$

Approximate Curvature Correction

It has been shown by Weston (1961) that a good approximation to the equation for excess pressure in an isothermal gravitating

spherical layer, assuming that the radial dimension of the atmosphere is small compared to the earth's radius, a_e , can be given for longitudinal symmetry by

$$\frac{1}{\sin\theta}\frac{\partial}{\partial\theta}\left(\sin\theta\frac{\partial p_m}{\partial\theta}\right) + \nu(\nu+1)p_m = 0 \qquad (70)$$

and

$$\frac{\partial^2 p_m}{\partial z^2} + \gamma\frac{g_m}{\alpha_m^2}\frac{\partial p_m}{\partial z} + \left(\frac{\omega^2}{\alpha_m^2} - h_m k^2\right)p_m = 0 \qquad (71)$$

where z is the radial coordinate, θ is the colatitude, and

$$k^2 a_e^2 = \nu(\nu+1) \qquad (72)$$

To this approximation the θ dependence of p_m is given by the Legendre functions $P_\nu(\cos\theta)$ and $Q_\nu(\cos\theta)$, and the radial dependence is determined by the same differential equation as 15 which governed the vertical dependence of p_m for the horizontal layer. In addition the approximate radial boundary conditions across spherical layers are the same as for the horizontal layers. Thus we have the

same relation for the spherically layered atmosphere as equation 52 with the $J_0(k_j r)$ dependence of δW_s replaced by some linear combination of $P_\nu(\cos\theta)$ and $Q_\nu(\cos\theta)$.

Now, near the source, the residue contribution, equation 69, should be valid for k_j large, i.e., small horizontal wave lengths. Thus for an approximate curvature correction to equation 69, valid for large $k_j a_e$, we will use an asymptotic expansion, valid for large ν , of the Legendre functions which reduces to $H_0^{(2)}(k_j r)$ near the source, i.e., θ small. Such an expansion was given by Szegö (1933)

$$P_\nu(\cos\theta) + i\frac{2}{\pi} Q_\nu(\cos\theta) \cong \left(\frac{\theta}{\sin\theta}\right)^{1/2} H_0^{(2)}[(\nu+1/2)\theta] \qquad (73)$$

For ν large, $k_j a_e \cong \nu + 1/2$ and equation 73 yields

$$P_\nu(\cos\theta) + i\frac{2}{\pi} Q_\nu(\cos\theta) \cong \left(\frac{r}{a_e \sin\theta}\right)^{1/2} H_0^{(2)}(k_j r) \qquad (74)$$

where r is the distance from the source measured on the

surface of the earth, i.e., $r = \frac{\theta}{a_e}$.

Therefore including the above approximation for curvature, our solution is

$$\{\bar{p}_o\}_{a_j} = 2\pi \hat{a}_s \frac{\rho_{as}}{\rho_s^o(0)} \frac{e^{(\lambda_s - \lambda_s)\hat{a}_s}}{(b_s + i\omega)^2} k_j \frac{\left[\frac{\rho_s(0)}{\rho_o}\right]_{H_j}}{\left[\frac{\rho_{n-1}}{\rho_o}\right]_{H_j} \left(\frac{\partial F_a}{\partial k}\right)_{\omega,j}} \left(\frac{r}{a_e \sin\theta}\right)^{1/2} H_0^{(2)}(k_j r)\, e^{i\omega(t - t_{as})} \tag{75}$$

Furthermore since we are interested in waves at large r from the source, we now make use of the asymptotic expansion for large arguments of $H_0^{(2)}(k_j r)$ and obtain from equation 75

$$\{\bar{p}_o\}_{a_j} = 2\pi \hat{a}_s \frac{\rho_{as}}{\rho_s^o(0)} \frac{e^{(\lambda_s - \lambda_s)\hat{a}_s}}{(b_s + i\omega)^2} k_j \frac{\left[\frac{\rho_s(0)}{\rho_o}\right]_{H_j}}{\left[\frac{\rho_{n-1}}{\rho_o}\right]_{H_j} \left(\frac{\partial F_a}{\partial k}\right)_{\omega,j}} \left(\frac{r}{a_e \sin\theta}\right)^{1/2} \left(\frac{2}{\pi k_j r}\right)^{1/2} \cdot$$

$$\cdot\, e^{i\omega\left(t - t_{as} - \frac{k_j r}{\omega} + \frac{\pi}{4\omega}\right)} \tag{76}$$

From this form of the solution, we see that our curvature correction factor

$$\left(\frac{r}{a_e \sin\theta}\right)^{1/2}$$

alters the amplitude in order to compensate for the effect of energy spreading over a spherical surface instead of a flat surface.

Barograph Response and Calibration

The type of microbarograph at Donnelley Seismological Laboratory has been previously described in the literature by Ewing and Press, (1953), and Donn, Rommer, Press, and Ewing, (1954). The frequency response of this instrument is given by the following equations

$$R(\omega) = \frac{X_p\,\omega}{\left[\left\{\omega^4 - \omega^2\left[\omega_p^2 + \omega_g^2 + 4\epsilon_p\epsilon_g(1-\sigma^2)\right] + \omega_p^2\omega_g^2\right\}^2 + \left\{2\omega^3(\epsilon_p+\epsilon_g) - 2\omega(\omega_g^2\epsilon_p + \omega_p^2\epsilon_g)\right\}^2\right]^{1/2}}$$

$$= X_p \; R_{np} \qquad (77)$$

$$\varphi_I = \tan^{-1}\left\{\frac{\omega^4 - \omega^2[\omega_F^2+\omega_G^2+4\epsilon_F\epsilon_G(1-\sigma^2)]+\omega_F^2\omega_G^2}{2\omega(\omega_G^2\epsilon_F+\omega_F^2\epsilon_G)-2\omega^3(\epsilon_F+\epsilon_G)}\right\} - \pi$$

where

$R(\omega)e^{-i\varphi_I}$	is the barograph frequency response
ω	is the angular frequency of the pressure disturbance
ω_F	is the natural frequency of the float transducer
ω_G	is the natural frequency of the galvanometer
ϵ_F	is the damping constant of the float transducer
ϵ_G	is the damping constant of the galvanometer
σ	is the coupling factor

The instrument constants are such that the galvanometer and float systems are critically damped, $\epsilon_F = \epsilon_G = 1$ and the coupling factor is negligible, $\sigma = 0$.

Since there was no record of an absolute response calibration for the instrument, it was decided that the best method of determining the frequency independent X_p was to compare responses with a well calibrated barograph at the U.S. Naval Electronics Laboratory, San Diego, California. At our request, they sent us their calibrated

record of the 4 October 1961 Russian explosion. In addition we received NEL/Report 773 which contained a description and frequency response of their barograph.

Performing Fourier analyses of the explosion recorded at NEL and the same event recorded here, we see from equation 76 that X_p can be found by

$$X_p = \frac{\mathcal{R}_{NEL}}{\mathcal{R}_{mp}} \left(\frac{\sin \Theta_p}{\sin \Theta_{NEL}} \right)^{1/2} \frac{S_p}{S_{NEL}} \qquad (78)$$

where S is the absolute value of the Fourier analysis, $\mathcal{R}_{NEL}$ is the amplitude response for the NEL barograph, $\mathcal{R}_{mp}$ is as defined in equation 77, and NEL and p subscripts denote NEL and Pasadena respectively.

In the actual analysis, we used the same window length and digital interval for each record. A value of X_p was then calculated using equations 77 and 78 for 40 frequencies, and the resulting mean value of X_p was used in the barogram synthesis program.

A resulting $X_p = .53$ was determined for the microbarograph with a critically damped 15 second period float and a critically damped 90 second galvonometer.

Barogram Synthesis

For spherical boundary value problems with harmonic time dependence, the requirement that the solutions be periodic in θ causes ν to be an integer. This requirement by equation 72 restricts k_j to particular values reducing our continuous (ω, k_j) phase spectra for $F_a = 0$ to discrete points. For this problem, we use the continuous (ω, k_j) or (ω, c_j) curves when we integrate our solution over ω to obtain theoretical barograms. Using the continuous (ω, k_j) curves has been shown by Weston (1961) to be equivalent to only keeping terms in the spherical solution which represent waves which have arrived at the detector without encircling the earth.

The flat earth result given by equation 76 is obviously the wave which has come directly to the detector by way of the shortest route without passing the antipode. For reference purposes and to be consistent with other authors we designate this arrival in the time domain as A_1. This solution is very similar in form to the result given by Weston (1961) for the spherical problem assuming a flat earth approximation. In fact the θ or π dependence for spectral amplitude and phase are identical. The solution differs from ours in the manner of calculating the homogeneous solutions,

the mode excitation, source normalization, and the detail in modeling the atmosphere realistically. Moreover he showed that for the A_2 arrival, which had traveled by way of the antipodal route, the spectral amplitude was the same as for the shorter route and had a phase corresponding to the longer route with a positive phase shift of $\frac{\pi}{2}$.

Since the derivation used here is for a horizontally stratified atmosphere with an approximate curvature correction, our solution cannot possibly give A_2 . Therefore using Weston's result as a justification, we obtain the A_2 arrival by replacing r in the phase of equation 76 by r_2 and by adding a positive phase shift of $\pi/2$, where r_2 is given by

$$r_2 = a_e(2\pi - \theta) = 2\pi a_e - r \qquad (79)$$

Leaving the spectral amplitude the same for A_2 as A_1 after A_2 has traveled a longer route can be physically interpreted as a refocusing of the spectral energy at the antipode with a resultant shift in phase of $\pi/2$ which often occurs in problems involving a focus.

Now performing the integration over ω so that the source

used in the derivation of equation 76 has the observed pressure-variation in the time domain, we have for A_1 from equation 76

$$[p(R,0;t)]_{a_j} \equiv [p_0]_{a_j} = \frac{1}{2\pi}\int_{-\infty}^{\infty} \{\bar{p}_0\}_{a_j}\, d\omega$$

$$= \left(\frac{2}{\pi R_e}\right)^{1/2} \frac{e^{-\lambda_s \hat{a}_s}}{\rho_s^{\circ}(D)}\, \hat{a}_s\, \rho_{as} \cdot (I_1 + I_2) \qquad (80)$$

$$R_e = a_e \sin\Theta$$

where

$$I_1 = \int_0^{\tilde{a}_1} \tilde{\mathcal{F}}_a^{(1)}(\omega)\, e^{i\omega(t-\tau_a)}\, d\omega + \int_{-\tilde{a}_1}^{0} \tilde{\mathcal{F}}_a^{(1)}(\omega)\, e^{i\omega(t-\tau_a)}\, d\omega$$

$$I_2 = \int_{\tilde{a}_1}^{\infty} \tilde{\mathcal{F}}_a^{(2)}\, e^{i\omega(t-\tau_a')}\, d\omega + \int_{-\infty}^{-\tilde{a}_1} \tilde{\mathcal{F}}_a^{(2)}(\omega)\, e^{i\omega(t-\tau_a')}\, d\omega \qquad (81)$$

$$\tilde{\mathcal{F}}_a^{(1)} = e^{\chi_s \hat{a}_s}\, \frac{A_{a_j}(\omega)}{(b_s^2+\omega^2)}\, |k_j|^{1/2} \left[\frac{\rho_s(D)}{\rho_0}\right]_{H_j} = e^{\chi_s \hat{a}_s}\, \tilde{\mathcal{F}}_a^{(2)}$$

$$A_{a_j}(\omega) = \frac{1}{\left[\frac{p_{n-1}}{p_o}\right]_{H_j} \left(\frac{\partial F_a}{\partial k}\right)_{\omega, j}}$$

$$\tau_a = t_{as} + \frac{k_j}{\omega} R - \frac{\pi}{4|\omega|} + 2\frac{\theta_s}{\omega} \qquad , \frac{k_j}{\omega} = \frac{1}{C_j}$$

$$\theta_s = \tan^{-1}\left(\frac{\omega}{b_s}\right) \qquad \tau_a' = \tau_a + \tau_x$$

$$\tau_x = -\frac{\hat{a}_s}{\alpha_s} \frac{(\omega^2 - \tilde{a}_1^2)^{1/2}}{\omega}$$

and where the phase velocity, C_j , and $\left[\frac{p_o(0)}{p_o}\right]_{H_j} A_{a_j}(\omega)$ are even functions of ω . Thus from the criteria of equation 9 and the fact that $\omega(t - \tau_a)$ is odd about $\omega = 0$, we have for calculating purposes

$$I_1 = 2 \int_0^{\tilde{a}_1} \left[\frac{p_s(0)}{p_o}\right]_{H_j} \frac{A_{a_j}(\omega)}{(b_s^2 + \omega^2)} k_j^{1/2} e^{\frac{\hat{a}_s}{\alpha_s}(\tilde{a}_1^2 - \omega^2)^{1/2}} \cos\omega[t - \tau_a]\, d\omega$$

and (82)

$$I_2 = 2 \int_{\tilde{a}_1}^{\infty} \left[\frac{\rho_s(D)}{\rho_o}\right]_{H_j} A_{a_j}(\omega) \frac{k_j^{1/2}}{(b_s^2+\omega^2)} \cos\omega[t-(\tau_a+\tau_x)]\, d\omega$$

where $$\tau_x = -\frac{\hat{a}_s}{\alpha_s} \frac{(\omega^2-\tilde{a}_1^2)^{1/2}}{\omega}$$

For A_2 the above equations remain the same with the exception that τ_a is now given by

$$\tau_a = t_{as} + \frac{k_j}{\omega} h_2 - \frac{3\pi}{4\omega d} + 2\frac{\theta_s}{\omega} \qquad (83)$$

where h_2 is given by equation 79.

For the A_1 barogram, we include the instrument response $R(\omega)$ and ϕ_I/ω given by equation 77, and obtain

$$I_1 = 2 \int_0^{\tilde{a}_1} R(\omega) \left[\frac{\rho_s(D)}{\rho_o}\right]_{H_j} A_{a_j}(\omega) \frac{k_j^{1/2}}{(b_s^2+\omega^2)} e^{\frac{\hat{a}_s}{\alpha_s}(\tilde{a}_1^2-\omega^2)^{1/2}} \cos\omega[t-(\tau_a+\tfrac{\phi_I}{\omega})]\, d\omega$$

(84)

$$I_2 = 2 \int_{\tilde{a}_1}^{\infty} R(\omega) \left[\frac{p_s(0)}{p_0}\right]_{H_j} A_{a_j}(\omega) \frac{k_j^{1/2}}{(b_s^2+\omega^2)^{1/2}} \cos\omega\left[t-(\tau_a+\tau_x+\phi_z(\omega))\right] d\omega$$

The barogram for A_2 is obtained by the same modification.

III. COMPUTATIONAL METHOD

The calculation of theoretical barograms is accomplished by means of two FORTRAN programs written for the IBM 7090 computer. The first is a modification of the air wave dispersion program described in Press and Harkrider (1962). Its purpose is to calculate all the quantities in equation 82 which depend on layering alone. These quantities are $A_{a_j}(\omega)$, k_j, and the group velocity, $U_j = \frac{d\omega}{dk_j}$.

In order to reduce the number of calculations for a given root, we find the zero's of the function F_a in terms of C_j and k_j instead of k_j and ω. There is further economy of calculation if we specify C_j and use trial k's until a zero of F_a is found. This is due to the large number of terms in F_a which are a function of C_j and the layer constants alone. Thus once calculated for a given C_j, they remain the same for every trial k used in computing F_a.

Therefore for the computation of F_a we use the following form of equation 51

$$F_a = A_{12}^{*} + (kc)^3 \frac{\left[q_m \left(\frac{\alpha_m^2}{c^2} - \frac{\gamma}{2} \right) - i\alpha_m^2 (k/\alpha_m) \right]}{\rho_m^{o} (z_{m-1}) \alpha_m^2 \delta_m} \cdot A_{22} \qquad (85)$$

All quantities in equation 85 are always real for all (c, k) real except for $i(k/\alpha_m)$ which is real or imaginary depending on the values of real (c, k). Since in this paper we are interested in undamped propagation, we now make the requirement that $(k/\alpha_m)^2$ be < 0 . This excludes leaking or complex modes of propagation. Under this condition, equation 85 is real and takes the form used in numerical calculation of dispersion curves:

$$F_a = A_{12}^{*} + (kc)^3 \frac{\left[q_m \left(\frac{\alpha_m^2}{c^2} - \frac{\gamma}{2} \right) - \alpha_m^2 |k/\alpha_m| \right]}{\rho_m^{o} (z_{m-1}) \alpha_m^2 \delta_m} \cdot A_{22} \qquad (86)$$

The condition that $(k/\alpha_m)^2 < 0$ now prescribes a cutoff region in the (c, k) plane defined by $(k/\alpha_m) = 0$. The boundary of this region is obtained in terms of c and period T by setting equation 22 equal to zero. This yields

$$T = T_{Bm} \frac{\left(\frac{c^2}{\alpha_m^2} - 1\right)^{1/2}}{\left(\frac{c^2}{\beta_m^2} - 1\right)^{1/2}} \qquad (87)$$

where

T_{Bm} is the Brunt resonant period of the halfspace and is given by

$$T_{Bm} = \frac{2\pi}{\sigma_{Bm}}$$

From equation 85 we have the following asymptotic values of the boundaries of the cutoff region

$$T \rightarrow \left(\frac{\beta_m}{\alpha_m}\right) T_{Bm} \qquad \text{for} \quad c \rightarrow \infty$$

$$T = 0 \qquad \text{for} \quad c = \alpha_m$$

No cutoff region occurs for $\beta_m \leq c \leq \alpha_m$

(88)

$$T \rightarrow \infty \qquad \text{for} \quad c \rightarrow \beta_m$$

$$T = T_{Bm} \qquad \text{for} \quad c = 0$$

No cutoff region occurs for

$$\left(\frac{\beta_m}{\alpha_m}\right) T_{Bm} \leq T \leq T_{Bm}$$

The flow of this program is similar to that in the programs described in Press, Harkrider and Seafeldt (1961) and Harkrider and Anderson (1962). The zeros of F_a are determined by initially specifying the phase velocity, C_j, and a trial value of the wave number, k. The elements of the A_m matrix are formed at

each layer and then multiplied by the matrix of the layer above it, starting with the layer at the surface. After the matrix product for all layers has been calculated, the program then combines these numerical quantities to obtain a value for F_a . New trial values of k (of increasing or decreasing size depending on the sign of the initial F_a value) specified by an input Δ k are used to calculate new k values until the root is bracketed by a change of sign in F_a. Linear interpolation and extrapolation are then repeatedly used to find small F values until k's of different F_a signs are within the precision interval desired. The resulting interpolated value of k is the output value given as the root for the input c_j.

The program has an additional feature in that as an input option, the first or second roots (two smallest k roots) will be found for a given c. This is accomplished by starting at the smallest k outside of the cutoff region (F_a complex) and finding either the first or second sign changes of F. The roots associated with either mode are then computed. For $c \geq \beta_m$ in the isothermal halfspace model, this initial k is zero. For $c < \beta_m$ the initial k is determined by equation 87.

In all models calculated we found that each continuous dispersion

curve or mode was a monotonic decreasing function of c versus k or T and always had the same F_a sign change through the root region. This made it easy to track all of the roots of a preselected mode. In order to save computer time and keep from jumping modes, the k root for the previous c is used as the starting point for the new c. Further details about root hunting procedures can be found in papers by Press et al (1961) and Harkrider and Anderson (1962).

Once a root is found by the computer, the homogeneous velocity and pressure ratios given by equation 68 are calculated at the midpoint in each layer. The vertical distribution of these ratios is generally diagnostic of the particular mode and provides a check against mode jumping.

Next the program computes the root values of $A_{a_j}(\omega)$ and U_j. In order to calculate $A_{a_j}(\omega)$, we need the value of $\left(\frac{\partial F_a}{\partial k}\right)_{\omega,j}$. This is accomplished by defining a layer derivative matrix $\left(\frac{\partial a_m}{\partial k}\right)_\omega$ where

$$\left[\left(\frac{\partial a_m}{\partial k}\right)_\omega\right]_{lk} = \left[\frac{\partial (a_m)_{lk}}{\partial k}\right]_\omega \qquad (89)$$

is the definition of the $\ell\pi^{th}$ matrix element. From equation 89 and the definition of matrix multiplication, we see that the matrix

$\left(\frac{\partial A_m}{\partial k}\right)_\omega$ can be given by the matrix products

$$\left(\frac{\partial A_m}{\partial k}\right)_\omega = \left(\frac{\partial a_m}{\partial k}\right)_\omega A_{m-1} + a_m \left(\frac{\partial A_{m-1}}{\partial k}\right)_\omega \qquad (90)$$

Therefore using equation 90 and analytic expressions for equation 89 in each layer starting from the surface layer, we can calculate the matrix $\left(\frac{\partial A}{\partial k}\right)_\omega$. With the elements from this matrix, we compute $\left(\frac{\partial F_a}{\partial k}\right)_\omega$ from equation 86. Similarly we calculate $\left(\frac{\partial F_a}{\partial \omega}\right)_k$ and form the group velocity U_j by the relation

$$U_j = -\left(\frac{\partial F_a}{\partial k}\right)_\omega \Big/ \left(\frac{\partial F_a}{\partial \omega}\right)_k \qquad (91)$$

The form of $A_{a_j}(\omega)$ given by equation 81 is due to a simplification in the numerator of the integral expression 62 evaluated at the zeros of the denominator. This simplification is

based on the fact that F_a is exactly zero at the poles of the integrand. But since a root is designated by the significance in k and not in how close F_a is to zero for root k, we felt that it would be desirable to calculate two A_{a_j}'s. The first, $A_{a_j}^{(1)}$, is defined by equation 81. The second, $A_{a_j}^{(2)}$, is calculated using the numerator of equation 51 of the integrand prior to the residue evaluation. The advisability of calculating two is demonstrated in the following paragraphs.

The value of $\left(\frac{\partial F_a}{\partial k}\right)_\omega$ depends on the number of layers used in calculating the roots of F_a. But since A_{a_j} is the frequency response at the surface for a source infinitesimally near the surface, one would expect it to be relatively insensitive to the higher layers especially at high frequencies. The same is true for c_j and U_j as long as the number of layers is such that all the minimum velocity layers are represented and the halfspace used in the root calculation is the highest velocity used in the calculating array. With this in mind the program calculates a "pseudo" $A_{a_j}^{(1)}$, $A_{a_j}^{(2)}$, and U_j at each layer starting from the surface by assuming that the next higher layer is the halfspace. For some layers this is impossible since the "pseudo" F_a at that altitude is complex. For these layers the machine prints out zero for $A_{a_j}^{(1)}$, $A_{a_j}^{(2)}$, and U_j.

As the "pseudo" calculations approach the root halfspace, we found that $A_{a_j}^{(2)}$ and U_j converge rapidly to their value at the root halfspace. (Here and later we designate the halfspace or last layer used in the root calculation as the root halfspace.) The difference in significance was often outside the "print out" value. As expected, we found that the higher the frequency the lower the altitude at which this convergence occured. Once "pseudo" $A_{a_j}^{(2)}$ and U_j begin to converge, they never "blow up" with increasing altitude, even at very high frequencies. This was not true for "pseudo" $A_{a_j}^{(1)}$ which converged slowly with altitude until it was near the convergent value indicated by $A_{a_j}^{(2)}$ at the root halfspace. It then began to diverge rapidly as the layer number or altitude increased. At long periods where the convergence for $A_{a_j}^{(1)}$ and $A_{a_j}^{(2)}$ was slow, the root halfspace values for $A_{a_j}^{(1)}$ and $A_{a_j}^{(2)}$ agreed to "print out" significance.

Because of the above, we used for A_{a_j} the root halfspace value of $A_{a_j}^{(2)}$ for all frequencies. The rapid convergence at high frequencies and the $A_{a_j}^{(1)}$ and $A_{a_j}^{(2)}$ agreement at small frequencies gave us confidence that our computed values of A_{a_j} and U_j were correct. As a further

check, we calculated a rough group velocity in two ways. The first is by numerical differentiation of the phase velocity. $\Delta c/\Delta k$ is obtained by perturbing c slightly and then finding a new k root. The second method is by numerical differentiation of F_a and using equation 91.

Before going on to a new root, the program stores k_j, c_j, U_j, A_{a_j}, and $\left[\frac{p_m - v_2}{p_o}\right]_{H_j}$, the pressure ratios at each layer mid-point, on a magnetic tape to be used in the barogram synthesis program. The location or file number of this data on the tape is printed out and the process is repeated for a new c_j until all the requested roots are determined.

The program has two options for input of layer constants. The first reads d_m and K_m° from data cards. From equations 17 and 18 we then calculate α_m and ρ_m° where for calculation purposes ρ_m° is given by

$$\rho_m^\circ = \rho_o^\circ \frac{K_o^\circ}{K_m^\circ} \exp\left(-\sum_{j=1}^{m-1} 2\lambda_j d_j - \lambda_m d_m\right) \qquad (92)$$

Here ρ_o° and K_o° are the equilibrium values for surface density and temperature. The second input option is to read

in d_m , α_m , and ρ_m^o directly.

From equation 18 we see that in order to obtain λ_m and in turn equation 92, we must calculate the layer gravity g_m . In the cases given in this paper the constant gravity in layer m , g_m , was chosen to be the value of gravity for a spherical earth at an altitude equal to the layer midpoint $z_{m-1/2}$.

As in previous dispersion programs, numbers of the order of $\exp\left(k \sum_{j}^{m-1} d_j\right)$ are involved in the calculation of F_a. Therefore, as c decreases and k increases, the larger root values of k will lead to machine overflow, if the total number of layers remains constant. When this occurs, the program will automatically reduce layers starting at high altitudes until F_a no longer overflows. The program then recalculates the root for the previous larger c in order to verify that no loss in precision of the k root was caused by layer reduction.

It can be shown that the determinants of the a_m matrices are identically equal to unity for all values of (c, k). It follows that the determinant of the product matrix A is also equal to one. Therefore, if loss in significance occurs due to machine round-off during the matrix multiplication loop, the numerical values of the

product matrix determinant differs greatly from one. As a check on the validity of roots, the program calculates and prints this determinant for each root.

From equation 26 we see that certain matrix elements are infinite at $\delta_m = 0$. For each layer, $\delta_m = 0$ defines a straight line in the (c, T) plane given by

$$T_m = \frac{2\pi c}{q_m}$$

Since q_m is bounded by $q_0 \geq q_m \geq q_n$, the δ_m's=0 for all layers fall in the region bounded by $T = \frac{2\pi c}{q_0}$ and $T = \frac{2\pi c}{q_0}$. This region will be shown on the dispersion curve figures as a stippled wedge starting at (c, T)=(0, 0) and extending to the top of the figures. In order to keep the programs from needlessly reducing layers due to overflow caused by a trial k being close to the zeros of δ_m , the computation is programed to keep c and k out of this region.

The purpose of the second program is to take the quantities calculated by the dispersion program and synthesize the pressure and barogram time variations at some surface detector. This is accomplished by applying the Aki approximation with linear amplitude intervals to equations 82 and 84. The approximation is given in appendix C by equation C11. Rearranging equation 82 into the form of equation C 11,

we see that the group delay, t_g , not previously defined, is

$$t_{g_i} = t_{as} + \frac{\pi}{U_i} + 2\left(\frac{d\theta_s}{d\omega}\right) \qquad \text{for} \quad 0 < \omega_i < \tilde{a}_1$$

and

(93)

$$t_{g_i} = t_{as} + \frac{\pi}{U_i} + 2\left(\frac{d\theta_s}{d\omega}\right)_i - \frac{\hat{a}_s}{\alpha_s}\frac{\omega_i}{(\omega_i^2 - \tilde{a}_1^2)^{1/2}} \qquad \text{for} \quad \omega_i > \tilde{a}_1$$

Similarly for equation 84, we obtain

$$t_{g_i} = t_{as} + \frac{\pi}{U_i} + 2\left(\frac{d\theta_s}{d\omega}\right)_i + \left(\frac{d\phi_I}{d\omega}\right)_i \qquad \text{for} \quad 0 < \omega_i < \tilde{a}_1$$

and

(94)

$$t_{g_i} = t_{as} + \frac{\pi}{U_i} + 2\left(\frac{d\theta_s}{d\omega}\right)_i - \frac{\hat{a}_s}{\alpha_s}\frac{\omega_i}{(\omega_i^2 - \tilde{a}_1^2)^{1/2}} + \left(\frac{d\phi_I}{d\omega}\right)_i \qquad \text{for} \quad \omega_i > \tilde{a}_1$$

For convenience the input layer parameters are in the same format as the dispersion program. Along with the model or layer parameters we have as input the "standard" bomb characteristics and the barograph constants. From this point on the program input

is divided into cases. As many of these cases can be run as desired depending on available machine time. Each case consists of input cards stating the number of modes, the source height, bomb yield, detector distance, approximate frequency interval, initial time at the detector, time interval between points, and the number of points to be calculated in the time series. From the source height, the program determines the source layer and the density at the source altitude. Thus with the yield, density, and source layer velocity, the distance scaling factor ξ is calculated by equation 13. Using ξ we obtain the needed bomb characteristics for the given case.

Each case is divided into modes. The mode input cards contain the number of frequencies previously calculated and the location of each frequency result on the dispersion storage tape. The location or file number order is by increasing frequency. Using the input file locations the computer reads k_j, C_j, U_j, A_{a_j}, and $\left[\frac{\rho_m}{\rho_0} - 1/2\right]_{H_j}$, where m is the layer containing the source, from this tape. Using the input layer constants for the source layer and the source altitude, the homogeneous pressure ratios at the source layer midpoint are corrected to the ratios at the source altitude, $\left[\frac{\rho_s(0)}{\rho_0}\right]_{H_j}$. With the frequencies, $\omega_j = \frac{k_j}{C_j}$,

tables of c_j, U_j, and $A_{sj} = k_j^{1/2} A_{aj} \left[\frac{\rho_s(0)}{\rho_0}\right]_{H_j}$

are formed and stored for later use.

Using the initial frequency, the final frequency, the approximate $\Delta\omega_i$ and $\tilde{a}_1$ calculated from the source layer constants, the program computes new frequency intervals subdividing the mode frequency band into equal intervals on each side of $\tilde{a}_1$. The new intervals are formed under the restriction that at most their width is less than the input interval and that there are at least 10 intervals for synthesis. For each interval midpoint, ω_i, the program calculates the exact values of the following source dependent quantities and their first derivatives with respect to ω.

$$A_{so} = \frac{e^{\hat{a}_s (\tilde{a}_1^2 - \omega_i^2)^{1/2}}}{(b_s^2 + \omega_i^2)} \qquad \text{for} \quad 0 < \omega_i < \tilde{a}_1$$

$$\theta_s = \tan^{-1}\left(\frac{\omega_i}{b_s}\right)$$

(95)

$$A_{s0} = \frac{1}{(b_s^2 + \omega_i^2)}$$

$$\theta_s = \tan^{-1}\left(\frac{\omega_i}{b_s}\right) \qquad \text{for} \quad \omega_i > \tilde{a}_1$$

$$\tau_\chi = -\frac{\hat{a}_s}{\alpha_s}\,\frac{(\omega_i^2 - \tilde{a}_1^2)^{1/2}}{\omega_i}$$

Using linear interpolation between the stored tape values, we obtain c_i, U_i, A_{si} and $\left(\frac{dA_s}{d\omega}\right)_i$ at the frequency midpoints. Combining these quantities with R, equations 93, 94, 95 and their evaluated derivatives, we obtain the values of $\bar{A}_i$, $\left(\frac{d\bar{A}}{d\omega}\right)_i$, τ_i and tg_i to be used in equation C11. When R is greater than the half circumference of the earth the program automatically corrects the phase delay and group delay to correspond to waves traveling the long way around the earth. The pressure at the detector is then calculated for an initial time and as many time increments as specified by the input. Next we calculate the exact barograph quantities $R(\omega_i)$, $\left(\frac{dR}{d\omega}\right)_i$, $\frac{\varphi_I}{\omega_i}$, and $\left(\frac{d\varphi_I}{d\omega}\right)_i$. With these we modify the previous frequency values to obtain the barogram time series by means of equation C11.

The process is repeated for each mode specified by input. In addition, an accumulated pressure and barogram time series is obtained by adding the time series of this mode to the previous mode. The time series values are printed out and graphically displayed by the printer and a Mosley Plotter. As soon as all modes have been computed the program goes to the next case.

IV. DISCUSSION

Frequency Domain

The vertical temperature structure used to model the earth's atmosphere is the ARDC standard atmosphere (Figure 1) used in Press and Harkrider (1962). This model is chosen since it was shown to explain adequately all the significant group-frequency arrivals in the observed barograms from the Russian Nuclear Tests (Figures 2 and 3).

The ARDC standard model of the atmosphere is characterized by the presence of two temperature minimums; one at 18.5 km and the other at 85 km. For computation it is represented by a digital model with 39 layers and is terminated with an isothermal half-space beginning at an elevation of 220 km. In addition to this model, we show dispersion curves for the following modifications of the ARDC standard atmosphere: an atmosphere terminated with a free surface at 220 km; an atmosphere with the upper temperature minimum removed; an atmosphere with the lower temperature minimum removed. The temperature structures for these models are shown in Figures 1 and 5. The atmosphere terminated by a free surface is studied to see how dispersion curves and spectral amplitude are effected by the method of termination. The remaining models are studied in order to estimate the effect of upper and lower temperature

minimums.

The following is a discussion of the dispersion curves for the various models. A more detailed discussion for these and other models can be found in Press and Harkrider (1962). Phase and group velocity curves are presented as a function of period for several modes of propagation in each model.

Dispersion curves are plotted in Figures 6 and 7 for the ARDC atmosphere terminated with an isothermal halfspace at 200 km. Figure 8 contains dispersion curves for this model terminated with a free surface at 220 km. The hatched areas in the upper half and lower right portions of Figures 6 and 7 are the cutoff regions within which lossless propagation does not occur because of radiation into the halfspace. Radiation losses do not occur for the model with a free surface termination. The oblique stippled band represents a region of singular values of F_a corresponding to $\delta_m = 0$. The program avoids these regions.

The dispersion curves are separated into modes S_0 and S_1, S_2 and GR_0, GR_1. The S modes are the first three of an infinite set, analogous to the corresponding acoustic modes of a non-gravitating model. This correspondence is based on the similarity in dispersion curves for T<4 min; it also follows from the fact that

in both cases the pressure-height curve has no nodes for S_0 , one node for S_1 , and two nodes for S_2 .

The high frequency limit of the S_0 , S_1 , and S_2 curves is the sound velocity in the upper channel. At infinite period phase and group velocities of S_0 reach values of about .75 km/sec. S_1 and S_2 have long period cutoffs near 4 and 3 minutes respectively with limiting phase and group velocities somewhat higher than the halfspace sound velocity (Figures 6 and 7). For the free surface model (Figure 8) S_0 , S_1 and S_2 approach infinite phase velocities and zero group velocities at long period cutoffs.

The modes GR_0 and GR_1 are not present for a non-gravitating model. GR_0 is characterized by vertical particle displacement with no nodes, GR_1 has one node, etc. A large number of GR modes have been found, but only a few are plotted. It is unusual that with increasing mode number (as defined by an increasing number of nodal surfaces) the period increases. With decreasing period the GR modes are characterized by phase and group velocities which reach zero. For increasing periods, phase velocity curves run into cutoffs for the

halfspace models. Group velocity maximums for GR_0 and GR_1 form flat plateaus at 312 meters/sec. For the model with a free surface termination phase and group velocity for the GR modes have no long period cutoffs. GR_0 shows the same plateau in group velocity at 312 meters/sec. The higher GR modes have plateaus below this. Dispersion curves corresponding to GR modes were first shown by Gazaryan (1961).

These two models have the following features in common: (1) Phase and group velocities between 400 and 200 meters/sec are essentially the same for S_0, S_1, S_2 and GR_0 modes for periods less than 5 minutes; (2) Between 5 and 15 minutes, a broad flat maximum in group velocity occurs at a value of 312 meters/sec. For the standard ARDC this plateau is formed by GR_0 and GR_1 with a "hole" in the plateau between 13 1/2 and 14 minutes. For the free surface model GR_0 forms the entire plateau and no "hole" is present. The dispersion curves for the two models differ for periods greater than 4 1/2 minutes in the regions of steeply rising phase and group velocities. From the study of other cases we have found that these portions of the dispersion curves are sensitive to the precise manner in which the very low density atmosphere above 100 km is specified.

It is interesting that flat segments of phase and group velocity

of S_2, S_1, S_0, GR_0, GR_1 for the ARDC standard model are nearly connected to form a common dispersion curve. The steep segments of the phase velocity curves are similarly related. The character of the propagating disturbance at any time is perhaps better represented by pseudo-dispersion curves formed from segments of several modes. The segments which form a pseudo-mode are all particularly sensitive to a given region of the waveguide. It will be shown that the sequence of maxima in group velocity are all associated with the properties of the lower channel of the atmosphere. This phenomenon has also been observed for multilayered elastic wave guides (Tolstoy, 1959).

The ARDC model with no upper temperature minimum (Figures 5 and 9) was studied to see how the upper channel of the atmosphere affects the dispersion curve. The major changes which occur are: (1) very short period energy now travels with sound velocity in the lower channel; (2) the minima in group velocity for the S_0 and S_1 modes shown in Figure 6 almost disappear. The time of arrival of the first waves, corresponding to the group velocity maxima of GR_1, S_0, S_1 is almost unchanged, and is therefore

unaffected by the properties of the atmosphere above 50 km.

The ARDC model with no lower temperature model (Figures 5 and 10) demonstrates that the arrival time of the first waves is particularly sensitive to the properties of the lower atmospheric channel which occupies the region 0-50 km. The maxima in group velocity associated with the first waves are shifted from 305 - 312 meters/sec to 320-335 meters/sec. GR_0 and GR_1 are otherwise unchanged. The minima in group velocity of S_0 and S_1 are deepened but the short period limit of phase and group velocity is unchanged.

In Press and Harkrider (1962) the ARDC models of tropical, artic winter and arctic summer atmospheres were studied to explore seasonal and geographic influences on dispersion (Figure 4). In these models the properties of the atmosphere below 40 or 50 km were varied. Of these models the dispersion results for the arctic winter model (Figures 4 and 11) deviated most from the ARDC standard. As might be expected from the previous section, the major difference between the ARDC standard and the arctic winter results (Figures 2 and 3) is the arrival time of the first waves. The group velocity plateau is reduced from 312 m/sec to 302 m/sec. The steeply rising portions of the group velocity which form the "legs" of the plateau are shifted to shorter periods.

This shift occurs for all modes with the exception of the short period "leg" of GR_0 and the long period "leg" of S_0 . This has the effect of increasing the width of the S_0 plateau at the expense of GR_0 .

The effect of lower portions of the wave guide on spectral amplitude can best be seen in the following. From Chapter II we know that the response of the medium for a surface source and receiver is given by $A_a(\omega)$. This response for S_2 , S_1 , S_0 , GR_0 , and GR_1 for the ARDC standard and arctic winter models are illustrated in Figure 12. The most striking feature is the similarity in shape between group velocity and amplitude. This similarity in shape demonstrates that the early arriving waves are more efficiently excited by near ground disturbances recorded by ground based detectors than the later arrivals corresponding to the group velocity minima. This effect was predicted in Press and Harkrider (1962) on the grounds that the early arrivals corresponding to the group velocity plateaus were controlled by the atmosphere structure below 50 km where as the group velocity minima were sensitive to the atmosphere above 50 km.

Another interesting feature of the response curves is the secondary plateaus of S_2 and S_1 (shown as A and B on Figure 12) at frequencies corresponding to later long period group arrivals. The secondary plateaus of S_2 and S_1 extend from a period of 2 and 3 minutes respectively to the long period cutoff of each mode.

For the S_2 mode this plateau for the late arriving 2 - 3 1/2 minute wave yields an excitation equivalent to the earlier arriving 1 - 1 1/4 minute wave. The effect of terminating the model with a free surface instead of a half space is to eliminate the hole in the spectrum near 14 minutes with a continuation of GR_o at an amplitude equal to that shown for GR_i . A similar effect is shown for the group velocity plateau in figures 7 and 8. Superimposed on the mode response curves is the amplitude response of the microbarograph with a peak amplitude of .021 inches/μ bar at a period of 1.6 minutes.

The effect of source and receiver height on spectral amplitude can be determined by the vertical distribution of the homogeneous pressure ratios. The distribution of this ratio as a function of period at a particular altitude is given in Figures 13, 14, and 15 for the ARDC standard model. The spectral amplitude is given by the product of A_a and the homogeneous pressure ratios at the source and receiver elevation. Thus a horizontal line in Figures 13, 14, and 15 with a constant value less than one would indicate a uniform reduction in amplitude over surface amplitudes.

In Figure 13, we display the ratio for an altitude of 18.5 km corresponding to the midpoint of the lower velocity channel. Other than a uniform reduction in amplitude as compared to surface excitation, this ratio shows the following effects on amplitude. (1) There is very little change in the general shape of GR_0 and GR_1. The late arriving waves for GR_1 are decreased slightly. The late arriving GR_0 are increased slightly especially at the short period end. (2) The early arriving waves for the acoustic modes corresponding to the group velocity plateaus show an increase in amplitude relative to the gravity modes. With either the source or detector at this altitude the peak amplitudes of the S_2, S_1, and S_0 modes are equal to the peak amplitudes of the and GR_1 modes. With both source and detector at this altitude the GR_0 peak amplitudes of the acoustic modes are greater than the gravity modes in the following order $S_2 > S_1 > S_0$. (3) The secondary plateaus of S_2 and S_1 are reduced relative to the plateaus of early arriving waves of all the modes. (4) The high frequency late arriving waves for the acoustic modes show an increase in excitation and the long period late arriving waves for S_2 and S_1 show a decrease.

A detailed discussion on the amplitude or excitation effects of placing the source or receiver in the more interesting parts of the atmosphere is beyond the scope of this paper. This is in part due to the fact that the observed barograms used in this paper were

produced by nuclear explosions at an altitude of less than 4 km.

The ratios necessary for determining these effects are given in Figures 13, 14, and 15 and can be summarized as follows: (1) In the lower velocity miminum, the gravity modes are comparatively unaffected as to shape. The excitation of the early arriving waves for the acoustic modes are increased relative to early arriving gravity waves. (2) In the relative velocity maximum between the minima, the early arriving acoustic waves are less excited than the corresponding gravity waves. (3) The effect of increasing altitude is to increase the excitation of the late arriving waves relative to the early arriving waves for each mode. For the short period acoustic waves which travel near the acoustic velocity of the upper minimum, the relative increase in excitation is maximum in this channel while the excitation of the long period late arrivals continues to increase with altitude. The majority of these results were postulated in Press and Harkrider (1962) from the manner in which different portions of the atmosphere affected the dispersion results. In addition, it must be remembered that these results hold for a "white" source only. The effect of the scaling laws for nuclear weapons is such that some of these effects will not be apparent for theoretical barograms in the time domain. This

will be discussed in greater detail later.

Time Domain

In order to study the effect of source yield and altitude in the time domain under realistic bomb test conditions, we constructed theoretical barograms using the amplitude and dispersion results for the ARDC model, terminated by a half space at 220 km. As a check on the conclusions drawn in the following paragraphs, selected barograms were made for an ARDC arctic winter model.

From seismic evidence the approximate location of the Russian tests gives a path of $r = 8000$ km for A_1 and an antipodal path of $r_2 =$ 32000 km for A_2 to the microbarograph at Donnelley Seismological Laboratory, Pasadena, California. The constants used for the bomb characteristics of a one kiloton explosion from The Effects of Nuclear Weapons, 1962 are as follows; a peak excess pressure of $p_a = 34.45$ milibars at a range of $\hat{a}_o = 1.61$ km, and a positive phase duration of $T_{+a_o} = .48$ sec.

All theoretical barograms given in this section are on the same horizontal time scale and have a common fiducial time at the left hand margin of the figure. Since the plotting scale is determined internally by the program, the scales for various traces may differ even in the same figure. Therefore in order to facilitate

amplitude comparisons, we have indicated certain vertical amplitudes in the figures by means of numbers, arrows and a horizontal dash at a peak and trough. The vertical scale for pressure waves is given in μ bars of pressure and the vertical scale for barograms is given in inches of barograph recording.

The most significant features of the theoretical barogram for the ARDC standard and arctic winter models are given by the summation of five modes, S_2 , S_1 , S_0 , GR_0 and GR_1 . Of these, the least significant contribution was that of GR_1 . In Figure 16 we show the theoretical pressure variation of A_1 for a 4 megaton nuclear explosion at 7000 feet elevation. The first four traces are the individual modes GR_0 , S_0 , S_1 , and S_2 . The fifth trace is the summation of all the modes. It also contains GR_1 whose contribution is negligible. In Figure 17, we have the corresponding A_1 theoretical barograms for the same explosion. Comparison of Figures 16 and 17 demonstrates the response of the barograph to the pressure wave arriving at the detector. This is seen in the relative increase in response of the higher frequency modes S_2 , S_1 , and S_0 to GR_0 .

In both Figures 16 and 17 we see that mode interference in the time domain significantly changes the character of the composite barogram. This is especially evident in the pressure variation where the super-position of modes results in spurious period arrival.

For determining the effect of yield with source altitude constant, five barograms were synthesized for the following yields at an altitude of 7000 feet; 1, 5, 10, 30, and 60 megatons (Figure 18). The most striking qualitative effect of increasing yield at the same source altitude other than the obvious increase in amplitude is the relative increase in the long period part of the wave train to the shorter period arrivals. This is especially noticeable in the extremes of the chosen yields. For 1 megaton blasts the S_1 mode is the major mode with S_0 and GR_0 almost equal to each other and somewhat less than S_1. For the 60 megaton explosion the GR_0 mode is by far the largest while S_0 is almost non-existant and S_1 gives the only high frequency character of the wave albeit small. This effect occurs despite the instrument response which accentuates the higher frequency modes S_0 and especially S_1.

From equation 82 we see that the only terms which could emphasize this mode with yield changes are the source terms in

the spectral amplitude

$$\frac{e^{\frac{\hat{a}_s}{\alpha_s}(\tilde{a}_1^2-\omega^2)^{1/2}}}{(b_s^2+\omega^2)}$$

for the long period modes

and

$$\frac{1}{(b_s^2+\omega^2)}$$

for the short period modes

where $\tilde{a}_1$ is the acoustic cutoff for the medium surrounding the source. Since $\tilde{a}_1 = \lambda_s \alpha_s$ is independent of the yield and by equations 11 and 12 $\hat{a}_s$ increases with yield so that the exponential term increases the relative excitation of the longer periods relative to the short periods with a yield increase. Similarly b_s decreases with increasing yield and thus increases the spectral amplitude at long periods while decreasing the short periods. From these factors we see that the scaling laws induce a "pseudo" non-linearity to the problem. This is especially true for the time scale of the initial pressure variation as the bomb size increases. Figure 19 shows the increase in amplitude and fundamental period with increasing yield for A_1 barograms of a

single mode, GR_o .

The effect of altitude for a constant yield is illustrated in Figure 20. For this purpose, we constructed three A_1 barograms for 5 megaton explosions at altitudes of 3500, 7000 and 14000 feet. In addition we made three more A_1 barograms for 30 megaton explosions at altitudes of 7000, 28000 and 56000 feet. With an increase of altitude from 3500 to 1400 feet for a 5 megaton bomb the barograms show an increase in amplitude of almost 50% in the portion of the wave train corresponding to group arrival of GR_o . For a group arrival corresponding to S_1 amplitude change is negligible. Both the overall amplitude increase and the relative increase of the long waves to the short waves with increasing altitude are due to the scaling laws used. This phenomenon is similar to the effect caused by increasing the yield at constant altitude discussed previously since $\hat{a}_s$ increases and b_s decreases with either an increase in yield or altitude.

For the early arriving short periods such as S_2 the decrease in short period due to decreasing b_s is compensated in this altitude range by the inverse effect of the wave guide itself.

In the frequency domain discussion it was pointed out that in the portion of the wave guide from the surface to the low velocity channel the effect of increasing altitude is to increase the relative excitation of the acoustic modes relative to the longer period GR modes.

For the 30 megaton bombs, the increase in altitude shows as increase in the long period arrivals and a decrease in the short period arrivals. From an altitude of 28000 feet to 56000 feet the short period part of train is negligible in amplitude. In this region of the atmosphere the long period emphasis of the scaling laws is increased by the wave guide since at altitudes near the relative temperature maximum the long period gravity modes are more easily excited than the short period acoustic modes.

Figure 21 shows A' barograms for an ARDC arctic winter atmosphere under various conditions of yield and bomb altitude. A comparison with theoretical barograms for the ARDC standard atmosphere yields the following observations: (1) The arctic winter wave train arrives at a later time than the ARDC standard corresponding to its lower group velocity plateaus. (2) The qualitative effects of varying yield and source altitude are the same as the ARDC standard model. (3) The major difference in wave train character is caused by mode interference. This is due to

the shift in phase for each mode caused by different phase velocities for the two models. (4) The amplitudes are essentially the same for the two models. Quantitative estimates of amplitudes for the composite barograms are complicated by mode interference.

Because of mode interference and the "pseudo" non-linearity induced by scaling laws, it is difficult to recover bomb yield and altitude from measurements on an observed or experimental barogram. Another method of attack is to compare observed barograms with theoretical barograms constructed from estimates of approximate yield and altitude.

Comparison of Theoretical and Observed Barograms

In this section we compare theoretical barograms with observed barograms at Pasadena produced by the Soviet nuclear explosions in Novaya Zemlya during the fall of 1961. The yields of the explosions are taken from the reported seismic estimations given by Bäth (1962). The altitudes for the 60 megaton explosion on October 30 and the 25 megaton explosion on 23 October were reported in the newspapers as being 12000 feet. Bäth (1962) classified the altitudes as low, intermediate and high for the 1961 explosions, with the 23 and 30 October being classifed as high. With this in mind we have arbitrarily assigned the following

altitudes to Bäth's qualitative estimates; 12000 feet for high altitude explosions, 8000 feet for intermediate altitude explosions, and 4000 feet for low altitude explosions.

In the following figures the theoretical and experimental records have been aligned on the time scale for the best fit. The arrows indicate where a fiducial time would fall on each record.

In Figure 22 the first two traces are the theoretical and observed recordings of A_1 waves from a 9 megaton explosion at 8000 feet on 10 September. In comparing the records we see that there is good agreement in phase, group and amplitude except in the region corresponding to the S_o group arrival. In this region between the numbers .8 and .85 on the theoretical trace we have a slight phase shift and mode interference resulting in a spurious long period. On the observed trace the 3 1/2 minute S_o arrival is well developed. In this figure and the following Figures 23 and 24, the S_o arrival is distorted, while on the observed records the arrival is well developed. The relative excitation between early group arrivals is consistent on both traces.

The last two traces are the observed and theoretical recordings of A_1 waves from an 8 megaton explosion at 8000 feet on 4 October. The overall amplitude is in fair agreement

There is a disagreement in the relative excitation of the early group arrivals. Comparing the observed barogram with the theoretical recording of A_1 for 5 megatons at 7000 feet in Figure 20 and the third trace in this figure gives a much better fit in relative excitation.

In Figure 23 the first two traces are the theoretical and observed recordings of A_1 for 11 megatons at 8000 feet on 6 October. The third and fourth traces are the theoretical and observed recordings respectively for 5 megatons at 4000 feet on 20 October. The theoretical and observed records for both explosions show reasonably good agreement in overall amplitude of the early portion of the wave train. The fifth trace is a theoretical recording of A_1 for an explosion of 1 megaton at 7000 feet. The bomb yield and elevation were chosen so as to match the amplitude with the observed recording of 20 October. This change in yield and altitude reduces the amplitude of the long period component at the beginning of the wave train relative to S_1.

In the previous comparisons of theoretical and observed A_1 recordings, there is one major discrepancy. The observed recording shows a late arriving wave train of an almost constant

period of from 1 to 2 minutes. This train is not found on the theoretical barograms. From the dispersion curves in Figure 6 this arrival could well be the steep portion of the group velocity curves of S_2 and S_1 which coincide at about 1 1/4. The portion at the far right of the record might correspond to the relative maximum in group velocity of 268 m/sec at a period of 2 minutes for the S_2 mode. This late arrival would correspond to the secondary plateau in amplitude for S_2 .

For the large explosions of 23 and 30 October, there were no complete A_1 recordings at Pasadena. In Figure 24 the first two traces are the theoretical and the incomplete portion of the observed A_1 recording respectively for the 25 megaton explosion at 12000 feet on 23 October. The theoretical amplitude is down by a factor of at least ten. The group and phase character show very little if any agreement.

Theoretical and observed recordings for A_2 are shown in Figure 25. These records are for the large explosions on 23 and 30 October. For the 25 megaton explosion shown in the top two traces the agreement in phase, group, and amplitude characteristics is excellent for the early arriving waves. For the 60 megaton explosion shown in the third and fourth traces the

the agreement is still good. The distortion is period between the number .51 and 2.1 for the observed record appears to be due to some sort of interference.

The differences in arrival times between the theoretical and observed A_1 and A_2 records leads to at most discrepancies in times of 3 per cent. The discrepancy in excitation between the acoustic modes and gravity modes for large yields and altitudes is due to the scaling laws.which are not valid for large yields and altitudes.

V. CONCLUSIONS

The conclusions reached in this paper are summarized as follows:

(1) The major features on the barogram can be explained by the super-positinn of four modes S_0 , S_1 , S_2 and GR_0 .

(2) Different portions of the vertical temperature structure of the atmosphere control the excitation of these modes. The zone with a velocity minimum near 20 km controls the early arriving acoustic modes. The region with a velocity maximum at about 50 km controls the early arriving gravity modes. The minimum velocity region at about 85 km controls the short period acoustic modes which travel at a group velocity equal to the acoustic velocity of this channel. The upper atmosphere controls the late arriving long period waves of each mode.

(3) A normalized point source is sufficient to model thermonuclear explosions.

(4) The observed shift in dominance of certain frequencies with yield and altitude can in general be explained using the empirical scaling laws derived from the direct wave near the explosion.

(5) Mode interference in the time domain and the "pseudo"

non-linearity induced by scaling laws makes it difficult to determine bomb yield and altitude from observed barograms. If elevation is provided, rough estimates of yield can be obtained with this theory.

(6) For large yields and altitudes the scaling laws seem to over-excite the long period gravity arrivals relative to the short period acoustic arrivals. Thus, some changes in scaling laws are indicated for these large events, a result which does not surprise us in view of the use of low yield data in deriving these laws.

APPENDIX A

Derivation of the Linearized Equations of Motion in Terms of the Perturbation Pressure for a Gravitating Constant Velocity Plane of Atmosphere

The initial part of this appendix follows closely the derivation given by Lamb (1879) and Pekeris (1948) and only deviates in the latter stages in order to obtain an equation of motion in terms of perturbation pressure rather than the first time derivative of the dilatation. The derivation assumes azimuthal symmetry using a cylindrical coordinate system (r, z) with the positive direction of the z axis to be taken upward.

The Eulerian equations of small motion are

$$\rho^{\circ} \frac{\partial u}{\partial t} = - \frac{\partial p}{\partial r} \qquad (1)$$

$$\rho^{\circ} \frac{\partial w}{\partial t} = - \frac{\partial p}{\partial z} - g\rho \qquad (2)$$

where the particle velocity is $\hat{v} = (u, w)$ and from the equation of continuity we have

$$\frac{d\rho^{\tau}}{dt} + \rho^{\circ} \, div \, \hat{v} = 0 \qquad (3)$$

where $$div\,\hat{v} = \frac{\partial(ru)}{r\partial r} + \frac{\partial w}{\partial z}$$

and $$\frac{d}{dt} = \frac{\partial}{\partial t} + \hat{v}\cdot\text{grad}$$

Then rewriting equation 3 gives

$$\frac{d\rho^T}{dt} = \frac{\partial\rho}{\partial t} + \hat{v}\cdot grad\,\rho^T = -\rho^\circ div\,\hat{v} \qquad (4)$$

or

$$\frac{\partial\rho}{\partial t} + w\frac{d\rho^\circ}{dz} = -\rho^\circ div\,\hat{v} \qquad (4')$$

where $\rho^T = \rho^\circ + \rho$ and $p^T = p^\circ + p$

and small quantities of second order have been neglected.

Now we assume that the perturbations of the pressure and density are connected by the adiabatic relation

$$\frac{dp^T}{dt} = \alpha^2\frac{d\rho^T}{dt} \qquad (5)$$

where

$$\alpha^2 = \gamma\frac{p^\circ}{\rho^\circ} = \gamma RK^\circ$$

Substituting equation 4 into 5 yields

$$\frac{\partial p}{\partial t} + w \frac{dp^\circ}{dz} = -\alpha^2 \rho^\circ \, div \, \hat{v} \tag{6}$$

In addition, the pressure distribution in the equilibrium state is

$$\frac{dp^\circ}{dz} = -g\rho^\circ \tag{7}$$

and with equation 7 we may rewrite equation 6 as

$$\frac{\partial p}{\partial t} - g\rho^\circ w = -\alpha^2 \rho^\circ \, div \, \hat{v} \tag{8}$$

Assuming all the perturbation quantities have an $e^{i\omega t}$ time dependence, we obtain from equation 8

$$\rho^\circ \alpha^2 \, div \, \hat{v} - \rho^\circ g w + i\omega p = 0 \tag{9}$$

and from equation 4′ and equation 8

$$-\alpha^2 \rho = \frac{w}{i\omega}\left[\alpha^2 \frac{dp^\circ}{dz} + g\rho^\circ\right] - p \tag{10}$$

Using equation 10 to eliminate ρ from equation 2 yields

$$i\omega\rho^{\circ}w = -\frac{\partial p}{\partial z} + g\alpha^{2}\left\{\frac{w}{i\omega}\left(\alpha^{2}\frac{d\rho^{\circ}}{dz} + g\rho^{\circ}\right) - p\right\} \qquad (11)$$

or
$$i\omega w\rho^{\circ} = -\frac{1}{h}\left(\frac{\partial p}{\partial z} + g\alpha^{2}p\right) \qquad (12)$$

where
$$h = 1 + \frac{g}{\omega^{2}}\left(\frac{d\rho^{\circ}}{dz}/\rho^{\circ} + g\alpha^{2}\right) = 1 - \frac{g^{2}}{\omega^{2}}\frac{(\gamma-1)}{\alpha^{2}}$$

since for an isothermal or constant velocity layer

$$\frac{d\rho^{\circ}}{dz} = -\frac{g\gamma}{\alpha^{2}}\rho^{\circ}$$

Now
$$div\,\hat{v} = \frac{\partial(ru)}{r\partial r} + \frac{\partial w}{\partial z}$$

Then from equation 1

$$\frac{\partial(ru)}{r\partial r} = \frac{1}{r}\frac{\partial}{\partial r}\left[-\frac{r}{i\omega\rho^\circ}\frac{\partial p}{\partial r}\right] = \frac{i}{\omega\rho^\circ r}\frac{\partial}{\partial r}\left(r\frac{\partial p}{\partial r}\right) \qquad (13)$$

and from equation 12

$$\frac{\partial w}{\partial z} = \frac{i}{\omega}\frac{1}{h}\left[\frac{\partial}{\partial z}\left(\frac{\partial p}{\partial z}/\rho^\circ\right) + \frac{q}{\alpha^2}\frac{\partial}{\partial z}\left(p/\rho^\circ\right)\right] \qquad (14)$$

Substituting in equation 8 we obtain

$$i\omega p - \frac{iq}{\omega h}\left(\frac{\partial p}{\partial z} + \frac{q}{\alpha^2}p\right) = -\alpha^2\rho^\circ \operatorname{div}\hat{v}$$

$$= -i\frac{\alpha^2}{\omega}\left[\frac{1}{r}\frac{\partial}{\partial r}\left(r\frac{\partial p}{\partial r}\right) + \frac{1}{h}\frac{q\gamma}{\alpha^2}\frac{\partial p}{\partial z} + \frac{1}{h}\frac{\partial^2 p}{\partial z^2} + \frac{\gamma q^2}{\alpha^2 h^2}p + \frac{q}{\alpha^2 h}\frac{\partial p}{\partial z}\right]$$

or

$$\frac{g}{\alpha^2 h}\frac{\partial p}{\partial z} - \frac{1}{\alpha^2}\left(\omega^2 - \frac{g^2}{\alpha^2 h}\right)p = \frac{1}{\pi}\frac{\partial}{\partial \pi}\left(\pi\frac{\partial p}{\partial \pi}\right) + \frac{1}{h}\left(\frac{g\gamma}{\alpha^2} + \frac{g}{\alpha^2}\right)\frac{\partial p}{\partial z} + \frac{\gamma g^2}{\alpha^4 h}p + \frac{1}{h}\frac{\partial^2 p}{\partial z^2}$$

thus

$$\frac{1}{\pi}\frac{\partial}{\partial \pi}\left(\pi\frac{\partial p}{\partial \pi}\right) + \frac{1}{h}\frac{\partial^2 p}{\partial z^2} + \frac{g\gamma}{h\alpha^2}\frac{\partial p}{\partial z} + \left[\frac{(\gamma-1)g^2}{\alpha^4 h} + \frac{\omega^2}{\alpha^2}\right]p = 0$$

or

$$\frac{1}{\pi}\frac{\partial}{\partial \pi}\left(\pi\frac{\partial p}{\partial \pi}\right) + \frac{1}{h}\left(\frac{\partial^2 p}{\partial z^2} + \frac{g\gamma}{\alpha^2}\frac{\partial p}{\partial z} + \frac{\omega^2}{\alpha^2}p\right) = 0 \qquad (15)$$

since

$$\frac{(\gamma-1)}{\alpha^4}g^2 + h\frac{\omega^2}{\alpha^2} = \frac{\omega^2}{\alpha^2}$$

APPENDIX B

Green's Function for an Isothermal Gravitating Atmosphere

The equation of pressure perturbation for a spatially unlimited isothermal gravitating atmosphere is given in cylindrical coordinates by equation A15 as

$$\frac{1}{r}\frac{\partial}{\partial r}\left(r\frac{\partial \bar{p}}{\partial r}\right)+\frac{1}{h}\left(\frac{\partial^2 \bar{p}}{\partial z^2}+\frac{\gamma g}{a^2}\frac{\partial \bar{p}}{\partial z}+\frac{\omega^2}{a^2}\bar{p}\right)=0 \qquad (1)$$

where

$$h=1-\frac{(\gamma-1)g^2}{\omega^2 a^2}=1-\frac{\sigma_B^2}{\omega^2}$$

and a time dependence of $e^{i\omega t}$ has been assumed.

We will define the Green's Function as the particular solution of the elementary inhomogeneous form of equation 1, or

$$\frac{1}{r}\frac{\partial}{\partial r}\left(r\frac{\partial \bar{p}}{\partial r}\right)+\frac{1}{h}\left(\frac{\partial^2 \bar{p}}{\partial z^2}+\frac{\gamma g}{a^2}\frac{\partial \bar{p}}{\partial z}+\frac{\omega^2}{a^2}\bar{p}\right)=\frac{\delta(r)\,\delta(z-d)}{r}e^{i\omega t} \qquad (2)$$

which corresponds to a point source located at $r=0,\ z=d$

Now applying the double spatial transform

$$\bar{\bar{p}}(k,\eta;\omega) = \frac{1}{(2\pi)^{1/2}} \int_0^\infty J_0(kr) r\, dr \int_{-\infty}^{\infty} e^{-i\eta z} \bar{p}(r,z;\omega)\, dz \qquad (3)$$

where the inverse is given by

$$\bar{p}(r,z;\omega) = \frac{1}{(2\pi)^{1/2}} \int_0^\infty J_0(kr) k\, dk \int_{-\infty}^{\infty} e^{i\eta z} \bar{\bar{p}}(k,\eta;\omega)\, d\eta \qquad (4)$$

to equation 2, we obtain

$$-k^2 \bar{\bar{p}} + \frac{1}{h}\left(-\eta^2 \bar{\bar{p}} + i\eta \frac{\gamma g}{\alpha^2} \bar{\bar{p}} + \frac{\omega^2}{\alpha^2} \bar{\bar{p}}\right) = \frac{e^{-i\eta d}}{(2\pi)^{1/2}} e^{i\omega t} \qquad (5)$$

Solving equation 5 yields

$$\bar{\bar{p}} = - \frac{h e^{-i\eta d} e^{i\omega t}}{(2\pi)^{1/2} \hat{A}(k,\eta;\omega)} \qquad (6)$$

where $\hat{A}(k,\eta;\omega) = hk^2 + \eta^2 - \frac{\omega^2}{\alpha^2} - i\frac{\eta\gamma g}{\alpha^2\pi}$

Now inverting by equation 4, we have the integral

$$\bar{\bar{p}} = - \frac{1}{(2\pi)^{1/2}} \int_0^\infty J_0(kr)\, k\, dk \int_{-\infty}^{\infty} \frac{h}{(2\pi)^{1/2}} \frac{e^{-i\eta d} e^{+i\eta z}}{\hat{A}(k,\eta;\omega)}\, d\eta\, e^{i\omega t}$$

$$= - \frac{h e^{i\omega t}}{(2\pi)} \int_0^\infty J_0(kr)\, k\, dk \int_{-\infty}^{\infty} \frac{e^{i\eta(z-d)}}{\hat{A}(k,\eta;\omega)}\, d\eta \qquad (7)$$

since $h = 1 - \frac{(\gamma-1)g^2}{\omega^2\alpha^2}$ is independent of k and η .

The poles of $\hat{A}^{-1}(k, \eta; \omega)$ are given by

$$\eta^2 - i\eta\frac{\gamma g}{\alpha^2} + \left(hk^2 - \frac{\omega^2}{\alpha^2}\right) = 0$$

or

$$\eta_{p\pm} = i\frac{\gamma g}{2\alpha^2} \pm i\left\{\frac{\gamma^2 g^2}{4\alpha^4} + \left(hk^2 - \frac{\omega^2}{\alpha^2}\right)\right\}^{1/2}$$

$$= i(\lambda \pm \nu_\alpha) \qquad (8)$$

where $\lambda = \frac{\gamma g}{2\alpha^2}$ and $\nu_\alpha = \left\{\frac{\gamma^2 g^2}{4\alpha^4} + \left(hk^2 - \frac{\omega^2}{\alpha^2}\right)\right\}^{1/2}$

To evaluate, for $z > d$ we close the η contour by a semi-infinite arc in the upper η half plane or $\mathrm{Im}(\eta) > 0$. The contribution along this arc to the integral is zero and by Cauch's Theorem

$$\int_{-\infty}^{\infty} \frac{e^{i\eta(z-d)}}{\hat{A}(k,\eta;\omega)}\, d\eta + \int \frac{e^{i\eta(z-d)}}{\hat{A}(k,\eta;\omega)}\, d\eta = 2\pi i \operatorname{Res}\left[\frac{e^{i\eta(z-d)}}{\hat{A}(k,\eta;\omega)}\right] \qquad (10)$$

or $$\int_{-\infty}^{\infty} \frac{e^{i\eta(z-d)}}{\hat{A}(k,\eta;\omega)}\, d\eta = 2\pi i \operatorname{Res}\left[\frac{e^{i\eta(z-d)}}{\hat{A}(k,\eta;\omega)}\right]$$

$$= 2\pi i \frac{e^{i\eta_{p+}(z-d)}}{\left(\frac{\partial \hat{A}}{\partial \eta}\right)_{k,\eta_{p+}}} \qquad (11)$$

and

$$\frac{\partial \hat{A}}{\partial \eta} = 2\eta - i\frac{q}{\alpha^2}$$

or

$$\left(\frac{\partial \hat{A}}{\partial \eta}\right)_{k,\eta_{pt}} = i2\lambda + i2\nu_\alpha - i2\lambda = i2\nu_\alpha \qquad (12)$$

and

$$\int_{-\infty}^{\infty} \frac{e^{i\eta(z-d}}{\hat{A}(k,\eta;\omega)}\, d\eta = \pi e^{-\lambda(z-d)} \frac{e^{-\nu_\alpha(z-d)}}{\nu_\alpha} \qquad \text{for } z > d \quad (13)$$

Now for $z < d$ we close the contour in the lower η half plane or $Im(\eta) < 0$ and obtain

$$\int_{-\infty}^{\infty} \frac{e^{i\eta(z-d)}}{\hat{A}(k,\eta;\omega)}\, d\eta = \pi e^{-\lambda(z-d)} \frac{e^{-\nu_\alpha(d-z)}}{\nu_\alpha} \qquad \text{for } z < d \quad (14)$$

From inspection of equation 13 and equation 14, we can write

$$\int_{-\infty}^{\infty} \frac{e^{i\eta(z-d)}}{\hat{A}(k,\eta;\omega)}\, d\eta = \pi e^{-\lambda(z-d)} \frac{e^{-\nu_\alpha|z-d|}}{\nu_\alpha} \qquad (15)$$

for all z

and we obtain for out solution in integral form

$$\bar{p} = -\frac{h}{2} e^{i\omega t} \int_0^\infty e^{-\lambda(z-d)} \frac{e^{-\nu_\alpha |z-d|}}{\nu_\alpha} J_0(k\pi)\, k\, dk$$

$$= -\frac{h}{2} e^{i\omega t} e^{-\lambda(z-d)} \int_0^\infty \frac{e^{-\nu_\alpha |z-d|}}{\nu_\alpha} J_0(k\pi)\, k\, dk \qquad (16)$$

Now $$\nu_\alpha^2 = h k^2 + \frac{\gamma^2 g^2}{4\alpha^4} - \frac{\omega^2}{\alpha^2} = -(k\pi_\alpha)^2$$

or $$\nu_\alpha^2 = h(k^2 + K^2) \qquad \text{where } K^2 = \frac{1}{h\alpha^2}\left(\frac{\gamma g^2}{4\alpha^2} - \omega^2\right)$$

giving us an integral of the form

$$\int_0^\infty \frac{e^{-h^{1/2}(k^2+K^2)^{1/2}|z-d|}}{h^{1/2}\sqrt{k^2+K^2}} J_0(k\pi)\, k\, dk \qquad (17)$$

and from Erdelyi et al. Tables of Integral Transforms, II we have

$$\int_0^\infty \frac{e^{-a(k^2+K^2)^{1/2}}}{(k^2+K^2)^{1/2}} J_0(kr)\, k\, dk = \frac{e^{-K(r^2+a^2)^{1/2}}}{(r^2+a^2)^{1/2}} \qquad (18)$$

for $Re\ a > 0$ and $Re\ K > 0$

Thus identifying a with $h^{1/2}|z-d|$ we obtain as our Green's function

$$\bar{p} = -\frac{h^{1/2}}{2} e^{i\omega t} e^{-\lambda(z-d)} \int_0^\infty \frac{e^{-h^{1/2}|z-d|(k^2+K^2)^{1/2}}}{(k^2+K^2)^{1/2}} J_0(kr)\, k\, dk \qquad (18')$$

or

$$\bar{p} = -\frac{h}{2}^{1/2} e^{-\lambda(z-d)} \frac{e^{-K[r^2+h(z-d)^2]^{1/2}}}{[r^2+h(z-d)^2]^{1/2}} e^{i\omega t} \qquad (19)$$

It is easy to verify by direct substitution that the Green's Function, equation 19, is a solution of the homogeneous equation 1 for all (r, z) except at the point (o, d). In addition if we let

$q = o$, the Green's Function reduces to the well known point source for outgoing spherical pressure waves in a liquid.

$$\bar{p} = -\frac{1}{2} \frac{e}{R} e^{i\omega(t-\frac{R}{\alpha})} \qquad (20)$$

where

$$R = [r^2 + (z-d)^2]^{1/2}$$

APPENDIX C

The Aki Approximation with Linear Amplitude Intervals

This appendix is an extension of an approximate evaluation developed by K. Aki (1960) of the following integral.

$$h(t) = 2\int_0^\infty \bar{A}(\omega)\ \cos \omega[t - \tau(\omega)]\, d\omega \qquad (1)$$

where $\bar{A}(\omega)$ is real in the frequency interval $\omega_1 < \omega_2$ and zero outside the interval. In Aki's evaluation it was also assumed that $\bar{A}(\omega)$ was constant in this interval.

The first step in the evaluation is to divide the integration interval ω_1 to ω_2 into subintervals over which phase and amplitude are approximately linear in ω. With this approximation, equation 1 takes the form

$$h(t) = 2\sum_i \int_{\omega_i - \frac{\Delta\omega_i}{2}}^{\omega_i + \frac{\Delta\omega_i}{2}} \bar{A}(\omega)\ \cos \varphi(\omega)\, d\omega \qquad (2)$$

where

$$\bar{A}(\omega) = \bar{A}_i + (\omega-\omega_i)\left(\frac{\partial \bar{A}}{\partial \omega}\right)_i \equiv \bar{A}_i + (\omega-\omega_i)\bar{a}_i$$

$$\varphi(\omega) = \omega t - \omega T(\omega) = \varphi_i + (\omega-\omega_i)\left(\frac{\partial \varphi}{\partial \omega}\right)_i \qquad (3)$$

with the i subscripted variables evaluated at the midpoint of the i th frequency interval $\Delta\omega_i$.

Defining t_q by $t_q = T + \omega\frac{\partial T}{\partial \omega}$ (4)

we see that

$$\left(\frac{\partial \varphi}{\partial \omega}\right)_i = \left[t - \left(T + \omega\frac{dT}{d\omega}\right)\right]_i = t - t_{qi} \qquad (5)$$

Thus expanding $\cos\varphi$ in terms of these quantities yields

$$\cos\varphi = \cos\left[\omega_i (t-\tau_i) + (t-t_{gi})(\omega-\omega_i)\right]$$

$$= \cos\omega_i(t-\tau_i)\cdot\cos\left[(t-t_{gi})(\omega-\omega_i)\right]$$

$$- \sin\omega_i(t-\tau_i)\ \sin\left[(t-t_{gi})(\omega-\omega_i)\right] \qquad (6)$$

and
$$\bar{A}(\omega)\cos\varphi = \bar{A}_i \cos\omega_i(t-\tau_i)\cos\left[(t-t_{gi})(\omega-\omega_i)\right]$$

$$- \bar{A}_i \sin\omega_i(t-\tau_i)\sin\left[(t-t_{gi})(\omega-\omega_i)\right]$$

$$+ \bar{a}_i(\omega-\omega_i)\cos\omega_i(t-\tau_i)\cos\left[(t-t_{gi})(\omega-\omega_i)\right]$$

$$- \bar{a}_i(\omega-\omega_i)\sin\omega_i(t-\tau_i)\sin\left[(t-t_{gi})(\omega-\omega_i)\right]$$

(7)

Now since the second and third terms in equation 7 are odd in ω about ω_i, the resultant integration over this interval is zero and the integral over the i th interval is

$$\int_{\omega_i - \frac{\Delta\omega_i}{2}}^{\omega_i + \frac{\Delta\omega_i}{2}} \bar{A}(\omega)\cos\varphi(\omega)\,d\omega = \bar{A}_i \cos\omega_i(t-\tau_i)\int_{\omega_i - \frac{\Delta\omega_i}{2}}^{\omega_i + \frac{\Delta\omega_i}{2}} \cos[(t-t_{g_i})(\omega-\omega_i)]\,d\omega$$

$$- \bar{a}_i \sin\omega_i(t-\tau_i)\int_{\omega_i - \frac{\Delta\omega_i}{2}}^{\omega_i + \frac{\Delta\omega_i}{2}} (\omega-\omega_i)\sin[(t-t_{g_i})(\omega-\omega_i)]\,d\omega$$

(8)

Changing the variable of integration from ω to $\chi = \omega - \omega_i$, we obtain

$$\int_{\omega_i - \frac{\Delta\omega_i}{2}}^{\omega_i + \frac{\Delta\omega_i}{2}} \cos\left[(t-t_{q_i})(\omega-\omega_i)\right] d\omega = \int_{-\frac{\Delta\omega_i}{2}}^{\frac{\Delta\omega_i}{2}} \cos\left[(t-t_{q_i})\chi\right] d\chi$$

$$= \frac{\sin\left[(t-t_{q_i})\chi\right]}{(t-t_{q_i})} \Bigg]_{-\frac{\Delta\omega_i}{2}}^{\frac{\Delta\omega_i}{2}}$$

$$= \Delta\omega_i \; \frac{\sin\left[\frac{\Delta\omega_i}{2}(t-t_{q_i})\right]}{\left[\frac{\Delta\omega_i}{2}(t-t_{q_i})\right]} \qquad (9)$$

and

$$\int_{\omega_i - \frac{\Delta\omega_i}{2}}^{\omega_i + \frac{\Delta\omega_i}{2}} (\omega - \omega_i) \sin[(t - t_{g_i})(\omega - \omega_i)]\, d\omega = \int_{-\frac{\Delta\omega_i}{2}}^{+\frac{\Delta\omega_i}{2}} \chi \sin[(t - t_{g_i})\chi]\, d\chi$$

$$= \frac{\Delta\omega_i}{(t - t_{g_i})} \left\{ \frac{\sin\left[\frac{\Delta\omega_i}{2}(t - t_{g_i})\right]}{\left[\frac{\Delta\omega_i}{2}(t - t_{g_i})\right]} - \cos\left[\frac{\Delta\omega_i}{2}(t - t_{g_i})\right] \right\} \qquad (10)$$

In equation 10 as $t \to t_{g_i}$ the expression approaches

$$\frac{\Delta\omega_i}{(t-t_{g_i})} - \frac{\Delta\omega_i}{(t-t_{g_i})} \to 0$$

so that equation 10 is bounded and approaches zero as $t \to t_{g_i}$.

Substituting equations 9 and 10 in equation 8, we obtain the approximate evaluation of equation 1.

$$h(t) = 2\sum_i \left\{ \bar{A}_i \, \Delta\omega_i \cos\omega_i(t-\tau_i) \, \frac{\sin\left[\frac{\Delta\omega_i}{2}(t-t_{g_i})\right]}{\left[\frac{\Delta\omega_i}{2}(t-t_{g_i})\right]} \right.$$

$$\left. - \left(\frac{\partial \bar{A}}{\partial\omega}\right)_i \Delta\omega_i \, \frac{\sin\omega_i(t-\tau_i)}{(t-t_{g_i})} \left[\frac{\sin\left[\frac{\Delta\omega_i}{2}(t-t_{g_i})\right]}{\left[\frac{\Delta\omega_i}{2}(t-t_{g_i})\right]} - \cos\left[\frac{\Delta\omega_i}{2}(t-t_{g_i})\right] \right] \right\}$$

(11)

APPENDIX D

List of Symbols not Defined in Text

Symbol	Definition
m	subscript indicating m^{th} layer constants
α	layer sound velocity
g	gravitational constant
ω	angular frequency
k	wave number in horizontal direction
c	$= \omega/k$: horizontal phase velocity
r	horizontal cylindrical coordinate
γ	C_p/C_v : specific heat ratio
R^*	universal gas constant
M_o	molecular weight at ground
R	R^*/M_o
K^*	real kinetic temperature in degrees Kelvin
K	$(M_o/M)K^*$: molecular scale temperature
u	radial particle velocity perturbation
w	vertical particle velocity perturbation
p	excess pressure
ρ	density perturbation
o	superscript denotes the static equilibrium quantity

Symbol	Definition
z_m	the altitude at the top of the $m^{\underline{th}}$ layer
d_m	$z_m - z_{m-1}$: layer thickness
t	time variable
T	$= \frac{2\pi}{kc}$: period
j	subscript denotes the roots of $F_a = 0$
s	subscript denotes the source layer
$\tilde{a}_1$	Acoustic cutoff frequency
$\tilde{a}_2$	Brunt cutoff frequency
2λ	exponential decay factor of density with altitude in isothermal layer.
W_s	yield for layers
W_o	standard yield
$\hat{a}_s$	normalizing distance for direct wave in layer
$\hat{a}_o$	standard normalizing distance
T_{+as}	positive phase duration time in layer s
T_{+a_o}	standard positive phase duration time.
iK_s	horizontal wave number of direct wave
$i\chi_s$	vertical wave number of direct wave.
$\{\ \}_{a_j}$	residue contribution of integral solution
$[\ ]_{H_j}$	homogeneous ratio evaluated at $j^{\underline{th}}$ root of $F_a = 0$.

REFERENCES

Aki, K., Study of earthquake mechanism by a method of phase equalization applied to Rayleigh and Love waves, J. Geophys. Research, 65, 729-740, 1960.

Båth, M., Seismic records of explosions - especially nuclear explosions, Part III, Forsvarets Forskningsanstalt Avdelning, 4, A4270-4721, 1962.

Carpenter, E. W., G. Harwood, and T. Whiteside, Microbarograph records from the Russian large nuclear explosions, Nature, 4805, 857, 1961.

Donn, W. L., and M. Ewing, Atmospheric waves from nuclear explosions, J. Geophys. Research, 67, 1855-1866, 1962.

Donn, W. L., and M. Ewing, The Soviet test of October 30, 1961, J. Atmospheric Sciences, in press, 1962.

Donn, W., R. Rommer, F. Press, and M. Ewing, Atmospheric Oscillations and related synoptic patterns, Bull. Amer. Meterol. Soc., 35, 301-309, 1954.

Dorman, J., Period equation for waves of Rayleigh type on a layered, liquid-solid half space, Bull. Seism. Soc. Am., 52, 389-397, 1962.

Erdelyi, A., W. Magnus, F. Oberhettinger, and F. Tricomi, Tables of Integral Transforms, 2, 9, 1954.

Ewing, M., and F. Press, Further study of atmospheric pressure fluctuations recorded on seismographs, Trans. Amer. Geophys. Un. 34, 95-100, 1953.

Gazaryn, Yu. L., Infra sonic normal modes in the atmosphere, Soviet Physics - Acoustics, 7, 17-22, 1961

Glasstone, S., The Effects of Nuclear Weapons, U.S. Government Printing Office, Washington 25, D. C., 1962.

Harkrider, D. G., and D. L. Anderson, Computation of surface wave dispersion for multilayered anisotropic media, Bull. Seism. Soc. Am., 52, 321-332, 1962.

Haskell, N. A., The dispersion of surface waves on multilayered media, Bull. Seism. Soc. Am., 43, 17-34, 1953.

Hunt, J. N., R. Palmer, and Sir William Penney, Atmospheric waves caused by large explosions, Phil. Trans. Roy. Soc. London, Ser. A., No. 1011, 252, 275-315, 1960.

Johnson, C. T., and J. R. Chiles, Jr., The NEL T21 microbarographic recording system, NEL/Report 773, 1957.

Lamb, H., Hydrodynamics, Dover Publications, New York, 1945.

Oksman, J., and E. Kataja, Round the world sound waves produced by the nuclear explosion on October 30, 1961, and their effect on the ionosphere at Sodankyla, Nature, 4808, 1173-1174, 1961.

Pekeris, C. L., The propagation of a pulse in the atmosphere, Part II, Phys. Rev., 73, 145-154, 1948.

Pfeffer, R. L., and J. Zarichny, Acoustic gravity wave propagation from nuclear explosions in the earth's atmosphere, Scientific Report No. 3, Dynamic meteorology project, Lamont Geological Observatory of Columbia University, 1962.

Press, F., D. Harkrider, and C. A. Seafeldt, A fast, convenient program for computation of surface-wave dispersion curves on multilayered media, Bull. Seism. Soc. Am., 51, 495-502, 1961.

Press, F., and D. Harkrider, Propagation of acoustic-gravity waves in the atmosphere, J. Geophys. Research, 67, 3889-3908, 1962.

Scorer, R. S., The dispersion of a pressure pulse in the atmosphere, Proc. Roy. Soc. London, Series A, 201, 137-157, 1950.

Tolstoy, I., Modes, rays and travel times, J. Geophys. Research, 64, 815-821, 1959.

Szego, G., Proc. London Math. Soc., 36, 427-450, 1933.

Wares, G. W., K. W. Champion, H. L. Pond, and A. E. Cole, Model atmospheres, Handbook of Geophysics, 1-1-1-37, The Macmillan Co., 1960.

Wexler, H., and W. A. Hass, Global atmospheric pressure effects of the October 30, 1961 explosion, J. Geophys. Research, XX, XXX-XXX, 1962.

Weston, V. H., Pressure pulse received due to an explosion in the atmosphere at an arbitrary altitude, Part I, The University of Michigan Radiation Laboratory Report, 2886-1-T, 1960.

Weston, V. H., The pressure pulse produced by a large explosion in the atmosphere, Con. J. Physics, 39, 993-1009, 1961a.

Weston, H. V., The pressure pulse produced by a large explosion in the atmosphere, Part II. The University of Michigan Radiation Laboratory Contract Report, AF 19 (60A) 5470, 1961b.

Weston, H. V., Intermediate results for thermosphere model, The University of Michigan Radiation Laboratory Memo, 2886-521-M, 1961c.

Yamomoto, R., The microbarographic oscillations produced by the explosions of hydrogen bombs in the Marshall Islands, Bull. Am. Meterol. Soc., 37, 406, 1956.

Yamomoto, R., A dynamical theory of the microbarographic oscillations produced by the explosions of hydrogen bombs, J. Meterol. Soc. Japan, 35, 1947.

FIGURE CAPTIONS

Figure 1. ARDC standard atmosphere and its approximation by isothermal layers.

Figure 2. Comparison of experimental group velocities for A_1 waves from Novaya Zemlya explosions with standard and extreme ARDC models. Data curves 1-8 from Donn and Ewing (1962).

Figure 3. Comparison of experimental and theoretical curves for A_2 and A_3 waves from Novaya Zemlya explosions. Data curves 1-4 from Donn and Ewing (1962).

Figure 4. Standard and extreme ARDC atmospheres.

Figure 5. Modifications to the standard atmosphere made in order to study the effect of different zones.

Figure 6. Phase and group velocity dispersion curves for $S_{o,1,2}$ and $GR_{o,1}$ modes of ARDC standard atmosphere with half-space beginning at 220 km. Stippled region indicates where singular values of F occur. Cutoffs indicated by hatch region.

Figure 7. Same as Figure 6 with different scale.

Figure 8. Phase and group velocity dispersion curves for $S_{o,1}$ and $GR_{o,1,2,3,}$ modes of ARDC standard atmosphere with free surface at 220 km.

Figure 9. Dispersion curves for modified ARDC model with no upper temperature minimum.

Figure 10. Dispersion curves for modified ARDC model with no lower temperature minimum.

Figure 11. Dispersion curves for ARDC arctic winter atmosphere.

Figure 12. Spectral amplitude of $\mathcal{A}_a$ for the ARDC standard and arctic winter atmospheres. Spectral amplitude of the barograph is superimposed.

Figure 13. Homogeneous pressure ratios at an altitude of 18.5 and 50 km for $S_{o,1,2}$ and $GR_{o,1}$ modes.

Figure 14. Homogeneous pressure ratios at an altitude of 85 km for $S_{o,1,2,}$ and $GR_{o,1}$ modes.

Figure 15. Homogeneous pressure ratios at an altitude of 125 km for $S_{o,1,2}$ and $GR_{o,1}$ modes.

Figure 16. Theoretical pressure variations of A_1 waves for the individual modes GR_o and $S_{o,1,2}$. The fifth trace is the resultant wave for $GR_o+S_o+S_1+S_2$

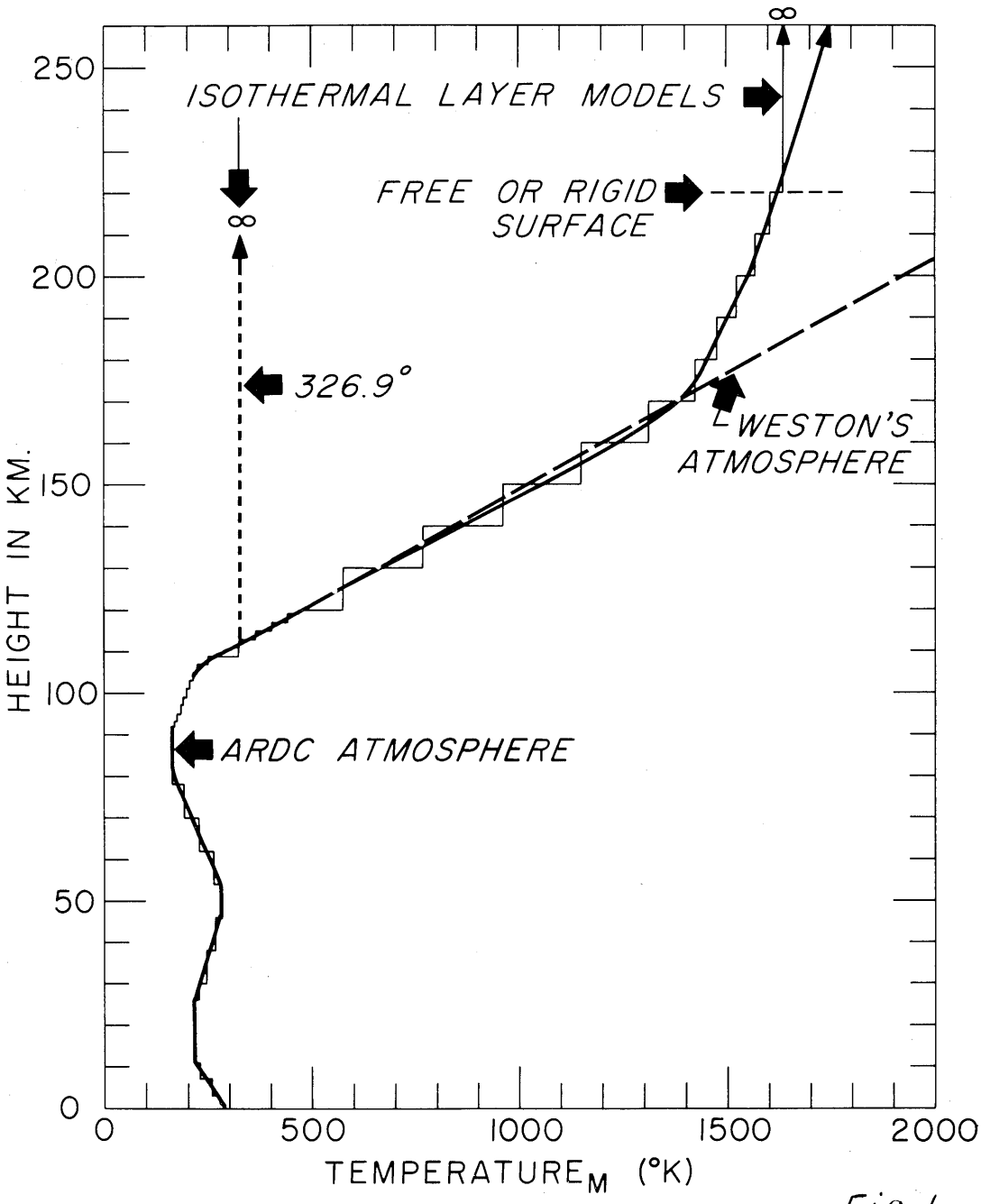
250
200
150
100
50
0
HEIGHT IN KM.
ISOTHERMAL LAYER MODELS
∞
FREE OR RIGID SURFACE
326.9°
WESTON'S ATMOSPHERE
ARDC ATMOSPHERE
0
500
1000
1500
2000
TEMPERATURE$_M$ (°K)

Fig. 1

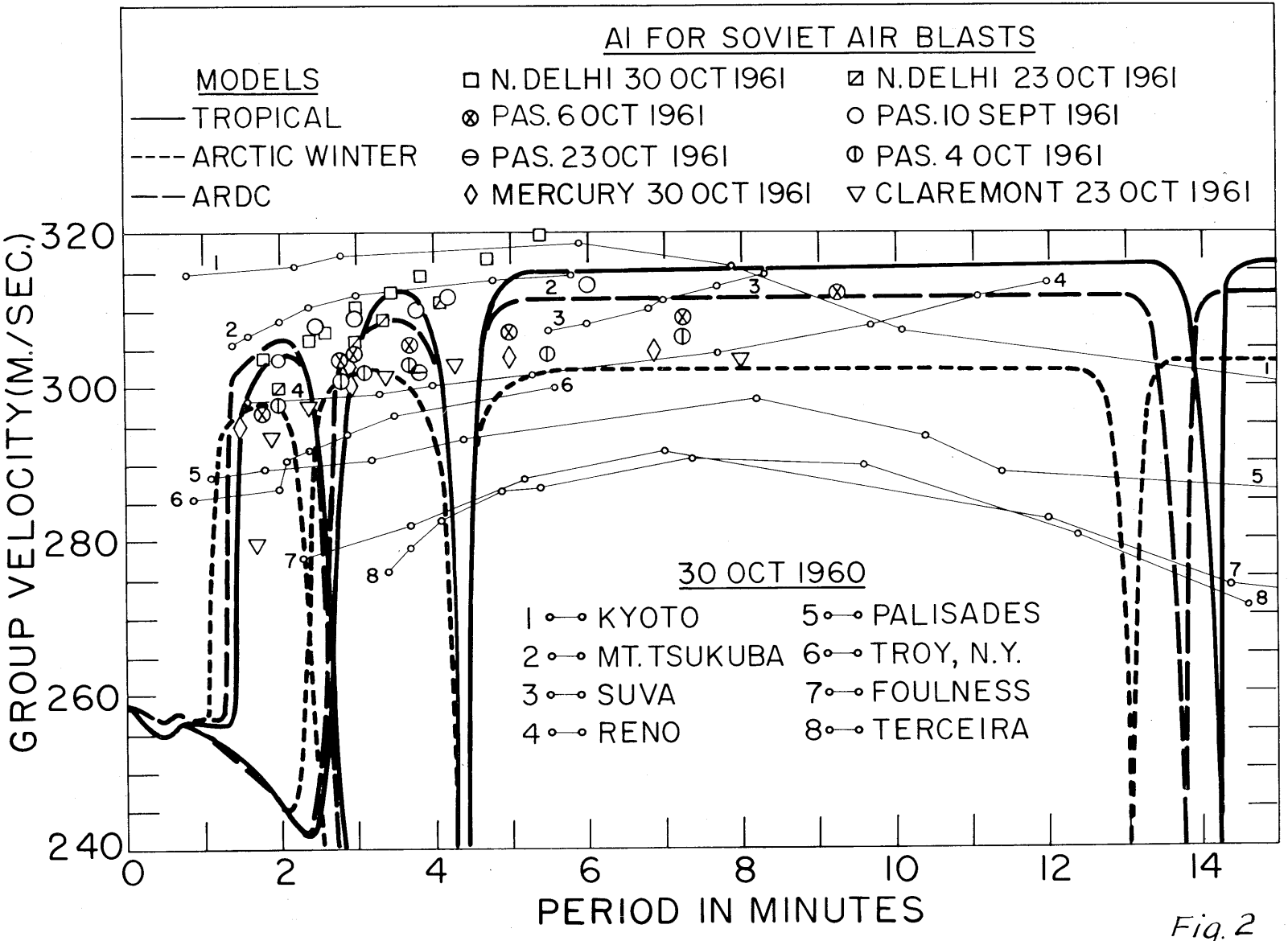
AI FOR SOVIET AIR BLASTS
MODELS
TROPICAL
ARCTIC WINTER
ARDC
N. DELHI 30 OCT 1961
PAS. 6 OCT 1961
PAS. 23 OCT 1961
MERCURY 30 OCT 1961
N. DELHI 23 OCT 1961
PAS. 10 SEPT 1961
PAS. 4 OCT 1961
CLAREMONT 23 OCT 1961
30 OCT 1960
1 KYOTO
2 MT. TSUKUBA
3 SUVA
4 RENO
5 PALISADES
6 TROY, N.Y.
7 FOULNESS
8 TERCEIRA
GROUP VELOCITY (M./SEC.)
320
300
280
260
240
0
2
4
6
8
10
12
14
PERIOD IN MINUTES

Fig. 2

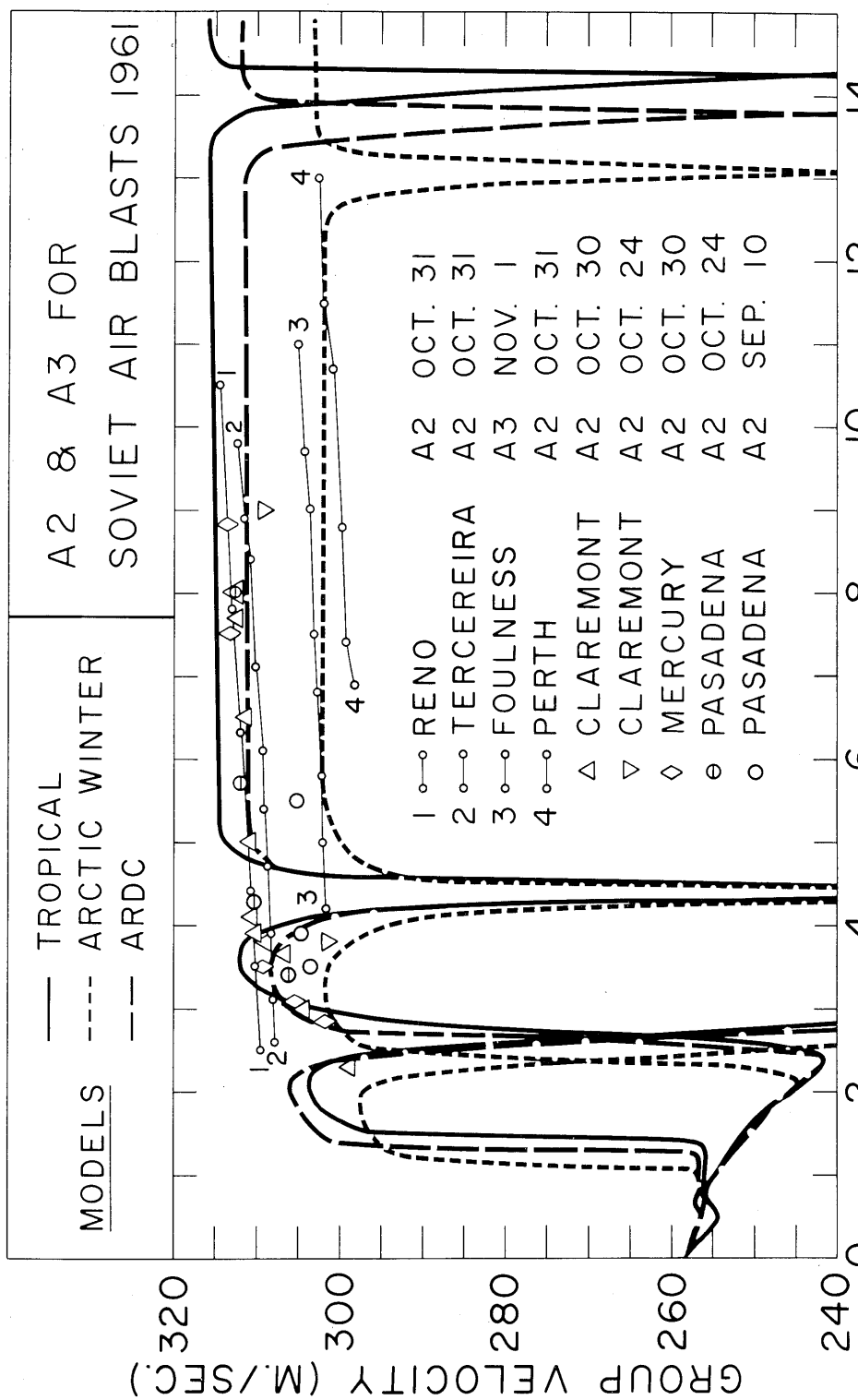
A2 & A3 FOR
SOVIET AIR BLASTS 1961
MODELS
TROPICAL
ARCTIC WINTER
ARDC
1 RENO A2 OCT. 31
2 TERCEREIRA A2 OCT. 31
3 FOULNESS A3 NOV. 1
4 PERTH A2 OCT. 31
CLAREMONT A2 OCT. 30
CLAREMONT A2 OCT. 24
MERCURY A2 OCT. 30
PASADENA A2 OCT. 24
PASADENA A2 SEP. 10
GROUP VELOCITY (M./SEC.)
320
300
280
260
240
0
2
4
6
8
10
12
14
PERIOD IN MINUTES

Fig. 3

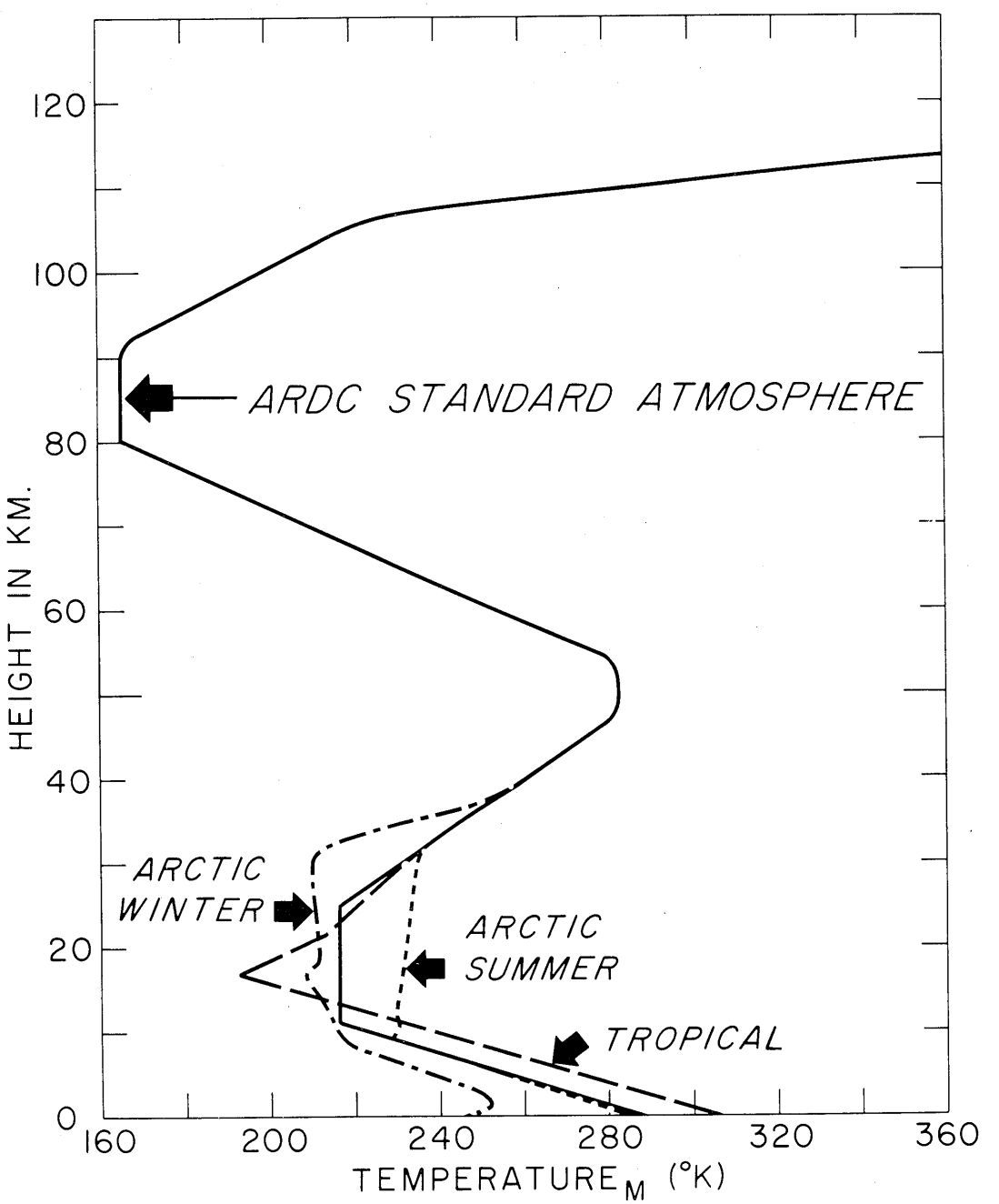
120
100
80
60
40
20
0
HEIGHT IN KM.
ARDC STANDARD ATMOSPHERE
ARCTIC
WINTER
ARCTIC
SUMMER
TROPICAL
160
200
240
280
320
360
TEMPERATURE M (°K)

Fig. 4

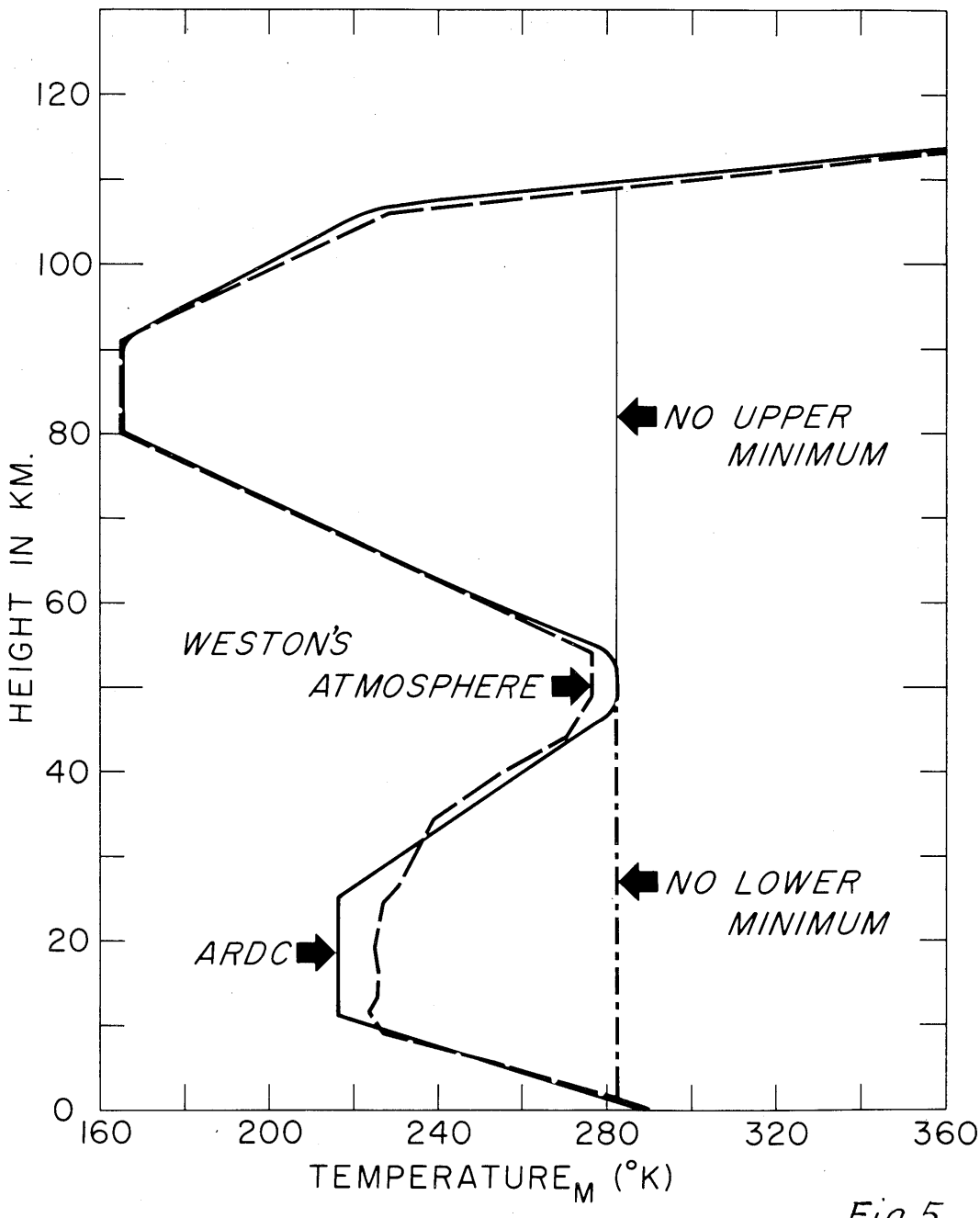
120
100
80
60
40
20
0
HEIGHT IN KM.
NO UPPER MINIMUM
WESTON'S ATMOSPHERE
NO LOWER MINIMUM
ARDC
160
200
240
280
320
360
TEMPERATURE$_M$ (°K)

Fig. 5

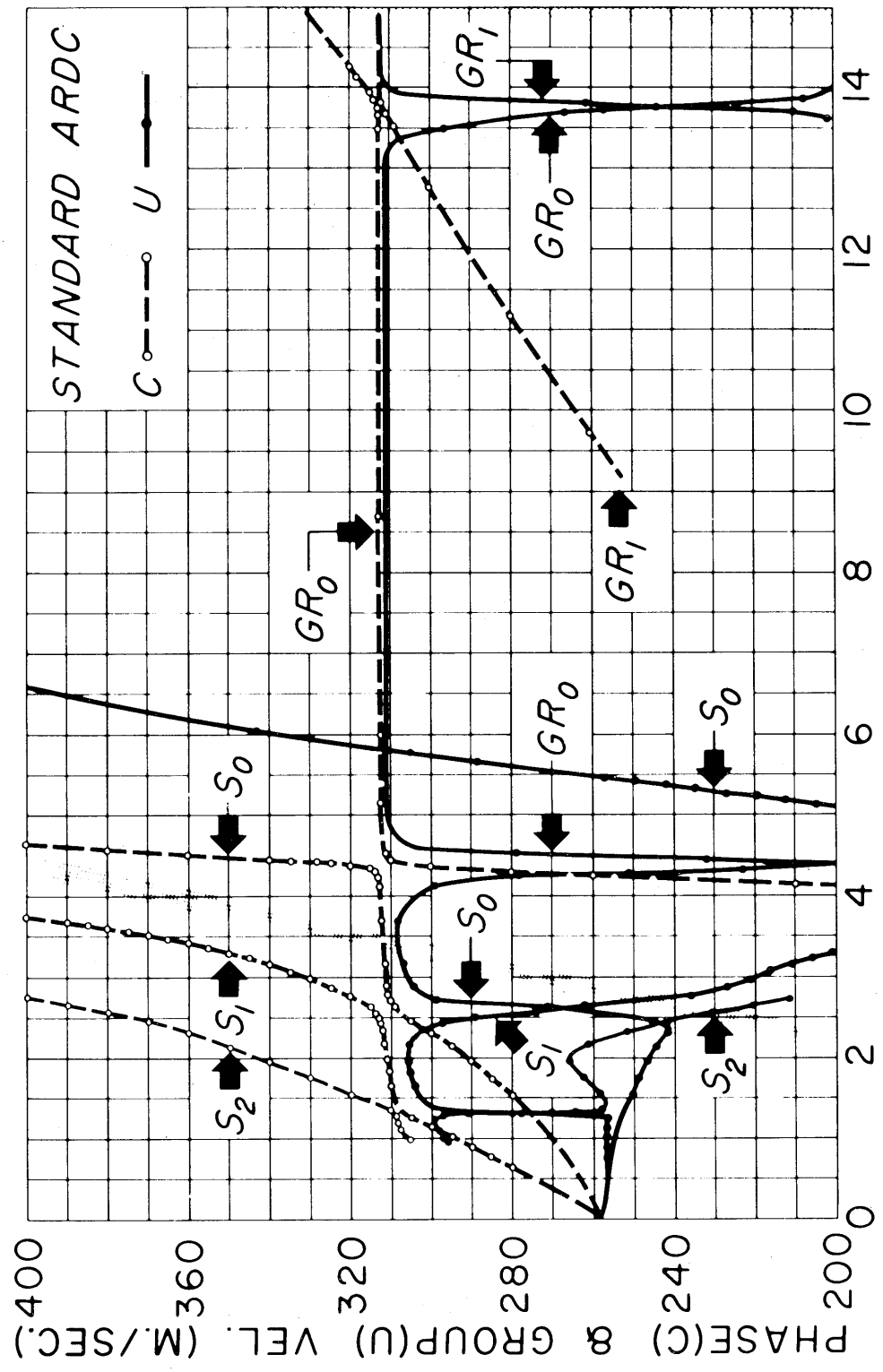
STANDARD ARDC
C
U
S_0
S_1
S_2
GR_0
GR_1
PERIOD IN MINUTES
PHASE(C) & GROUP(U) VEL. (M./SEC.)
0
2
4
6
8
10
12
14
200
240
280
320
360
400

Fig. 6

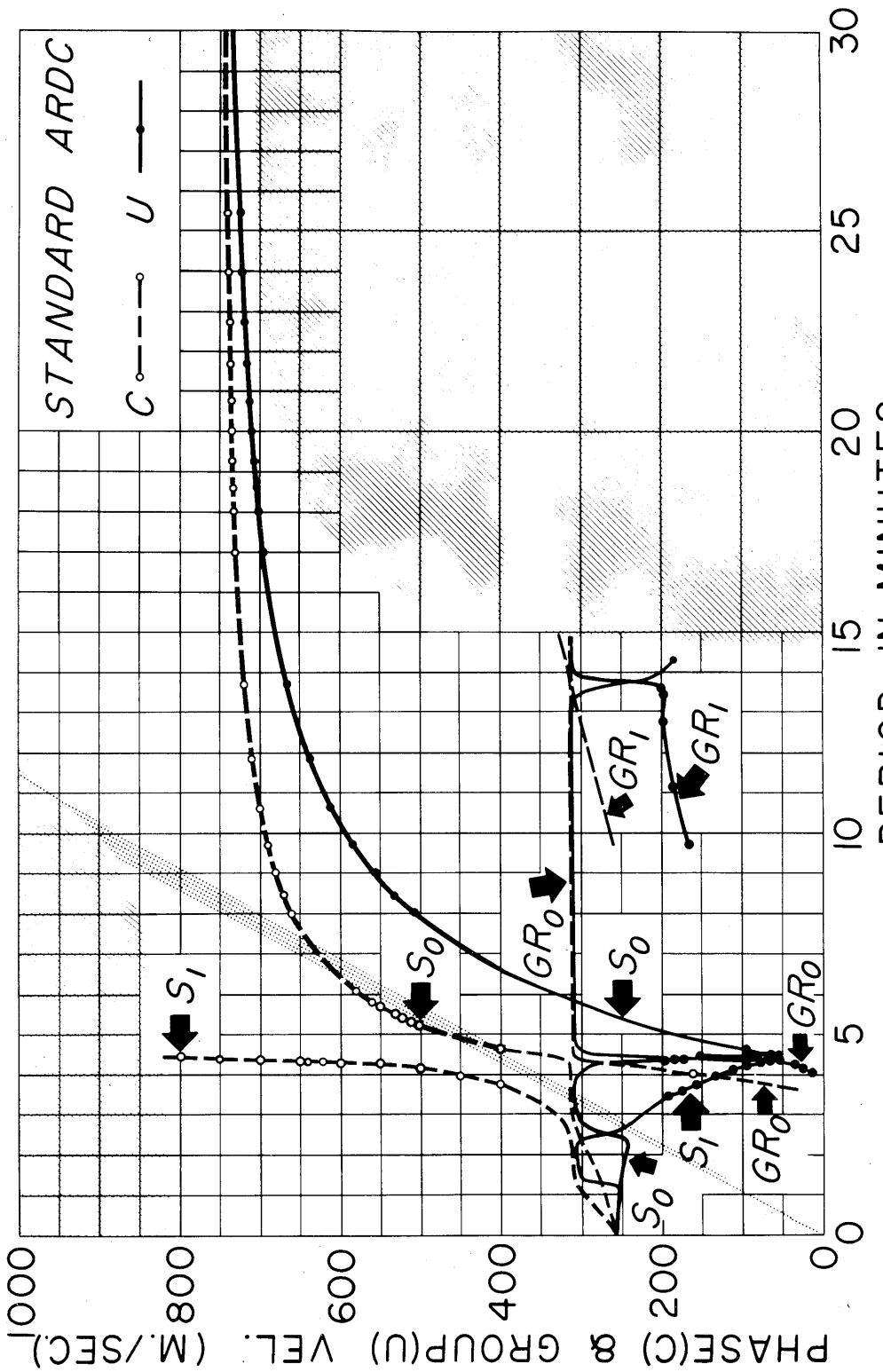
STANDARD ARDC
C
U
PHASE(C) & GROUP(U) VEL. (M./SEC.)
PERIOD IN MINUTES
0
200
400
600
800
1000
0
5
10
15
20
25
30
S_1
S_0
GR_0
GR_1

Fig. 7

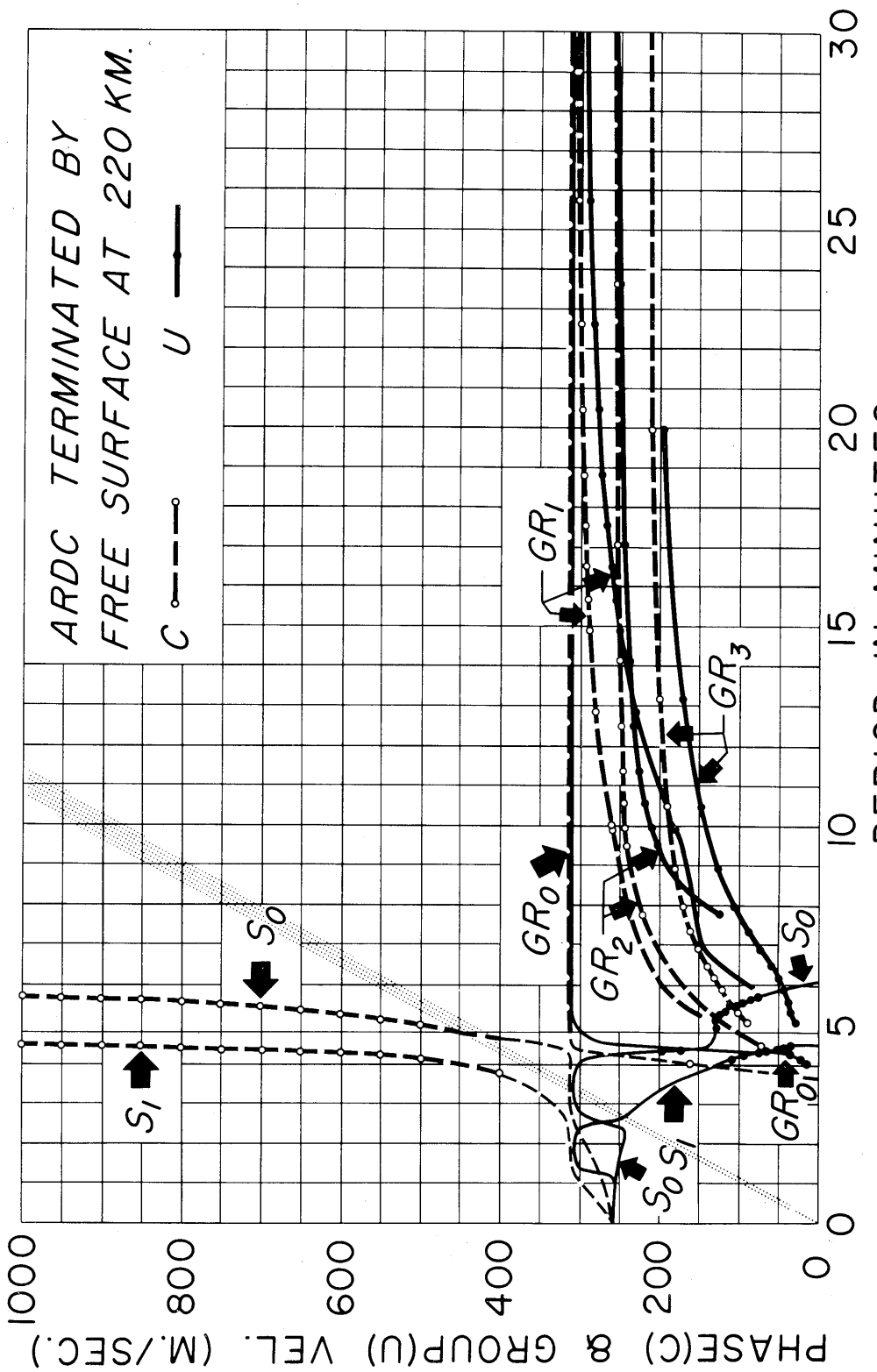
ARDC TERMINATED BY
FREE SURFACE AT 220 KM.
C
U
PHASE(C) & GROUP(U) VEL. (M./SEC.)
PERIOD IN MINUTES
0
200
400
600
800
1000
0
5
10
15
20
25
30
S_1
S_0
GR_0
GR_1
GR_2
GR_3
GR_{01}
S_0S_1

Fig. 8

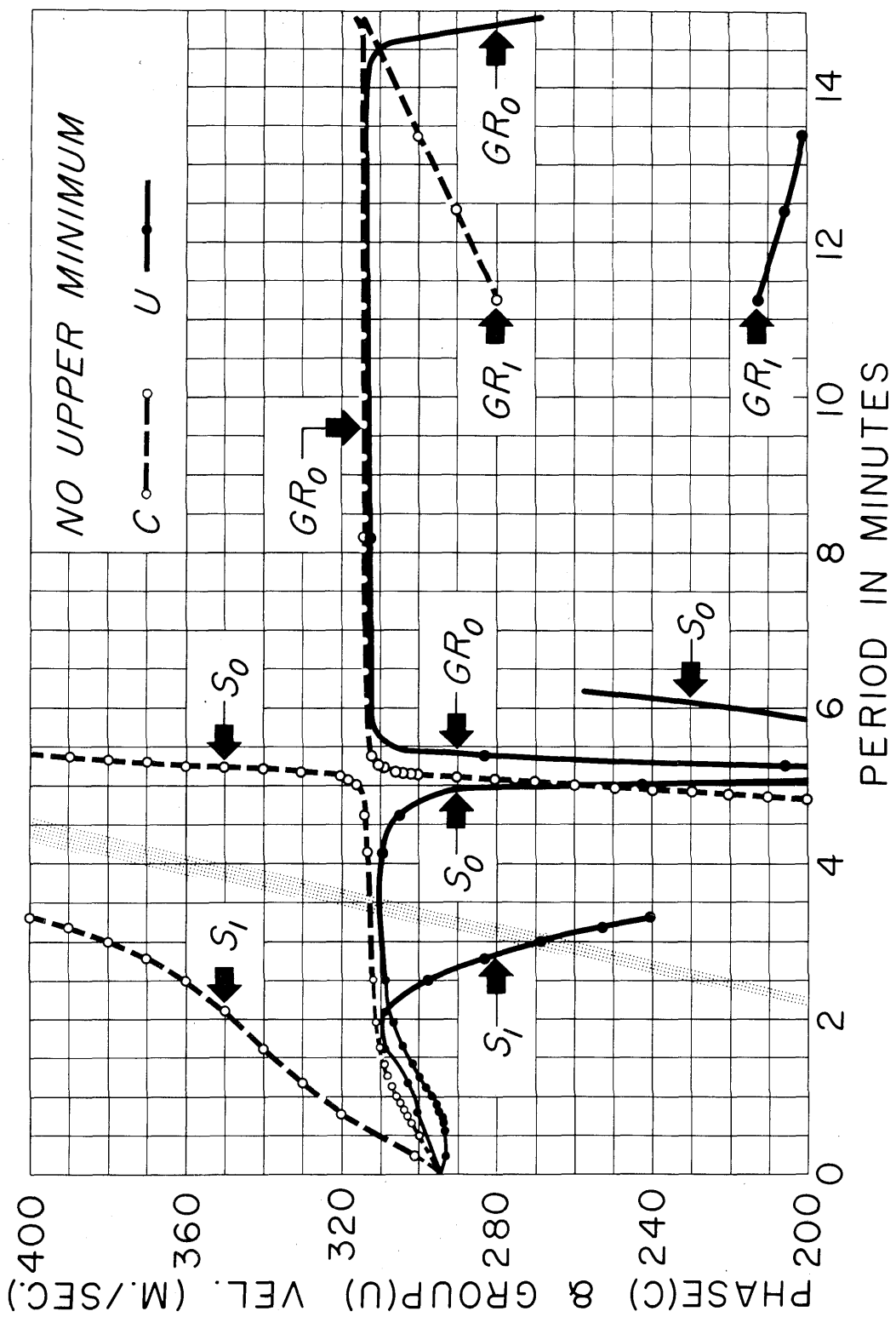
NO UPPER MINIMUM
C
U
S_0
S_1
GR_0
GR_1
PERIOD IN MINUTES
PHASE(C) & GROUP(U) VEL. (M./SEC.)
0
2
4
6
8
10
12
14
200
240
280
320
360
400

Fig. 9

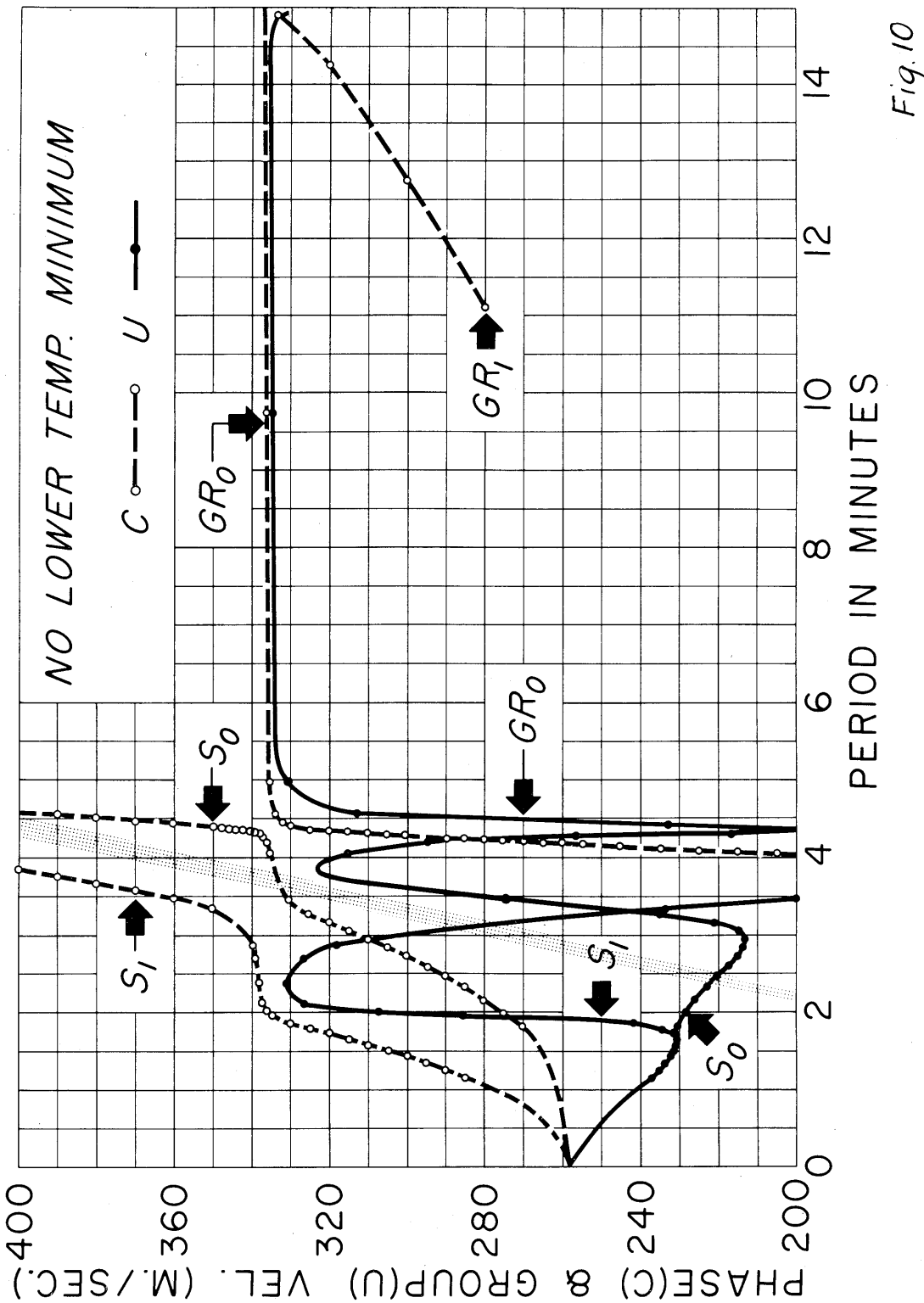
NO LOWER TEMP. MINIMUM
C
U
S_1
S_0
GR_0
GR_1
GR_0
S_1
S_0
PHASE(C) & GROUP(U) VEL. (M./SEC.)
400
360
320
280
240
200
0
2
4
6
8
10
12
14
PERIOD IN MINUTES

Fig. 10

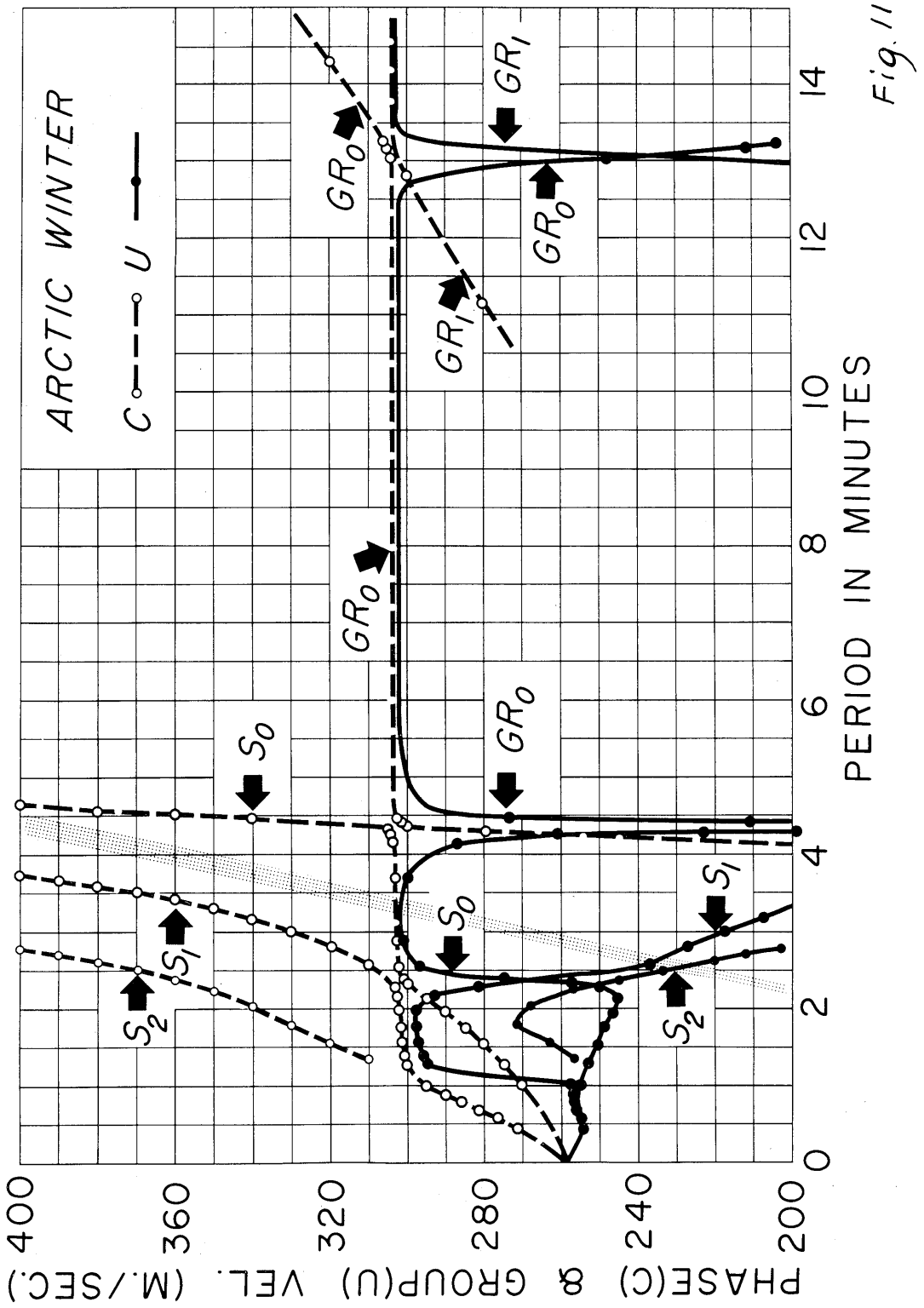
ARCTIC WINTER
C
U
PHASE(C) & GROUP(U) VEL. (M./SEC.)
400
360
320
280
240
200
0
2
4
6
8
10
12
14
PERIOD IN MINUTES
S_2
S_1
S_0
GR_0
GR_1

Fig. 11

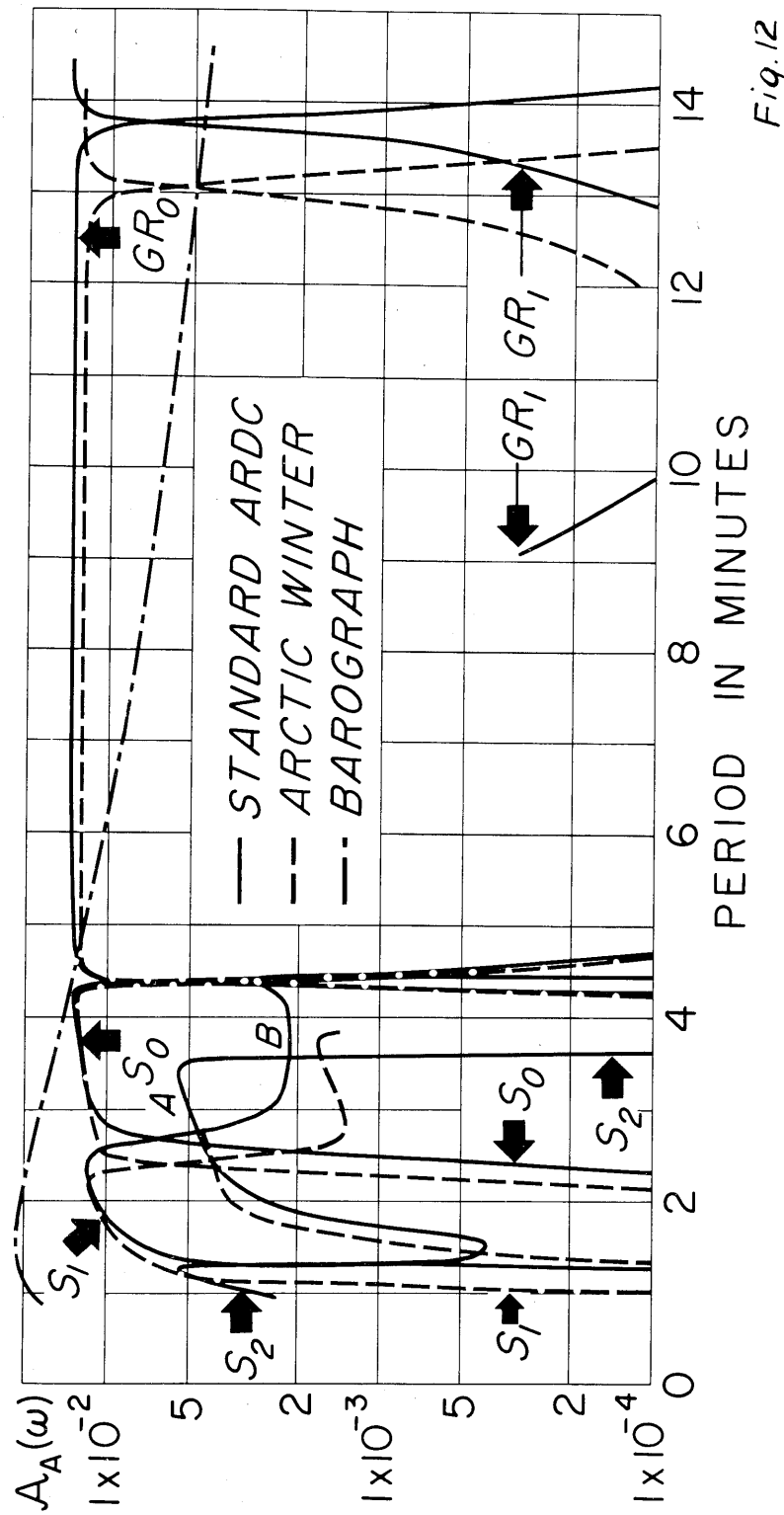
STANDARD ARDC
ARCTIC WINTER
BAROGRAPH
GR_0
GR_1
GR_1
S_0
S_1
S_2
A
B
S_0
S_2
S_1
$A_A(\omega)$
1×10^{-2}
5
2
1×10^{-3}
5
2
1×10^{-4}
0
2
4
6
8
10
12
14
PERIOD IN MINUTES

Fig. 12

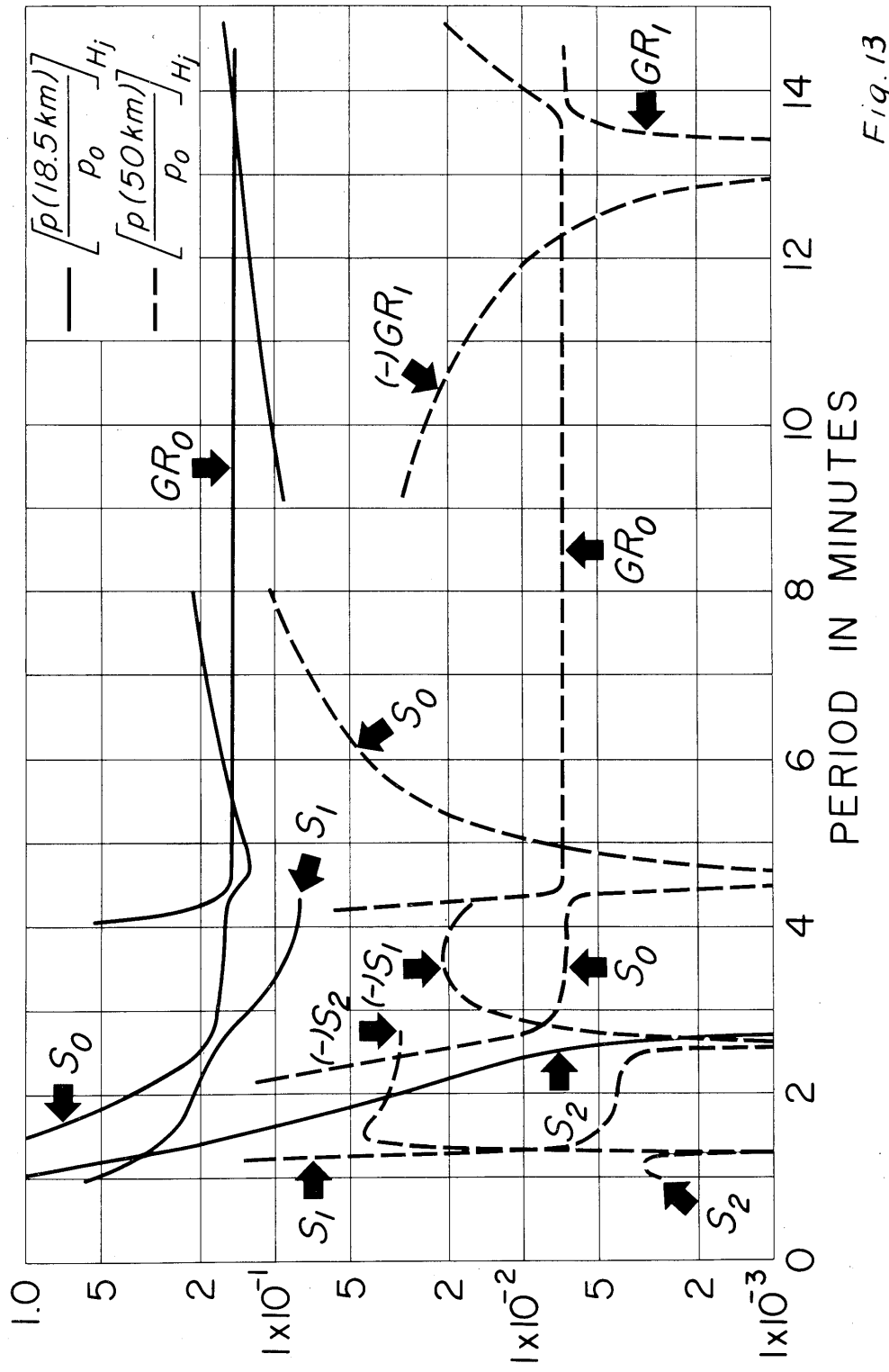
$\left[\frac{p(18.5\,km)}{p_o}\right]_{Hj}$
$\left[\frac{p(50\,km)}{p_o}\right]_{Hj}$
GR_0
S_0
S_1
$(-)S_2$
$(-)S_1$
S_2
$(-)GR_1$
GR_1
1.0
5
2
1×10^{-1}
5
2
1×10^{-2}
5
2
1×10^{-3}
0
2
4
6
8
10
12
14
PERIOD IN MINUTES

Fig. 13

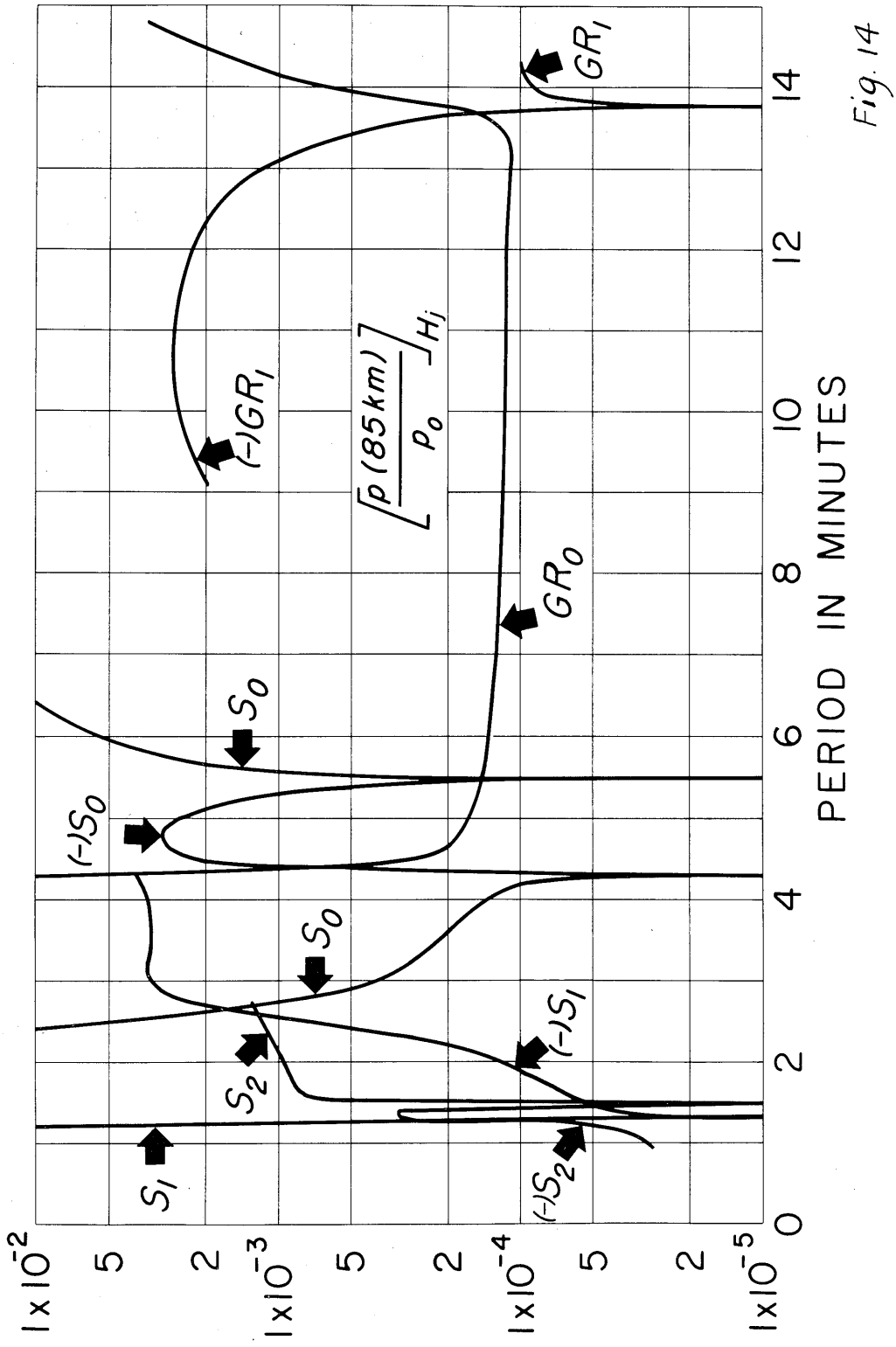
1x10^-2
5
2
1x10^-3
5
2
1x10^-4
5
2
1x10^-5
0
2
4
6
8
10
12
14
PERIOD IN MINUTES
S1
S2
S0
S0
(-)S0
(-)S1
(-)S2
GR0
GR1
(-)GR1
[p(85km)/p0]Hj

Fig. 14

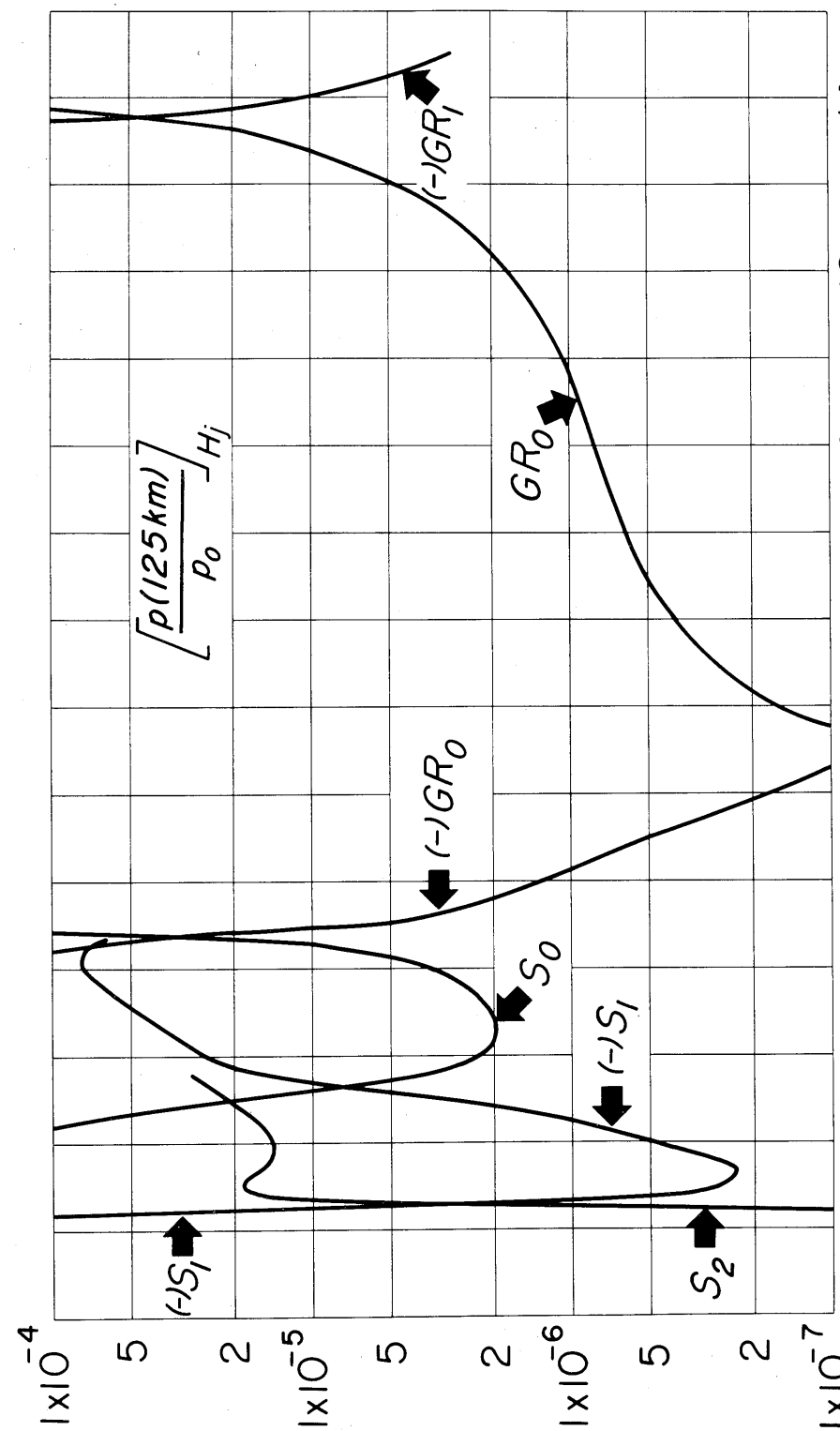
$\left[\frac{p(125km)}{p_o}\right]_{Hj}$
$(-)S_1$
S_0
$(-)GR_0$
$(-)S_1$
S_2
GR_0
$(-)GR_1$
1x10^{-4}
5
2
1x10^{-5}
5
2
1x10^{-6}
5
2
1x10^{-7}
0
2
4
6
8
10
12
14
PERIOD IN MINUTES

Fig. 15

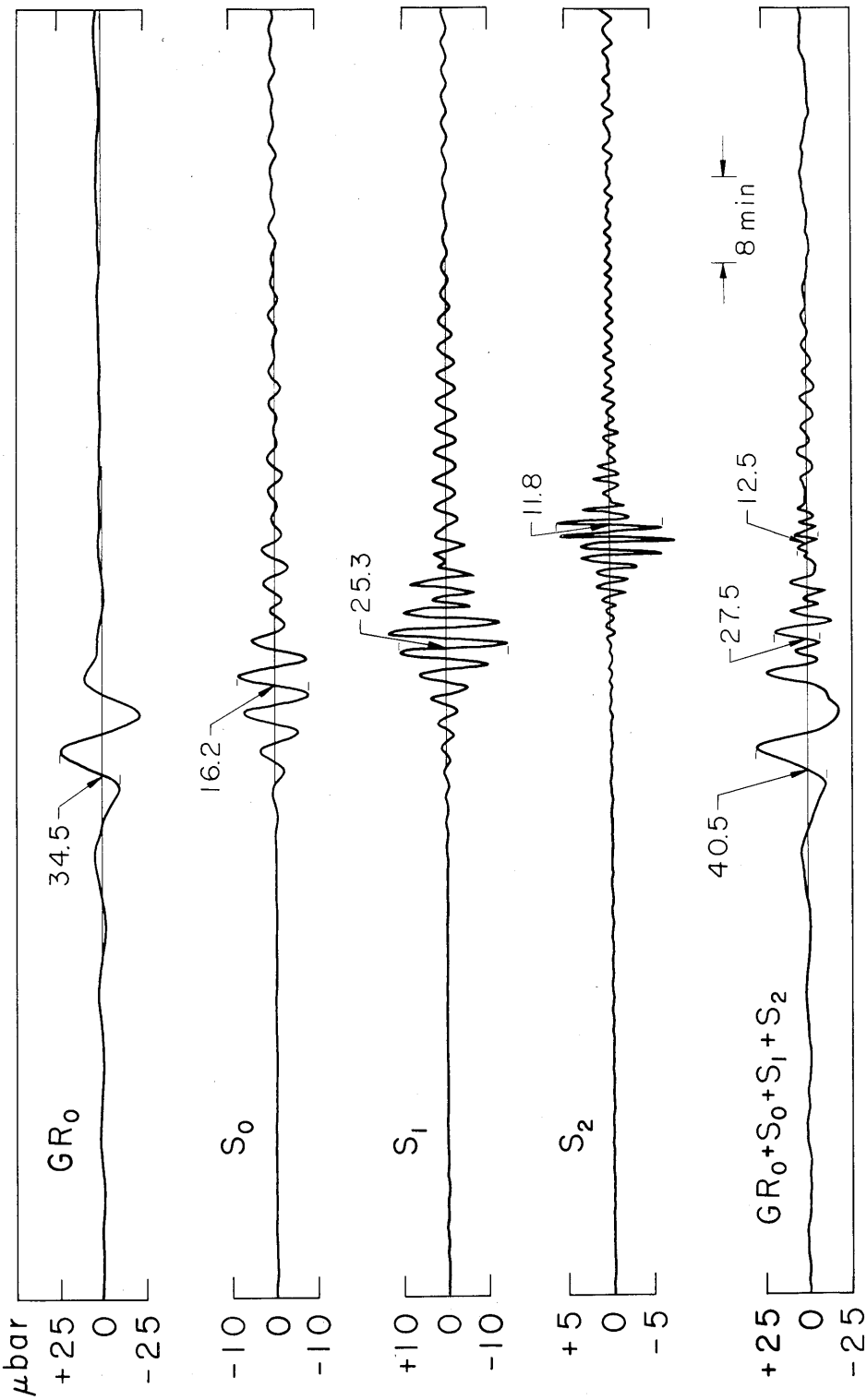
μbar
+25
0
-25
GR0
34.5
-10
0
-10
S0
16.2
+10
0
-10
S1
25.3
+5
0
-5
S2
11.8
+25
0
-25
GR0+S0+S1+S2
40.5
27.5
12.5
8 min
4 MT at 7 kft 8023 km

Fig. 16

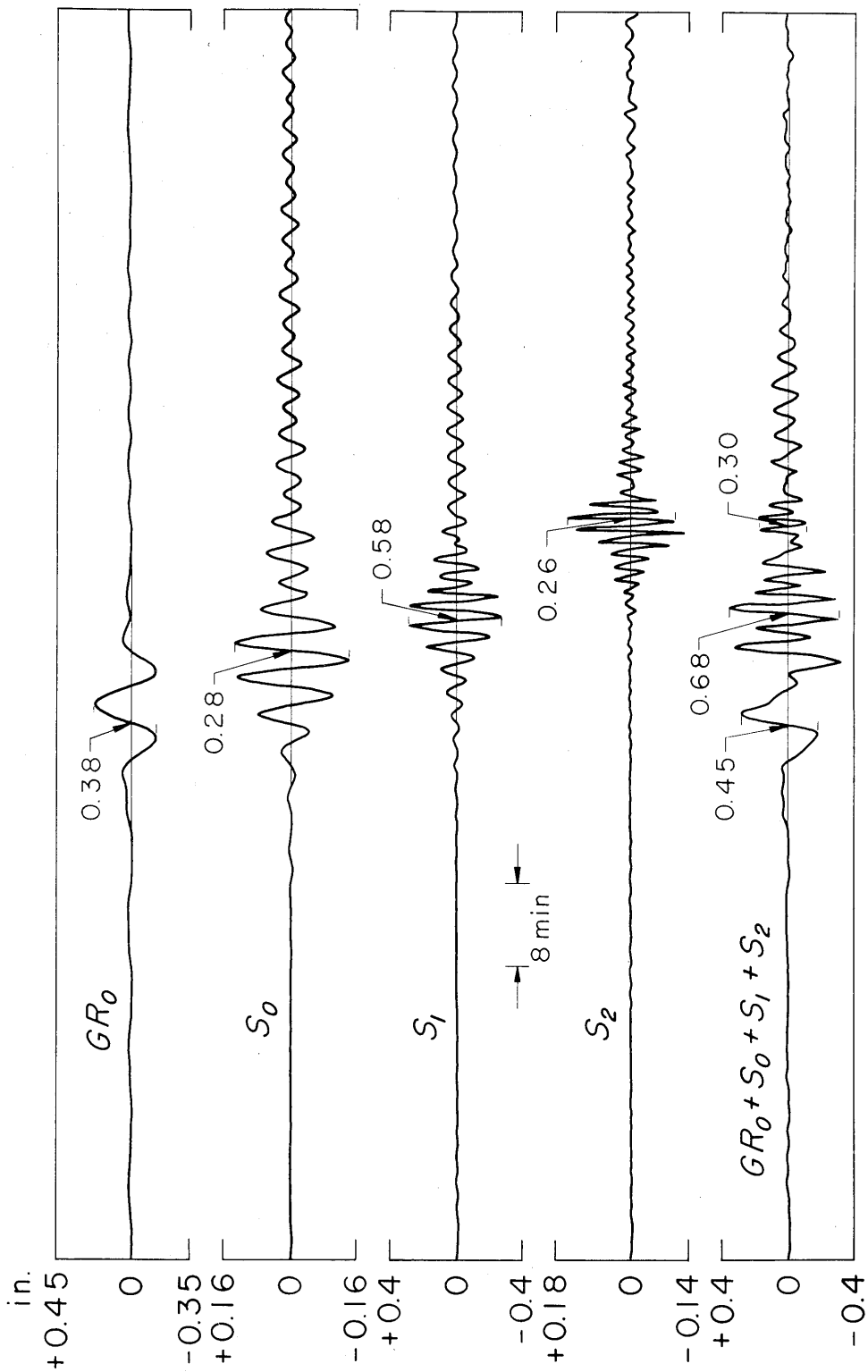
in.
+0.45
0
-0.35
+0.16
0
-0.16
+0.4
0
-0.4
+0.18
0
-0.14
+0.4
0
-0.4
GR_0
S_0
S_1
S_2
$GR_0 + S_0 + S_1 + S_2$
0.38
0.28
0.58
0.26
0.68
0.45
0.30
8 min
4 MT at 7 kft 8023 km

Fig.17

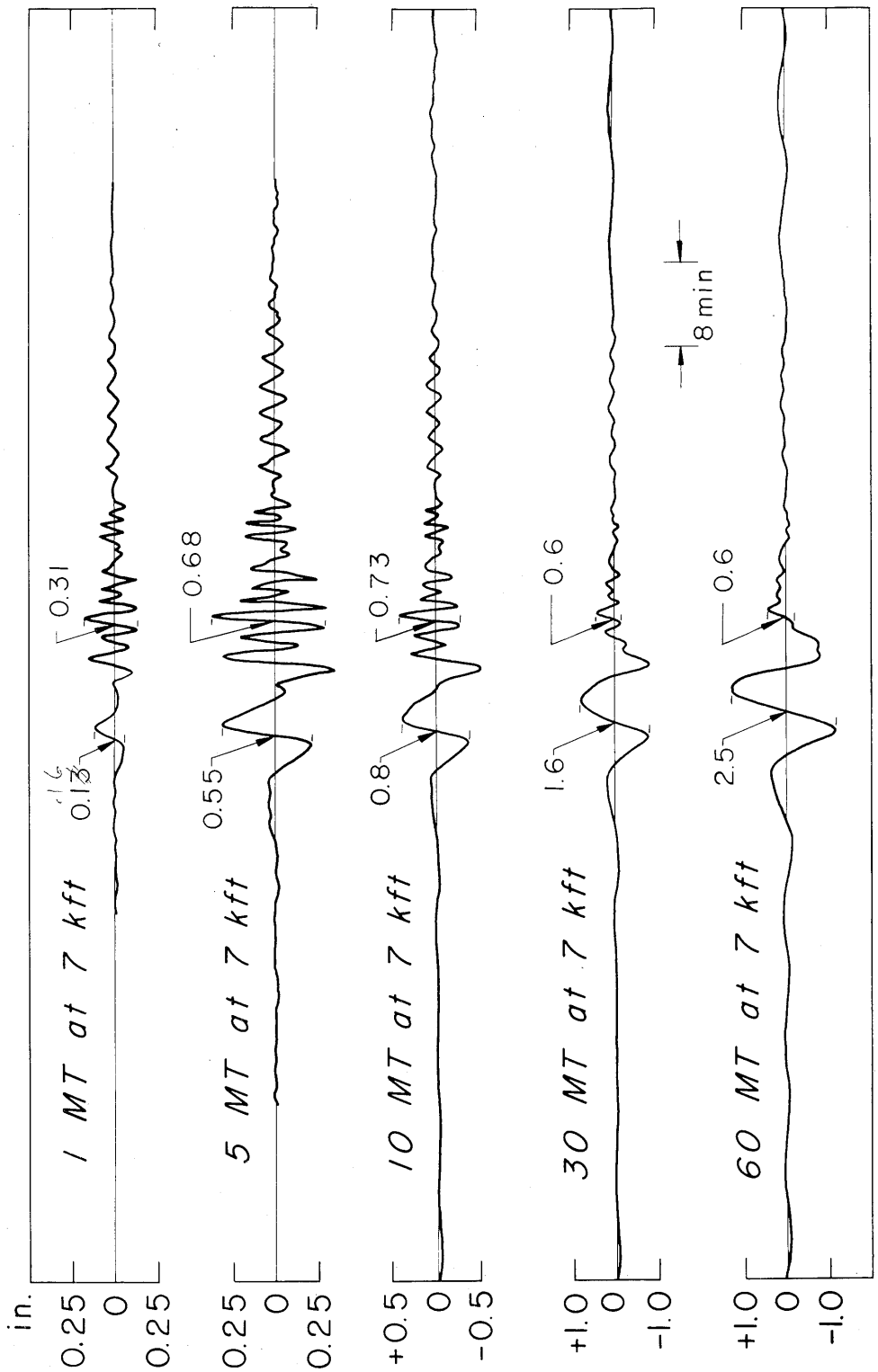

EFFECT OF YIELD

Fig. 18

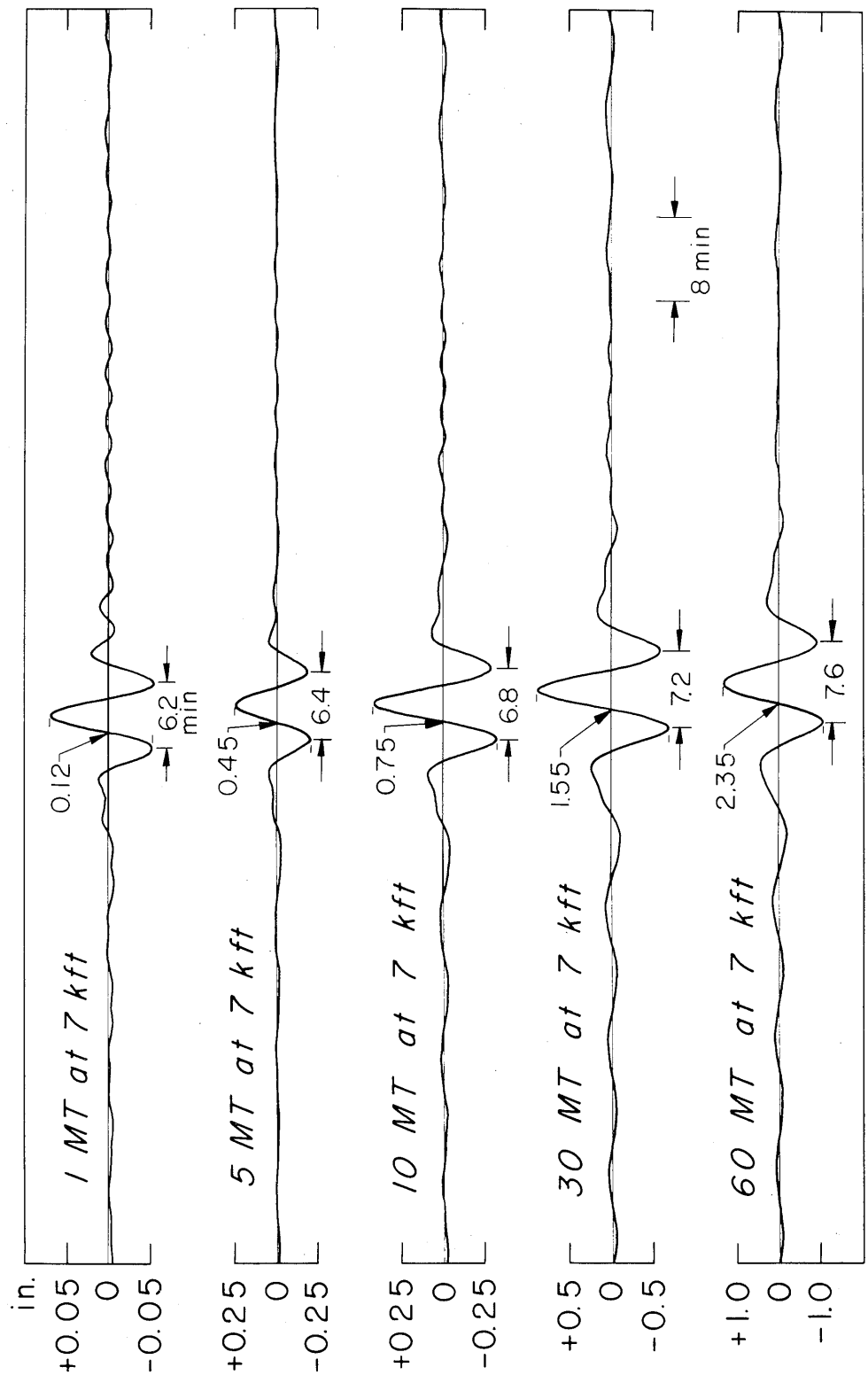

EFFECT OF YIELD ON GR.

Fig. 19

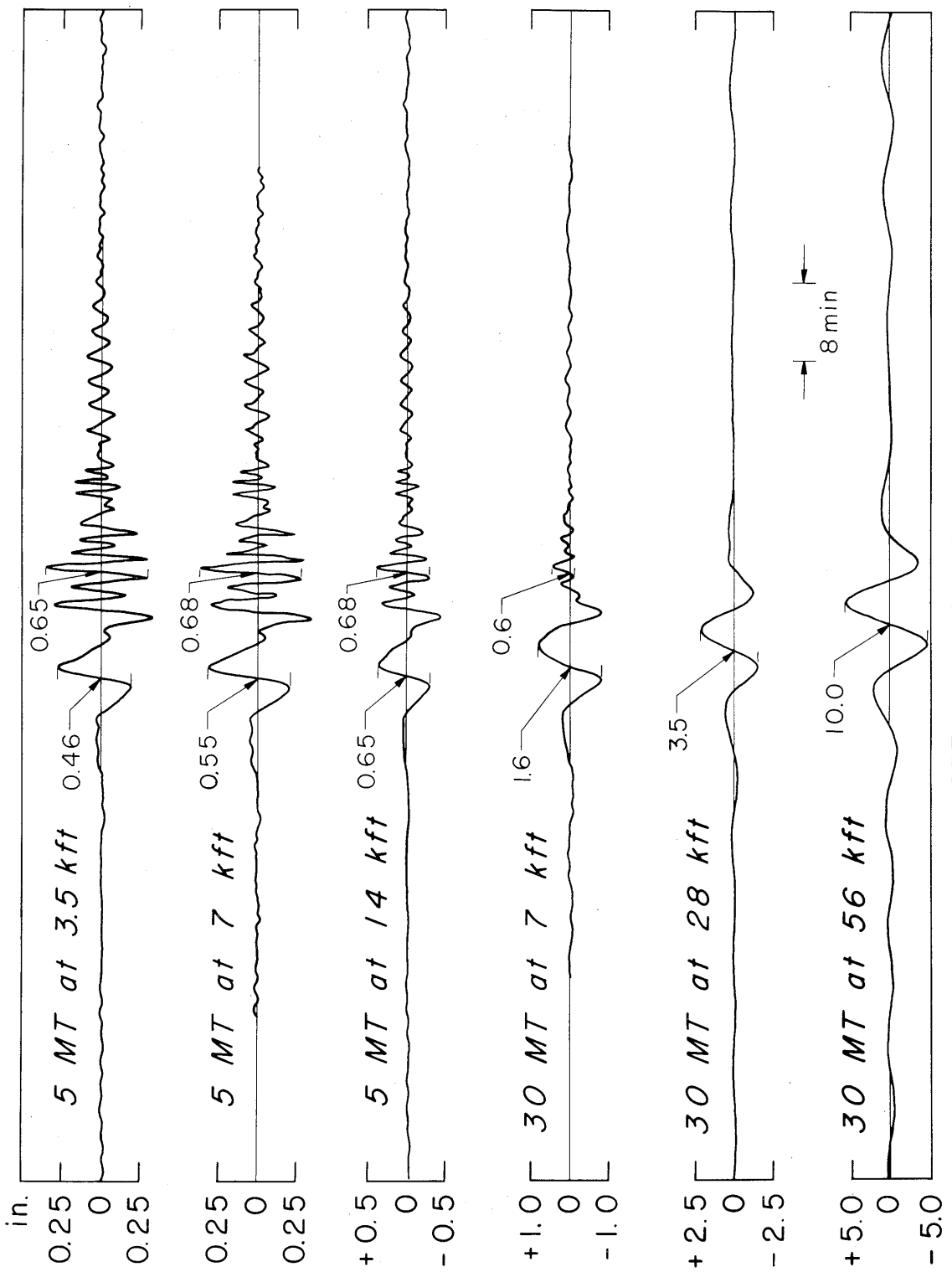
in.
+0.25
0
-0.25
5 MT at 3.5 kft
0.46
0.65
+0.25
0
-0.25
5 MT at 7 kft
0.55
0.68
+0.5
0
-0.5
5 MT at 14 kft
0.65
0.68
+1.0
0
-1.0
30 MT at 7 kft
1.6
0.6
+2.5
0
-2.5
30 MT at 28 kft
3.5
8 min
+5.0
0
-5.0
30 MT at 56 kft
10.0
EFFECT OF ALTITUDE

Fig. 20

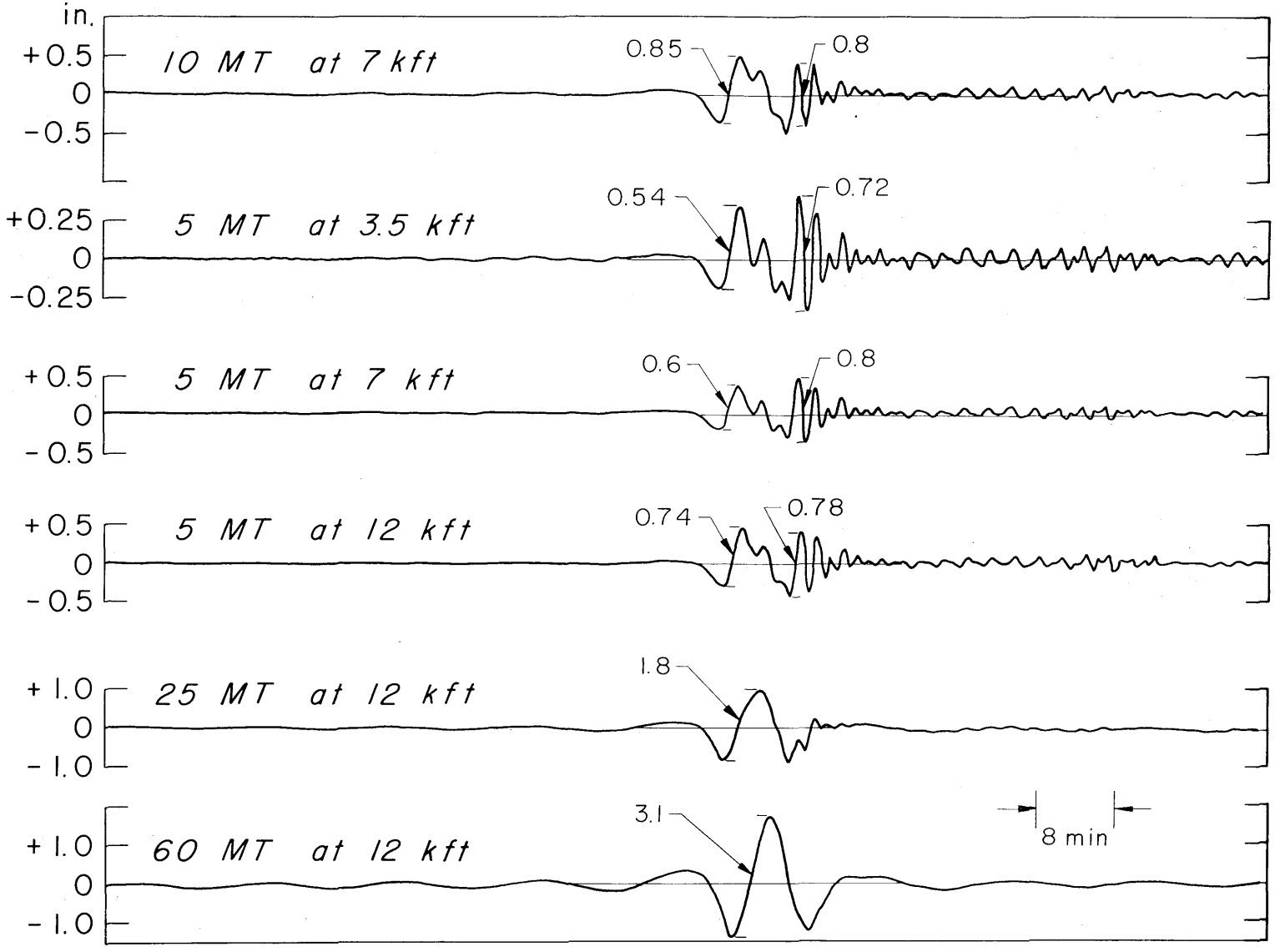

EFFECT OF YIELD AND ALTITUDE ON ARCTIC WINTER MODEL

Fig. 21

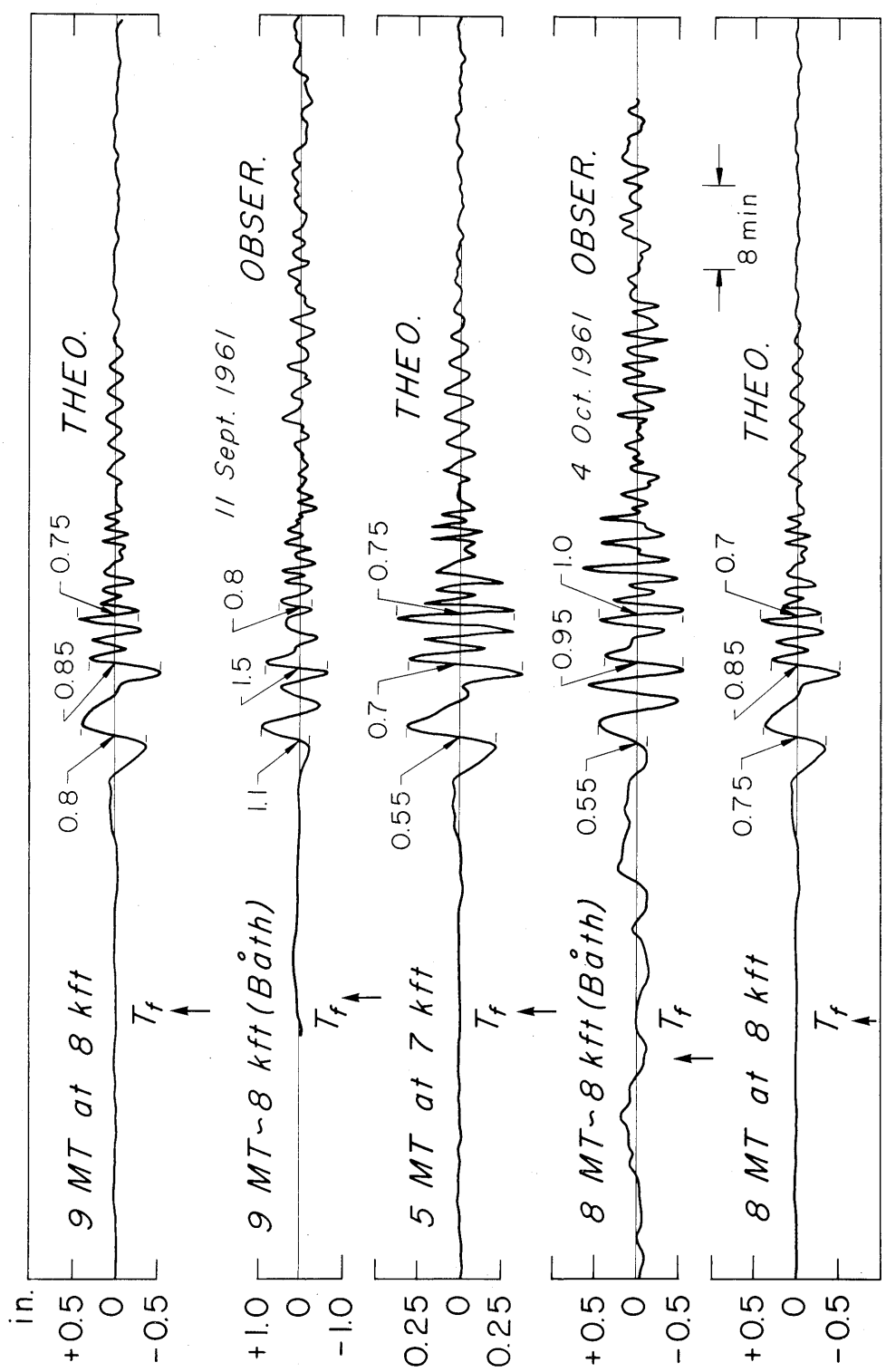
in.
+0.5
0
-0.5
9 MT at 8 kft
0.8
0.85
0.75
THEO.
T_f
+1.0
0
-1.0
9 MT~8 kft (Båth)
1.1
1.5
0.8
11 Sept. 1961
OBSER.
T_f
+0.25
0
-0.25
5 MT at 7 kft
0.55
0.7
0.75
THEO.
T_f
+0.5
0
-0.5
8 MT~8 kft (Båth)
0.55
0.95
1.0
4 Oct. 1961
OBSER.
T_f
+0.5
0
-0.5
8 MT at 8 kft
0.75
0.85
0.7
THEO.
8 min
T_f
PASADENA AI

Fig. 22

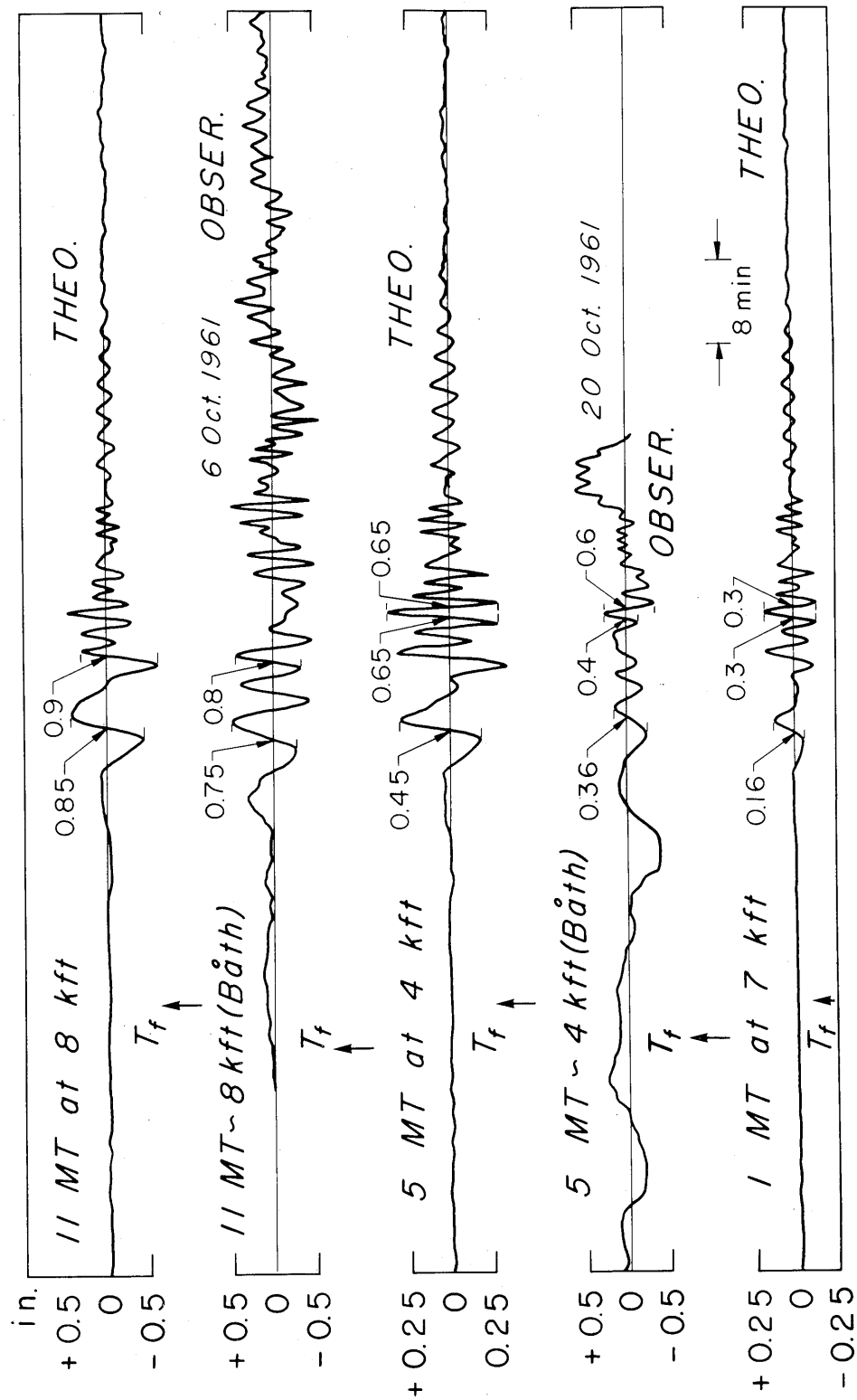
in.
+0.5
0
-0.5
11 MT at 8 kft
0.85
0.9
THEO.
T_f
+0.5
0
-0.5
11 MT~8 kft (Båth)
0.75
0.8
6 Oct. 1961
OBSER.
T_f
+0.25
0
0.25
5 MT at 4 kft
0.45
0.65
0.65
THEO.
T_f
+0.5
0
-0.5
5 MT~4 kft (Båth)
0.36
0.4
0.6
20 Oct. 1961
OBSER.
T_f
8 min
+0.25
0
-0.25
1 MT at 7 kft
0.16
0.3
0.3
THEO.
T_f
PASADENA AI

Fig. 23

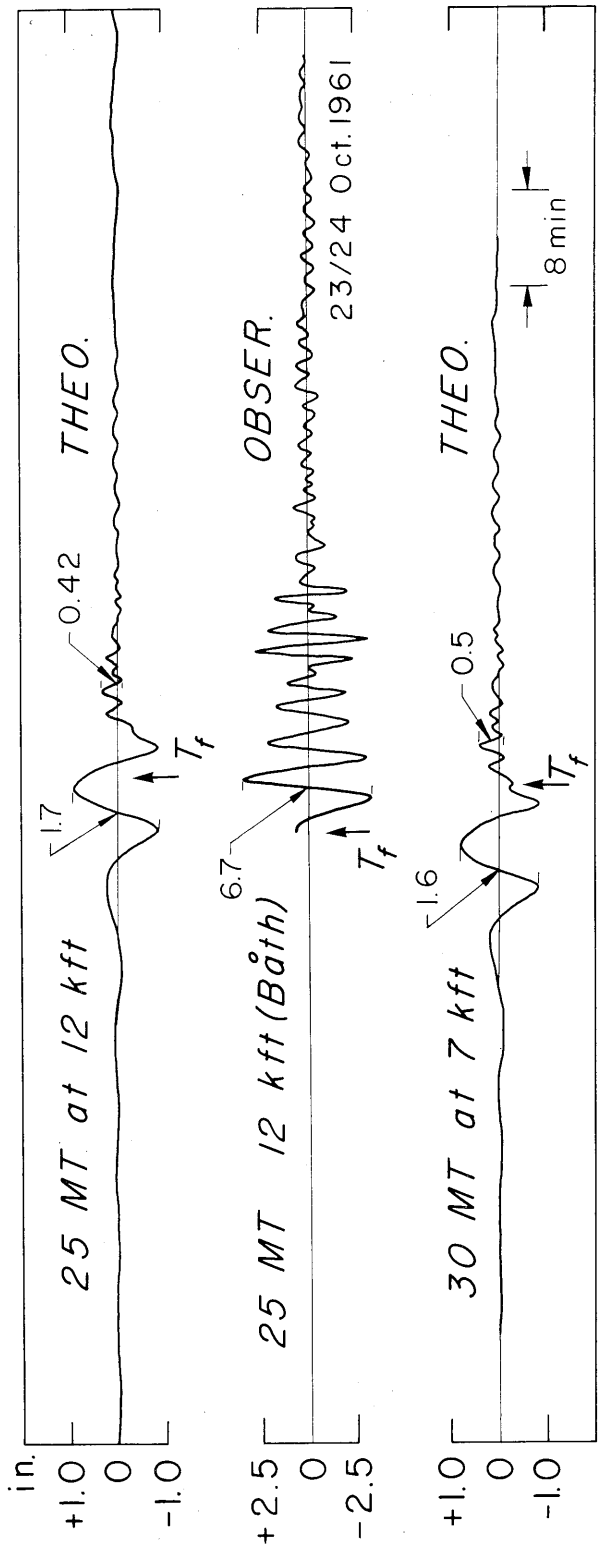
in.
+1.0
0
-1.0
25 MT at 12 kft
THEO.
1.7
0.42
T_f
+2.5
0
-2.5
25 MT 12 kft (Båth)
OBSER.
23/24 Oct. 1961
6.7
T_f
+1.0
0
-1.0
30 MT at 7 kft
THEO.
1.6
0.5
T_f
8 min
PASADENA AI

Fig. 24

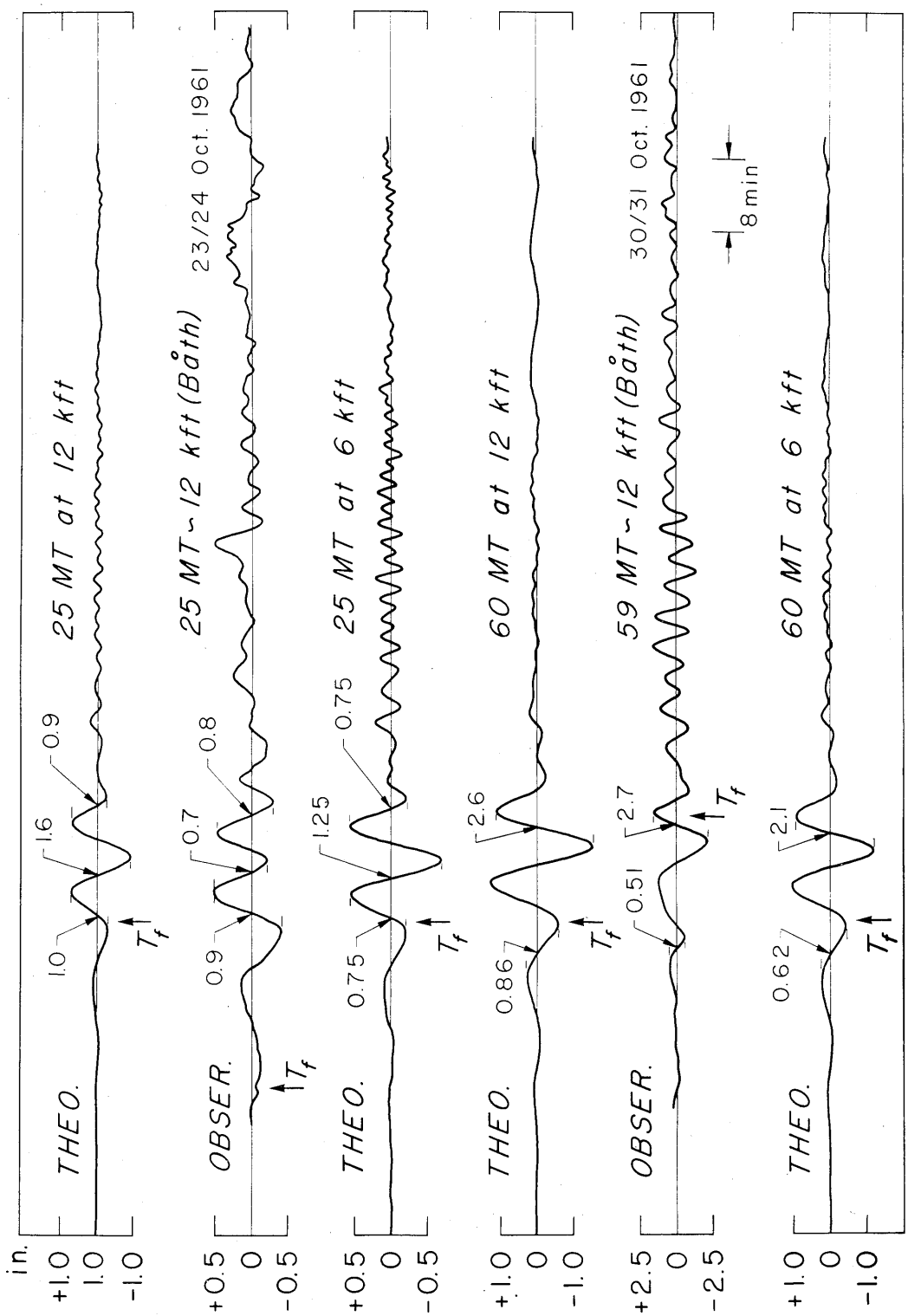
in.
+1.0
1.0
-1.0
THEO.
1.0
1.6
0.9
T_f
25 MT at 12 kft
+0.5
0
-0.5
OBSER.
0.9
0.7
0.8
T_f
25 MT ~ 12 kft (Båth)
23/24 Oct. 1961
+0.5
0
-0.5
THEO.
0.75
1.25
0.75
T_f
25 MT at 6 kft
+1.0
0
-1.0
THEO.
0.86
2.6
T_f
60 MT at 12 kft
+2.5
0
-2.5
OBSER.
0.51
2.7
T_f
59 MT ~ 12 kft (Båth)
30/31 Oct. 1961
8 min
+1.0
0
-1.0
THEO.
0.62
2.1
T_f
60 MT at 6 kft
PASADENA A2

Fig. 25

PART II

RAYLEIGH AND LOVE WAVES FROM SOURCES IN A MULTILAYERED ELASTIC HALF-SPACE

ABSTRACT

A matrix formulation is used to derive integral expressions for the time transformed displacement fields produced by simple sources at depth in a multilayered elastic isotropic halfspace. The integrals are evaluated for their residue contribution to obtain surface wave displacements in the frequency domain. The theory includes the effect of layering and source depth for the following: (1) Rayleigh waves from an explosive source, (2) Rayleigh waves from a vertical point source, (3) Rayleigh and Love waves from a vertical strike slip fault model. The latter source also includes the effect of fault dimensions and rupture velocity. The theory presented here is the ground work for the numerical computation of theoretical seismograms for use in a later paper in which a comparison will be made between observations and theory in both the time and frequency domain. A discussion is included on how these comparisons might be used in the frequency domain to estimate source depth.

ACKNOWLEDGEMENTS

The author is grateful to Professor Frank Press for his support and encouragement throughout this study. Many valuable discussions were held with Dr. D. L. Anderson and Mr. C. B. Archambeau. Their cooperation and support is acknowledged with gratitude. The author also wishes to thank Dr. R. A. Phinney for reading and critizing a rough draft of appendix A.

This research was supported by Grant No. AF-AFOSR-25-63 of the Air Force Office of Scientific Research as part of the Advanced Research Projects Agency Project VELA.

Mr. L. Lenches' help in preparation of the figures is acknowledged with special thanks.

TABLE OF CONTENTS

I. INTRODUCTION

Several years ago Dorman, Ewing, and Oliver (1960) successfully adapted the THOMSON-HASKELL matrix formulation to calculating dispersion of surface waves on multilayered elastic media using a high speed computer. Since that time surface wave dispersion has been used extensively in the interpretation of the earth's structure. Dorman et al. were able to establish the presence of the mantle's low velocity zone under the oceans. The presence of this zone under continents had long been postulated from the amplitude and travel time of body waves, but this was the first independent evidence of its existence. Calculation of dispersion had previously been limited to simple earth models consisting of at most three layers. This early work also established the fact that complex earth structures could be modelled by replacing the actual structure with a large number of isotropic, homogeneous layers.

The matrix methodology which made possible the systematic and straightforward computation of surface wave dispersion on multilayered elastic media for any number of plane parallel isotropic layers, was first introduced by Thomson (1950). He developed the technique in order to determine the reflection and transmission coefficients for plane body waves propagating through a stratified solid medium. Haskell (1953) realized that the dispersion relation between period and phase velocity in plane layered elastic media appears in the same form regardless of the source type. With this in mind he developed this plane wave formulation into a technique for determining dispersion of

surface waves. Since no source was involved, the dispersion relation was obtained by solving a set of homogeneous simultaneous linear equations. The resulting ratios of plane wave displacements and stresses, which are a by-product of the dispersion computation, play an important part in the source formulation and will be referred to in subsequent discussions as the homogeneous motion stress ratios. The usage of the terms inhomogeneous and homogeneous stems from the fact that the equations of motion can be reduced to inhomogeneous or homogeneous, second order, linear equations depending on whether a driving force is present or not present respectively in the elastic system.

The success of surface wave dispersion in yielding additional knowledge on the earth's upper mantle structure and on the earthquake source mechanism has given hope to seismologists that the amplitude spectra of surface waves may provide further information concerning the mechanism of seismic sources. This is especially true for source depth which has no influence on dispersion. In order to determine the effect of source depth on surface wave amplitudes it is necessary to include a source at depth in the multilayered formulation. Also without a specific sour ce one is unable to determine the relative excitation between modes as a function of frequency.

There are two methods of attacking the source problem for an n-layered medium. The classical technique uses the determinants that result from Cramer's rule for solving a set of inhomogeneous linear equations. One expresses the source as an integration of homogeneous solutions to which have been added homogeneous layer solutions with

arbitrary coefficients so as to be able to satisfy the boundary conditions at each interface. In this way one arrives at a formal integral solution with an integrand given in terms of the ratios of two determinants of order (4n-2) for Rayleigh waves and (2n-2) for Love waves.

This method, although easy to formulate, is extremely cumbersome if not dangerous to evaluate numerically on a computer. The danger involved results from the fact that determinants in general are not slowly varying functions of their elements. The determinant solution was obtained by Jaedetsky (1953) and Kellis-Borok (1953). Besides the numerical difficulties inherent in solving larger order determinants there is the practical difficulty of reordering or simplifying the determinants into a form which provides insight as to the individual effects of receiver depth, source depth, and layering on the spectral amplitude.

The second method is to use a matrix formulation. Previously this has been done in two ways. Using the THOMSON-HASKELL matrices to obtain the reflection and transmission coefficients for plane waves in multilayered media, and an integral representation of a point source in terms of plane waves, Gilbert (1956) obtained a formal integral solution for the compressional point source, but made no effort to evaluate the integral for the surface wave contribution.

Gilbert and MacDonald (1961) applied the THOMSON-HASKELL matrix method to a layered sphere using the solutions of the equations of motion for an elastic shell. They obtained the solution to the source-at-depth problem of the sphere by operating on the source vector equation with a matrix product of the shell matrices. The source vector equation

was obtained by evaluating the source at positions infinitesimally above and below the source depth.

The theory presented here is the ground work for the numerical computation of seismograms in a later paper. In that paper we will synthesize seismograms under various conditions of source type, structure, and source depth. Then by comparing seismograms, we will see if the various parameters have qualitative characteristics in the time domain. In addition we will attempt to use the techniques suggested in this paper as a means of estimating source depth in the frequency domain. In both cases the theory will be compared to observed seismograms in both frequency and time domains.

This paper derives in detail an integral solution for the time transformed displacements for certain elementary sources at depth in a multilayered isotropic halfspace. The integrands are expressed in terms of elements from the matrix product of the THOMSON-HASKELL layer matrices in the layered array. These integrands are obtained by a technique similar to that used by Gilbert and MacDonald, namely, by a matrix operation on a general source vector equation. The elements of the vector equation depend on the integrand of the particular type of source under investigation. The transformed sources considered are as follows: (1) An explosive or spherical pressure source, (2) A horizontal and vertical point force, (3) A model of vertical strike slip fault sources formed by integration of a time lagged horizontal singlet or doublet point force over the fault surface.

The vertical and horizontal point forces are not as restrictive

as one might surmize. Their generality was shown by Kellis-Borok (1953) who pointed out that the field due to a point force, F, of arbitrary direction in a multilayered media can be obtained by the superposition of the fields due to a vertical point force, $F \sin\Delta$, and a horizontal point force, $F \cos\Delta$, where Δ is the vertical angle between F and the horizontal. Furthermore, displacement fields for multipole sources can be determined by spatial differentiation.

From the residue contribution of the integral solutions, we obtain the Rayleigh and Love wave displacements for various source types. If we had stopped here this problem would have been merely an extension of the matrix technique of Gilbert and MacDonald to Rayleigh and Love waves on a multilayered media for different types of sources. Extensive programming and numerical analysis would have been needed to compute amplitude spectra or theoretical seismograms. However by obtaining a simple form of the inverse of the product matrix in terms of the elements of the product matrix itself and simplifying the residue numerator we are able to separate the solution into factors representing source depth, receiver depth, layering, and path of propagation. The necessary simplification of the numerator is accomplished by using relations determined by setting the integrand denominator to zero. The factors representing source and receiver depth are shown to be simple functions of quantities calculated in the plane wave problem. Using the numerical techniques described in Part I, the excitation function for the layered medium can be calculated analytically by adapting the computer programs which are currently used in seismology to

calculate dispersion for Rayleigh and Love surface waves.

From these results we are also able to show certain reciprocity relations for surface waves which had been previously proved for the total displacement field. In addition we discuss how numerical calculations in the frequency domain might be used to estimate source depth from a Fourier analysis of observed seismograms.

II. THEORY

Introduction

The adaption of the plane wave matrix formulation to the point source theory is accomplished by using a general source vector equation. The source vector equation is general in that it can be used for a wider variety of point sources than considered in this paper. The vector equation is composed of elements which correspond to a discontinuity in the plane of the source of the motion-stress elements of the plane wave theory. These motion-stress elements are shown to be the vertically dependent parts of the integrand for the general solution of the problem. The discontinuity at the source results from the fact that point sources can be expressed as an integral over the horizontal wave number of an integrand which has a first or second order discontinuity across the horizontal source plane

For sources defined by potentials instead of vectors, we use an alternate method. Here the integrands of the source potentials are expressed in the following form

$$\varphi_{so}(z) = S_{01}^{\pm} e^{-ikr_{\alpha_s}|z-D|}$$

$$\psi_{so}(z) = S_{02}^{\pm} e^{-ikr_{\beta_s}|z-D|} \qquad \pm \text{ as } z \gtrless D$$

and

$$\chi_{so}(z) = S_{03}^{\pm} e^{-ikr_{\rho_s}|z-D|}$$

where

z is the vertical coordinate

D is the source depth

$\varphi_{so}(z)$ is the z dependent part of the dilatational potential source integrand

$\psi_{so}(z)$ is the z dependent part of the shear potential source integrand for Rayleigh type motion

$\chi_{so}(z)$ is the z dependent part of the shear potential source integrand for Love type motion

and $S_{01}^{\pm}$, $S_{02}^{\pm}$, $S_{03}^{\pm}$ are spatially independent constants which depend on the source type. Quantitites not defined in the text are defined in Appendix E. Substituting these relations in the THOMSON-HASKELL relations, we obtain the necessary discontinuity in the motion stress elements in terms of $S_{01}^{\pm}$, $S_{02}^{\pm}$, $S_{03}^{\pm}$ and the elastic constants of layer containing the source. This method is used in the formulation of an explosive source at depth.

In order to retain a continuity of presentation, the following parts of this paper are given in the appendices:

Appendix A: This appendix derives the vector and matrix relations for the z dependent motion-stress elements in each layer, which form the integrands of the solutions and are characteristic of Rayleigh and Love type motion. The derivation is in an appendix since it is essentially a reorganization of the matrix formulation given by Haskell (1953). The reorganization is presented in such a manner as to make the inclusion of a general point source in the layer a simple and straightforward extension of the formulation.

Appendices B and C: These appendices contain the derivation of source expressions in an integral form suitable for the matrix formulation.

Appendices D and E: These appendices contain the inversion of the Rayleigh layer and product matrix, and the derivation of relations obtained from the zeros of the integrand denominator.

All of the above appendices except A contain a large number of algebraic steps. Their results are necessary for the solution of the problem but their derivation is not essential to understanding the theory.

Rayleigh Waves From an Explosive Source At Depth

For an explosive source, we use the Fourier time transformed spherical compressional potential derived in Appendix C for a pressure suddenly applied to the walls of a spherical cavity in medium s. It must be pointed out that only the source term "sees" the spherical cavity. In other words, we do not impose on the multilayer problem the boundary condition that normal and tangential stress over the cavity walls vanish for the homogeneous terms; thus waves reflected and scattered by the cavity are not considered.

We consider a semi infinite elastic medium made up of n parallel solid homogeneous, isotropic layers (Figure 1). We number the array such that the layer at the free surface is layer o and the half space is layer n. Consider a compressional point source in layer s at a depth D from the free surface. The potential of this explosive source is given by equation C8 as

$$\bar{\varphi}_{so}(R) = -\frac{\bar{p}_{os}}{4\mu_s} a_s^3 \frac{e^{i(k_{\alpha_s} a_s - \theta_{SP})}}{\left[\left(1 - \frac{a_s^2 k_{\beta_s}^2}{4}\right)^2 + k_{\alpha_s}^2 a_s^2\right]^{\frac{1}{2}}} \frac{e^{-ik_{\alpha_s} R}}{R} \tag{1}$$

where R is the distance from the source and

$$\theta_{SP} = \tan^{-1} \frac{k_{\alpha_s} a_s}{\left(1 - \frac{a_s^2 k_{\beta_s}^2}{4}\right)}$$

Other terms are defined in Appendix F.

Placing the origin of a cylindrical coordinate system (r, θ, z) at the free surface the layer interfaces are defined by z constant and layer s is bounded by z_{s-1} and z_s with $z_s > D > z_{s-1}$. We can write R as

$$R = \left[r^2 + (z - D)^2\right]^{1/2} \tag{2}$$

By means of the Sommerfeldt integral, we can rewrite equation 1 as

$$\bar{\varphi}_{so}(r, z) = \int_0^\infty S_{01} e^{-ikr_{\alpha_s} |z-D|} J_o(kr)\, dk \tag{3}$$

where

$$S_{01} = i \frac{\bar{p}_{os} a_s^3 e^{i(k_{\alpha_s} a_s - \theta_{SP})}}{4\mu_s r_{\alpha_s} \left[\left(1 - \frac{a_s^2 k_{\beta_s}^2}{4}\right)^2 + k_{\alpha_s}^2 a_s^2\right]^{\frac{1}{2}}} \tag{4}$$

and

$$k^2 r_{\alpha_s}^2 = k_{\alpha_s}^2 - k^2$$

Since the source is symmetric and the only boundary conditions are at the layer interfaces, z constant, the problem is axially symmetric. The displacements and stresses for this symmetry are given in terms of potentials $\overline{\varphi}_m(r,z)$ and $\overline{\psi}_m(r,z)$ for layer m by

$$\overline{q}_m(r,z) = \frac{\partial\overline{\varphi}_m}{\partial r} + \frac{\partial^2\overline{\psi}_m}{\partial r\partial z}$$

$$\overline{w}_m(r,z) = \frac{\partial\overline{\varphi}_m}{\partial z} + \frac{\partial^2\overline{\psi}_m}{\partial z^2} + k^2_{\beta_m}\overline{\psi}_m$$

$$\overline{P}_{zz_m}(r,z) = 2\mu_m\left[\frac{\partial^2\overline{\varphi}_m}{\partial z^2} + \frac{\partial^3\overline{\psi}_m}{\partial z^3} + k^2_{\beta_m}\frac{\partial\overline{\psi}_m}{\partial z}\right] - \lambda_m k^2_{a_m}\overline{\varphi}_m \qquad (5)$$

$$\overline{P}_{rz_m}(r,z) = \mu_m\left[2\frac{\partial^2\overline{\varphi}_m}{\partial z\partial r} + 2\frac{\partial^3\overline{\psi}_m}{\partial r\partial z^3} + k^2_{\beta_m}\frac{\partial\overline{\psi}_m}{\partial r}\right]$$

where $\overline{q}_m$, $\overline{w}_m$, $\overline{P}_{zz_m}$ and $\overline{P}_{rz_m}$ are the radial displacement, normal displacement, normal stress, and radial tangential stress to the z plane respectively and where the potentials are solutions of

$$\frac{1}{r}\frac{\partial}{\partial r}\left(r\frac{\partial\overline{\varphi}_m}{\partial r}\right) + \frac{\partial^2\overline{\varphi}_m}{\partial z^2} = -k^2_{a_m}\overline{\varphi}_m$$

and (6)

$$\frac{1}{r}\frac{\partial}{\partial r}\left(r\frac{\partial\overline{\psi}_m}{\partial r}\right) + \frac{\partial^2\overline{\psi}_m}{\partial z^2} = -k^2_{\beta_m}\overline{\psi}_m$$

We define

$$\overline{q}_m(r,z) = \int_0^\infty q_m(r,z;k)\,dk\,, \qquad \overline{w}_m(r,z) = \int_0^\infty w_m(r,z;k)\,dk\,,$$

$$\overline{P}_{zz_m}(r,z) = \int P_{zz_m}(r,z;k)\,dk\,, \qquad \overline{P}_{rz_m}(r,z) = \int_0^\infty P_{rz_m}(r,z;k)\,dk \tag{7}$$

$$\overline{\varphi}_m(r,z) = \int_0^\infty \varphi_m(r,z;k)\,dk \qquad \text{and} \quad \overline{\psi}_m(r,z) = \int_0^\infty \psi_m(r,z;k)\,dk$$

and assume the same radial dependence as the source integrand for $\varphi_m(r,z;k)$ and $\psi_m(r,z;k)$, i.e.

$$\begin{aligned} \varphi_m(r,z;k) &= \psi_m(z)\,J_o(kr) \\ \psi_m(r,z;k) &= \psi_m(z)\,J_o(kr) \end{aligned} \tag{8}$$

Substituting equations 7 and 8 in 5, and equating integrands, we obtain the following;

$$\begin{aligned} q_m(r,z;k) &= -k\left[\varphi_m(z) + \frac{d\psi_m}{dz}(z)\right] J_1(kr) \\ &\equiv -\frac{1}{k}\,\frac{\overset{u}{R}_m}{c}(z)\,J_1(kr) \\ w_m(r,z;k) &= \left[\frac{d\varphi_m}{dz}(z) + \frac{d^2\psi_m}{dz^2}(z) + k^2\beta_m\,\psi_m(z)\right] J_o(kr) \\ &\equiv -\frac{i}{k}\,\frac{\overset{\cdot}{w}_{R_m}}{c}(z)\,J_o(kr) \\ P_{zz_m}(r,z;k) &= \left\{2\mu_m\left[\frac{d^2\varphi_m}{dz^2}(z) + \frac{d^3\psi_m}{dz^3}(z) + k^2\beta_m\,\frac{d\psi_m}{dz}(z)\right]\right. \\ &\qquad \left. - \lambda_m k^2 a_m\,\varphi_m(z)\right\} J_o(kr) \equiv \sigma_{R_m}(z)\,J_o(kr) \end{aligned} \tag{9}$$

$$P_{rz_m}(r, z;k) = - k\mu_m\left[2 \frac{d\varphi_m}{dz}(z) + 2 \frac{d^2\psi_m}{dz^2}(z) + k^2_{\beta_m} \frac{d\psi_m}{dz}(z) \right] J_1(kr)$$

$$\equiv - i\tau_{R_m}(z)\, J_1(kr)$$

Similarly, from equation 6, $\varphi_m(z)$ and $\psi_m(z)$ are solutions of

$$\frac{d^2\varphi_m}{dz^2}(z) = (k^2 - k^2_{\alpha_m})\varphi_m(z) \equiv - k^2 r^2_{\alpha_m} \varphi_m(z)$$

$$\frac{d^2\psi_m}{dz^2}(z) = (k^2 - k^2_{\beta_m})\psi_m(z) \equiv - k^2 r^2_{\beta_m} \psi_m(z) \qquad (10)$$

Using the definition of phase velocity $c = \frac{\omega}{k}$ we can write

$$(kr_{\alpha_m})^2 = k^2_{\alpha_m} - k^2 = k^2\left[\frac{c^2}{\alpha^2_m} - 1\right]$$

$$(kr_{\beta_m})^2 = k^2_{\beta_m} - k^2 = k^2\left[\frac{c^2}{\beta^2_m} - 1\right]$$

where $k_{\alpha_m} = \frac{\omega}{\alpha_m}$, $k_{\beta_m} = \frac{\omega}{\beta_m}$ and α_m and β_m are the compressional and shear velocities respectively of layer m. We use the following sign criteria for r_{α_m} and r_{β_m} as given in Haskell (1953);

$$r_{\alpha_m} = \left[\frac{c^2}{\alpha^2_m} - 1\right]^{\frac{1}{2}} \qquad \text{for } c > \alpha_m$$

$$r_{\alpha_m} = - i\left[1 - \frac{c^2}{\alpha^2_m}\right]^{\frac{1}{2}} \qquad \text{for } c < \alpha_m$$

$$r_{\beta_m} = \left[\frac{c^2}{\beta^2_m} - 1\right]^{\frac{1}{2}} \qquad \text{for } c > \beta_m$$

$$r_{\beta_m} = -i\left[1 - \frac{c^2}{\beta_m^2}\right]^{\frac{1}{2}} \qquad \text{for } c < \beta_m$$

At the interface between two layers, we impose the conditions of continuity of displacement and stress. In order that this be true for all r along the boundary, the integrands of displacement and stress show that the z dependent quantities defined by equation 9 must also be continuous. In vector notation this boundary condition can be expressed as

$$\begin{bmatrix} \frac{\dot{u}_{R_m}(z_{m-1})}{c} \\ \frac{\dot{w}_{R_m}(z_{m-1})}{c} \\ \sigma_{R_m}(z_{m-1}) \\ \tau_{R_m}(z_{m-1}) \end{bmatrix} = \begin{bmatrix} \frac{\dot{u}_{R_{m-1}}(z_{m-1})}{c} \\ \frac{\dot{w}_{R_{m-1}}(z_{m-1})}{c} \\ \sigma_{R_{m-1}}(z_{m-1}) \\ \tau_{R_{m-1}}(z_{m-1}) \end{bmatrix} \tag{11}$$

The vector used in equation 11 will be referred to as the motion-stress vector. In Appendix A, it is shown that the motion-stress vectors at the top and bottom of a layer are related by the linear transformation equation A11

$$\begin{bmatrix} \frac{\dot{u}_{R_m}(z_m)}{c} \\ \frac{\dot{w}_{R_m}(z_m)}{c} \\ \sigma_{R_m}(z_m) \\ \tau_{R_m}(z_m) \end{bmatrix} = a_{R_m} \begin{bmatrix} \frac{\dot{u}_{R_m}(z_{m-1})}{c} \\ \frac{\dot{w}_{R_m}(z_{m-1})}{c} \\ \sigma_{R_m}(z_{m-1}) \\ \tau_{R_m}(z_{m-1}) \end{bmatrix} \tag{12}$$

where the elements of the layer matrix a_{R_m} are given by equation A13.

For the source layer, s, the integrand of the source term is from equation 3

$$\varphi_{so}(r, z;k) = \varphi_{so}(z)\, J_o(kr) \tag{13}$$

where

$$\varphi_{so}(z) = S_{01} e^{-ikr_{a_s}|z-D|} \tag{14}$$

For a point source of this form, the vector equations for a general point source derived in Appendix A, equations A19 and A20, reduce to

$$\begin{bmatrix} \frac{\dot{u}_{R_{s2}}(z_s)}{c} \\ \frac{\dot{w}_{R_{s2}}(z_s)}{c} \\ \sigma_{R_{s2}}(z_s) \\ \tau_{R_{s2}}(z_s) \end{bmatrix} = a_{R_{s2}} \begin{bmatrix} \frac{\dot{u}_{R_{s2}}(D)}{c} \\ \frac{\dot{w}_{R_{s2}}(D)}{c} \\ \sigma_{R_{s2}}(D) \\ \tau_{R_{s2}}(D) \end{bmatrix}$$

$$\begin{bmatrix} \frac{\dot{u}_{R_{s1}}(D)}{c} \\ \frac{\dot{w}_{R_{s1}}(D)}{c} \\ \sigma_{R_{s1}}(D) \\ \tau_{R_{s1}}(D) \end{bmatrix} = a_{R_{s1}} \begin{bmatrix} \frac{\dot{u}_{R_{s1}}(z_{s-1})}{c} \\ \frac{\dot{w}_{R_{s1}}(z_{s-1})}{c} \\ \sigma_{R_{s1}}(z_{s-1}) \\ \tau_{R_{s1}}(z_{s-1}) \end{bmatrix} \tag{15}$$

and

$$\begin{bmatrix} \frac{\dot{u}_{R_{s2}}}{c}(D) \\ \frac{\dot{w}_{R_{s2}}}{c}(D) \\ \sigma_{R_{s2}}(D) \\ \tau_{R_{s2}}(D) \end{bmatrix} = \begin{bmatrix} \frac{\dot{u}_{R_{s1}}}{c}(D) \\ \frac{\dot{w}_{R_{s1}}}{c}(D) \\ \sigma_{R_{s1}}(D) \\ \tau_{R_{s1}}(D) \end{bmatrix} + \begin{bmatrix} \delta\left(\frac{\dot{u}_{R_s}}{c}\right) \\ \delta\left(\frac{\dot{w}_{R_s}}{c}\right) \\ \delta\sigma_{R_s} \\ \delta\tau_{R_s} \end{bmatrix} \tag{16}$$

Comparing equations 14 and A14, we see that $S_{01}^{+} = S_{01}^{-} = S_{01}$ and $S_{02}^{\pm} = 2$ and thus, by equation A21,

$$\begin{aligned} \delta\left(\frac{\dot{u}_{R_s}}{c}\right) &= 0 \\ \delta\left(\frac{\dot{w}_{R_s}}{c}\right) &= 2k^2 r_{a_s} S_{01} \\ \delta\sigma_{R_s} &= 0 \\ \delta\tau_{R_s} &= -2k^2 c^2 \rho_s \gamma_s r_{a_s} S_{01} = -4k^2 \mu_s r_{a_s} S_{01} \end{aligned} \tag{17}$$

or

$$\begin{bmatrix} \frac{\dot{u}_{R_{s2}}}{c}(D) \\ \frac{\dot{w}_{R_{s2}}}{c}(D) \\ \sigma_{R_{s2}}(D) \\ \tau_{R_{s2}}(D) \end{bmatrix} = \begin{bmatrix} \frac{\dot{u}_{R_{s1}}}{c}(D) \\ \frac{\dot{w}_{R_{s1}}}{c}(D) \\ \sigma_{R_{s1}}(D) \\ \tau_{R_{s1}}(D) \end{bmatrix} + \begin{bmatrix} 0 \\ \delta\left(\frac{\dot{w}_{R_s}}{c}\right) \\ 0 \\ \delta\tau_{R_s} \end{bmatrix} \tag{18}$$

Combining equations 11 and 12, we have

$$\begin{bmatrix} \frac{\dot{u}_{R_{n-1}}}{c}(z_{n-1}) \\ \frac{\dot{w}_{R_{n-1}}}{c}(z_{n-1}) \\ \sigma_{R_{n-1}}(z_{n-1}) \\ \tau_{R_{n-1}}(z_{n-1}) \end{bmatrix} = A_R^{s2} \begin{bmatrix} \frac{\dot{u}_{R_{s2}}}{c}(D) \\ \frac{\dot{w}_{R_{s2}}}{c}(D) \\ \sigma_{R_{s2}}(D) \\ \tau_{R_{s2}}(D) \end{bmatrix} \tag{19}$$

$$\begin{bmatrix} \frac{\dot{u}_{R_{s1}}}{c}(D) \\ \frac{\dot{w}_{R_{s1}}}{c}(D) \\ \sigma_{R_{s1}}(D) \\ \tau_{R_{s1}}(D) \end{bmatrix} = A_{R_{s1}} \begin{bmatrix} \frac{\dot{u}_{R1}}{c}(0) \\ \frac{\dot{w}_{R1}}{c}(0) \\ \sigma_{R1}(0) \\ \tau_{R1}(0) \end{bmatrix} \tag{20}$$

where $A_R^{s2} = a_{R_{n-1}} \cdots a_{R_{s2}}$ and $A_{R_{s1}} = a_{R_{s1}} \cdots a_1$. At the free surface $z = 0$, we require that the stresses vanish. Thus by equation 9, equation 20 reduces to

$$\begin{bmatrix} \frac{\dot{u}_{R_{s1}}}{c}(D) \\ \frac{\dot{w}_{R_{s1}}}{c}(D) \\ \sigma_{R_{s1}}(D) \\ \tau_{R_{s1}}(D) \end{bmatrix} = A_{R_{s1}} \begin{bmatrix} \frac{\dot{u}_{R_o}}{c} \\ \frac{\dot{w}_{R_o}}{c} \\ 0 \\ 0 \end{bmatrix} \tag{21}$$

where $\frac{\dot{u}_{R_o}}{c} \equiv \frac{\dot{u}_{R_1}}{c}(0)$ and $\frac{\dot{w}_{R_o}}{c} \equiv \frac{\dot{w}_{R_1}}{c}(0)$

We now define W, X, Y and Z by the matrix operation

$$\begin{bmatrix} W \\ X \\ Y \\ Z \end{bmatrix} \equiv A^{-1}_{R_{s1}} \begin{bmatrix} \frac{\dot{u}_{R_{s1}}}{c}(D) \\ \frac{\dot{w}_{R_{s1}}}{c}(D) \\ \sigma_{R_{s1}}(D) \\ \tau_{R_{s1}}(D) \end{bmatrix} \tag{22}$$

Multiplying the vector source equation 18 by $A^{-1}_{R_{s1}}$ and using equations 22 and 21, we have

$$\begin{bmatrix} W \\ X \\ Y \\ Z \end{bmatrix} = \begin{bmatrix} \frac{\dot{u}_{R_o}}{c} \\ \frac{\dot{w}_{R_o}}{c} \\ 0 \\ 0 \end{bmatrix} + A^{-1}_{R_{s1}} \begin{bmatrix} 0 \\ \delta\left(\frac{\dot{w}_{R_s}}{c}\right) \\ 0 \\ \delta\tau_{R_s} \end{bmatrix} \tag{23}$$

or

$$\begin{aligned} \frac{\dot{u}_{R_o}}{c} &= W - \left[\delta\left(\frac{\dot{w}_{R_s}}{c}\right)\left(A^{-1}_{R_{s1}}\right)_{12} + \delta\tau_{R_s}\left(A^{-1}_{R_{s1}}\right)_{14}\right] \\ \frac{\dot{w}_{R_o}}{c} &= X - \left[\delta\left(\frac{\dot{w}_{R_s}}{c}\right)\left(A^{-1}_{R_{s1}}\right)_{22} + \delta\tau_{R_s}\left(A^{-1}_{R_{s1}}\right)_{24}\right] \\ Y &= \left[\delta\left(\frac{\dot{w}_{R_s}}{c}\right)\left(A^{-1}_{R_{s1}}\right)_{32} + \delta\tau_{R_s}\left(A^{-1}_{R_{s1}}\right)_{34}\right] \\ Z &= \left[\delta\left(\frac{\dot{w}_{R_s}}{c}\right)\left(A^{-1}_{R_{s1}}\right)_{42} + \delta\tau_{R_s}\left(A^{-1}_{R_{s1}}\right)_{44}\right] \end{aligned} \tag{24}$$

From Appendix D the inverse of $A_{R_{s1}}$ is given by

$$A^{-1}_{R_{s1}} = \begin{bmatrix} \left(A_{R_{s1}}\right)_{44} & -\left(A_{R_{s1}}\right)_{34} & \left(A_{R_{s1}}\right)_{24} & -\left(A_{R_{s1}}\right)_{14} \\ -\left(A_{R_{s1}}\right)_{43} & \left(A_{R_{s1}}\right)_{33} & -\left(A_{R_{21}}\right)_{23} & \left(A_{R_{s1}}\right)_{13} \\ \left(A_{R_{s1}}\right)_{42} & -\left(A_{R_{s1}}\right)_{32} & \left(A_{R_{s1}}\right)_{22} & -\left(A_{R_{s1}}\right)_{12} \\ -\left(A_{R_{s1}}\right)_{41} & \left(A_{R_{s1}}\right)_{31} & -\left(A_{R_{s1}}\right)_{21} & \left(A_{R_{s1}}\right)_{11} \end{bmatrix} \tag{25}$$

Replacing the $\left(A^{-1}_{R_{s1}}\right)$ elements in equation 24 by their $A_{R_{s1}}$ equivalents, yields

$$\begin{aligned} \frac{\dot{u}_{R_o}}{c} &= W + \left[\delta\left(\frac{\dot{w}_{R_s}}{c}\right)\left(A_{R_{s1}}\right)_{34} + \delta\tau_{R_s}\left(A_{R_{s1}}\right)_{14}\right] \\ \frac{\dot{w}_{R_o}}{c} &= X - \left[\delta\left(\frac{\dot{w}_{R_s}}{c}\right)\left(A_{R_{s1}}\right)_{33} + \delta\tau_{R_s}\left(A_{R_{s1}}\right)_{13}\right] \\ Y &= -\left[\delta\left(\frac{\dot{w}_{R_s}}{c}\right)\left(A_{R_{s1}}\right)_{32} + \delta\tau_{R_s}\left(A_{R_{s1}}\right)_{12}\right] \\ Z &= \left[\delta\left(\frac{\dot{w}_{R_s}}{c}\right)\left(A_{R_{s1}}\right)_{31} + \delta\tau_{R_s}\left(A_{R_{s1}}\right)_{11}\right] \end{aligned} \tag{26}$$

From equation D7, we have for the halfspace or layer n

$$\begin{bmatrix} \underline{\Delta}'_n + \underline{\Delta}''_n \\ \underline{\Delta}'_n - \underline{\Delta}''_n \\ \underline{\omega}'_n - \underline{\omega}'_n \\ \underline{\omega}'_n + \underline{\omega}''_n \end{bmatrix} = E^{-1}_{R_n} \begin{bmatrix} \frac{\dot{u}_{R_n}(z_{n-1})}{c} \\ \frac{\dot{w}_{R_n}(z_{n-1})}{c} \\ \sigma_{R_n}(z_{n-1}) \\ \tau_{R_n}(z_{n-1}) \end{bmatrix} \tag{27}$$

As a boundary condition for the halfspace, we require that the coefficients $\underline{\Delta}''_n$ and $\underline{\omega}''_n$ vanish. For c greater than either of the halfspace body velocities, this is equivalent to requiring that there be no radiation from infinity into the wave guide due to equation A5 and the sign criteria of r_{α_n} and r_{β_n}. Similarly, for c less than either of the body velocities, this is equivalent to requiring that displacements and stress remain finite as the depth becomes infinite. With this boundary condition, equation 27 reduces to

$$\begin{bmatrix} \underline{\Delta}'_n \\ \underline{\Delta}'_n \\ \underline{\omega}'_n \\ \underline{\omega}'_n \end{bmatrix} = E^{-1}_{R_n} \begin{bmatrix} \frac{\dot{u}_{R_n}(z_{n-1})}{c} \\ \frac{\dot{w}_{R_n}(z_{n-1})}{c} \\ \sigma_{R_n}(z_{n-1}) \\ \tau_{R_n}(z_{n-1}) \end{bmatrix} \tag{28}$$

Defining the matrix A_R by the matrix product

$$A_R = A_R^{s2} A_{R_{s1}} = a_{R_{n-1}} \cdots a_{R_{s2}} a_{R_{s1}} \cdots a_{R_1} = a_{R_{n-1}} \cdots a_{R_s} \cdots a_{R_1}$$

since it can be shown that $a_{R_s} = a_{R_{s2}} a_{R_{s1}}$, and in turn defining J by

$$J = E_{R_n}^{-1} A_R \tag{29}$$

we obtain from equations 28, 19, and 22

$$\begin{bmatrix} \underline{\Delta}'_n \\ \underline{\Delta}'_n \\ \underline{\omega}'_n \\ \underline{\omega}'_n \end{bmatrix} = J \begin{bmatrix} W \\ X \\ Y \\ Z \end{bmatrix} \tag{30}$$

Eliminating $\underline{\Delta}'_n$ from the linear equations given by equation 30 yields

$$0 = (J_{11} - J_{21})W + (J_{12} - J_{22})X + (J_{12} - J_{23})Y + (J_{14} - J_{24})Z \tag{31}$$

Similarly eliminating $\underline{\omega}'_n$ yields

$$0 = (J_{31} - J_{41})W + (J_{32} - J_{42})X + (J_{33} - J_{43})Y + (J_{34} - J_{44})Z \tag{32}$$

Combining equations 31 and 32 to eliminate W we obtain

$$X = - \frac{[GN - LH]Y + [RN - SL]Z}{[NK - LM]} \tag{33}$$

where

$$\frac{G}{L} = \frac{J_{13} - J_{23}}{J_{11} - J_{21}}, \qquad \frac{H}{N} = \frac{J_{33} - J_{43}}{J_{31} - J_{41}}, \qquad \frac{R}{L} = \frac{J_{14} - J_{24}}{J_{11} - J_{21}}$$

$$\frac{S}{N} = \frac{J_{34} - J_{44}}{J_{31} - J_{41}}, \qquad \frac{K}{L} = \frac{J_{12} - J_{22}}{J_{11} - J_{21}} \quad \text{and} \quad \frac{M}{N} = \frac{J_{32} - J_{42}}{J_{31} - J_{41}} \tag{34}$$

Using the definition of J and the elements of $E_{R_n}^{-1}$ given in equation A12, we can write the following

$$
\begin{aligned}
L &= \gamma_n r_{\alpha_n} (A_R)_{11} + (\gamma_n - 1)(A_R)_{21} - \frac{r_{\alpha_n}}{\rho_n c^2}(A_R)_{31} + \frac{(A_R)_{41}}{\rho_n c^2} \\
K &= \gamma_n r_{\alpha_n} (A_R)_{12} + (\gamma_n - 1)(A_R)_{22} - \frac{r_{\alpha_n}}{\rho_n c^2}(A_R)_{32} + \frac{(A_R)_{42}}{\rho_n c^2} \\
G &= \gamma_n r_{\alpha_n} (A_R)_{13} + (\gamma_n - 1)(A_R)_{23} - \frac{r_{\alpha_n}}{\rho_n c^2}(A_R)_{33} + \frac{(A_R)_{43}}{\rho_n c^2} \\
R &= \gamma_n r_{\alpha_n} (A_R)_{14} + (\gamma_n - 1)(A_R)_{24} - \frac{r_{\alpha_n}}{\rho_n c^2}(A_R)_{34} + \frac{(A_R)_{44}}{\rho_n c^2} \\
N &= -(\gamma_n - 1)(A_R)_{11} + \gamma_n r_{\beta_n} (A_R)_{21} + \frac{(A_R)_{31}}{\rho_n c^2} + \frac{r_{\beta_n}}{\rho_n c^2}(A_R)_{41} \\
M &= -(\gamma_n - 1)(A_R)_{12} + \gamma_n r_{\beta_n} (A_R)_{22} + \frac{(A_R)_{32}}{\rho_n c^2} + \frac{r_{\beta_n}}{\rho_n c^2}(A_R)_{42} \\
H &= -(\gamma_n - 1)(A_R)_{13} + \gamma_n r_{\beta_n} (A_R)_{23} + \frac{(A_R)_{33}}{\rho_n c^2} + \frac{r_{\beta_n}}{\rho_n c^2}(A_R)_{43} \\
S &= -(\gamma_n - 1)(A_R)_{14} + \gamma_n r_{\beta_n} (A_R)_{24} + \frac{(A_R)_{34}}{\rho_n c^2} + \frac{r_{\beta_n}}{\rho_n c^2}(A_R)_{44}
\end{aligned}
\tag{35}
$$

Similarly

$$
W = \frac{\left[GN\left(\frac{M}{N}\right) - LH\left(\frac{K}{L}\right)\right] Y + \left[RN\left(\frac{M}{N}\right) - SL\left(\frac{K}{L}\right)\right] Z}{[NK - LM]} \tag{36}
$$

Using equations 33 and 36, we have from equation 26

$$\frac{\dot{w}_{R_o}}{c} = - \frac{N_R^{(1)} N_R^{(2)}}{F_R} \tag{37}$$

and

$$\frac{\dot{u}_{R_o}}{c} = \frac{N_R^{(3)} N_R^{(4)}}{F_R} \tag{38}$$

where

$$F_R \equiv [NK - LM]$$

$$N_R^{(1)} \equiv [GN - LH] \left\{ Y + \frac{[RN - SL]}{[GN - LH]} Z \right\}$$

$$N_R^{(2)} \equiv 1 + \frac{F_R}{N_R^{(1)}} \left[\delta \left(\frac{\dot{w}_{R_s}}{c} \right) \left(A_{R_s} \right)_{33} + \delta\tau_{R_s} \left(A_{R_s} \right)_{13} \right] \tag{39}$$

$$N_R^{(3)} \equiv [GN(\tfrac{M}{N}) - LH(\tfrac{K}{L})] \left\{ Y + \frac{[RN(\tfrac{M}{N}) - SL(\tfrac{K}{L})]}{[GN(\tfrac{M}{N}) - LH(\tfrac{K}{L})]} Z \right\}$$

$$N_R^{(4)} \equiv 1 + \frac{F_R}{N_R^{(3)}} \left[\delta \left(\frac{\dot{w}_{R_s}}{c} \right) \left(A_{R_s} \right)_{34} + \delta\tau_{R_s} \left(A_{R_s} \right)_{14} \right]$$

It is convenient at this point to examine equations 39 when F_R is equal to zero. In Appendix E, it was shown that when $F_R = 0$ the following is true

$$\frac{RN - SL}{GN - HL} = \frac{K}{L} \tag{40}$$

In addition, from the definition of F_R in equation 39, we have

$$\frac{M}{N} = \frac{K}{L} \tag{41}$$

and thus for the case of $F_R = 0$, equations 39 reduce to

$$N_R^{(1)} = [GN - LH)\{Y + \frac{K}{L} Z\}$$

$$N_R^{(2)} = 1 \tag{42}$$

$$N_R^{(3)} = \frac{K}{L} N_R^{(1)}$$

and

$$N_R^{(4)} = 1$$

Thus by equations 7, 9, 37, and 38, the displacements at the free surface are given by

$$\overline{w}_o = i \int_0^\infty \frac{1}{k} \frac{N_R^{(1)} N_R^{(2)}}{F_R} J_o(kr)\, dk \tag{43}$$

and

$$\overline{q}_o = - \int_0^\infty \frac{1}{k} \frac{N_R^{(3)} N_R^{(4)}}{F_R} J_o(kr)\, dk \tag{44}$$

Evaluating equations 43 and 44 for the residue contribution, we obtain for each j^{th} mode or root, ω fixed, at $F_R(\omega, k_{R_j}) = 0$

$$\{\overline{w}_o\}_{R_j} = \frac{\pi}{k_{R_j}} \frac{N_{R_j}^{(1)} N_{R_j}^{(2)}}{\left(\frac{\partial F_R}{\partial k}\right)_{\omega, j}} H_o^{(2)}(k_{R_j} r)$$

$$\{\overline{q}_o\}_{R_j} = i \frac{\pi}{k_{R_j}} \frac{N_{R_j}^{(3)} N_{R_j}^{(4)}}{\left(\frac{\partial F_R}{\partial k}\right)_{\omega, j}} H_1^{(2)}(k_{R_j} r) \tag{45}$$

or by equation 42

$$\{\overline{w}_o\}_{R_j} = \frac{\pi}{k_{R_j}} \frac{N^{(1)}_{R_j}}{\left(\frac{\partial F_R}{\partial k}\right)_{\omega, j}} H_o^{(2)}(k_{R_j} r)$$

$$\{\overline{q}_o\}_{R_j} = i \frac{K}{L} \frac{\pi}{k_{R_j}} \frac{N^{(1)}_{R_j}}{\left(\frac{\partial F_R}{\partial k}\right)_{\omega, j}} H_1^{(2)}(k_{R_j} r) \qquad (46)$$

where $\left(\frac{\partial F_R}{\partial k}\right)_{\omega, j}$, $N^{(1)}_{R_j}$, $N^{(2)}_{R_j}$, $N^{(3)}_{R_j}$ and $N^{(4)}_{R_j}$ are evaluated at (ω, k_{R_j}) such that $F_R(\omega, k_{R_j}) = 0$.

$F_R(\omega, k_{R_j}) = 0$ is a form of the period equation for Rayleigh wave propagation in plane multilayered isotropic solids (Haskell, 1953; Dorman, M. Ewing, and Oliver, 1960; Press, Harkrider and Seafeldt, 1961; Dorman, 1962; Harkrider and Anderson, 1962). For all real (ω, k) or (c, k) the elements in the a_{R_m} matrix are either always real or always imaginary according to the following criteria (Haskell, 1953).

$$\text{Real } (a_{R_m})_{jk} \qquad \text{if } j + k \text{ even integer}$$

$$\text{Imaginary } (a_{R_m})_{jk} \text{ if } j + k \text{ odd integer}$$

The same is true also for the product matrix A_R. For a phase velocity less than or equal to the halfspace shear velocity β_n, we see that the quantities defined in equation 35 are also real or imaginary for all real k. We now express the imaginary quantities as a real quantity (designated by an asterisk superscript) multiplied by i or

$$L = iL^*, \quad G = iG^*, \quad M = iM^* \quad \text{and} \quad S = iS^*$$

and thus

$$F_R(\omega, k) \equiv NK + L^* M^*$$

which is real for all real k and $c \leq \beta_n$.

Taking the ratio of $\{\overline{q}_o\}_{R_j}$ to $\{\overline{w}_o\}_{R_j}$, we obtain from equation 46

$$\frac{\{\overline{q}_o\}_{R_j}}{\{\overline{w}_o\}_{R_j}} = i \frac{K}{L} \frac{H_1^{(2)}(k_{R_j} r)}{H_o^{(2)}(k_{R_j} r)}$$

or

$$\frac{\{\overline{q}_o\}_{R_j}}{\{\overline{w}_o\}_{R_j}} \rightarrow - \frac{K}{L} = i \frac{K}{L^*} \quad \text{as} \quad k_{R_j} r \rightarrow \infty$$

Thus at horizontal ranges large compared to the wavelength, the surface displacements are either prograde elliptical or retrograde elliptical dependent on whetehr the real ratio $(\frac{K}{L^*})$ is positive or negative respectively. This large distance result is the same as obtained by Haskell (1953) for the homogeneous case of plane two-dimensional Rayleigh waves:

$$\left[\frac{\dot{u}_o}{\dot{w}_o} \right]_H = - \frac{K}{L}$$

Rewriting equation 46 in Haskell's notation

$$\{\overline{q}_o\}_{R_j} = - i \left[\frac{u_o}{\dot{w}_o} \right]_H \{\overline{w}_o\}_{R_j} \; H_1^{(2)}(k_{R_j} r) \Big/ H_o^{(2)}(k_{R_j} r)$$

Evaluating the residue contributions of the integral representations for $\overline{q}_{s1}(D)$, $\overline{P}_{zz_{s1}}(D)$, $\overline{P}_{rz_{s1}}(D)$, $\overline{q}_{s2}(D)$, $\overline{w}_{s2}(D)$, $\overline{P}_{zz_{s2}}(D)$

and $\overline{P}_{rz_{s2}}(D)$ by using equations 21 and 18 we find that

$$\{\overline{q}_{s1}(D)\}_{R_j} = -i\left\{\left(A_{R_{s1}}\right)_{12} + \left[\frac{\dot{u}_o}{\dot{w}_o}\right]_{H_j}\left(A_{R_{s1}}\right)_{11}\right\}\{\overline{w}_o\}_{R_j} H_1^{(2)}(k_{R_j} r)/H_o^{(2)}(k_{R_j} r)$$

$$\equiv -i\left[\frac{\dot{u}_{s1}(D)}{\dot{w}_o}\right]_{H_j}\{\overline{w}_o\}_{R_j} H_1^{(2)}(k_{R_j} r)/H_o^{(2)}(k_{R_j} r)$$

$$\{\overline{w}_{s1}(D)\}_{R_j} = \left\{\left(A_{R_{s1}}\right)_{22} + \left[\frac{\dot{u}_o}{\dot{w}_o}\right]_{H_j}\left(A_{R_{s1}}\right)_{21}\right\}\{\overline{w}_o\}_{R_j}$$

$$\equiv \left[\frac{\dot{w}_{s1}(D)}{\dot{w}_o}\right]_{H_j}\{\overline{w}_o\}_{R_j} \qquad (47)$$

$$\{\overline{P}_{zz_{s1}}(D)\}_{R_j} = ik_{R_j}\left(A_{R_{s1}}\right)_{32} + \left[\frac{\dot{u}_o}{\dot{w}_o}\right]_{H_j}\left(A_{R_{s1}}\right)_{31}\{\overline{w}_o\}_{R_j}$$

$$\equiv ik_{R_j}\left[\frac{\sigma_{s1}(D)}{\frac{\dot{w}_o}{c}}\right]_{H_j}\{\overline{w}_o\}_{R_j}$$

$$\{\overline{P}_{rz_{s1}}(D)\}_{R_j} = k_{R_j}\left\{\left(A_{R_{s1}}\right)_{42} + \left[\frac{\dot{u}_o}{\dot{w}_o}\right]_{H}\left(A_{R_{s1}}\right)_{41}\right\}\{\overline{w}_o\}_{R_j} H_1^{(2)}(k_{R_j} r)/H_o^{(2)}(k_{R_j} r)$$

$$\equiv k_{R_j}\left[\frac{\tau_{s1}(D)}{\frac{\dot{w}_o}{c}}\right]_{H_j}\{\overline{w}_o\}_{R_j} H_1^{(2)}(k_{R_j} r)/H_o^{(2)}(k_{R_j} r)$$

and

$$\{\overline{q}_{s2}(D)\}_{R_j} = \{\overline{q}_{s1}(D)\}_{R_j}$$

$$\{\overline{w}_{s2}(D)\}_{R_j} = \{\overline{w}_{s1}(D)\}_{R_j} \qquad (48)$$

$$\{\overline{P}_{zz_{s2}}(D)\}_{R_j} = \{\overline{P}_{zz_{s1}}(D)\}_{R_j}$$

$$\{\overline{P}_{rz_{s2}}(D)\}_{R_j} = \{\overline{P}_{rz_{s1}}(D)\}_{R_j}$$

From the set of equations 48, we see that there is no discontinuity in displacement or stress across the source plane $z = D$, for the residue contributions. Thus from equation 47 we obtain

$$\begin{aligned}
\{\overline{q}_m(z)\} &= -i\left[\frac{\dot{u}_m(z)}{\dot{w}_o}\right]_{H_j}\{\overline{w}_o\}_{R_j} H_1^{(2)}(k_{R_j}r)\Big/H_o^{(2)}(k_{R_j}r) \\
\{\overline{w}_m(z)\} &= \left[\frac{\dot{w}_m(z)}{\dot{w}_o}\right]_{H_j}\{\overline{w}_o\}_{R_j} \\
\{\overline{P}_{zz_m}(z)\} &= ik_{R_j}\left[\frac{\sigma_m(z)}{\frac{\dot{w}_o}{c}}\right]_{H_j}\{\overline{w}_o\}_{R_j} \\
\{\overline{P}_{rz_m}(z)\} &= k_{R_j}\left[\frac{\tau_m(z)}{\frac{\dot{w}_o}{c}}\right]_{H_j}\{\overline{w}_o\}_{R_j} H_1^{(2)}(k_{R_j}r)\Big/H_o^{(2)}(k_{R_j}r)
\end{aligned} \tag{49}$$

where the homogeneous ratios (H subscripts) are given for all m in terms of

$$A_{R_m}(z) = a_{R_m}(z)a_{R_{m-1}}\cdots a_{R_1}$$

and where $a_{R_m}(z)$ is the layer matrix for a sublayer in m of thickness $d_m(z) = z - z_{m-1}$.

From equation 26 and the definitions of the homogeneous ratios implied in equations 47 and 49, we have

$$[\,Y + \frac{K}{L} Z] = - \left\{ \delta \left(\frac{\dot{w}_{R_s}}{c} \right) \left[\frac{\sigma_s(D)}{\frac{\dot{w}_o}{c}} \right]_{H_j} + \delta \tau_{R_s} \left[\frac{\dot{u}_s(D)}{\dot{w}_o} \right]_{H_j} \right\} \qquad (50)$$

Inserting real quantities (asterisked) and using equations 4, 18 and 42, yields

$$\frac{N^{(1)}_{R_j}}{\left(\frac{\partial F_R}{\partial k}\right)_{\omega, j}} = ik_{R_j} a_s^3 \bar{p}_{os} \frac{\left\{ \frac{1}{2\mu_s} \left[\frac{\sigma^*_s(D)}{\frac{\dot{w}_o}{c}} \right]_{H_j} - \left[\frac{\dot{u}_s(D)}{\dot{w}_o} \right]_{H_j} \right\}}{\left[\left(1 - \frac{a_s^2 k_{\beta_s}^2}{4} \right)^2 + k_{\alpha_s}^2 a_s^2 \right]^{\frac{1}{2}}} \mathcal{A}_{R_j}(\omega) e^{i(k_{\alpha_s} a_s - \theta_{SP})}$$

where

$$\mathcal{A}_{R_j}(\omega) = \frac{[\,G^* N - L^* H]}{\left(\frac{\partial F_R}{\partial k}\right)_{\omega, j}}$$

Therefore the Fourier time transformed Rayleigh wave surface displacements for an explosive spherical source at depth D are

$$\{\bar{w}_o\}_{R_j} = i\, k_{R_j} \bar{p}_{os} a_s^3 \frac{\left\{ \frac{1}{2\mu_s} \left[\frac{\sigma^*_s(D)}{\frac{\dot{w}_o}{c}} \right]_{H_j} - \left[\frac{\dot{u}^*_s(D)}{\dot{w}_o} \right]_{H_j} \right\}}{\left[\left(1 - \frac{a_s^2 k_{\beta_s}^2}{4} \right)^2 + k_{\alpha_s}^2 a_s^2 \right]^{\frac{1}{2}}} \mathcal{A}_{R_j} e^{i(k_{\alpha_s} a_s - \theta_{SP})}$$

$$\times H_o^{(2)}(k_{R_j} r)$$

$$\{\bar{q}_o\}_{R_j} = \left[\frac{\dot{u}_o^*}{\dot{w}_o}\right]_{H_j} i\pi k_{R_j} \bar{p}_{os} a_s^3 \frac{\left\{\frac{1}{2\mu_s}\left[\frac{\sigma_s^*(D)}{\frac{\dot{w}_o}{c}}\right]_{H_j} - \left[\frac{u_s^*(D)}{\dot{w}_o}\right]_{H_j}\right\}}{\left[\left(1 - \frac{a_s^2 k^2 \beta_s}{4}\right)^2 + k_{\alpha_s}^2 a_s^2\right]^{\frac{1}{2}}}$$

$$\times A_{R_j} e^{i(k_{\alpha_s} a_2 - \theta_{SP})} H_1^{(2)}(k_{R_j} r)$$

Before proceeding to the next section, it should be noted that by means of equations 9, the part of our solution dependent on source depth D can be written as

$$\left\{\frac{1}{2\mu_s}\left[\frac{\sigma_s^*(D)}{\frac{\dot{w}_o}{c}}\right]_{H_j} - \left[\frac{u_s^*(D)}{\dot{w}_o}\right]_{H_j}\right\} = -\frac{k^2}{\gamma_s}\left[\frac{\varphi_s(D)}{\frac{\dot{w}_o}{c}}\right]_{H_j}$$

Rayleigh Waves From a Vertical Point Force at Depth

Consider the same elastic medium as before but with a vertical point force in layer s at (0, 0. The Fourier time transformed vertical point force $\bar{L}(\omega)$, positive in the downward or positive z direction is defined (Pekeris, 1955) in terms of the transformed normal stress to z = D plane as

$$2\pi \int_0^\infty [\bar{P}_{zz_s}(r, D^+) - \bar{P}_{zz_s}(r, D^-)]\, r\, dr = -\bar{L} \qquad (53)$$

or

$$[\bar{P}_{zz_s}(r, D^+) - \bar{P}_{zz_s}(r, D^-)] = -\frac{\bar{L}}{2\pi} \int_0^\infty J_o(kr) k\, dk$$

with continuous $\overline{q}_s$, $\overline{w}_s$ and $\overline{P}_{rz_s}$ for all r along z = D.

Since this source is aximuthally symmetric about the z axis and the boundary conditions are at the z constant plane interfaces this problem reduces, as before, to cylindrical symmetry. All the definitions and relations used in the previous section apply here up to equations 17. Comparing equation 53 with equation 5, we obtain

$$\begin{aligned} &\delta\left(\frac{\dot{u}_{R_s}}{c}\right) = 0 \\ &\delta\left(\frac{\dot{w}_{R_s}}{c}\right) = 0 \\ &\delta\sigma_{R_s} = -\frac{\overline{Lk}}{2\pi} \\ &\delta\tau_{R_s} = 0 \end{aligned} \tag{54}$$

Thus the vector equation in the source layer s for the vertical point force is

$$\begin{bmatrix} \frac{\dot{u}_{R_{s2}}(D)}{c} \\ \frac{\dot{w}_{R_{s2}}(D)}{c} \\ \sigma_{R_{s2}}(D) \\ \tau_{R_{s2}}(D) \end{bmatrix} = \begin{bmatrix} \frac{\dot{u}_{R_{s1}}(D)}{c} \\ \frac{\dot{w}_{R_{s1}}(D)}{c} \\ \sigma_{R_{s1}}(D) \\ \tau_{R_{s1}}(D) \end{bmatrix} + \begin{bmatrix} 0 \\ 0 \\ \delta\sigma_{R_s} \\ 0 \end{bmatrix} \tag{55}$$

Following the same procedure of the first section we obtain

$$\frac{\dot{u}_{R_o}}{c} = W - \delta\sigma_{R_s}\left(A^{-1}_{R_{s1}}\right)_{13}$$

$$\frac{\dot{w}_{R_o}}{c} = X - \delta\sigma_{R_s}\left(A^{-1}_{R_{s1}}\right)_{23}$$

$$Y = \delta\sigma_{R_s}\left(A^{-1}_{R_{s1}}\right)_{33} \qquad (56)$$

$$Z = \delta\sigma_{R_s}\left(A^{-1}_{R_{s1}}\right)_{43}$$

and by equation 25, the inverse of $A_{R_{s1}}$,

$$\frac{\dot{u}_{R_o}}{c} = W - \delta\sigma_{R_s}\left(A_{R_{s1}}\right)_{24}$$

$$\frac{\dot{w}_{R_o}}{c} = X - \delta\sigma_{R_s}\left(A_{R_{s1}}\right)_{23}$$

$$Y = \delta\sigma_{R_s}\left(A_{R_{s1}}\right)_{22} \qquad (57)$$

$$Z = -\delta\sigma_{R_s}\left(A_{R_{s1}}\right)_{21}$$

Using equations 27 through 38 yields

$$\frac{\dot{w}_{R_o}}{c} = -\frac{N_R^{(1)} N_R^{(2)}}{F_R} \qquad (58)$$

and

$$\frac{\dot{u}_{R_o}}{c} = \frac{N_R^{(3)} N_R^{(4)}}{F_R} \qquad (59)$$

where from equations 57

$$N_R^{(2)} = 1 - \frac{F_R}{N_R^{(1)}} \delta\sigma_{R_s} \left(A_{R_{s1}}\right)_{23}$$

$$N_R^{(4)} = 1 - \frac{F_R}{N_R^{(3)}} \delta\sigma_{R_s} \left(A_{R_{s1}}\right)_{24} \tag{60}$$

As before the displacements at the free surface are

$$\overline{w}_o = i \int_0^\infty \frac{1}{k} \frac{N_R^{(1)} N_R^{(2)}}{F_R} J_o(kr)\, dk \tag{61}$$

and

$$\overline{q}_o = - \int_0^\infty \frac{1}{k} \frac{N_R^{(3)} N_R^{(4)}}{F_R} J_1(kr)\, dk \tag{62}$$

The residue contribution of equations 61 and 62 are thus

$$\{\overline{w}_o\}_{R_j} = \frac{\pi}{k_{R_j}} \frac{N_{R_j}^{(1)}}{\left(\frac{\partial F_R}{\partial k}\right)_{\omega, j}} H_o^{(2)}(k_{R_j} r)$$

$$\{\overline{q}_o\}_{R_j} = i \frac{K}{L} \frac{\pi}{k_{R_j}} \frac{N_{R_j}^{(1)}}{\left(\frac{\partial F_R}{\partial k}\right)_{\omega, j}} H_1^{(2)}(k_{R_j} r) \tag{63}$$

where $N_{R_j}^{(1)}$ is, as before,

$$N_{R_j}^{(1)} = [\, GN - LH] \left\{ Y + \frac{K}{L} Z \right\}$$

but now from equation 57

$$N_{R_j}^{(1)} = [\, GN - LH]\, \delta\sigma_{R_s} \left\{ \left(A_{R_{s1}}\right)_{22} - \frac{K}{L} \left(A_{R_{s1}}\right)_{21} \right\} \tag{64}$$

All the relations concerning F_R and the displacements and stresses at depth in terms of the homogeneous solutions shown for the

explosive source are also true for the vertical point force. With these relations $N^{(1)}_{R_j}$ can be rewritten as

$$N^{(1)}_{R_j} = - \frac{\overline{L} k_{R_j}}{2\pi} [GN - LH] \left[\frac{\dot{w}_s}{\dot{w}_o} (D) \right]_{H_j} \tag{65}$$

Therefore the Fourier time transformed Rayleigh wave displacements for a vertical point force at depth D are

$$\begin{aligned} \{\overline{w}_o\}_{R_j} &= - i \frac{\overline{L}}{2} \left[\frac{\dot{w}_s}{\dot{w}_o} (D) \right]_{H_j} A_{R_j} H_o^{(2)}(k_{R_j} r) \\ \{\overline{q}_o\}_{R_j} &= - i \frac{\overline{L}}{2} \left[\frac{\dot{u}_o^*}{\dot{w}_o} \right]_{H_j} \left[\frac{\dot{w}_s}{\dot{w}_o} \right]_{H_j} A_{R_j} H_1^{(2)}(k_{R_j} r) \end{aligned} \tag{66}$$

where, as in equation 51,

$$A_{R_j} = \frac{[G^* N - L^* H]}{\left(\frac{\partial F_R}{\partial k} \right)_{\omega, j}}$$

Rayleigh and Love Waves From a Horizontal Point Force at Depth

We now consider a Fourier time transformed horizontal point force in layer s at depth D directed in the $\theta = 0$ direction. As our source displacement field, we use the displacements due to a horizontal point force of strength $\overline{L}(\omega)$ in an elastic space with the same elastic properties as layer s. The displacements as derived in Appendix B are

$$\bar{q}_{so}(r,\theta,z) = \frac{\bar{L}}{4\pi\omega^2\rho_s}\cos\theta\left[\frac{\partial}{\partial r^2}\left(\frac{e^{-ik_{\beta_s}R} - e^{-ik_{\alpha_s}R}}{R}\right) + k_{\beta_s}^2\frac{e^{-ik_{\beta_s}R}}{R}\right]$$

$$\bar{v}_{so}(r,\theta,z) = \frac{\bar{L}}{4\pi\omega^2\rho_s}\sin\theta\left[\frac{1}{r}\frac{\partial}{\partial r}\left(\frac{e^{-ik_{\beta_s}R} - e^{-ik_{\alpha_s}R}}{R}\right) + k_{\beta_s}^2 e^{-ik_{\beta_s}R}\right] \quad (67)$$

$$\bar{w}_{so}(r,\theta,z) = \frac{\bar{L}}{4\pi\omega^2\rho_s}\cos\theta\frac{\partial^2}{\partial z\partial r}\left(\frac{e^{-ik_{\beta_s}R} - e^{-ik_{\alpha_s}R}}{R}\right)$$

where

$$R^2 = r^2 + (z - D)^2$$

Rewriting as an integral representation, yields

$$\bar{q}_{so}(r,\theta,z) = -i\frac{\bar{L}}{4\pi\omega^2\rho_s}\cos\theta\int_0^\infty\left[k^2\left(\frac{e^{-ikr_{\alpha_s}|z-D|}}{r_{\alpha_s}} + r_{\beta_s}e^{-ikr_{\beta_s}|z-D|}\right)\frac{dJ_1(kr)}{dkr} + k_{\beta_s}^2 e^{ikr_{\beta_s}|z-D|}\frac{J_1(kr)}{kr}\right]dk$$

$$\bar{v}_{so}(r,\theta,z) = i\frac{\bar{L}}{4\pi\omega^2\rho_s}\sin\theta\int_0^\infty\left[k^2\left(\frac{e^{-ikr_{\alpha_s}|z-D|}}{r_{\alpha_s}} + r_{\beta_s}e^{-ikr_{\beta_s}|z-D|}\right)\frac{J_1(kr)}{kr} + k_{\beta_s}^2 e^{-ikr_{\alpha_s}|z-D|}\frac{dJ_1(kr)}{dkr}\right]dk \quad (68)$$

$$\bar{w}_{so}(r,\theta,z) = \frac{\bar{L}}{4\pi\omega^2\rho_s}\cos\theta\frac{|z-D|}{z-D}\int_0^\infty\left[k^2\left(e^{-ikr_{\beta_s}|z-D|} - e^{-ikr_{\alpha_s}|z-D|}\right)J_1(kr)\right]dk$$

In our cylindrical coordinate system, the problem no longer exhibits azimuthal symmetry. We now have a θ dependence caused by the directed horizontal point force. In order to include the aximuthal dependence, we add to the cylindrical set of potentials $(\overline{\varphi}, \overline{\psi})$ a new potential $\overline{\chi}$ such that

$$\begin{aligned}
\overline{q}_m(r,\theta,z) &= \frac{\partial \overline{\varphi}_m}{\partial r} + \frac{\partial^2 \overline{\psi}_m}{\partial r \partial z} + \frac{1}{r}\frac{\partial \overline{\chi}_m}{\partial \theta} \\
\overline{v}_m(r,\theta,z) &= \frac{1}{r}\frac{\partial \overline{\varphi}_m}{\partial \theta} + \frac{1}{r}\frac{\partial^2 \overline{\psi}_m}{\partial z \partial \theta} - \frac{\partial \overline{\chi}_m}{\partial r} \\
\overline{w}_m(r,\theta,z) &= \frac{\partial \overline{\varphi}_m}{\partial z} - \frac{1}{r}\frac{\partial}{\partial r}\left(r\frac{\partial \overline{\psi}_m}{\partial r}\right) + \frac{1}{r^2}\frac{\partial^2 \overline{\psi}_m}{\partial \theta^2}
\end{aligned} \tag{69}$$

By substition of equations 69 into the transformed vector equation of motion

$$(\lambda_m + 2\mu_m)\,\text{grad div}\,\hat{\overline{S}}_m - \mu_m \text{curl}\,(\text{curl}\,\hat{\overline{S}}_m) = -\omega^2 \rho_m \hat{\overline{S}}_m \tag{70}$$

where

$$\hat{\overline{S}}_m = (\overline{q}_m, \overline{v}_m, \overline{w}_m)$$

we see that

$$\text{div}\,\hat{\overline{S}}_m = \nabla^2 \overline{\varphi}_m$$

and that equation 70 is satisfied if $\overline{\varphi}_m$, $\overline{\psi}_m$ and $\overline{\chi}_m$ are the solutions of

$$\begin{aligned}
\nabla^2 \overline{\varphi}_m &\equiv \frac{1}{r}\frac{\partial}{\partial r}\left(r\frac{\partial \overline{\varphi}_m}{\partial r}\right) + \frac{1}{r^2}\frac{\partial^2 \overline{\varphi}_m}{\partial \theta^2} + \frac{\partial^2 \overline{\varphi}_m}{\partial z^2} = -k_{\alpha_m}^2 \overline{\varphi}_m \\
\nabla^2 \overline{\psi}_m &= -k_{\beta_m}^2 \overline{\psi}_m \\
\nabla^2 \overline{\chi}_m &= -k_{\beta_m}^2 \overline{\chi}_m
\end{aligned} \tag{71}$$

With equations 69 and 71, the definitions of stress yields

$$\overline{q}_m(r,\theta,z) = \frac{\partial\overline{\varphi}_m}{\partial r} + \frac{\partial^2\overline{\psi}_m}{\partial r\partial z} + \frac{1}{r}\frac{\partial\overline{\chi}_m}{\partial\theta}$$

$$\overline{v}_m(r,\theta,z) = \frac{1}{r}\frac{\partial\overline{\varphi}_m}{\partial\theta} + \frac{1}{r}\frac{\partial^2\overline{\psi}_m}{\partial z\partial\theta} - \frac{\partial\overline{\chi}_m}{\partial r}$$

$$\overline{w}_m(r,\theta,z) = \frac{\partial\overline{\varphi}_m}{\partial z} + \frac{\partial^2\overline{\psi}_m}{\partial z^2} + k_{\beta_m}^2\overline{\psi}_m$$

$$\overline{P}_{zz_m}(r,\theta,z) = 2\mu_m\frac{\partial\overline{w}_m}{\partial z} + \lambda_m \operatorname{div}\hat{S}_m \qquad (72)$$

$$= 2\mu_m\left[\frac{\partial^2\overline{\varphi}_m}{\partial z^2} + \frac{\partial^3\overline{\psi}_m}{\partial z^3} + k_{\beta_m}^2\frac{\partial\overline{\psi}_m}{\partial z}\right] - \lambda_m k_{\alpha_m}^2\overline{\varphi}_m$$

$$\overline{P}_{\theta z_m}(r,\theta,z) = \mu_m\left(\frac{1}{r}\frac{\partial\overline{w}_m}{\partial\theta} + \frac{\partial\overline{v}_m}{\partial z}\right)$$

$$= \mu_m\left[\frac{2}{r}\frac{\partial^2\overline{\varphi}_m}{\partial z\partial\theta} + \frac{2}{r}\frac{\partial^3\overline{\psi}_m}{\partial z^2\partial\theta} + \frac{k_{\beta_m}^2}{r}\frac{\partial\overline{\psi}_m}{\partial\theta} - \frac{\partial^2\overline{\chi}_m}{\partial r\partial\theta}\right]$$

$$\overline{P}_{rz_m}(r,\theta,z) = \mu_m\left(\frac{\partial\overline{w}_m}{\partial r} + \frac{\partial\overline{q}_m}{\partial z}\right)$$

$$= \mu_m\left[2\frac{\partial^2\overline{\varphi}_m}{\partial z\partial r} + 2\frac{\partial^3\overline{\psi}_m}{\partial z^2\partial r} + k_{\beta_m}^2\frac{\partial\overline{\psi}_m}{\partial r} + \frac{1}{r}\frac{\partial^2\overline{\chi}_m}{\partial z\partial\theta}\right]$$

In passing, we note that if $\overline{\chi}_m$ is independent of r and if $\overline{\varphi}_m$, $\overline{\psi}_m$ and $\overline{\chi}_m$ are independent of θ, equations 72 reduce to the azimuthal symmetric equations 5.

Using the integral definitions of equations 7 and extending them to $\overline{v}_m$, $\overline{P}_{\theta z_m}$ and $\overline{\chi}_m$, we have after separating the solutions of

equations 71

$$\varphi_m(r, \theta, z;k) = \varphi_m(z) J_1(kr) \cos \theta$$

$$\psi_m(r, \theta, z;k) = \psi_m(z) J_1(kr) \cos \theta \qquad (73)$$

$$\chi_m(r, \theta, z;k) = \chi_m(z) J_1(kr) \sin \theta$$

where

$$\frac{d^2\varphi_m(z)}{dz^2} = -k^2 r_{a_m}^2 \varphi_m(z)$$

$$\frac{d^2\psi_m(z)}{dz^2} = -k^2 r_{\beta_m}^2 \psi_m(z)$$

$$\frac{d^2\chi_m(z)}{dz^2} = -k^2 r_{\beta_m}^2 \chi_m(z)$$

Since there are no boundaries at r or θ constant, the solutions to this problem will have the same r and θ dependence as the source integrand. The r and θ dependence of equations 73 were chosen for this reason as we will now demonstrate. Substituting the integral representations into equations 72 using 73, and equating integrands we obtain

$$q_m(r, \theta, z;k) = \left\{ \left[\varphi_m(z) + \frac{d\psi_m(z)}{dz} \right] \frac{dJ_1(kr)}{dr} + \chi_m(z) \frac{J_1(kr)}{r} \right\} \cos \theta$$

$$\equiv \left\{ \frac{1}{k} \left[\frac{\dot{u}_{R_m}(z)}{c} \right] \frac{dJ_1(kr)}{dkr} - \frac{i}{k} \left[\frac{\dot{v}_{L_m}(z)}{c} \right] \frac{J_1(kr)}{kr} \right\} \cos \theta$$

$$v_m(r,\theta,z;k) = \left\{ -\left[\varphi_m(z) + \frac{d\psi_m(z)}{dz}\right]\frac{J_1(kr)}{r} - \chi_m(z)\frac{dJ_1(kr)}{dr}\right\}\sin\theta$$

$$\equiv \left\{ -\frac{1}{k}\frac{\dot{u}_{R_m}(z)}{c}\frac{J_1(kr)}{kr} + \frac{i}{k}\frac{\dot{v}_{L_m}(z)}{c}\frac{dJ_1(kr)}{dkr}\right\}\sin\theta$$

$$w_m(r,\theta,z;k) = \left[\frac{d\bar{\varphi}_m(z)}{dz} + \frac{d^2\psi_m(z)}{dz^2} + k^2\beta_m\psi_m(z)\right] J_1(kr)\cos\theta$$

$$\equiv -\frac{i}{k}\frac{\dot{w}_{R_m}(z)}{c} J_1(kr)\cos\theta$$

$$P_{zz_m}(r,\theta,z;k) = \left\{ 2\mu_m\left[\frac{d^2\varphi_m(z)}{dz^2} + \frac{d^3\psi_m(z)}{dz^3} + k^2\beta_m\frac{d\psi_m(z)}{dz}\right]\right.$$

$$\left. - \lambda_m k^2\alpha_m\varphi_m(z)\right\} J_1(kr)\cos\theta$$

$$\equiv \sigma_{R_m}(z)\, J_1(kr)\cos\theta \qquad (74)$$

$$P_{\theta z_m}(r,\theta,z;k) = -\mu_m\left\{\left[2\frac{d\bar{\varphi}_m(z)}{dz} + 2\frac{d^2\psi_m(z)}{dz^2} + k^2\beta_m\psi_m(z)\right]\frac{J_1(kr)}{r}\right.$$

$$\left. + \frac{d\chi_m(z)}{dz}\frac{dJ_1(kr)}{dr}\right\}\sin\theta$$

$$\equiv \left\{ -i\tau_{R_m}(z)\frac{J_1(kr)}{kr} - \tau_{L_m}(z)\frac{dJ_1(kr)}{dkr}\right\}\sin\theta$$

$$P_{rz_m}(r,\theta,z;k) = \mu_m\left\{\left[2\frac{d\varphi_m(z)}{dz} + 2\frac{d^2\psi_m(z)}{dz^2} + k^2\beta_m\psi_m(k)\right]\frac{dJ_1(kr)}{dkr}\right.$$

$$\left. + \frac{d\chi_m}{dz}(z)\frac{J_1(kr)}{r}\right\}\cos\theta$$

$$\equiv \left\{ i\tau_{R_m}(z)\frac{dJ_1(kr)}{dkr} + \tau_{L_m}(z)\frac{J_1(kr)}{kr}\right\}\cos\theta$$

We see from equations 74 that two new z dependent quantities have been introduced into our boundary value problem; i.e. $v_{L_m}(z)$ and $\tau_{L_m}(z)$. These quantities are defined in equations A22 and are associated with Love type surface waves as will be demonstrated later.

As before the boundary conditions are continuity of displacement and stress at the welded interfaces. Since $\frac{J_1(kr)}{kr}$ and $\frac{dJ_1(kr)}{dkr}$ are linearly independent and continuous across interfaces, we must impose continuity on their individual coefficients in order that continuity of displacement and stress be satisfied for all r. From equations 74, we see that the following must be continuous at the z_{m-1} interface;

$$\begin{bmatrix} \frac{\dot{u}_{R_m}(z_{m-1})}{c} \\ \frac{\dot{w}_{R_m}(z_{m-1})}{c} \\ \frac{\sigma_{R_m}(z_{m-1})}{c} \\ \tau_{R_m}(z_{m-1}) \end{bmatrix} = \begin{bmatrix} \frac{\dot{u}_{R_{m-1}}(z_{m-1})}{c} \\ \frac{\dot{w}_{R_{m-1}}(z_{m-1})}{c} \\ \frac{\sigma_{R_{m-1}}(z_{m-1})}{c} \\ \tau_{R_{m-1}}(z_{m-1}) \end{bmatrix}$$

and

$$\begin{bmatrix} \frac{\dot{v}_{L_m}(z_{m-1})}{c} \\ \tau_{L_m}(z_{m-1}) \end{bmatrix} = \begin{bmatrix} \frac{\dot{v}_{L_{m-1}}(z_{m-1})}{c} \\ \tau_{L_{m-1}}(z_{m-1}) \end{bmatrix} \qquad (77)$$

The above boundary conditions are written as two vector equations since the two motions stress vectors 76 and 77 at one side of a layer are related to those at the other side by the following linear transformations.

$$\begin{bmatrix} \frac{\dot{u}_{R_m}(z_m)}{c} \\ \frac{\dot{w}_{R_m}(z_m)}{c} \\ \sigma_{R_m}(z_m) \\ \tau_{R_m}(z_m) \end{bmatrix} = a_{R_m} \begin{bmatrix} \frac{\dot{u}_{R_m}(z_{m-1})}{c} \\ \frac{\dot{w}_{R_m}(z_{m-1})}{c} \\ \sigma_{R_m}(z_{m-1}) \\ \tau_{R_m}(z_{m-1}) \end{bmatrix} \tag{78}$$

and

$$\begin{bmatrix} \frac{\dot{v}_{L_m}(z_m)}{c} \\ \tau_{L_m}(z_m) \end{bmatrix} = a_{L_m} \begin{bmatrix} \frac{\dot{v}_{L_m}(z_{m-1})}{c} \\ \tau_{L_m}(z_{m-1}) \end{bmatrix} \tag{79}$$

given in Appendix A as equations A11 and A31.

Comparing equations 74 with the source integrands, equations 68, we obtain

$$\frac{\dot{u}_{R_{so}}(z)}{c} = -i \frac{\overline{L}}{4\pi\omega^2\rho_s} k^3 \left(\frac{e^{-ikr_{\alpha_s}|z-D|}}{r_{\alpha_s}} + r_{\beta_s} e^{-ikr_{\beta_s}|z-D|} \right)$$

$$\frac{\dot{v}_{L_{so}}(z)}{c} = \frac{\overline{L}}{4\pi\omega^2\rho_s} kk_{\beta_s}^2 e^{-ikr_{\beta_s}|z-D|} \tag{80}$$

$$\frac{\dot{w}_{R_{so}}(z)}{c} = i \frac{\overline{L}}{4\pi\omega^2\rho_s} \left\{ \frac{|z-D|}{z-D} \right\} k^3 \left(e^{-ikr_{\beta_s}|z-D|} - e^{-ikr_{\alpha_s}|z-D|} \right)$$

Evaluating the source stresses from equations 68 and comparing the

integrands with equations 74, we obtain

$$\sigma_{R_{so}}(z) = -i\frac{k\bar{L}}{4\pi}\left[(\gamma_s - 1)\frac{e^{-ikr_{\alpha_s}|z-D|}}{r_{\alpha_s}} - \gamma_s r_{\beta_s} e^{-ikr_{\beta_s}|z-D|}\right]$$

$$\tau_{R_{so}}(z) = i\frac{k\bar{L}}{4\pi}\left\{\frac{|z-D|}{z-D}\right\}\left[\gamma_s e^{-ikr_{\alpha_s}|z-D|} - (\gamma_s - 1)e^{-ikr_{\beta_s}|z-D|}\right] \quad (81)$$

$$\tau_{L_{so}}(z) = -\frac{k\bar{L}}{4\pi}\left\{\frac{|z-D|}{z-D}\right\} e^{-ikr_{\beta_s}|z-D|}$$

Evaluation of equations 80 and 81 leads to the vector equations for the source layer at $z = D$,

$$\begin{bmatrix} \frac{\dot{u}_{R_{s2}}(D)}{c} \\ \frac{\dot{w}_{R_{s2}}(D)}{c} \\ \sigma_{R_{s2}}(D) \\ \tau_{R_{s2}}(D) \end{bmatrix} = \begin{bmatrix} \frac{\dot{u}_{R_{s1}}(D)}{c} \\ \frac{\dot{w}_{R_{s1}}(D)}{c} \\ \sigma_{R_{s1}}(D) \\ \tau_{R_{s1}}(D) \end{bmatrix} + \begin{bmatrix} 0 \\ 0 \\ 0 \\ \delta\tau_{R_s} \end{bmatrix} \quad (82)$$

where

$$\delta\tau_{R_s} = i\frac{k\bar{L}}{2\pi}$$

and

$$\begin{bmatrix} \frac{\dot{v}_{L_{s2}}(D)}{c} \\ \tau_{L_{32}}(D) \end{bmatrix} = \begin{bmatrix} \frac{\dot{v}_{L_{s1}}(D)}{c} \\ \tau_{L_{s1}}(D) \end{bmatrix} + \begin{bmatrix} 0 \\ \delta\tau_{L_s} \end{bmatrix} \quad (83)$$

where

$$\delta\tau_{L_s} = -\frac{k\bar{L}}{2\pi}$$

The same result can be derived by noting that the source displacements can be obtained from the source potentials

$$\varphi_{so}(z) = -i\frac{k\bar{L}}{4\pi\omega^2\rho_s}\frac{e^{-ikr_{\alpha_s}|z-D|}}{k\,r_{\alpha_s}}$$

$$\psi_{so}(z) = \frac{\bar{L}}{4\pi\omega^2\rho_s}\left\{\frac{|z-D|}{z-D}\right\}e^{-ikr_{\beta_s}|z-D|} \tag{84}$$

$$\chi_{so}(z) = -i\frac{\bar{L}}{4\pi\omega^2\rho_s}\frac{k_{\beta_s}^2}{kr_{\beta_s}}e^{-ikr_{\beta_s}|z-D|}$$

And by comparison with equations A14 and A33 we have

$$S_{01}^{+} = S_{01}^{-} = -i\frac{\bar{L}}{4\pi\omega^2\rho_s}\frac{k}{r_{\alpha_s}}$$

$$S_{02}^{+} = -S_{02}^{-} = \frac{\bar{L}}{4\pi\omega^2\rho_s} \tag{85}$$

$$S_{03}^{+} = S_{03}^{-} = -i\frac{\bar{L}}{4\pi\omega^2\rho_s}\frac{k_{\beta_s}^2}{kr_{\beta_s}}$$

Substitution of equations 85 into equations A21 and A36 yields the same result as above.

$$\delta\tau_{R_s} = i\frac{k\bar{L}}{2\pi} \quad \text{and} \quad \delta\tau_{L_s} = -\frac{k\bar{L}}{2\pi}$$

The horizontal force problem has now separated into two sets of vector relations independent of each other, the first set given by equations 76, 78, and 82 and the second set by 77, 79, and 83. The The first set represents Rayleigh type surface waves and the second

set, Love type surface waves when the residue contributions are obtained. Following the procedure of the previous sections, we obtain for the first set

$$\frac{\dot{u}_{R_o}}{c} = W + \delta\tau_{R_s}\left(A_{R_{s1}}\right)_{14}$$

$$\frac{\dot{w}_{R_o}}{c} = X - \delta\tau_{R_s}\left(A_{R_{s1}}\right)_{13} \tag{86}$$

$$Y = -\delta\tau_{R_s}\left(A_{R_{s1}}\right)_{12}$$

$$Z = \delta\tau_{R_s}\left(A_{R_{s1}}\right)_{11}$$

Solving equations 86 yields

$$\frac{\dot{w}_{R_o}}{c} = -\frac{N_R^{(1)}N_R^{(2)}}{F_R} \tag{87}$$

and

$$\frac{\dot{u}_{R_o}}{c} = \frac{N_R^{(3)}N_R^{(4)}}{F_R} \tag{88}$$

where

$$N_R^{(2)} = 1 + \frac{F_R}{N_R^{(1)}}\,\delta\tau_{R_s}\left(A_{R_{s1}}\right)_{13}$$

$$N_R^{(4)} = 1 + \frac{F_R}{N_R^{(3)}}\,\delta\tau_{R_s}\left(A_{R_{s1}}\right)_{14} \tag{89}$$

For the second set, we have similar to equations 19 and 20

$$\begin{bmatrix} \frac{\dot{v}_{L_{n-1}}(z_{n-1})}{c} \\ \tau_{L_{n-1}}(z_{n-1}) \end{bmatrix} = A_L^{s2} \begin{bmatrix} \frac{\dot{v}_{L_{s2}}(D)}{c} \\ \tau_{L_{s2}}(D) \end{bmatrix} \tag{90}$$

and

$$\begin{bmatrix} \frac{\dot{v}_{L_{s1}}(D)}{c} \\ \tau_{L_{s1}}(D) \end{bmatrix} = A_{L_{s1}} \begin{bmatrix} \frac{\dot{v}_{L_o}(0)}{c} \\ 0 \end{bmatrix} \tag{91}$$

where

$$A_L^{s2} = a_{L_{n-1}} \cdots a_{L_{s2}}$$

$$A_{L_{s1}} = a_{L_{s1}} \cdots a_1$$

and

$$\frac{\dot{v}_{L_o}}{c} \equiv \frac{\dot{v}_{L_1}(0)}{c}$$

Using the following definition

$$\begin{bmatrix} V \\ T \end{bmatrix} = A_{L_{s1}}^{-1} \begin{bmatrix} \frac{\dot{v}_{L_{s2}}(D)}{c} \\ \tau_{L_{s2}}(D) \end{bmatrix} \tag{92}$$

and multiplying the source layer vector equation 83 by $A_{L_{s1}}^{-1}$ yields

$$\begin{bmatrix} V \\ T \end{bmatrix} = \begin{bmatrix} \frac{\dot{v}_{L_o}}{c} \\ 0 \end{bmatrix} + A_{L_{s1}}^{-1} \begin{bmatrix} 0 \\ \delta\tau_{L_s} \end{bmatrix}$$

or

$$\frac{\dot{v}_{L_o}}{c} = V - \delta\tau_{L_s}\left(A^{-1}_{L_{s1}}\right)_{12}$$

$$T = \delta\tau_{L_s}\left(A^{-1}_{L_{s1}}\right)_{22} \tag{93}$$

From the elements of a_{L_m}, equation A32, we see that the determinant of a_{L_m} is unity. Therefore the determinant of the product matrices is equal to one and thus the inverse of $A_{L_{s1}}$ can be written immediately as

$$A^{-1}_{L_{s1}} = \begin{bmatrix} \left(A_{L_{s1}}\right)_{22} & -\left(A_{L_{s1}}\right)_{12} \\ -\left(A_{L_{s1}}\right)_{21} & \left(A_{L_{s1}}\right)_{11} \end{bmatrix} \tag{94}$$

Using equations 94, equations 93 can be rewritten as

$$\frac{\dot{v}_{L_o}}{c} = V + \delta\tau_{L_s}\left(A_{L_{s1}}\right)_{12}$$

$$T = \delta\tau_{L_s}\left(A_{L_{s1}}\right)_{11} \tag{95}$$

From equations A26, we have for the halfspace or layer n

$$\begin{bmatrix} \underline{\epsilon}'_n + \underline{\epsilon}''_n \\ \underline{\epsilon}'_n - \underline{\epsilon}''_n \end{bmatrix} = E^{-1}_{L_n} \begin{bmatrix} \frac{\dot{v}_{L_n}(z_{n-1})}{c} \\ \tau_{L_n}(z_{n-1}) \end{bmatrix} \tag{96}$$

Our boundary conditions at infinity in the halfspace as before requires that $\underline{\epsilon}''_n = 0$. Defining

$$A_L \equiv A_L^{s2} A_{L_{s1}} = a_{L_{n-1}} \cdots a_{L_{s2}} a_{L_{s1}} \cdots a_{L_1} = a_{L_{n-1}} \cdots a_{L_s} \cdots a_{L_1}$$

where it can be shown that $a_{L_{s2}} a_{L_{s1}} = a_{L_s}$, we obtain using equations 96, 90, and 91

$$\begin{bmatrix} \underline{\epsilon}'_n \\ \\ \underline{\epsilon}'_n \end{bmatrix} = E_{L_n}^{-1} A_L \begin{bmatrix} V \\ \\ T \end{bmatrix} \tag{97}$$

or

$$V = - \frac{[(J_L)_{12} - (J_L)_{22}]}{[(J_L)_{11} - (J_L)_{21}]} \; T \tag{98}$$

where

$$J \equiv E_{L_n}^{-1} A_L = \begin{bmatrix} (ik)^{-1} & 0 \\ \\ 0 & -(ik\mu_n r \beta_n)^{-1} \end{bmatrix} \begin{bmatrix} (A_L)_{11} & (A_L)_{12} \\ \\ (A_L)_{21} & (A_L)_{22} \end{bmatrix} \tag{99}$$

Evaluation of equation 99 and substitution of equation 98 in 95, yields

$$\frac{\dot{v}_{L_o}}{c} = \frac{N_L^{(1)} N_L^{(2)}}{F_L} \tag{100}$$

where

$$F_L = - (A_L)_{12}^* - (A_L)_{11} \mu_n r_n^* \beta_n$$

$$N_L^{(1)} = i \frac{k\overline{L}}{2\pi} [(A_L)_{22} - (A_L)_{12}^* \mu_n r_n^* \beta_n] \left(A_{L_{s1}}\right)_{11} \tag{101}$$

and

$$N_L^{(2)} = 1 - i \frac{k\overline{L}}{2\pi} \frac{F_L}{N_L^{(1)}} \left(A_{L_{s1}}\right)_{21}^*$$

since

$$\delta\tau_{L_s} = -\frac{k\overline{L}}{2\pi}$$

The matrix elements of a_{L_m} are real or imaginary by the same criteria as a_{R_m}. These criteria will also hold for the matrix product elements. In addition for $c \leq \beta_n$ we have as before that r_{β_n} is imaginary. The imaginary quantities are expressed as real quantities (designated by asterisks) multiplied by i. This notation was used in equations 101.

$F_L(\omega, k) = 0$ is a form of the period equation for Love wave propagation in plane multilayered isotropic solids. Since we are interested in the residue contribution we note that when $F_L = 0$, equations 101 reduce to

$$\mu_n r^*_{\beta_n} = -\frac{(A_L)^*_{21}}{(A_L)_{11}}$$

$$N_L^{(2)} = 1 \qquad (102)$$

and

$$N_L^{(1)} = i\frac{k\overline{L}}{2\pi}\frac{[(A_L)_{11}(A_L)_{22}+(A_L)^*_{12}(A_L)^*_{21}]}{(A_L)_{11}}\left(A_{L_{s1}}\right)_{11}$$

And since the determinant of $A_L = 1$, we have

$$|A_L| \equiv (A_L)_{11}(A_L)_{22} + (A_L)^*_{12}(A_L)^*_{21} = 1$$

and (103)

$$N_L^{(1)} = i\frac{k\overline{L}}{2\pi}\frac{1}{(A_L)_{11}}\left(A_{L_{s1}}\right)_{11}$$

Thus by equations 87, 88, 103, and 74 for $m = 0$, the Fourier displacements at the free surface are

$$\overline{q}_o(r,\theta,z) = \int_0^\infty \left\{ \frac{1}{k} \frac{N_R^{(3)} N_R^{(4)}}{F_R} \frac{dJ_1(kr)}{dkr} - \frac{i}{k} \frac{N_L^{(1)} N_L^{(2)}}{F_L} \frac{J_1(kr)}{kr} \right\} dk \cos\theta$$

$$\overline{v}_o(r,\theta,z) = \int_0^\infty \left\{ -\frac{1}{k} \frac{N_R^{(3)} N_R^{(4)}}{F_R} \frac{J_1(kr)}{kr} + \frac{i}{k} \frac{N_L^{(1)} N_L^{(2)}}{F_L} \frac{dJ_1(kr)}{dkr} \right\} dk \sin\theta \qquad (104)$$

$$\overline{w}_o(r,\theta,z) = \int_0^\infty \frac{i}{k} \frac{N_R^{(1)} N_R^{(2)}}{F_R} J_1(kr)\, dk \cos\theta$$

Evaluating the residue contribution of equations 104 for the zeros of F_R we obtain for each j^{th} mode

$$\{\overline{w}_o\}_{R_j} = \frac{\pi}{k_{R_j}} \frac{N_{R_j}^{(1)} N_{R_j}^{(2)}}{\left(\frac{\partial F_R}{\partial k}\right)_{\omega, j}} H_1^{(2)}(k_{R_j} r) \cos\theta$$

$$\{\overline{q}_o\}_{R_j} = -i \frac{\pi}{k_{R_j}} \frac{N_{R_j}^{(3)} N_{R_j}^{(4)}}{\left(\frac{\partial F_R}{\partial k}\right)_{\omega, j}} \left\{ H_o^{(2)}(k_{R_j} r) - \frac{H_1^{(2)}(k_{R_j} r)}{k_{R_j} r} \right\} \cos\theta \qquad (105)$$

$$\{\overline{v}_o\}_{R_j} = i \frac{\pi}{k_{R_j}} \frac{N_{R_j}^{(3)} N_{R_j}^{(4)}}{\left(\frac{\partial F_R}{\partial k}\right)_{\omega, j}} \frac{H_1^{(2)}(k_{R_j} r)}{k_{R_j} r} \sin\theta$$

As shown before

$$N_{R_j}^{(2)} = N_{R_j}^{(4)} = 1$$

$$N_{R_j}^{(3)} = \frac{K}{L} N_{R_j}^{(1)} = -i \left[\frac{\dot{u}_o^*}{\dot{w}_o} \right]_{H_j} N_{R_j}^{(1)}$$

$$N_{R_j}^{(1)} = [GN - LH]\{Y + \frac{K}{L} Z\}$$

and by equations 86 and 82

$$N_{R_j}^{(1)} = k_{R_j} \frac{\overline{L}}{2\pi} [G^*N - L^*H] \left\{ \left(A_{R_{s1}}\right)_{12} - \frac{K}{L} \left(A_{R_{s1}}\right)_{11} \right\} \tag{106}$$

Using the homogeneous solution notation, we write equation 106 as

$$N_{R_j}^{(1)} = i\, k_{R_j} \frac{\overline{L}}{2\pi} [G^*N - L^*H] \left[\begin{matrix} \dot{u}_s^* \\ \dot{w}_o \end{matrix} (D) \right]_{H_j}$$

yielding the Rayleigh contribution for a horizontal point force at depth D

$$\{\overline{w}_o\}_{R_j} = i \frac{\overline{L}}{2} \left[\begin{matrix} \dot{u}_s^* \\ \dot{w}_o \end{matrix} (D) \right]_{H_j} A_{R_j} H_1^{(2)}(k_{R_j} r) \cos\theta$$

$$\{\overline{q}_o\}_{R_j} = - i \frac{\overline{L}}{2} \left[\begin{matrix} \dot{u}_o^* \\ \dot{w}_o \end{matrix} \right]_{H_j} \left[\begin{matrix} \dot{u}_s^* \\ \dot{w}_o \end{matrix} (D) \right]_{H_j} A_{R_j} \left\{ H_o^{(2)}(k_{R_j} r) - \frac{H_1^{(2)}(k_{R_j} r)}{k_{R_j} r} \right\} \cos\theta \tag{107}$$

$$\{\overline{v}_o\}_{R_j} = i \frac{\overline{L}}{2} \left[\begin{matrix} \dot{u}_o^* \\ \dot{w}_o \end{matrix} \right]_{H_j} \left[\begin{matrix} \dot{u}_o^* \\ \dot{w}_o \end{matrix} (D) \right]_{H_j} A_R \frac{H_1^{(2)}(k_{R_j} r)}{k_{R_j} r} \sin\theta$$

where A_R is given by equation 51.

Evaluating the residue of equations 104 for the zeros of F_L, we obtain for each j^{th} mode

$$\{\overline{v}_o\}_{L_j} = \frac{\pi}{k_{L_j}} \frac{N_{L_j}^{(1)} N_{L_j}^{(2)}}{\left(\frac{\partial F_L}{\partial k}\right)_{\omega, j}} \left\{ H_o^{(2)}(k_{L_j} r) - \frac{H_1^{(2)}(k_{L_j} r)}{k_{L_j} r} \right\} \sin\theta$$

$$\{\overline{q}_o\}_{L_j} = - \frac{\pi}{k_{L_j}} \frac{N_{L_j}^{(1)} N_{L_j}^{(2)}}{\left(\frac{\partial F_L}{\partial k}\right)_{\omega, j}} \frac{H_1^{(2)}(k_{L_j} r)}{k_{L_j} r} \cos\theta \tag{108}$$

$$\{\overline{w}_o\}_{L_j} = 0$$

where from equations 103 we have

$$N_{L_1}^{(2)} = 1$$

and

$$N_{L_j}^{(1)} = ik_{L_j}\frac{\overline{L}}{2\pi}\frac{1}{(A_L)_{11}}\left(A_{L_{s1}}\right)_{11} \tag{109}$$

In terms of the homogeneous notation we have

$$\left[\frac{\dot{v}_s(D)}{\dot{v}_o}\right]_{H_j} \equiv \left(A_{L_{s1}}\right)_{11}$$

and

$$\left[\frac{\dot{v}_{n-1}}{\dot{v}_o}\right]_{H_j} \equiv \left[\frac{\dot{v}_n(z_n-1)}{\dot{v}_o}\right]_{H_j} \equiv (A_L)_{11}$$

Thus, for the Love contribution

$$\{\overline{v}_o\}_{L_j} = i\frac{\overline{L}}{2}\left[\frac{\dot{v}_s(D)}{\dot{v}_o}\right]_{H_j} \mathcal{A}_{L_j}\left\{H_o^{(2)}(k_{L_j}r) - \frac{H_1^{(2)}(k_{L_j}r)}{k_{L_j}r}\right\}\sin\theta$$

$$\{\overline{q}_o\}_{L_j} = -i\frac{\overline{L}}{2}\left[\frac{\dot{v}_s(D)}{\dot{v}_o}\right]_{H_j} \mathcal{A}_{L_j}\frac{H_1^{(2)}(k_{L_j}r)}{k_{L_j}r}\cos\theta \tag{110}$$

where

$$\mathcal{A}_{L_j} = \frac{1}{\left[\frac{\dot{v}_{n-1}}{\dot{v}_o}\right]_{H_j}\left(\frac{\partial F_L}{\partial k}\right)_{\omega,j}}$$

As in previous sections the residue contributions are continuous through the source plane, and it follows that the residue displacements

at depth for the horizontal point force are

$$\{\bar{q}_m(z)\}_{R_j} = i\left[\frac{\dot{u}_m(z)}{\dot{w}_o}\right]_{H_j} \{\bar{w}_o\}_{R_j}\left\{H_o^{(2)}(k_{R_j}r) - \frac{H_1^{(2)}(k_{R_j}r)}{k_{R_j}r}\right\}\Big/ H_1^{(2)}(k_{R_j}r)$$

$$\{\bar{w}_m(z)\}_{R_j} = \left[\frac{\dot{w}_m(z)}{\dot{w}_o}\right]_{H_j} \{\bar{w}_o\}_{R_j} \tag{111}$$

and

$$\{\bar{v}_m(z)\}_{L_j} = \left[\frac{\dot{v}_m(z)}{\dot{v}_o}\right]_{H_j} \{\bar{v}_o\}_{L_j}$$

for all m. The homogeneous ratios are given for Rayleigh in terms of $A_{R_m}(z)$ as before. The Love ratios are similarly given in terms of

$$A_{L_m}(z) = a_{L_m}(z)\, a_{L_{m-1}} \cdots a_{L_1}$$

where $A_{L_m}(z)$ is the matrix for a sublayer in m of thickness $d_m = z - z_{m-1}$.

In the remainder of this paper, we will be interested in Rayleigh and Love waves at large r. Neglecting terms in $r^{-3/2}$ which are small compared to terms in $r^{-1/2}$, we have as the dominant surface displacements,

$$\{\bar{w}_o\}_{R_j} = i\frac{\bar{L}}{2}\left[\frac{\dot{u}_s^*(D)}{\dot{w}_o}\right]_{H_j} \mathcal{A}_{R_j} H_1^{(2)}(k_{R_j}r)\cos\theta$$

$$\{\bar{q}_o\}_{R_j} = -i\frac{\bar{L}}{2}\left[\frac{\dot{u}_o^*}{\dot{w}_o}\right]_{H_j}\left[\frac{\dot{u}_s^*(D)}{\dot{w}_o}\right]_{H_j} \mathcal{A}_{R_j} H_o^{(2)}(k_{R_j}r)\cos\theta \tag{112}$$

$$\{\bar{v}_o\}_{L_j} = i\frac{\bar{L}}{2}\left[\frac{\dot{v}_s(D)}{v_o}\right]_{H_j} \mathcal{A}_{L_j} H_o^{(2)}(k_{L_j}r)\sin\theta$$

Extension of the Horizontal Point Force Solutions To a Model of a Vertical Strike Fault

In this section, we take the solutions for a horizontal point force at depth in a multilayered medium and extend them by spatial integration to represent a model for a vertical strike fault. This method of integration over a finite vertical fault plane was used by Ben-Menahem (1961). For Rayleigh waves he used the horizontal point force solutions of an elastic halfspace and for the Love waves the corresponding solutions for one layer over a halfspace. In this multilayered formulation, the vertical integration is evaluated exactly. For the time lagged integration over the horizontal fault dimension, we use the approximate evaluation given by Ben-Menahem.

Now consider, in phase, horizontal point forces distributed continuously on the vertical z axis for the interval $h_1 \leq z \leq h_2$. The strength is adjusted so that as $\Delta h = h_2 - h_1$ approaches zero, the integrated effect reverts to the point force solution at $z = h_1 = h_2$. Then using equations 112, we obtain for a vertical segment of horizontal forces in a single source layer s,

$$\{\overline{w}_o\}_{R_j}^{\Delta h} = i\frac{\overline{L}}{2} A_{R_j} H_1^{(2)}(k_{R_j} r)\cos\theta \frac{1}{\Delta h}\int_{h_1}^{h_2}\left[\begin{matrix}\dot{u}_s^*(h)\\ \dot{w}_o\end{matrix}\right]_{H_j} dh \qquad (113)$$

where

$$\left[\begin{matrix}\dot{u}_s^*(h)\\ \dot{w}_o\end{matrix}\right]_{H_j} = \left[A_{R_s}(h)\right]_{12}^* + \left[\begin{matrix}\dot{u}_o^*\\ \dot{w}_o\end{matrix}\right]_{H_j}\left[A_{R_s}(h)\right]_{11}$$

and $\left[\begin{matrix}\dot{u}_o^*\\ \dot{w}_o\end{matrix}\right]_{H_j}$ is a function of the layer array and hot h.

Now since a given layer can be divided into as many sublayers as desired by the matrix relations of Appendix A, we can write

$$A_{R_s}(h) = a_{R_s}(\ell)\, A_{R_s}(h_1) \qquad \text{where} \quad \ell = h - h_1$$

Performing the integration, we obtain

$$\int_{h_1}^{h_2} \left[\frac{\dot{u}_s^*(h)}{\dot{w}_o}\right]_{H_j} dh = \left[\frac{\dot{u}_s^*(h_1)}{\dot{w}_o}\right]_{H_j} I_{11}(\Delta h) + \left[\frac{\dot{w}_s(h_1)}{\dot{w}_o}\right]_{H_j} I_{12}^*(\Delta h) + \left[\frac{\sigma_s^*(h_1)}{\frac{\dot{w}_o}{c}}\right]_{H_j} I_{13}(\Delta h) + \left[\frac{\tau_{R_s}(h_1)}{\frac{\dot{w}_o}{c}}\right]_{H_j} I_{14}^*(\Delta h) \qquad (114)$$

where

$$I_{11}(\Delta h) = \int_0^{\Delta h} \left[a_{R_s}(\ell)\right]_{11} d\ell = \gamma_s \frac{\sin \Delta P_s}{k r_{\alpha_s}} - (\gamma_s - 1) \frac{\sin \Delta Q_s}{k r_{\beta_s}}$$

$$I_{12}^*(\Delta h) = \int_0^{\Delta h} \left[a_{R_s}(\ell)\right]_{12}^* d\ell = (\gamma_s - 1) \frac{1}{k_{R_j} r_{\alpha_s}^2} (1 - \cos \Delta P_s) + \frac{\gamma_s}{k_{R_j}} (1 - \cos \Delta Q_s) \qquad (115)$$

$$I_{13}(\Delta h) = \int_0^{\Delta h} \left[a_{R_s}(\ell)\right]_{13} d\ell = -\frac{1}{\rho_s c_{R_j}^2} \left[\frac{\sin \Delta P_s}{k_{R_j} r_{\alpha_s}} - \frac{\sin \Delta Q_s}{k_{R_j} r_{\beta_s}}\right]$$

$$I_{14}^*(\Delta h) = \int_0^{\Delta h} \left[a_{R_s}(\ell)\right]_{14}^* d\ell = \frac{1}{\rho_s c_{R_j}^2} \left[\frac{1}{k_{R_j} r_{\alpha_s}^2} (1 - \cos \Delta P_s + \frac{1}{k_{R_j}} (1 - \cos \Delta Q_s)\right]$$

$$\Delta P_s = k_{R_j} r_{\alpha_s} \Delta h \qquad \text{and} \quad \Delta P_s = k_{R_j} r_{\beta_s} \Delta h$$

When the line of sources extends through the interface between layers say S_k: k = 1, m , we generalize our result to

$$\{\overline{w}_o\}_{R_j}^{\Delta h} = i \frac{\overline{L}}{2} A_{R_j} O_{R_s} H_1^{(2)}(k_{R_j} r) \cos \theta$$

where

$$O_{R_s} = \frac{1}{\Delta h} \left\{ \int_{h_1}^{z_{s_1}} \left[\frac{\dot{u}^*_{s_1}(h)}{\dot{w}_o} \right]_{H_j} dh + \sum_{k=2}^{m-1} \int_{z_{s_{k-1}}}^{z_{s_k}} \left[\frac{\dot{u}^*_{s_k}(h)}{\dot{w}_o} \right]_{H_j} dh \right.$$

$$\left. + \int_{z_{s_{m-1}}}^{h_2} \left[\frac{\dot{u}^*_{s_m}(h)}{\dot{w}_o} \right]_{H_j} dh \right.$$

The $\frac{1}{\Delta h}$ is carried outside the summation, instead of $\frac{1}{\Delta h_{s_k}}$ with each element, so that if all the layers were the same material the result would be consistent with a single layer. Similarly

$$\{\overline{q}_o\}_{R_j}^{\Delta h} = - i \frac{\overline{L}}{2} \left[\frac{\dot{u}^*_o}{\dot{w}_o} \right]_{H_j} A_{R_j} O_{R_s} H_o^{(2)}(k_{R_j} r) \cos \theta \qquad (117)$$

Now for Love waves, the integrated effect for a single source layer is

$$\{\overline{v}_o\}_{L_j}^{\Delta h} = i \frac{\overline{L}}{2} A_{L_j} H_o^{(2)}(k_{L_j} r) \sin \theta \frac{1}{\Delta h} \int_{h_1}^{h_2} \left[\frac{\dot{v}_s(h)}{\dot{v}_o} \right]_{H_j} dh \qquad (118)$$

where

$$\left[\frac{\dot{v}_s(h)}{\dot{v}_o}\right]_{H_j} = \left[A_{L_s}(h)\right]_{11}$$

Decomposing $A_{L_s}(h)$ to

$$A_{L_s}(h) = a_{L_s}(\ell) A_{L_s}(h_1)$$

where

$$\ell = h - h_1$$

the integration yields

$$\int_{h_1}^{h_2} \left[\frac{\dot{v}_s(h)}{\dot{v}_o}\right]_{H_j} dh = \left[\frac{\dot{v}_s(h_1)}{\dot{v}_o}\right]_{H_j} I_{11}(\Delta h) - \left[\frac{\tau^*_{L_s}(h_1)}{\frac{\dot{v}_o}{c}}\right]_{H_j} I^*_{12}(\Delta h) \qquad (119)$$

where

$$I_{11}(\Delta h) = \int_0^{\Delta h} \left[a_{L_s}(\ell)\right]_{11} d\ell = \frac{\sin \Delta Q_s}{k_{L_j} r \beta_s}$$

$$I^*_{12}(\Delta h) = \int_0^{\Delta h} \left[a_{L_s}(\ell)\right]^*_{12} d\ell = \frac{1}{\mu_s k_{L_j} r \beta_s} (1 - \cos \Delta Q_s) \qquad (120)$$

When the segment extends vertically through many layers, we generalize to

$$O_{L_s} = \frac{1}{\Delta h} \int_{h_1}^{z_{s_1}} \left[\frac{\dot{v}_{s_1}(h)}{\dot{v}_o}\right]_{H_j} dh + \sum_{k=2}^{m-1} \int_{z_{s_{k-1}}}^{z_{s_k}} \left[\frac{\dot{v}_{s_k}(h)}{\dot{v}_o}\right]_{H_j} dh$$

$$+ \int_{z_{s_{m-1}}}^{h_2} \left[\frac{\dot{v}_{s_m}(h)}{\dot{v}_o}\right]_{H_j} dh \qquad (121)$$

and obtain

$$\{\bar{v}_o\}^{\Delta h}_{L_j} = i\frac{\bar{L}}{2} A_{L_j} H_o^{(2)}(k_{L_j} r) O_{L_s} \sin\theta$$

We now shift the vertical line of horizontal forces in the horizontal direction from 0 to b with velocity v. We take into consideration the necessary phase shift corresponding to a time shift in the source time function at each source point. We obtain

$$\{\bar{q}_o\}^{\Delta h,\, b}_{R_j} = -i\frac{\bar{L}}{2}\left[\frac{\dot{u}_o^*}{\dot{v}_o}\right]_{H_j} A_{R_j} O_{R_s} J^c_{0R}$$

$$\{\bar{w}_o\}_{R_j} = i\frac{\bar{L}}{2} A_{R_j} O_{R_s} J^c_{1R} \qquad (122)$$

where by Ben-Menahem (1961)

$$J^c_{0R} = \frac{1}{b}\int_0^b \cos\theta\, H_o^{(2)}(k_{R_j} r) e^{-i\xi/v}\, d\xi$$

$$= \frac{\cos\theta_o}{(k_{R_j} r)^{1/2}} \left(\frac{2}{\pi}\right)^{1/2} \left\{\frac{\sin X_R}{X_R}\right\} e^{-i\left(\omega \frac{r_o}{c_{R_j}} + X_R - \frac{\pi}{4}\right)}$$

and

$$J^c_{1R} = \frac{1}{b}\int_0^b \cos\theta\, H_1^{(2)}(k_{R_j} r) e^{-i\xi/v}\, d\xi \qquad (123)$$

$$= \frac{\cos\theta_o}{(k_{R_j} r)^{1/2}} \left(\frac{2}{\pi}\right)^{1/2} \left\{\frac{\sin X_R}{X_R}\right\} e^{-i\left(\frac{\omega r_o}{c_{R_j}} + X_R - \frac{3\pi}{4}\right)}$$

where

$$X_R = \frac{\omega b}{c_{r_j}}\left(\frac{c_{R_j}}{v} - \cos\theta_o\right) \quad \text{and} \quad c_{R_j} = \frac{\omega}{k_{R_j}}$$

For the Love wave contribution, we obtain

$$\{\bar{v}_o\}_{L_j}^{\Delta h, b} = i\frac{\bar{L}}{2} A_L O_{L_s} J_{0L}^{s} \tag{124}$$

where

$$\begin{aligned} J_{0L}^{s} &= \frac{1}{b}\int_0^b \sin\theta\, H_o^{(2)}(k_{L_j} r) e^{-i\xi/v}\, d\xi \\ &= \frac{\sin\theta_o}{(k_{L_j} r_o)^{1/2}} \left(\frac{2}{\pi}\right)^{1/2} \left\{\frac{\sin X_L}{X_L}\right\} e^{-i\left(\frac{\omega r_o}{c_{L_j}} + X_L - \frac{\pi}{4}\right)} \end{aligned} \tag{125}$$

and

$$X_L = \frac{\omega b}{c_{L_j}}\left(\frac{c_{L_j}}{v} - \cos\theta_o\right) \qquad \text{and} \quad c_{L_j} = \frac{\omega}{k_{L_j}}$$

The source fault plane geometry, used in the above evaluation, is the same as in Ben-Menahem except that ours is a right-hand coordinate system with θ being the negative of his (figures 2 and 3). The r and θ in the integrals are given by

$$\begin{aligned} r &= r_o\left[1 - 2\left(\frac{\xi}{r_o}\right)\cos\theta_o + \left(\frac{\xi}{r_o}\right)^2\right]^{1/2} \\ \theta &= \cos^{-1}\left\{\frac{r_o\cos\theta_o - \xi}{r}\right\} \end{aligned} \tag{126}$$

The evaluation of the integrals is approximate and based on the assumption that the range r is large compared to the wavelength of the surface waves and the horizontal extent of the fault or

$$\begin{aligned} r_o &>> k_{R_j}, k_{L_j} \\ r_o &>> b \end{aligned} \tag{127}$$

$$\{\bar{q}_o\}^{\Delta h, b}_{R_j} = -i\left(\frac{2}{\pi r_o}\right)^{1/2} \cos\theta_o \frac{\bar{L}}{2} k^{-1/2}_{R_j} \begin{bmatrix} \dot{u}^*_o \\ \dot{w}_o \end{bmatrix}_{H_j} O_{R_s} A_{R_j} \left\{\frac{\sin X_R}{X_R}\right\} \times e^{-i\left(\frac{\omega r_o}{c_{R_j}} + X_R - \frac{\pi}{4}\right)}$$

$$\{\bar{w}_o\}^{\Delta h, b}_{R_j} = i\left(\frac{2}{\pi r_o}\right)^{1/2} \cos\theta_o \frac{\bar{L}}{2} k^{-1/2}_{R_j} O_{R_s} A_{R_j} \left\{\frac{\sin X_R}{X_R}\right\} e^{-i\left(\frac{\omega r_o}{c_{R_j}} + X_R - \frac{3\pi}{4}\right)} \tag{128}$$

$$\{\bar{v}_o\}_{L_j} = i\left(\frac{2}{\pi r_o}\right)^{1/2} \sin\theta_o \frac{\bar{L}}{2} k^{-1/2}_{R_j} O_{L_s} A_{L_j} \left\{\frac{\sin X_L}{X_L}\right\} e^{-i\left(\frac{\omega r_o}{c_{L_j}} + X_L - \frac{\pi}{4}\right)}$$

In addition we may extend our model to a strike slip fault by considering a point couple instead of a point force moving along the finite fault plane. We accomplish this by differentiating the point force results with respect to the horizontal coordinate η perpendicular to the fault plane where

$$\frac{\partial}{\partial \eta} = \sin\theta_o \left(\frac{\partial}{\partial r_o}\right) + \frac{\cos\theta_o}{r_o}\left(\frac{\partial}{\partial \theta_o}\right) \tag{129}$$

Equation 129 applies strictly to the single horizontal couple or the vertical line of couples. However, to our order of approximation in the horizontal integration, it can also be applied to the horizontal moving couples on a finite fault. As a result, neglecting all but the lowest order of r_o, we obtain from equations 128

$$\{\bar{q}_o\}^{c,\Delta h,b}_{R_j} = -\left(\frac{2}{\pi r_o}\right)^{1/2} \sin\theta_o \cos\theta_o \frac{\bar{L}'}{2} k^{1/2}_{R_j} \left[\frac{\dot{u}^*_o}{\dot{w}_o}\right]_{H_j} O_{R_s} A_{R_j}$$

$$\times\left\{\frac{\sin X_R}{X_R}\right\} e^{-i\left(\frac{\omega r_o}{c_{R_j}} + X_R - \frac{\pi}{4}\right)}$$

$$\{\bar{w}_o\}^{c,\Delta h,b}_{R_j} = \left(\frac{2}{\pi r_o}\right)^{1/2} \sin\theta_o \cos\theta_o \frac{\bar{L}'}{2} k^{1/2}_{R_j} O_{R_s} A_{R_j}$$

$$\times\left\{\frac{\sin X_R}{X_R}\right\} e^{-i\left(\frac{\omega r_o}{c_{R_j}} + X_R - \frac{3\pi}{4}\right)} \qquad (130)$$

$$\{\bar{v}_o\}^{c,\Delta h,b}_{L_j} = \left(\frac{2}{\pi r_o}\right)^{1/2} \sin^2\theta_o \frac{\bar{L}'}{2} k^{1/2}_{L_j} O_{L_s} A_{L_j} \left\{\frac{\sin X_L}{X_L}\right\} e^{-i\left(\frac{\omega r_o}{c_{L_j}} + X_L - \frac{\pi}{4}\right)}$$

where $\bar{L}'$, the time transformed couple strength has the dimensions of $\bar{L}$ × length or force × time × length.

Synthesis For Time Domain Displacements

In this section we write the displacements for a given source-time variation in such a form that the Fourier inversion can be accomplished numerically using the Aki synthesis with linear amplitude intervals described in Appendix C, Part 1.

We take the following as the time variation at the source for the various sources studied in the previous sections:

1. Pressure-time variation on a cavity of radius a_s

$$\left[p_{os}(t) \right] = \begin{cases} p_{as} e^{-\sigma(t-t_o)} & t > t_o \\ 0 & t < t_o \end{cases} \tag{131}$$

2. Force-time variation

$$\left[L(t) \right] = \begin{cases} L_o e^{-\sigma(t-t_o)} & t > t_o \\ 0 & t < t_o \end{cases} \tag{132}$$

3. Couple-time variation

$$\left[L'(t) \right] = \begin{cases} L'_o e^{-\sigma(t-t_o)} & t > t_o \\ 0 & t < t_o \end{cases} \tag{133}$$

Defining the time Fourier transform as

$$\overline{f} = \int f(t)\ e^{-i\omega t}\, dt$$

we obtain the transformed source functions

$$1.\quad \overline{p}_{os} = \frac{p_{as} e^{-i\omega t_o}}{\sigma + i\omega} \tag{134}$$

$$2.\quad \overline{L} = L_o \frac{e^{-i\omega t_o}}{\sigma + i\omega} \tag{135}$$

$$e.\quad \overline{L'} = L'_o \frac{e^{-i\omega t_o}}{\sigma + i\omega} \tag{136}$$

For use with the inversion program, we write the denominator as

$$\frac{1}{\sigma + i\omega} = \frac{e^{-i\theta_s}}{(\sigma^2 + \omega^2)^{1/2}} \tag{137}$$

where

$$\theta_s = \tan^{-1}\frac{\omega}{\sigma}$$

Substituting the above source transforms in the previous source solutions and inverting where

$$f(t) = \frac{1}{2\pi}\int_{-\infty}^{\infty} \bar{f}\, e^{i\omega t}\, d\omega$$

we obtain the following for large epicentral distances;

1. Buried spherical source, from equations 52,

$$\{W_0\}_{R_j} = \left(\frac{1}{2\pi R}\right)^{1/2} a_s^3 \rho_{as} \int_0^{\infty} 2k_{R_j}^{1/2} \frac{\left\{\frac{1}{2\mu_s}\left[\frac{\sigma_s^*(\omega)}{\frac{\dot{W}_0}{c}}\right]_{H_j} - \left[\frac{\dot{u}_s^*(\omega)}{\dot{W}_0}\right]_{H_j}\right\} A_{R_j} \cos\omega(t-\tau_w)\, d\omega}{(\sigma^2+\omega^2)^{1/2}\left[\left(1-\frac{a_s^2 k_{\beta s}^2}{4}\right)^2 + k_{\alpha s}^2 a_s^2\right]^{1/2}}$$

(138)

$$\{q_0\}_{R_j} = -\left(\frac{1}{2\pi R}\right)^{1/2} a_s^3 \rho_{as} \int_0^{\infty} 2k_{R_j}^{1/2} \left[\frac{\dot{u}_0^*}{\dot{W}_0}\right]_{H_j} \frac{\left\{\frac{1}{2\mu_s}\left[\frac{\sigma_s^*(\omega)}{\frac{\dot{W}_0}{c}}\right]_{H_j} - \left[\frac{\dot{u}_s^*(\omega)}{\dot{W}_0}\right]_{H_j}\right\} A_{R_j} \cos\omega(t-\tau_w)\, d\omega}{(\sigma^2+\omega^2)^{1/2}\left[\left(1-\frac{a_s^2 k_{\beta s}^2}{4}\right)^2 + k_{\alpha s}^2 a_s^2\right]^{1/2}}$$

where

$$\tau_w = t_o + \frac{r}{c_{R_j}} + \frac{\theta_s}{\omega} + \frac{\theta_{SP}}{\omega} - \frac{a_s}{a_s} - \frac{3\pi}{4\omega}$$

$$\tau_u = \tau_w + \frac{\pi}{2\omega}$$

2. Vertical point force at depth, from equations 66,

$$\{w_o\}_{R_j} = -\frac{L_o}{2\pi}\left(\frac{1}{2\pi r}\right)^{1/2}\int_0^\infty 2k_{R_j}^{-1/2}\frac{\left[\frac{\dot{w}_s(D)}{\dot{w}_o}\right]_{H_j} A_{R_j}\cos\omega(t-\tau_w)\,d\omega}{(\sigma^2+\omega^2)^{1/2}}$$

$$\{\bar{q}_o\}_{R_j} = \frac{L_o}{2\pi}\left(\frac{1}{2\pi r}\right)^{1/2}\int_0^\infty 2k_{R_j}^{-1/2}\left[\frac{\dot{u}_o^*}{\dot{w}_o}\right]_{H_j}\frac{\left[\frac{\dot{w}_s(D)}{\dot{w}_o}\right]_{H_j} A_{R_j}\cos\omega(t-\tau_u)\,d\omega}{(\sigma^2+\omega^2)^{1/2}} \qquad (139)$$

where

$$\tau_w = t_o + \frac{r}{c_{R_j}} + \frac{\theta_s}{\omega} - \frac{3\pi}{4\omega}$$

$$\tau_u = \tau_w + \frac{\pi}{2\omega}$$

3. Horizontal point force at depth, from equations 112,

$$\{w_o\}_{R_j} = -\frac{L_o}{2\pi}\left(\frac{1}{2\pi r}\right)^{1/2}\cos\theta\int_0^\infty 2k_{R_j}^{-1/2}\frac{\left[\frac{\dot{u}_s^*(D)}{\dot{w}_o}\right]_{H_j} A_{R_j}\cos\omega(t-\tau_w)\,d\omega}{(\sigma^2+\omega^2)^{1/2}}$$

$$\{q_o\}_{R_j} = -\frac{L_o}{2\pi}\left(\frac{1}{2\pi r}\right)^{1/2}\cos\theta\int_0^\infty 2k_{R_j}^{-1/2}\left[\frac{\dot{u}_o^*}{\dot{w}_o}\right]_{H_j}\frac{\left[\frac{\dot{u}_s^*(D)}{\dot{w}_o}\right]_{H_j} A_{R_j}\cos\omega(t-\tau_u)\,d\omega}{(\sigma^2+\omega^2)^{1/2}} \qquad (140)$$

$$\{v_o\}_{L_j} = \frac{L_o}{2\pi}\left(\frac{1}{2\pi r}\right)^{1/2}\sin\theta\int_0^\infty 2k_{L_j}^{-1/2}\frac{\left[\frac{\dot{v}_s(D)}{\dot{v}_o}\right]_{H_j} A_{L_j}\cos\omega(t-\tau_L)\,d\omega}{(\sigma^2+\omega^2)^{1/2}}$$

where

$$\tau_w = t_o + \frac{r}{c_{R_j}} + \frac{\theta_s}{\omega} - \frac{\pi}{4\omega}$$

$$\tau_u = \tau_w + \frac{\pi}{2\omega}$$

$$\tau_L = t_o + \frac{r}{c_{L_j}} + \frac{\theta_s}{\omega} - \frac{3\pi}{4}$$

where for the above, we have used the Hankel function expansion for ranges (r) large compared to the surface wave length $\left(\frac{2\pi}{k_{R_j}}, \frac{2\pi}{k_{L_j}}\right)$

$$H_m^{(2)}(kr) = \left(\frac{2}{\pi kr}\right)^{1/2} e^{-i\left(kr - \frac{m\pi}{2} - \frac{\pi}{4}\right)}$$

4. Model vertical strike fault, from equations 128,

$$\{W_o\}_{R_j}^{\Delta h, b} = -\frac{L_o}{2\pi}\left(\frac{1}{2\pi r_o}\right)^{1/2} \cos\theta_o \int_0^\infty 2k_{R_j}^{-1/2} A_{R_j} \frac{O_{R_s}}{(\sigma^2+\omega^2)^{1/2}} \left\{\frac{\sin X_R}{X_R}\right\} \cos\omega(t-\tau_w)\, d\omega$$

$$\{q_o\}_{R_t}^{\Delta h, b} = \frac{L_o}{2\pi}\left(\frac{1}{2\pi r_o}\right)^{1/2} \cos\theta_o \int_0^\infty 2k_{R_j}^{-1/2} \left[\frac{U_o}{W_o}^*\right]_{H_j} A_{R_j} \frac{O_{R_s}}{(\sigma^2+\omega^2)^{1/2}} \left\{\frac{\sin X_R}{X_R}\right\} \cos\omega(t-\tau_u)\, d\omega \tag{141}$$

$$\{V_o\}_{L_j}^{\Delta h, b} = \frac{L_o}{2\pi}\left(\frac{1}{2\pi r_o}\right)^{1/2} \sin\theta_o \int_0^\infty 2k_{L_j}^{-1/2} A_{L_j} \frac{O_{L_s}}{(\sigma^2+\omega^2)^{1/2}} \left\{\frac{\sin X_L}{X_L}\right\} \cos\omega(t-\tau_L)\, d\omega$$

where

$$\tau_w = t_o + \frac{r}{c_{R_j}} + \frac{X_R}{\omega} + \frac{\theta_s}{\omega} - \frac{\pi}{4\omega}$$

$$\tau_u = \tau_w + \frac{\pi}{2\omega}$$

$$\tau_L = t_o + \frac{r}{c_{L_j}} + \frac{X_L}{\omega} + \frac{\theta_s}{\omega} - \frac{3\pi}{4\omega}$$

5. Model strike slip fault

$$\{W_o\}_{R_j}^{c,\Delta h,b} = \frac{L_o'}{2\pi}\left(\frac{1}{2\pi r_o}\right)^{1/2} \sin\theta_o \cos\theta_o \int_0^\infty 2k_{R_j}^{1/2} A_{R_j} \frac{O_{RS}}{(\sigma^2+\omega^2)^{1/2}} \left\{\frac{\sin X_R}{X_R}\right\} \cos\omega(t-\tau_w)\, d\omega$$

$$\{q_o\}_{R_j}^{c,\Delta h,b} = \frac{L_o'}{2\pi}\left(\frac{1}{2\pi r_o}\right)^{1/2} \sin\theta_o \cos\theta_o \int_0^\infty 2k_{R_j}^{1/2} \left[\frac{\dot{u}_o^*}{\dot{w}_o}\right]_{H_j} \frac{A_{R_j} O_{RS}}{(\sigma^2+\omega^2)^{1/2}} \left\{\frac{\sin X_R}{X_R}\right\} \cos\omega(t-\tau_w)\, d\omega \quad (142)$$

$$\{V_o\}_{L_j}^{c,\Delta h,b} = \frac{L_o'}{2\pi}\left(\frac{1}{2\pi r_o}\right)^{1/2} \sin^2\theta_o \int_0^\infty 2k_{L_j}^{1/2} A_{L_j} \frac{O_{LS}}{(\sigma^2+\omega^2)^{1/2}} \left\{\frac{\sin X_L}{X_L}\right\} \cos\omega(t-\tau_L)\, d\omega$$

where

$$\tau_w = t_o + \frac{r_o}{c_{R_j}} + \frac{X_R}{\omega} + \frac{\theta_s}{\omega} + \frac{\pi}{4\omega}$$

$$\tau_u = \tau_w + \frac{\pi}{2\omega}$$

and

$$\tau_L = t_o + \frac{r_o}{c_{L_j}} + \frac{X_L}{\omega} + \frac{\theta_s}{\omega} - \frac{\pi}{4\omega}$$

III. DISCUSSION

Almost all previous work on sources in layered elastic media has been restricted to simple layer models. The frequency domain displacements derived in this paper exhibit many of the characteristics inferred from the work on simple models. Obviously, the radial and azimuthal dependence are the same as obtained for simple models. Therefore the factors obtained for a model of a vertical strike slip fault which depend on r and θ are identical to the ones obtained by Ben-Menahem (1960) for the same model. Their application in determining fault parameters such as fault length and rupture velocity is thoroughly described by Ben-Menahem and thus will not be discussed here.

We will restrict our discussion to the effects of source depth and layering on the spectral amplitude of displacements as derived in this paper. Jardetsky (1953) and Kellis-Borok (1953) have also given expressions for these effects in terms of ratios of determinants of order $(4n - 2)$. The significant difference in their formulation and the one given here, is that we are able to simplify the displacement expression so that the effects of layering, source depth and receiver depth are separated into independent factors.

For the various sources investigated, the factors are as follows

1. Explosive source

$$\{\overline{w}(z, D)\}_{R_j} \sim \left[\frac{\dot{w}_R(z)}{\dot{w}_o}\right]_{H_j} \left[\frac{\varphi_s(D)}{\frac{\dot{w}_o}{c}}\right]_{H_j} A_{R_j} k^{\frac{1}{2}} R_j \qquad (143)$$

$$\{\overline{q}(z, D)\}_{R_j} \sim \left[\frac{\dot{u}_R^*(z)}{\dot{w}_o}\right]_{H_j} \left[\frac{\varphi_s(D)}{\frac{\dot{w}_o}{c}}\right]_{H_j} \mathcal{A}_{R_j} k_{R_j}^{\frac{1}{2}}$$

2. Vertical point force

$$\{\overline{w}(z, D)\}_{R_j} \sim \left[\frac{\dot{w}_R(z)}{\dot{w}_o}\right]_{H_j} \left[\frac{\dot{w}_s(D)}{\dot{w}_o}\right]_{H_j} \mathcal{A}_{R_j} k_{R_j}^{-\frac{1}{2}}$$

$$\{\overline{q}(z, D)\}_{R_j} \sim \left[\frac{\dot{u}_R^*(z)}{\dot{w}_o}\right]_{H_j} \left[\frac{\dot{w}_s(D)}{\dot{w}_o}\right]_{H_j} \mathcal{A}_{R_j} k_{R_j}^{-\frac{1}{2}} \qquad (144)$$

3. Horizontal point force

$$\{\overline{w}(z, D)\}_{R_j} \sim \left[\frac{\dot{w}_R(z)}{\dot{w}_o}\right]_{H_j} \left[\frac{\dot{u}_s^*(D)}{\dot{w}_o}\right]_{H_j} \mathcal{A}_{R_j} k_{R_j}^{-\frac{1}{2}}$$

$$\{\overline{q}(z, D)\}_{R_j} \sim \left[\frac{\dot{u}_R^*(z)}{\dot{w}_o}\right]_{H_j} \left[\frac{\dot{u}_s^*(D)}{\dot{w}_o}\right]_{H_j} \mathcal{A}_{R_j} k_{R_j}^{-\frac{1}{2}} \qquad (145)$$

$$\{\overline{v}(z, D)\}_{L_j} \sim \left[\frac{\dot{v}_R(z)}{\dot{v}_o}\right]_{H_j} \left[\frac{\dot{v}_s(D)}{\dot{v}_o}\right]_{H_j} \mathcal{A}_{L_j} k_{L_j}^{-\frac{1}{2}}$$

where the R and s subscripts in the H_j subscripted brackets refer to receiver and source layers respectively. The H_j subscripted quantities in equations 144 and 145 refer to the ratios of velocity or displacement with depth for the homogeneous case in the j^{th} mode. The homogeneous ratio of dilation, φ_s, with depth used in equations 143 can also be given in terms of the homogeneous ratios of horizontal

displacement and normal stress with depth. In the vertical fault models, the source depth effect of equations 45 is replaced by the average value of the point force factor over the vertical dimension of the finite fault. The homogeneous ratios were defined in Chapter II in terms of the THOMSON-HASKELL matrix elements as

$$\left[\frac{\dot{u}_m^*(z)}{\dot{w}_o}\right]_{H_j} = \left[A_{R_m}(z)\right]_{12} + \left[\frac{\dot{u}_o^*}{\dot{w}_o}\right]_{H_j}\left[A_{R_m}(z)\right]_{11}$$

$$\left[\frac{\dot{w}_m(z)}{\dot{w}_o}\right]_{H_j} = \left[A_{R_m}(z)\right]_{22} - \left[\frac{\dot{u}_o^*}{\dot{w}_o}\right]_{H_j}\left[A_{R_m}(z)\right]_{21}^*$$

$$\left[\frac{\sigma_{R_m}^*(z)}{\frac{\dot{w}_o}{c}}\right]_{H_j} = \left[A_{R_m}(z)\right]_{32} + \left[\frac{\dot{u}_o^*}{\dot{w}_o}\right]_{H_j}\left[A_{R_m}(z)\right]_{31}$$

$$\left[\frac{\tau_{R_m}(z)}{\frac{\dot{w}}{c}}\right]_{H_j} = \left[A_{R_m}(z)\right]_{42} - \left[\frac{\dot{u}_o^*}{\dot{w}_o}\right]_{H_j}\left[A_{R_m}(z)\right]_{41}^*$$

$$\left[\frac{\dot{u}_o^*}{\dot{w}_o}\right]_{H_j} = \frac{K}{L^*}$$

$$\left[\frac{\varphi_m(z)}{\frac{\dot{w}_o}{c}}\right]_{H_j} = \frac{\gamma_m}{k_{R_j}^2}\left\{\left[\frac{\dot{u}_m^*(z)}{\dot{w}_o}\right]_{H_j} - \frac{1}{2\mu_m}\left[\frac{\sigma_m^*(z)}{\frac{\dot{w}_o}{c}}\right]_{H_j}\right\}$$

$$\left[\frac{\dot{v}_m(z)}{\dot{v}_o}\right]_{H_j} = \left[A_{L_m}(z)\right]_{11}$$

$$\left[\frac{\tau^{*}_{L_m}(z)}{\frac{\dot{v}_o}{c}}\right]_{H_j} = \left[A_{L_m}(z)\right]^{*}_{21}$$

From equations 143, 144, and 145 we see that the relations between displacement and receiver depth, z, are the same regardless of the type of source considered here. This fact was pointed out by Kellis-Borok and Yanovskaya (1962) as being true for all sources. They failed to realize though that for vector point forces and the explosive source, the relations between displacement and source depth, D, for a given mode j can be expressed by similar relations. From our results, we have as the source depth relations

1. Explosive source

$$\frac{\{\overline{w}(z,D)\}_{R_j}}{\{\overline{w}(z,0)\}_{R_j}} = \frac{\{\overline{q}(z,D)\}_{R_j}}{\{\overline{q}(z,0)\}_{R_j}} = \left[\frac{\varphi_s(D)}{\varphi_s(0)}\right]_{H_j}\left(\frac{\beta_s}{\beta_1}\right)^2\left[\frac{(1-\frac{a_1^2k_{\beta_1}^2}{4})^2 + k_{a_1}^2a_1^2}{(1-\frac{a_s^2k_{\beta_s}^2}{4})^2 + k_{a_s}^2a_s^2}\right]^{\frac{1}{2}}\frac{p_{os}}{p_{01}}\left(\frac{a_s}{a_1}\right)^3 \quad (146)$$

2. Vertical point force

$$\frac{\{\overline{w}(z,D)\}_{R_j}}{\{\overline{w}(z,0)\}_{R_j}} = \frac{\{\overline{q}(z,D)\}_{R_j}}{\{\overline{q}(z,0)\}_{R_j}} = \frac{\{\overline{w}(D,z)\}_{R_j}}{\{\overline{w}(0,z)\}_{R_j}} = \left[\frac{\dot{w}_s(D)}{\dot{w}_o}\right]_{H_j} \quad (147)$$

3. Horizontal point force

$$\frac{\{\overline{w}(z, D)\}_{R_j}}{\{\overline{w}(z, 0)\}_{R_j}} = \frac{\{\overline{q}(z, D)\}_{R_j}}{\{\overline{q}(z, 0)\}_{R_j}} = \frac{\{\overline{q}(D, z)\}_{R_j}}{\{\overline{q}(0, z)\}_{R_j}}$$
$$= \left[\frac{\dot{u}_s^*(D)}{\dot{w}_o}\right]_{H_j} \tag{148}$$

$$\frac{\{\overline{v}(z, D)\}_{L_j}}{\{\overline{v}(z, 0)\}_{L_j}} = \frac{\{v(D, z)\}_{L_j}}{\{v(0, z)\}_{L_j}}$$
$$= \left[\frac{\dot{v}_s(D)}{\dot{v}_o}\right]_{H_j}$$

For volume sources, not considered in this paper, Kellis-Borok and Yanovskaya (1962) give a set of formulas taken from M. G. Niegaus which allow one to calculate source depth relations. This is accomplished by performing integrations over the vertical coordinate of the homogeneous solutions weighted by the actual source forces.

Actually the source depth relations given in equations 147 and 148 could have been determined using theorems on scalar and elastic reciprocity given by, among others, Rayleigh (1855) and Knopoff and Gangi (1958). These theorems apply to the total motion but as seen from our results, they are also true for the surface wave contribution to the total motion. For Rayleigh waves we see that the vertical surface displacement at A due to an internal horizontal point force at B is equal to the horizontal displacement at B due to a surface vertical

point force of the same strength at A. Love waves obey scalar reciprocity in that the source and receiver depth factors are interchangeable.

Sherwood and Spencer (1962) using another reciprocity theorem by Rayleigh (1855) postulated that the surface displacement at A due to an internal dilatational source at B is identical to the dilatation at B produced by a vertical point force at A. From our results we see that this is true if the magnitude of the force is properly normalized to the dilatation source, that is, if we set the coefficient of the radial part of the dilatation source in equation 1 equal to unity then our vertical force, $\overline{L}$, must be of magnitude $i4\pi\omega^2\rho_s$.

The factors A_R and A_L for Rayleigh and Love waves respectively are independent of source and receiver depth and also the type of source and receiver. They depend only on the properties of the layers in the array. From equations 66, $\frac{A_R}{2}$ can be considered as the spectral vertical response of Rayleigh waves at the free surface to a unit vertical surface point force after removing the transmission effect in the r direction. Similarly from equations 110, $\frac{A_L}{2}$ is the spectral SH response of Love waves at the free surface to a unit horizontal surface point force.

Computer programs based on the THOMSON-HASKELL matrices for the computation of dispersion (c, T) in multilayered halfspaces yield the homogeneous motion stress ratios as a by product. Several such programs are described in the literature. Using the technique given in Part I to calculate analytic $(\frac{\partial F}{\partial k})_\omega$, it is therefore possible to modify these programs to compute analytically values of A_R and A_L as a function of phase velocity or frequency.

The estimation of source depth from surface wave data has intrigues seismologists for many years. Basically the methods were limited by not knowing the relative excitation from one frequency to another for a given mode and from one mode to another for a given frequency. This relative excitation is given by the variation in $\mathcal{A}_R$ and $\mathcal{A}_L$ with frequency and mode. All previous attempts have been based on the results of simple layer models. Now we may use values of $\mathcal{A}_R$ and $\mathcal{A}_L$ for more realistic earth models in these estimates.

With this possibility in mind, we now write down the spectral ratios of displacement for a vector point force at a vertical angle of δ with the horizontal

$$\frac{\left|\{\overline{w}_o\}_{R_\ell}\right|}{\left|\{\overline{w}_o\}_{R_j}\right|} = \frac{\cos\theta \left[\frac{\dot{u}_s^*(D)}{\dot{w}_o}\right]_{H_\ell} + \tan\delta \left[\frac{\dot{w}_s(D)}{\dot{w}_o}\right]_{H_\ell}}{\cos\theta \left[\frac{\dot{u}_s^*(D)}{\dot{w}_o}\right]_{H_j} + \tan\delta \left[\frac{\dot{w}_s(D)}{\dot{w}_o}\right]_{H_j}} \frac{\mathcal{A}_{R_\ell}}{\mathcal{A}_{R_j}} \left(\frac{c_{R_\ell}}{c_{R_j}}\right)^{\frac{1}{2}} \tag{149}$$

$$\frac{\left|\{\overline{v}_o\}_{L_\ell}\right|}{\left|\{\overline{v}_o\}_{L_j}\right|} = \frac{\left[\frac{\dot{v}_s(D)}{\dot{v}_o}\right]_{H_\ell}}{\left[\frac{\dot{v}_s(D)}{\dot{v}_o}\right]_{H_j}} \frac{\mathcal{A}_{L_\ell}}{\mathcal{A}_{L_j}} \left(\frac{c_{L_\ell}}{c_{L_j}}\right)^{\frac{1}{2}} \tag{150}$$

$$\frac{\left|\{\overline{w}_o\}_{R_j}\right|}{\left|\{\overline{v}_o\}_{L_j}\right|} = \frac{\cos\theta \left[\frac{\dot{u}_s^*(D)}{\dot{w}_o}\right]_{H_j} + \tan\delta \left[\frac{\dot{w}_s(D)}{\dot{w}_o}\right]_{H_j}}{\sin\theta \left[\frac{\dot{v}_s(D)}{\dot{v}_o}\right]_{H_j}} \frac{\mathcal{A}_{R_j}}{\mathcal{A}_{L_j}} \left(\frac{c_{R_j}}{c_{L_j}}\right)^{\frac{1}{2}} \tag{151}$$

where ℓ and j are different modes. The use of matched digital seismographs and computer programs for epicenter location and spectral analysis allow one to readily combine the horizontal components to form a horizontal tranverse component, v_o, and to obtain its spectral amplitude. Assuming that v_o can be obtained either by the above or a fortuitous alignment between horizontal seismographs and epicenter, equation 150 is the least effected by possibly unknown parameters such as θ and δ. Using group velocity windows and performing a series of narrow band spectral analyses to separate modes (Alexander, 1963) we can form the ratio given in equation 150 and obtain its frequency dependence. After a structure has been found which agrees with the observed dispersion, which is independent of depth, one can determine the mode order and then eliminate A_L and c_L from equation 150 leaving the homogeneous ratios for different modes. Comparing the resultant values with theoretical curves for various depths gives an estimate of the source depth.

If there is no appreciable Love type motion for any azimuth, we can assume that the event has either explosive or involved mostly vertical motion at the source. For a vertical point force, we let $\delta = 90^o$ in equation 149 and then can perform an analysis on w_o corresponding to equation 150 to obtain a fault depth estimate. If the source is explosive, we have a ratio similar to the $\delta = 90^o$ form of equation 150 involving the variation of dilatation with depth from mode to mode.

If the source involves primarily horizontal motion, equation 151 is especially attractive, particularly if θ can be determined by either after shocks or fault plane solutions. This is due to the fact that,

except for structures with extremely low velocity zones at depth (Harkrider, Hales, and Press, 1963), the quantity $\left[\frac{\dot{u}_s^*(D)}{\dot{w}_o}\right]_{H_j}$ for fundamental mode Rayleigh waves at a given depth has only one zero in the frequency domain, and the Love ratio none. Thus the presence of a strong minimum in the spectral ratios is then diagnostic of the source depth.

The above techniques hold strictly only for point sources and explosions. For finite faults with a rupture velocity and amplitude, the amplitude picture is complicated by the directivity or $\left\{\frac{\sin X_R}{X_R}\right\}$ and $\left\{\frac{\sin X_L}{X_L}\right\}$. If the epicenter is surrounded by enough matched instruments, it may be possible to remove this factor or give a reasonable bound on its effect.

Another technique is to construct theoretical seismograms for different structures, source types and source depths using the relations in the synthesis section. Then we compare the theoretical seismograms to see if the various parameters have qualitative characteristics in the time domain. This will be done in later papers.

Although the above techniques have all been suggested in the past by other authors they were never carried out because of the unwieldy formulation and the difficulties of numerical evaluation. The techniques developed here remove these difficulties and make possible direct comparison of theory and data to yield additional information about the source.

IV. CONCLUSIONS

The most important theoretical result obtained from this investigation of point sources is that the spectral amplitude can be factored into terms representing, separately, the effect of layering, source, and receiver. These factors may be summarized as follows;

1. The factor representing the layering, A_R or A_L depends on the layered earth structure and the type of surface wave motion under consideration. This term remains unchanged for the different types of source, source depth, receiver depth, epicentral distance, and azimuth.

2. The effect of source and receiver depth can be determined from the same set of relations. These relations are the motion-stress ratios for the homogeneous problem. The particular combination of ratios depends on the type of source and receiver.

For our models of the vertical fault, the above separation also holds. This is because, to our order of approximation, the horizontal source integration is equivalent to keeping the spectral amplitude constant while varying the phase over the fault surface. From the exact vertical integration over the extended source we introduce a concept of a mean value of the source depth. However one would expect that for more realistic volume sources this result would prove approximately valid especially at large epicentral distance compared to the wave length and source dimensions.

The obvious advantages of the factoring is that the homogeneous stress and displacement ratios, and the layering effect need be calculated only once for a given frequency and mode. Once these quantities are

plotted, they can easily be used to calculate the spectrum under many different conditions of source type, source depth, and receiver depth.

For many years the homogeneous stress and displacement ratios were calculated as a function of depth as standard procedure in computer programs used for calculating dispersion of Rayleigh and Love waves on multilayered elastic halfspaces. At the Cal Tech Seismological Laboratory as part of the research here described, the Rayleigh and Love dispersion programs have been converted to calculate also the layering effects A_R and A_L.

The use of digital seismographs in recent years has made possible the routine Fourier analysis of a large number of seismic events. Up to the present, only the phase and directivity information obtained from this data have been used to estimate source parameters. The use of directivity has been restricted to sources of large enough magnitudes to create waves which circle the world. The calculation of the effect of source depth on spectral amplitude using previous techniques was prohibitively slow and expensive, even on large computers. Now with stress and displacement ratios calculated for realistic earth structures, one can use a desk calculator to estimate source depth and type for relatively small events from their spectral amplitude.

APPENDIX A

MATRIX AND VECTOR RELATIONS FOR A GENERAL SOURCE IN AN ELASTIC LAYER

In obtaining expressions for Rayleigh and Love type surface waves generated by point sources in Chapter 11, we used vector and matrix relations for z dependent quantities characteristics of each type of wave. These relations are derived in this appendix. The derivation is essentially a reorganization of the matrix formulation given by Haskell (1953) for an elastic layer without a source. His results are rederived in such a manner as to make the inclusion of a general point source in the layer a simple and straightforward extension of the formulation.

Rayleigh

Consider an elastic layer m with the following z dependent quantities defined by

$$\frac{\dot{u}_{Rm}(z)}{c} = k^2\left[\varphi_m(z) + \frac{d\psi_m(z)}{dz}\right]$$

$$\frac{\dot{w}_{Rm}(z)}{c} = ik\left[\frac{d\varphi_m(z)}{dz} + \frac{d^2\psi_m(z)}{dz^2} + k_{\beta m}^2\,\psi_m(z)\right]$$

$$\sigma_{Rm}(z) = 2\mu_m\left[\frac{d^2\varphi_m(z)}{dz^2} + \frac{d^3\psi_m(z)}{dz^3} + k_{\beta m}^2\,\frac{d\psi_m(z)}{dz}\right] - \lambda_m k_{\alpha m}^2\,\varphi_m(z) \qquad (1)$$

$$\tau_{Rm}(z) = -ik\mu_m\left[2\frac{d\varphi_m(z)}{dz} + 2\frac{d^2\psi_m(z)}{dz^2} + k_{\beta m}^2\,\psi_m(z)\right]$$

where the potentials $\varphi_m(z)$ and $\psi_m(z)$ are solutions of

$$\frac{d^2\varphi_m(z)}{dz^2} = -k^2\Pi_{\alpha m}^2\,\varphi_m(z)$$
$$\frac{d^2\psi_m(z)}{dz^2} = -k^2\Pi_{\beta m}^2\,\psi_m(z) \qquad (2)$$

For layers not containing a source, we use for $\varphi_m(z)$ and $\psi_m(z)$ the general solutions of equations 2 with arbitrary coefficients.

$$\varphi_m(z) = \underline{\Delta}'_m\, e^{-ik\Pi_{\alpha m}z} + \underline{\Delta}''_m\, e^{ik\Pi_{\alpha m}z}$$
$$\psi_m(z) = \underline{\omega}'_m\, e^{-ik\Pi_{\beta m}z} + \underline{\omega}''_m\, e^{ik\Pi_{\beta m}z} \qquad (3)$$

Defining

$$\underline{\Delta}'_m = -k^2\left(\frac{c}{\alpha_m}\right)^2 e^{-ik\Pi_{\alpha m}z_{m-1}}\underline{\Delta}'_m,\quad \underline{\Delta}''_m = -k^2\left(\frac{c}{\alpha_m}\right)^2 e^{ik\Pi_{\alpha m}z_{m-1}}\underline{\Delta}''_m$$
$$\underline{\omega}'_m = i\frac{k^3}{\gamma_m}e^{-ik\Pi_{\beta m}z_{m-1}}\underline{\omega}'_m \quad\text{and}\quad \underline{\omega}''_m = i\frac{k^3}{\gamma_m}e^{ik\Pi_{\beta m}z_{m-1}}\underline{\omega}''_m \qquad (4)$$

and substituting equations 3 in equations 1, we obtain

$$\frac{\underline{u}_{Rm}(z)}{c} = -\left(\frac{\alpha_m}{c}\right)^2\Big[(\underline{\Delta}'_m + \underline{\Delta}''_m)\cos k\Pi_{\alpha m}(z-z_{m-1}) - i(\underline{\Delta}'_m - \underline{\Delta}''_m)\sin k\Pi_{\alpha m}(z-z_{m-1})\Big]$$
$$-\gamma_m\Pi_{\beta m}\Big[(\underline{\omega}'_m - \underline{\omega}''_m)\cos k\Pi_{\beta m}(z-z_{m-1}) - i(\underline{\omega}'_m + \underline{\omega}''_m)\sin k\Pi_{\beta m}(z-z_{m-1})\Big]$$

$$\frac{\underline{w}_{Rm}(z)}{c} = -\left(\frac{\alpha_m}{c}\right)^2\Pi_{\alpha m}\Big[-i(\underline{\Delta}'_m + \underline{\Delta}''_m)\sin k\Pi_{\alpha m}(z-z_{m-1}) + (\underline{\Delta}'_m - \underline{\Delta}''_m)\cos k\Pi_{\alpha m}(z-z_{m-1})\Big] \qquad (5)$$
$$+\gamma_m\Big[-i(\underline{\omega}'_m - \underline{\omega}''_m)\sin k\Pi_{\beta m}(z-z_{m-1}) + (\underline{\omega}'_m + \underline{\omega}''_m)\cos k\Pi_{\beta m}(z-z_{m-1})\Big]$$

$$\sigma_{Rm}(z) = -\rho_m \alpha_m^2 (\gamma_m - 1)\left[(\underline{\Delta}_m' + \underline{\Delta}_m'')\cos k\eta_{\alpha m}(z - z_{m-1}) - i(\underline{\Delta}_m' - \underline{\Delta}_m'')\sin k\eta_{\alpha m}(z - z_{m-1})\right]$$

$$-\rho_m c^2 \gamma_m \eta_{\beta m}\left[(\underline{\omega}_m' - \underline{\omega}_m'')\cos k\eta_{\beta m}(z - z_{m-1}) - i(\underline{\omega}_m' + \underline{\omega}_m'')\sin k\eta_{\beta m}(z - z_{m-1})\right]$$

$$\tau_{Rm}(z) = \rho_m \alpha_m^2 \gamma_m \eta_{\alpha m}\left[-i(\underline{\Delta}_m' + \underline{\Delta}_m'')\sin k\eta_{\alpha m}(z - z_{m-1}) + (\underline{\Delta}_m' - \underline{\Delta}_m'')\cos k\eta_{\alpha m}(z - z_{m-1})\right]$$

$$-\rho_m c^2 \gamma_m (\gamma_m - 1)\left[-i(\underline{\omega}_m' - \underline{\omega}_m'')\sin k\eta_{\beta m}(z - z_{m-1}) + (\underline{\omega}_m' + \underline{\omega}_m'')\cos k\eta_{\beta m}(z - z_{m-1})\right]$$

where we have made use of the following relations

$$k^2\eta_{\alpha m}^2 = k_{\alpha m}^2 - k^2 \quad , \qquad k^2\eta_{\beta m}^2 = k_{\beta m}^2 - k^2$$

$$k_{\alpha m}^2 = \frac{k^2 c^2}{\alpha_m^2} = \frac{k^2 c^2 \rho_m}{(\lambda_m + 2\mu_m)} \quad , \qquad k_{\beta m}^2 = \frac{k^2 c^2}{\beta_m^2} = \frac{k^2 c^2 \rho_m}{\mu_m} \tag{6}$$

and

$$\gamma_m = 2\left(\frac{\beta_m}{c}\right)^2$$

Evaluating equations 5 at $z = z_{m-1}$ and writing the result in vector notation, we have

$$\begin{bmatrix} \frac{\dot{\underline{u}}}{c}_{Rm}(z_{m-1}) \\ \frac{\dot{\underline{w}}}{c}_{Rm}(z_{m-1}) \\ \sigma_{Rm}(z_{m-1}) \\ \tau_{Rm}(z_{m-1}) \end{bmatrix} = E_{Rm} \begin{bmatrix} \underline{\Delta}_m' + \underline{\Delta}_m'' \\ \underline{\Delta}_m' - \underline{\Delta}_m'' \\ \underline{\omega}_m' - \underline{\omega}_m'' \\ \underline{\omega}_m' + \underline{\omega}_m'' \end{bmatrix} \tag{7}$$

where the matrix E_{R_m} is

$$E_{R_m} = \begin{bmatrix} -\left(\frac{\alpha_m}{c}\right)^2 & 0 & -\gamma_m \Pi_{\beta m} & 0 \\ 0 & -\left(\frac{\alpha_m}{c}\right)^2 \Pi_{\alpha m} & 0 & \gamma_m \\ -\rho_m \alpha_m^2 (\gamma_m - 1) & 0 & -\rho_m c^2 \gamma_m^2 \Pi_{\beta m} & 0 \\ 0 & \rho_m \alpha_m^2 \gamma_m \Pi_{\alpha m} & 0 & -\rho_m c^2 \gamma_m (\gamma_m - 1) \end{bmatrix} \tag{8}$$

Similarily, evaluating equations 5 at $z = z_m$ yields

$$\begin{bmatrix} \frac{\dot{u}_{R_m}(z_m)}{c} \\ \frac{\dot{w}_{R_m}(z_m)}{c} \\ \sigma_{R_m}(z_m) \\ \tau_{R_m}(z_m) \end{bmatrix} = D_{R_m} \begin{bmatrix} \underline{\Delta}'_m + \underline{\Delta}''_m \\ \underline{\Delta}'_m - \underline{\Delta}''_m \\ \underline{\omega}'_m - \underline{\omega}''_m \\ \underline{\omega}'_m + \underline{\omega}''_m \end{bmatrix} \tag{9}$$

where

$$D_{R_m} = \begin{bmatrix} -\left(\frac{\alpha_m}{c}\right)\cos P_m & i\left(\frac{\alpha_m}{c}\right)^2 \sin P_m & -\gamma_m \Pi_{\beta m} \cos Q_m & i\gamma_m \Pi_{\beta m} \sin Q_m \\ i\left(\frac{\alpha_m}{c}\right)^2 \Pi_{\alpha m} \sin P_m & -\left(\frac{\alpha_m}{c}\right)^2 \Pi_{\alpha m} \cos P_m & -i\gamma_m \sin Q_m & \gamma_m \cos Q_m \\ -\rho_m \alpha_m^2 (\gamma_m - 1)\cos P_m & i\rho_m \alpha_m^2 (\gamma_m - 1)\sin P_m & -\rho_m c^2 \gamma_m^2 \Pi_{\beta m} \cos Q_m & i\rho_m c^2 \gamma_m^2 \Pi_{\beta m} \sin Q_m \\ -i\rho_m \alpha_m^2 \gamma_m \Pi_{\alpha m} \sin P_m & \rho_m \alpha_m^2 \gamma_m \Pi_{\alpha m} \cos P_m & i\rho_m c^2 \gamma_m (\gamma_m - 1)\sin Q_m & -\rho_m c^2 \gamma_m (\gamma_m - 1)\cos Q_m \end{bmatrix} \tag{10}$$

$$P_m = k\Pi_{\alpha m} d_m \quad , \quad Q_m = k\Pi_{\beta m} d_m \qquad \text{and} \quad d_m = z_m - z_{m-1}$$

Combining equations 7 and 9, we obtain

$$\begin{bmatrix} \frac{u}{c}_{Rm}(z_m) \\ \frac{w}{c}_{Rm}(z_m) \\ \sigma_{Rm}(z_m) \\ T_{Rm}(z_m) \end{bmatrix} = a_{Rm} \begin{bmatrix} \frac{u}{c}_{Rm}(z_{m-1}) \\ \frac{w}{c}_{Rm}(z_{m-1}) \\ \sigma_{Rm}(z_{m-1}) \\ T_{Rm}(z_{m-1}) \end{bmatrix} \tag{11}$$

where

$$a_{Rm} = D_{Rm} E_{Rm}^{-1}$$

and the inverse of E_{R_m} is

$$E_{Rm}^{-1} = \begin{bmatrix} -2\left(\frac{\beta_m}{\alpha_m}\right)^2 & 0 & (\rho_m \alpha_m^2)^{-1} & 0 \\ 0 & c^2(\gamma_m - 1)/(\alpha_m^2 \Pi_{\alpha m}) & 0 & (\rho_m \alpha_m^2 \Pi_{\alpha m})^{-1} \\ (\gamma_m - 1)/(\gamma_m \Pi_{\beta m}) & 0 & -(\rho_m c^2 \gamma_m \Pi_{\beta m})^{-1} & 0 \\ 0 & 1 & 0 & (\rho_m c^2 \gamma_m)^{-1} \end{bmatrix} \tag{12}$$

From equations 10 and 12, the elements of the layer matrix a_{R_m} is

$$(a_{Rm})_{11} = (a_{Rm})_{44} = \gamma_m \cos P_m - (\gamma_m - 1)\cos Q_m$$

$$(a_{Rm})_{12} = (a_{Rm})_{34} = i\left[(\gamma_m - 1)\frac{\sin P_m}{\Pi_{\alpha m}} - \gamma_m \Pi_{\beta m} \sin Q_m\right.$$

$$(a_{Rm})_{13} = (a_{Rm})_{24} = -(\rho_m c^2)^{-1}\left[\cos P_m - \cos Q_m\right]$$

$$(a_{Rm})_{14} = i(\rho_m c^2)^{-1}\left[\frac{\sin P_m}{\Pi_{\alpha m}} + \Pi_{\beta m} \sin Q_m\right]$$

$$(a_{Rm})_{21} = (a_{Rm})_{43} = -i\left[\gamma_m \Pi_{\alpha m} \sin P_m + (\gamma_m - 1)\sin \frac{Q_m}{\Pi_{\beta m}}\right] \tag{13}$$

$$(a_{km})_{22} = (a_{km})_{33} = -(\gamma_m - 1)\cos P_m + \gamma_m \cos Q_m$$

$$(a_{km})_{23} = i(\rho_m c^2)^{-1}\left[\Pi_{\alpha m} \sin P_m + \frac{\sin Q_m}{\Pi_{\beta m}}\right]$$

$$(a_{km})_{31} = (a_{km})_{42} = \rho_m c^2 \gamma_m (\gamma_m - 1)\left[\cos P_m - \cos Q_m\right]$$

$$(a_{km})_{32} = i\rho_m c^2\left[(\gamma_m - 1)^2 \frac{\sin P_m}{\Pi_{\alpha m}} + \gamma_m^2 \Pi_{\beta m} \sin Q_m\right]$$

$$(a_{km})_{41} = i\rho_m c^2\left[\gamma_m^2 \Pi_{\alpha m} \sin P_m + (\gamma_m - 1)^2 \frac{\sin Q_m}{\Pi_{\beta m}}\right]$$

For the source layer s defined by the planes z_s and z_{s-1}, we use a general point source located at D ($z_s > D > z_{s-1}$) such that the source potentials $\varphi_{so}(z)$ and $\psi_{so}(z)$ are solutions of equations 2 everywhere in s and continuous with continuous derivatives except at D, or

$$\varphi_{so}(z) = S_{01}^{\pm} e^{-ik\Pi_{\alpha s}|z-D|} \qquad \pm \text{ as } z \gtrless D$$

$$\psi_{so}(z) = S_{02}^{\pm} e^{-ik\Pi_{\beta s}|z-D|} \qquad (14)$$

Combining equations 14 with the solutions of equations 2 with arbitrary coefficients, the general potentials for the source layer are

$$\varphi_s(z) = S_{01}^{\pm} e^{-ik\Pi_{\alpha s}|z-D|} + \underline{A}_s' e^{-ik\Pi_{\alpha s} z} + \underline{A}_s'' e^{ik\Pi_{\alpha s} z} \qquad (15)$$

$$\psi_s(z) = S_{02}^{\pm} e^{-ik\Pi_{\beta s}|z-D|} + \underline{\omega}_s' e^{-ik\Pi_{\beta s} z} + \underline{\omega}_s'' e^{ik\Pi_{\beta s} z}$$

or rewriting

$$\Phi_s(z) = (S_{01}^{+} e^{ik\eta_{\alpha s} D} + \underline{\underline{\Delta}}_s') e^{-ik\eta_{\alpha s} z} + \underline{\underline{\Delta}}_s'' e^{ik\eta_{\alpha s} z} \qquad z_s \geq z > D$$

$$\Psi_s(z) = (S_{02}^{+} e^{ik\eta_{\beta s} D} + \underline{\underline{\omega}}_s') e^{-ik\eta_{\beta s} z} + \underline{\underline{\omega}}_s'' e^{ik\eta_{\beta s} z}$$

$$\Phi_s(z) = \underline{\underline{\Delta}}_s' e^{-ik\eta_{\alpha s} z} + (\underline{\underline{\Delta}}_s'' + S_{01}^{-} e^{-ik\eta_{\alpha s} D}) e^{ik\eta_{\alpha s} z} \qquad D > z \geq z_{s-1} \tag{16}$$

$$\Psi_s(z) = \underline{\underline{\omega}}_s' e^{-ik\eta_{\beta s} z} + (\underline{\underline{\omega}}_s'' + S_{02}^{-} e^{-ik\eta_{\beta s} D}) e^{ik\eta_{\beta s} z}$$

Decomposing layer s into two layers with the same elastic constants; layer; layer s_2 for $z_s \geq z \geq D$ and layer s_1 for $D \geq z \geq z_{s-1}$, and defining new constants

$$\underline{\underline{\Delta}}_{s2}' = S_{01}^{+} e^{ik\eta_{\alpha s} D} + \underline{\underline{\Delta}}_s' \quad , \quad \underline{\underline{\Delta}}_{s2}'' = \underline{\underline{\Delta}}_{s2}'' = \underline{\underline{\Delta}}_s''$$

$$\underline{\underline{\omega}}_{s2}' = S_{02}^{+} e^{ik\eta_{\beta s} D} + \underline{\underline{\omega}}_s' \quad , \quad \underline{\underline{\omega}}_{s2}'' = \underline{\underline{\omega}}_s'' \tag{17}$$

$$\underline{\underline{\Delta}}_{s1}' = \underline{\underline{\Delta}}_s' \quad , \quad \underline{\underline{\Delta}}_{s1}'' = \underline{\underline{\Delta}}_s'' + S_{01}^{-} e^{-ik\eta_{\alpha s} D}$$

$$\underline{\underline{\omega}}_{s1}' = \underline{\underline{\omega}}_s' \quad \text{and} \quad \underline{\underline{\omega}}_{s1}'' = \underline{\underline{\omega}}_s'' + S_{02}^{-} e^{-ik\eta_{\beta s} D}$$

we can write equation 16

$$\Phi_{s2}(z) = \underline{\underline{\Delta}}_{s2}' e^{-ik\eta_{\alpha s} z} + \underline{\underline{\Delta}}_{s2}'' e^{ik\eta_{\alpha s} z} \qquad z_s \geq z \geq D$$

$$\Psi_{s2}(z) = \underline{\underline{\omega}}_{s2}' e^{-ik\eta_{\beta s} z} + \underline{\underline{\omega}}_{s2}'' e^{ik\eta_{\beta s} z} \tag{18}$$

$$\Phi_{s1}(z) = \underline{\underline{\Delta}}_{s1}' e^{-ik\eta_{\alpha s} z} + \underline{\underline{\Delta}}_{s1}'' e^{ik\eta_{\alpha s} z} \qquad D \geq z \geq z_{s-1}$$

$$\Psi_{s1}(z) = \underline{\underline{\omega}}_{s1}' e^{-ik\eta_{\beta s} z} + \underline{\underline{\omega}}_{s1}'' e^{ik\eta_{\beta s} z}$$

Comparing equations 18 with 3 and the relations derived from equation 3, we have the following relations for the source layer

$$\begin{bmatrix} \frac{\dot{u}_{R_{s2}}}{c}(z_s) \\ \frac{\dot{w}_{R_{s2}}}{c}(z_s) \\ \sigma_{R_{s2}}(z_s) \\ \tau_{R_{s2}}(z_s) \end{bmatrix} = a_{R_{s2}} \begin{bmatrix} \frac{\dot{u}_{R_{s2}}}{c}(D) \\ \frac{\dot{w}_{R_{s2}}}{c}(D) \\ \sigma_{R_{s2}}(D) \\ \tau_{R_{s2}}(D) \end{bmatrix}$$

$$\begin{bmatrix} \frac{\dot{u}_{R_{s1}}}{c}(D) \\ \frac{\dot{w}_{R_{s1}}}{c}(D) \\ \sigma_{R_{s1}}(D) \\ \tau_{R_{s1}}(D) \end{bmatrix} = a_{R_{s1}} \begin{bmatrix} \frac{\dot{u}_{R_{s1}}}{c}(z_{s-1}) \\ \frac{\dot{w}_{R_{s1}}}{c}(z_{s-1}) \\ \sigma_{R_{s1}}(z_{s-1}) \\ \tau_{R_{s1}}(z_{s-1}) \end{bmatrix} \qquad (19)$$

where the elements $a_{R_{s2}}$ and $a_{R_{s1}}$ are identical with the exception that

$$d_{s2} = z_s - D \qquad \text{and} \qquad d_{s1} = D - z_{s-1}$$

Furthermore it can be shown that their matrix product yields

$$a_{R_s} = a_{R_{s2}}\, a_{R_{s1}}$$

where a_{R_s} is the layer matrix for layer s if no source is present. In addition we have the vector equation

$$\begin{bmatrix} \frac{\dot{u}_{R_{s2}}}{c}(D) \\ \frac{\dot{w}_{R_{s2}}}{c}(D) \\ \sigma_{R_{s2}}(D) \\ \tau_{R_{s2}}(D) \end{bmatrix} = \begin{bmatrix} \frac{\dot{u}_{R_{s1}}}{c}(D) \\ \frac{\dot{w}_{R_{s1}}}{c}(D) \\ \sigma_{R_{s1}}(D) \\ \tau_{R_{s1}}(D) \end{bmatrix} + \begin{bmatrix} \delta\left(\frac{\dot{u}_{R_s}}{c}\right) \\ \delta\left(\frac{\dot{w}_{R_s}}{c}\right) \\ \delta\,\sigma_{R_s} \\ \delta\,\tau_{R_s} \end{bmatrix} \qquad (20)$$

where from equations 1 and 16

$$\delta\left(\frac{\dot{u}_{Rs}}{c}\right) = k^2\left[(S_{01}^{+} - S_{01}^{-}) - ik\eta_{\beta s}(S_{02}^{+} + S_{02}^{-})\right]$$

$$\delta\left(\frac{\dot{w}_{Rs}}{c}\right) = ik\left[-ik\eta_{\alpha s}(S_{01}^{+} + S_{01}^{-}) + k^2(S_{02}^{+} - S_{02}^{-})\right] \qquad (21)$$

$$\delta\sigma_{Rs} = k^2c^2\rho_s\left[(\gamma_s - 1)(S_{01}^{+} - S_{02}^{-}) - ik\eta_{\beta s}\gamma_s(S_{02}^{+} + S_{02}^{-})\right]$$

$$\delta\tau_{Rs} = k^2c^2\rho_s\left[-\gamma_s\eta_{\alpha s}(S_{01}^{+} + S_{01}^{-}) - ik(\gamma_s - 1)(S_{02}^{+} - S_{02}^{-})\right]$$

Love

For Love wave propagation, we are concerned with the following z dependent quantities defined by

$$\frac{\dot{v}_{Lm}}{c} = ik^2\chi_m(z)$$

$$\tau_{Lm} = k\mu_m\frac{d\chi_m(z)}{dz} \qquad (22)$$

where the potential $\chi_m(z)$ is a solution of

$$\frac{d^2\chi_m(z)}{dz^2} = -k^2\eta_{\beta m}^2\chi_m(z) \qquad (23)$$

Similar to the preceding section, we form $\chi_m(z)$ from the general solutions of equation 23 for layers without a source

$$\chi_m(z) = \underline{\underline{\epsilon}}_m' e^{-ik\eta_{\beta m}z} + \underline{\underline{\epsilon}}_m'' e^{ik\eta_{\beta m}z} \qquad (24)$$

and substitute into equation 22. Defining

$$\underline{\epsilon}_m' = k e^{-ik\eta_{\beta m}z_{m-1}}\underline{\underline{\epsilon}}_m' \qquad \text{and} \qquad \underline{\epsilon}_m'' = k e^{ik\eta_{\beta m}z_{m-1}}\underline{\underline{\epsilon}}_m''$$

we obtain

$$\frac{\dot{V}_{Lm}}{c}(z) = (\epsilon_m' + \epsilon_m'')ik\cos k\eta_{\beta m}(z-z_{m-1}) + (\epsilon_m' - \epsilon_m'')k\sin k\eta_{\beta m}(z-z_{m-1}) \tag{25}$$

$$T_{Lm}(z) = -(\epsilon_m' + \epsilon_m'')k\mu_m\eta_{\beta m}\sin k\eta_{\beta m}(z-z_{m-1}) - (\epsilon_m' - \epsilon_m'')ik\mu_m\eta_{\beta m}\cos k\eta_{\beta m}(z-z_{m-1})$$

Evaluating equations 25 at $z = z_{m-1}$, yields

$$\begin{bmatrix} \frac{\dot{V}_{Lm}}{c}(z_{m-1}) \\ T_{Lm}(z_{m-1}) \end{bmatrix} = E_{Lm} \begin{bmatrix} \epsilon_m' + \epsilon_m'' \\ \epsilon_m' - \epsilon_m'' \end{bmatrix} \tag{26}$$

where

$$E_{Lm} = \begin{bmatrix} (ik)^{+1} & 0 \\ 0 & (-ik\mu_m\eta_{\beta m})^{+1} \end{bmatrix} \tag{27}$$

and the inverse of E_{L_m} is

$$E_{Lm}^{-1} = \begin{bmatrix} (ik)^{-1} & 0 \\ 0 & -(ik\mu_m\eta_{\beta m})^{-1} \end{bmatrix} \tag{28}$$

Evaluating at $z = z_m$, we have

$$\begin{bmatrix} \frac{\dot{V}_{Lm}}{c}(z_m) \\ T_{Lm}(z_m) \end{bmatrix} = D_{Lm} \begin{bmatrix} \epsilon_m' + \epsilon_m'' \\ \epsilon_m' - \epsilon_m'' \end{bmatrix} \tag{29}$$

where

$$D_{Lm} = \begin{bmatrix} ik\cos Q_m & k\sin Q_m \\ -k\mu_m\eta_{\beta m}\sin Q_m & -ik\mu_m\eta_{\beta m}\cos Q_m \end{bmatrix} \tag{30}$$

With equations 27 and 30 we obtain

$$\begin{bmatrix} \frac{\dot{V}_{Lm}(z_m)}{c} \\ T_{Lm}(z_m) \end{bmatrix} = a_{Lm} \begin{bmatrix} \frac{\dot{V}_{Lm}(z_{m-1})}{c} \\ T_{Lm}(z_{m-1}) \end{bmatrix} \tag{31}$$

where

$$a_{Lm} = D_{Lm} E_{Lm}^{-1}$$

and the elements of a_{L_m} are

$$\begin{aligned} (a_{Lm})_{11} &= (a_{Lm})_{22} = \cos Q_m \\ (a_{Lm})_{12} &= \frac{i}{\mu_m \eta_{\beta m}} \sin Q_m \\ (a_{Lm})_{21} &= i \mu_m \eta_{\beta m} \sin Q_m \end{aligned} \tag{32}$$

As in the Rayleigh section, we have as our general point source in layer s at z = D

$$\chi_{s0}(z) = S_{03}^{\pm} \; e^{-ik\eta_{\beta s}|z-D|} \tag{33}$$

Performing operations similar to the preceding section we obtain

$$\begin{bmatrix} \frac{\dot{V}_{Ls2}(z_s)}{c} \\ T_{Ls2}(z_s) \end{bmatrix} = a_{Ls2} \begin{bmatrix} \frac{\dot{V}_{Ls2}(D)}{c} \\ T_{Ls2}(D) \end{bmatrix}$$

$$\begin{bmatrix} \frac{\dot{V}_{Ls1}(D)}{c} \\ T_{Ls1}(D) \end{bmatrix} = a_{Ls1} \begin{bmatrix} \frac{\dot{V}_{Ls1}(z_{s-1})}{c} \\ T_{Ls1}(z_{s-1}) \end{bmatrix} \tag{34}$$

and the vector equation

$$\begin{bmatrix} \frac{\dot{V}_{L52}(0)}{c} \\ T_{L52}(0) \end{bmatrix} = \begin{bmatrix} \frac{\dot{V}_{LS1}(0)}{c} \\ T_{LS1}(0) \end{bmatrix} + \begin{bmatrix} \delta\left(\frac{\dot{V}_{LS}}{c}\right) \\ \delta T_{LS} \end{bmatrix} \tag{35}$$

where by equations 22

$$\delta\left(\frac{\dot{V}_{LS}}{c}\right) = ik^2\left(S_{03}^{+} - S_{03}^{-}\right) \tag{36}$$

$$\delta T_{LS} = -ik^2 \mu_S \pi_{\beta S}\left(S_{03}^{+} + S_{03}^{-}\right)$$

APPENDIX B

THE DISPLACEMENTS FOR A POINT FORCE IN AN ELASTIC SPACE IN TERMS OF A CYLINDRICAL COORDINATE SYSTEM AT RIGHT ANGLES TO THE FORCE

In this appendix we first derive the solutions in terms of the natural coordinate system, i.e., a cylindrical coordinate system, (ξ, δ, x), coincident with the force in order to make use of the aximuthal symmetry of the force, then transform the solutions to a cylindrical coordinate system, (r, θ, z), perpendicular to the force. The coordinate systems are as shown in figure 4.

We now define a point force, $\bar{L}$, positive in the positive x direction, located at the origin by

$$2\pi \int_0^\infty [\bar{P}_{xx}(\xi, 0^+) - \bar{P}_{xx}(\xi, 0^-)]\, \xi\, d\xi = -\bar{L}$$

or

$$\bar{P}_{xx}(\xi, 0^+) - \bar{P}_{xx}(\xi, 0^-) = -\frac{\bar{L}}{2\pi} \int_0^\infty J_0(k\xi)\, k\, dk \tag{1}$$

and from the following definition

$$\bar{P}_{xx}(\xi, x) = \int_0^\infty P_{xx}(\xi, x; k)\, dk \tag{2}$$

we have

$$P_{xx}(\xi, 0^+; k) - P_{xx}(\xi, 0^-; k) = -\frac{\bar{L}}{2\pi} k J_0(k\xi) \tag{3}$$

where $\bar{P}_{xx}(\xi, x)$ is the time transformed normal stress in the x direction.

Using the potentials φ and ψ which satisfy

$$\nabla^2\varphi = -k_\alpha^2\,\varphi$$
$$\nabla^2\psi = -k_\beta^2\,\psi \tag{4}$$

it can be shown from the equations of motion that stress and displacement for aximuthal symmetry are given by (Ewing, Jardetzky, and Press; 1957)

$$P_{xx} = -\lambda k_\alpha^2\varphi + 2\mu\left(\frac{\partial^2\varphi}{\partial x^2} + \frac{\partial^3\psi}{\partial x^3} + k_\beta^2\frac{\partial\psi}{\partial x}\right)$$
$$P_{x\xi} = \mu\frac{\partial}{\partial\xi}\left(2\frac{\partial\varphi}{\partial x} + 2\frac{\partial^2\psi}{\partial x^2} + k_\beta^2\psi\right) \tag{5}$$
$$u_\xi = \frac{\partial}{\partial\xi}\left(\varphi + \frac{\partial\psi}{\partial x}\right)$$
$$u_x = \frac{\partial\varphi}{\partial x} + \frac{\partial^2\psi}{\partial x^2} + k_\beta^2\psi$$

where $P_{x\xi}$, u_ξ and u_x are defined similarly to P_{xx} in terms of $\overline{P}_{x\xi}$, $\overline{u}_\xi$, and $\overline{u}_x$; the tangential stress, the radial displacement and the normal displacement in the x direction respectively.

The general solutions for equations 4 are

$$\varphi = A_1 e^{-ik\eta_\alpha x}\,J_0(k\xi)$$
$$\psi = B_1 e^{-ik\eta_\beta x}\,J_0(k\xi) \qquad x>0$$

and (6)

$$\varphi = A_2 e^{ik\eta_\alpha x}\,J_0(k\xi)$$
$$\psi = B_2 e^{ik\eta_\beta x}\,J_0(k\xi) \qquad x<0$$

where

$$k\eta_{\alpha,\beta} = -i(k^2 - k_{\alpha,\beta}^2)^{1/2} \quad \text{for} \quad k > k_{\alpha,\beta}$$
$$= (k_{\alpha,\beta}^2 - k^2)^{1/2} \quad \text{for} \quad k < k_{\alpha,\beta}$$

Substituting equations 6 in the following boundary conditions at $x = 0$

$$
\begin{aligned}
&u_\xi(\xi, 0^+; k) - u_\xi(\xi, 0^-; k) = 0 \\
&u_x(\xi, 0^+; k) - u_x(\xi, 0^-; k) = 0 \\
&P_{x\xi}(\xi, 0^+; k) - P_{x\xi}(\xi, 0^-; k) = 0 \\
&P_{xx}(\xi, 0^+; k) - P_{xx}(\xi, 0^-; k) = -\frac{\bar{L}}{2\pi} k J_0(k\xi)
\end{aligned}
\tag{7}
$$

and solving for the constants A_1, A_2, B_1, and B_2 we obtain

$$
A_1 = \frac{\bar{L}k}{4\pi\omega^2\rho} \quad , A_2 = -\frac{\bar{L}k}{4\pi\omega^2\rho} \quad \text{and} \quad B_1 = B_2 = -i\frac{\bar{L}k}{4\pi\omega^2\rho\Pi_\beta} \tag{8}
$$

where we have made use of the relations

$$
k_\beta^2 = \frac{\omega^2\rho}{\mu} \quad \text{and} \quad k_\alpha^2 = \frac{\omega^2\rho}{(\lambda+2\mu)} \tag{9}
$$

Substituting equations 8 into equations 6 and 5 we have as our solutions

$$
\bar{u}_\xi = \frac{\bar{L}}{4\pi\omega^2\rho} \frac{\partial}{\partial\xi} \int_0^\infty \left[e^{-ik\Pi_\alpha x} - e^{-ik\Pi_\beta x} \right] J_0(k\xi)\, k\, dk \qquad x > 0
$$

$$
\bar{u}_x = \frac{\bar{L}}{4\pi\omega^2\rho} \int_0^\infty \left[-ik\Pi_\alpha e^{-ik\Pi_\alpha x} + \frac{k^2}{(ik\Pi_\beta)} e^{-ik\Pi_\beta x} \right] J_0(k\xi)\, dk
$$

and (10)

$$
\bar{u}_\xi = \frac{\bar{L}}{4\pi\omega^2\rho} \frac{\partial}{\partial\xi} \int_0^\infty \left[-e^{ik\Pi_\alpha x} + e^{ik\Pi_\beta x} \right] J_0(k\xi)\, dk \qquad x < 0
$$

$$
\bar{u}_x = \frac{\bar{L}}{4\pi\omega^2\rho} \int_0^\infty \left[-ik\Pi_\alpha e^{ik\Pi_\alpha x} + \frac{k^2}{(ik\Pi_\beta)} e^{ik\Pi_\beta x} \right] J_0(k\xi)\, dk
$$

From the well known integral relation

$$\frac{e^{-ik_{\alpha,\beta}R}}{R} = \int_0^\infty \frac{e^{-ik\eta_{\alpha,\beta}|x|}}{ik\eta_{\alpha,\beta}} J_0(k\xi)\, k\, dk \tag{11}$$

where

$$R = (\xi^2 + x^2)^{1/2} \qquad \text{and} \quad k\eta_{\alpha,\beta} = -i(k^2 - k_{\alpha,\beta}^2)^{1/2} \text{ for } k > k_{\alpha,\beta}$$

$$= (k_{\alpha,\beta}^2 - k^2)^{1/2} \text{ for } k < k_{\alpha,\beta}$$

we obtain the following relations.

$$\frac{\partial}{\partial x}\left(\frac{e^{-ik_{\alpha,\beta}R}}{R}\right) = -\left\{\frac{|x|}{x}\right\}\int_0^\infty e^{-ik\eta_{\alpha,\beta}|x|} J_0(k\xi)\, dk$$

and (12)

$$\frac{\partial^2}{\partial x^2}\left(\frac{e^{-ik_{\alpha,\beta}R}}{R}\right) = \int_0^\infty (ik\eta_{\alpha,\beta}) e^{-ik\eta_{\alpha,\beta}|x|} J_0(k\xi)\, dk$$

Comparing equations 11 and 12 with equations 10 we obtain for all x

$$\bar{u}_\xi = \frac{\bar{L}}{4\pi\omega^2\rho} \frac{\partial^2}{\partial\xi\partial x}\left(\frac{e^{-ik_\beta R} - e^{-ik_\alpha R}}{R}\right)$$

(13)

$$\bar{u}_x = \frac{\bar{L}}{4\pi\omega^2\rho}\left[\frac{\partial^2}{\partial x^2}\left(\frac{e^{-ik_\beta R} - e^{-ik_\alpha R}}{R}\right) + k_\beta^2 \frac{e^{-ik_\alpha R}}{R}\right]$$

Now defining

$$\hat{A} = \frac{e^{-ik_\beta R} - e^{-ik_\alpha R}}{R} \tag{14}$$

where

$$R = (x^2 + \xi^2)^{1/2} = (z^2 + r^2)^{1/2}$$

and making use of the fact that R is not a function of δ or θ we find that

$$\frac{\partial^2 \hat{A}}{\partial \xi \partial x} = \frac{\cos\theta}{\sin\delta} \frac{\partial^2 \hat{A}}{\partial r \partial z} \tag{15}$$

$$= \frac{\sin\theta \cos\theta}{\cos\delta} \left[\frac{\partial^2 \hat{A}}{\partial r^2} - \frac{1}{r} \frac{\partial \hat{A}}{\partial r} \right] \tag{16}$$

and

$$\frac{\partial^2 \hat{A}}{\partial x^2} = \cos^2\theta \frac{\partial^2 \hat{A}}{\partial r^2} + \frac{\sin^2\theta}{r} \frac{\partial \hat{A}}{\partial r} \tag{17}$$

The displacements $\bar{q}$, $\bar{v}$, and $\bar{w}$ in the r, θ, and z directions respectively from the geometry are given by

$$\begin{aligned} \bar{q} &= \cos\theta\, \bar{u}_x + \sin\theta \cos\delta\, \bar{u}_\xi \\ \bar{v} &= \cos\theta \cos\delta\, \bar{u}_\xi - \sin\theta\, \bar{u}_x \\ \bar{w} &= \sin\delta\, \bar{u}_\xi \end{aligned} \tag{18}$$

Substituting equations 13, 15, 16 and 17 into 18 we obtain for the displacements in the (r, θ, z) coordinates the following.

$$\begin{aligned} \bar{q} &= \frac{\bar{L}}{4\pi\omega^2\rho} \cos\theta \left[\frac{\partial^2 \hat{A}}{\partial r^2} + k_\beta^2 \frac{e^{-ik_\beta R}}{R} \right] \\ \bar{v} &= -\frac{\bar{L}}{4\pi\omega^2\rho} \sin\theta \left[\frac{1}{r} \frac{\partial \hat{A}}{\partial r} + k_\beta^2 \frac{e^{-ik_\beta R}}{R} \right] \\ \bar{w} &= \frac{\bar{L}}{4\pi\omega^2\rho} \cos\theta \frac{\partial^2 \hat{A}}{\partial z \partial r} \end{aligned} \tag{19}$$

Now using equations 11 in terms of r, z instead of ξ, x, equations 19 become

$$\bar{q} = -i\frac{\bar{L}}{4\pi\omega^2\rho}\cos\theta\int_0^\infty\left[k^2\left(\frac{e^{-ik\eta_\alpha|z|}}{\eta_\alpha}+\eta_\beta e^{-ik\eta_\beta|z|}\right)\frac{dJ_1(kr)}{kdr}+k_\beta^2\frac{e^{-ik\eta_\beta|z|}}{\eta_\beta}\frac{J_1(kr)}{kr}\right]dk$$

$$\bar{v} = i\frac{\bar{L}}{4\pi\omega^2\rho}\sin\theta\int_0^\infty\left[k^2\left(\frac{e^{-ik\eta_\alpha|z|}}{\eta_\alpha}+\eta_\beta e^{-ik\eta_\beta|z|}\right)\frac{J_1(kr)}{kr}+k_\beta^2\frac{e^{-ik\eta_\beta|z|}}{\eta_\beta}\frac{dJ_1(kr)}{kdr}\right]dk \tag{20}$$

$$\bar{w} = \frac{\bar{L}}{4\pi\omega^2\rho}\cos\theta\left\{\frac{|z|}{z}\right\}\int_0^\infty\left[k^2\left(e^{-ik\eta_\beta|z|}-e^{-ik\eta_\alpha|z|}\right)J_1(kr)\right]dk$$

Then using the stress-strain relations for the (r, θ, z) coordinates

$$\bar{P}_{rz} = \mu\left(\frac{\partial\bar{w}}{\partial r}+\frac{\partial\bar{q}}{\partial z}\right) \quad \text{and} \quad \bar{P}_{\theta z} = \mu\left(\frac{\partial\bar{w}}{r\partial\theta}+\frac{\partial\bar{v}}{\partial z}\right) \tag{21}$$

and evaluating at $z = 0$ we obtain

$$\bar{P}_{rz} = -\frac{\bar{L}}{4\pi}\cos\theta\int_0^\infty J_0(kr)\,k\,dk \qquad z = 0^+$$

$$\bar{P}_{\theta z} = \frac{\bar{L}}{4\pi}\sin\theta\int_0^\infty J_0(kr)\,k\,dk \tag{22}$$

and

$$\bar{P}_{rz} = \frac{\bar{L}}{4\pi}\cos\theta\int_0^\infty J_0(kr)\,k\,dk \qquad z = 0^-$$

$$\bar{P}_{\theta z} = -\frac{\bar{L}}{4\pi}\sin\theta\int_0^\infty J_0(kr)\,k\,dk$$

and therefore

$$\bar{P}_{rz}(r,0^+) - \bar{P}_{rz}(r,0^-) = -\frac{\bar{L}}{2\pi}\cos\theta \int_0^\infty J_0(kr)\,k\,dk$$

$$\bar{P}_{\theta z}(r,0^+) - \bar{P}_{\theta z}(r,0^-) = \frac{\bar{L}}{2\pi}\sin\theta \int_0^\infty J_0(kr)\,k\,dk \qquad (23)$$

In addition, inspection of equations 20 at z = 0 yield

$$\bar{q}(r,0^+) - \bar{q}(r,0^-) = 0$$

$$\bar{v}(r,0^+) - \bar{v}(r,0^-) = 0 \qquad (24)$$

and $$\bar{w}(r,0^+) - \bar{w}(r,0^-) = 0$$

since $$\bar{w}(r,0^+) = \bar{w}(r,0^-) = 0$$

Now

$$\bar{P}_{zz} = (\lambda+2\mu)\frac{\partial \bar{w}}{\partial z} + 2\mu\left(\frac{\partial \bar{q}}{\partial r} + \frac{\bar{q}}{r} + \frac{1}{r}\frac{\partial \bar{v}}{\partial \theta}\right) \qquad (25)$$

which from equations 19 involves either none or two differentials of $\hat{A}$ with respect to z. Therefore since $\hat{A}$ and its even derivatives with respect to z are continuous across z = 0, we find that

$$\bar{P}_{zz}(r,0^+) - \bar{P}_{zz}(r,0^-) = 0 \qquad (26)$$

For the horizontal point force in multilayered media, we will use relations 23, 24, and 26 as the boundary conditions representing the source in the matrix formulation. It is interesting to note that from the geometry

$$\bar{P}_{xz} = \cos\theta\,\bar{P}_{rz} - \sin\theta\,\bar{P}_{\theta z}$$

$$\bar{P}_{yz} = \sin\theta\, \bar{P}_{rz} + \cos\theta\, \bar{P}_{\theta z} \tag{27}$$

and by equations 23 we obtain

$$\bar{P}_{xz}(r,0^+) - \bar{P}_{xz}(r,0^-) = -\frac{\bar{L}}{2\pi}\int_0^\infty J_0(kr)\, k\, dk$$

$$\bar{P}_{yz}(r,0^+) = \bar{P}_{yz}(r,0^-) = 0 \tag{28}$$

And using the integral relation (Snedon 1950)

$$\int_0^\infty J_0(kr)\, k\, dk = \frac{1}{2\pi}\int_{-\infty}^{\infty}\int_{-\infty}^{\infty} e^{i(sx+py)}\, ds\, dp \tag{29}$$

where $k e^{i\gamma} = s + ip$

and $r e^{i\theta} = x + iy$

we finally obtain

$$\bar{P}_{xz}(r,0^+) - \bar{P}_{xz}(r,0^-) = -\frac{\bar{L}}{(2\pi)^2}\int_{-\infty}^{\infty}\int_{-\infty}^{\infty} e^{i(sx+py)}\, ds\, dp$$

$$\bar{P}_{yz}(r,0) = 0 \tag{30}$$

which except for a factor of $\frac{1}{2\pi}$ are the boundary conditions used to describe a horizontal point force by Yanovskaya (1958) and Ben-Menahem (1961).

APPENDIX C

TIME TRANSFORMED SOURCE POTENTIAL FOR A PRESSURE UNIFORMLY APPLIED TO THE WALLS OF A CAVITY IN AN ELASTIC SPACE

The following derivation has been given by many authors (Kawasumi and Yosiyama, 1935; Sharpe, 1942; Fu, 1945; Menzel, 1951; Blake, 1952). It is rederived here only for the purpose of rapid reference for those not familiar with the result.

Consider an elastic space s with a spherical cavity of radius a_s whose center is located at the origin of the spherical coordinate system (R, θ, φ). If a pressure is uniformly applied to the walls of the cavity, a spherical wave dependent only on R will radiate in the solid from the cavity walls. The radial displacement and stress with R dependence only can be expressed in terms of a potential $\varphi_s(R)$ by

$$U_{Rs}(R) = \frac{\partial \varphi_s}{\partial R}(R)$$

$$T_{RR_s}(R) = (\lambda_s + 2\mu_s)\frac{\partial U_{Rs}}{\partial R} + 2\lambda_s \frac{U_{Rs}}{R} \qquad (1)$$

$$= (\lambda_s + 2\mu_s)\frac{\partial^2 \varphi_s}{\partial^2 R} + 2\frac{\lambda_s}{R}\frac{\partial \varphi_s}{\partial R}$$

where

$$\frac{\partial^2 \varphi_s}{\partial R^2} = \frac{1}{\alpha_s^2}\frac{\partial^2 \varphi_s}{\partial t^2} \qquad (2)$$

Applying a Fourier time transformed pressure $\bar{p}_{os}$ at $R = a_s$ given by

$$\bar{p}_{os} = \int_{-\infty}^{\infty} [p_{os}(t)]\, e^{-i\omega t}\, dt \qquad (3)$$

we obtain for the transformed stress and potential at the cavity walls

$$\bar{T}_{RR_s}(a_s) = (\lambda_s + 2\mu_s)\frac{\partial^2 \bar{\varphi}_s(a_s)}{\partial R^2} + 2\frac{\lambda_s}{a_s}\frac{\partial \bar{\varphi}_s(a_s)}{\partial R} = -\bar{p}_{os} \tag{4}$$

where $\bar{\varphi}_s(R)$ satisfies the Fourier transform of equation 2

$$\frac{d^2 \bar{\varphi}_s(R)}{dR^2} = -k_{\alpha_s}^2 \bar{\varphi}_s(R) \tag{5}$$

with

$$k_{\alpha_s} = \frac{\omega}{\alpha_s}$$

The negative sign in equation 4 is the result of a positive pressure corresponding to a compression and a positive stress corresponding to a rarification.

Assuming that the medium is quiet before the pressure is applied, we have for the solution of equation 5

$$\bar{\varphi}_s(R) = \tilde{A}_s \frac{e^{-ik_{\alpha_s}R}}{R} \tag{6}$$

where $\tilde{A}_s$ is to be determined by the transformed boundary condition 4. We now substitute equation 6 in equation 4 and obtain

$$\tilde{A}_s = -\frac{\bar{p}_{os}}{4\mu_s} a_s^3 \frac{e^{i\omega\left(\frac{a_s}{\alpha_s} - \frac{\theta_{sp}}{\omega}\right)}}{\left[\left(1 - \frac{a_s k_{\beta s}^2}{4}\right)^2 + k_{\alpha s}^2 a_s^2\right]^{1/2}} \tag{7}$$

where

$$\theta_{sp} = \tan^{-1}\left[\frac{k_{\alpha s} a_s}{\left(1 - \frac{a_s^2 k_{\beta s}^2}{4}\right)}\right] \qquad \text{and} \qquad k_{\beta s}^2 = \frac{\omega^2}{\beta_s^2} = \omega^2 \frac{\rho_s}{\mu_s}$$

Rewriting equation 6 with equation 7 we have the desired result.

$$\bar{\Phi}_s(R) = -\frac{\bar{p}_{os}}{4\mu_s}\, a_s^3\, \frac{e^{-i\omega\left[\frac{(R-a_s)}{\alpha_s} + \frac{\theta_{sp}}{\omega}\right]}}{R\left[\left(1-\frac{a_s^2 k_{as}^2}{4}\right)^2 + k_{as}^2 a_s^2\right]^{1/2}} \tag{8}$$

APPENDIX D

INVERSION OF RAYLEIGH LAYER AND PRODUCT LAYER MATRICES

1. Layer Matrix Inverse

The inverse will be obtained by a physical argument using the elastic relations of azimuthal symmetry. This approach reduces the algebra considerably compared to a straight forward matrix inversion.

The elastic relations for azimuthal symmetry are as follows. The displacements in the positive z and r directions are w and q respectively, and the normal and tangential stress in planes perpendicular to the z axis are defined by

$$\begin{aligned} P_{zz} &= \lambda\theta + 2\mu \frac{\partial w}{\partial z} \\ P_{rz} &= \mu\left(\frac{\partial q}{\partial z} + \frac{\partial w}{\partial r}\right) \end{aligned} \tag{1}$$

respectively where

$$\theta = \frac{\partial q}{\partial r} + \frac{\partial w}{\partial z} + \frac{q}{r}$$

Now defining $\dot{u}_R(z)$, $\dot{w}_R(z)$, $\sigma_R(z)$ and $\tau_R(z)$ by

$$\begin{aligned} q &= -\frac{\dot{u}_R(z)}{\omega} J_1(kr) \\ w &= -i\frac{\dot{w}_R(z)}{\omega} J_o(kr) \\ P_{zz} &= \sigma_R(z)\, J_o(kr) \\ P_{rz} &= -i\tau_R(z) J_1(kr) \end{aligned} \tag{2}$$

It has been shown previously that these quantities evaluated at the

bounding surfaces $z = z_m, z_{m-1}$ of the m^{th} layer are related by the vector equation

$$\begin{bmatrix} \frac{\dot{u}_R(z_m)}{c} \\ \frac{\dot{w}_R(z_m)}{c} \\ \sigma_R(z_m) \\ \tau_R(z_m) \end{bmatrix} = a_{R_m} \begin{bmatrix} \frac{\dot{u}_R(z_{m-1})}{c} \\ \frac{\dot{w}_R(z_{m-1})}{c} \\ \sigma_R(z_{m-1}) \\ \tau_R(z_{m-1}) \end{bmatrix} \tag{3}$$

where $z_m - z_{m-1} = d_m$.

For the inverse of a_{R_m} we now consider the m layer with a new coordinate ξ in the negative z direction with the r coordinate unchanged. The new elastic relations with azimuthal symmetry are given by

$$\begin{aligned} \xi &= - z \\ \hat{q} &= q \\ \hat{w} &= - w \\ \hat{\theta} &= \frac{\partial \hat{q}}{\partial r} + \frac{\partial \hat{w}}{\partial \xi} + \frac{\hat{q}}{r} = \frac{\partial q}{\partial r} + \frac{\partial w}{\partial z} + \frac{q}{r} = \theta \\ \hat{P}_{zz} &= \lambda \hat{\theta} + 2\mu \frac{\partial \hat{w}}{\partial \xi} = \lambda \theta + 2\mu \frac{\partial w}{\partial z} \\ \hat{P}_{rz} &= \mu \left(\frac{\partial \hat{q}}{\partial \xi} + \frac{\partial \hat{w}}{\partial r} \right) = - \mu \left(\frac{\partial q}{\partial z} + \frac{\partial w}{\partial r} \right) = - P_{rz} \end{aligned} \tag{4}$$

Defining $\dot{\hat{u}}_R(z)$, $\dot{\hat{w}}_R(z)$, $\hat{\sigma}_R(z)$ and $\hat{\tau}_R(z)$ by equations 2 replacing q, w, P_{zz} and P_{rz} by $\hat{q}$, $\hat{w}$, $\hat{P}_{zz}$ and $\hat{P}_{rz}$ respectively, we have as a new vector equation

$$\begin{bmatrix} \frac{\dot{u}_R}{c}(z_{m-1}) \\ \frac{\dot{w}_R}{c}(z_{m-1}) \\ \sigma_R(z_{m-1}) \\ \tau_R(z_{m-1}) \end{bmatrix} = a_{R_m} \begin{bmatrix} \frac{\dot{u}_R}{c}(z_m) \\ \frac{\dot{w}_R}{c}(z_m) \\ \sigma_R(z_m) \\ \tau_R(z_m) \end{bmatrix} \tag{5}$$

The m layer matrix being the same as in equation 3, since the layer is elastically isotropic. In other words the expression for transforming displacement and stress from one side of the layer to the other side is the same as long as the displacement and stress are defined in the same sense as the direction of the transformation.

From equation 4 we see that equation 5 can be rewritten as

$$\begin{bmatrix} \frac{\dot{u}_R}{c}(z_{m-1}) \\ -\dot{w}_R(z_{m-1}) \\ \sigma_R(z_{m-1}) \\ -\tau_R(z_{m-1}) \end{bmatrix} = a_{R_m} \begin{bmatrix} \frac{\dot{u}_R}{c}(z_m) \\ -\dot{w}_R(z_m) \\ \sigma_R(z_m) \\ -\tau_R(z_m) \end{bmatrix} \tag{6}$$

or

$$\frac{\dot{u}_R}{c}(z_{m-1}) = \left(a_{R_m}\right)_{11} \frac{\dot{u}_R}{c}(z_m) - \left(a_{R_m}\right)_{12} \frac{\dot{w}_R}{c}(z_m) + \left(a_{R_m}\right)_{13} \sigma_R(z_m)$$

$$- \left(a_{R_m}\right)_{14} \tau_R(z_m)$$

$$\frac{\dot{w}_R}{c}(z_{m-1}) = -\left(a_{R_m}\right)_{21}\frac{\dot{u}_R}{c}(z_m) + \left(a_{R_m}\right)_{22}\frac{\dot{w}_R}{c}(z_m) - \left(a_{R_m}\right)_{23}\sigma_R(z_m) + \left(a_{R_m}\right)_{24}\tau_R(z_m)$$

$$\sigma_R(z_{m-1}) = \left(a_{R_m}\right)_{31}\frac{\dot{u}_R}{c}(z_m) - \left(a_{R_m}\right)_{32}\frac{\dot{w}_R}{c}(z_m) + \left(a_{R_m}\right)_{33}\sigma_R(z_m) - \left(a_{R_m}\right)_{34}\tau_R(z_m) \qquad (7)$$

$$\tau_R(z_{m-1}) = -\left(a_{R_m}\right)_{41}\frac{\dot{u}_R}{c}(z_m) + \left(a_{R_m}\right)_{42}\frac{\dot{w}_R}{c}(z_m) - \left(a_{R_m}\right)_{43}\sigma_R(z_m) + \left(a_{R_m}\right)_{44}\tau_R(z_m)$$

which in turn can be rewritten as

$$\begin{bmatrix} \frac{\dot{u}_R}{c}(z_{m-1}) \\ \frac{\dot{w}_R}{c}(z_{m-1}) \\ \sigma_R(z_{m-1}) \\ \tau_R(z_{m-1}) \end{bmatrix} = \begin{bmatrix} \left(a_{R_m}\right)_{11} & -\left(a_{R_m}\right)_{12} & \left(a_{R_m}\right)_{13} & -\left(a_{R_m}\right)_{14} \\ -\left(a_{R_m}\right)_{21} & \left(a_{R_m}\right)_{22} & -\left(a_{R_m}\right)_{23} & \left(a_{R_m}\right)_{24} \\ \left(a_{R_m}\right)_{31} & -\left(a_{R_m}\right)_{32} & \left(a_{R_m}\right)_{33} & -\left(a_{R_m}\right)_{34} \\ -\left(a_{R_m}\right)_{41} & \left(a_{R_m}\right)_{42} & -\left(a_{R_m}\right)_{43} & \left(a_{R_m}\right)_{44} \end{bmatrix} \begin{bmatrix} \frac{\dot{u}_R}{c}(z_m) \\ \frac{\dot{w}_R}{c}(z_m) \\ \sigma_R(z_m) \\ \tau_R(z_m) \end{bmatrix} \qquad (8)$$

and by definition

$$\begin{bmatrix} \frac{\dot{u}_R(z_{m-1})}{c} \\ \frac{\dot{w}_R(z_{m-1})}{c} \\ \sigma_R(z_{m-1}) \\ \tau_R(z_{m-1}) \end{bmatrix} = a_{R_m}^{-1} \begin{bmatrix} \frac{\dot{u}_R(z_m)}{c} \\ \frac{\dot{w}_R(z_m)}{c} \\ \sigma_R(z_m) \\ \tau_R(z_m) \end{bmatrix} \tag{9}$$

Therefore comparing equations 8 and 9, we have for the inverse of a_{R_m}

$$\left(a_{R_m}^{-1}\right)_{jk} = (-1)^{j+k}\left(a_{R_m}\right)_{jk} \tag{10}$$

On inspecting the matrix elements we see that this result could have been obtained by replacing d_m by $-d_m$ in the a_{R_m} matrix.

In order to obtain a simple expression for the inverse of the layer product matrix in the next section we now rewrite the inverse of a_{R_m} making use of relations between individual a_{R_m} elements.

$$\left(a_{R_m}^{-1}\right)_{11} = \left(a_{R_m}\right)_{11} = \left(a_{R_m}\right)_{44}$$

$$\left(a_{R_m}^{-1}\right)_{12} = -\left(a_{R_m}\right)_{12} = -\left(a_{R_m}\right)_{34}$$

$$\left(a_{R_m}^{-1}\right)_{13} = \left(a_{R_m}\right)_{13} = \left(a_{R_m}\right)_{24}$$

$$\left(a_{R_m}^{-1}\right)_{14} = -\left(a_{R_m}\right)_{14}$$

$$\left(a_{R_m}^{-1}\right)_{21} = -\left(a_{R_m}\right)_{21} = -\left(a_{R_m}\right)_{43}$$

$$\left(a_{R_m}^{-1}\right)_{22} = \left(a_{R_m}\right)_{22} = \left(a_{R_m}\right)_{33}$$

$$\left(a_{R_m}^{-1}\right)_{31} = \left(a_{R_m}\right)_{21} = \left(a_{R_m}\right)_{42}$$

$$\left(a_{R_m}^{-1}\right)_{32} = -\left(a_{R_m}\right)_{32}$$

$$\left(a_{R_m}^{-1}\right)_{33} = \left(a_{R_m}\right)_{33} = \left(a_{R_m}\right)_{22}$$

$$\left(a_{R_m}^{-1}\right)_{34} = -\left(a_{R_m}\right)_{34} = -\left(a_{R_m}\right)_{12}$$

$$\left(a_{R_m}^{-1}\right)_{41} = -\left(a_{R_m}\right)_{41}$$

$$\left(a_{R_m}^{-1}\right)_{42} = \left(a_{R_m}\right)_{42} = \left(a_{R_m}\right)_{31}$$

$$\left(a^{-1}_{R_m}\right)_{23} = -\left(a_{R_m}\right)_{23} \qquad \left(a^{-1}_{R_m}\right)_{43} = -\left(a_{R_m}\right)_{43} = -\left(a_{R_m}\right)_{21}$$

$$\left(a^{-1}_{R_m}\right)_{24} = \left(a_{R_m}\right)_{24} = \left(a_{R_m}\right)_{13} \qquad \left(a^{-1}_{R_m}\right)_{44} = \left(a_{R_m}\right)_{44} = \left(a_{R_m}\right)_{11}$$

(11)

2. Product Matrix Inverse

The product matrix is defined by the product

$$A_{R_m} = a_{R_m} \cdot a_{R_{m-1}} \cdots a_2 \cdot a_1 = a_{R_m} A_{R_{m-1}} \tag{12}$$

and its inverse is the same in terms of the product matrix as the layer matrix inverse given in equation 11. In order to prove this we will use induction.

First we assume that it is true for $A^{-1}_{R_{m-1}}$. Then forming the product $A^{-1}_{R_m} = A^{-1}_{R_{m-1}} a^{-1}_{R_m}$ and using equations 11 for the inverses $a^{-1}_{R_m}$ and $A^{-1}_{R_{m-1}}$ we obtain

$$\begin{aligned}\left(A^{-1}_{R_m}\right)_{11} &= \left(A^{-1}_{R_{m-1}}\right)_{11}\left(a^{-1}_{R_m}\right)_{11} + \left(A^{-1}_{R_{m-1}}\right)_{12}\left(a^{-1}_{R_m}\right)_{21} + \left(A^{-1}_{R_{m-1}}\right)_{13}\left(a^{-1}_{R_m}\right)_{31} \\ &\quad + \left(A^{-1}_{R_{m-1}}\right)_{14}\left(a^{-1}_{R_m}\right)_{41} \\ &= \left(a_{R_m}\right)_{44}\left(A^{-1}_{R_{m-1}}\right)_{44} + \left(a_{R_m}\right)_{43}\left(A^{-1}_{R_{m-1}}\right)_{34} + \left(a_{R_m}\right)_{42}\left(A^{-1}_{R_{m-1}}\right)_{24} \\ &\quad + \left(a_{R_m}\right)_{41}\left(A^{-1}_{R_{m-1}}\right)_{14} \\ &= \left(A_{R_m}\right)_{44}\end{aligned}$$

$$\left(A^{-1}_{R_m}\right)_{12} = \left(A^{-1}_{R_{m-1}}\right)_{11}\left(a^{-1}_{R_m}\right)_{12} + \left(A^{-1}_{R_{m-1}}\right)_{12}\left(a^{-1}_{R_m}\right)_{22} + \left(A^{-1}_{R_{m-1}}\right)_{13}\left(a^{-1}_{R_m}\right)_{32} + \left(A^{-1}_{R_{m-1}}\right)_{14}\left(a^{-1}_{R_m}\right)_{42}$$

$$= -\left(a_{R_m}\right)_{34}\left(A_{R_{m-1}}\right)_{44} - \left(a_{R_m}\right)_{33}\left(A_{R_{m-1}}\right)_{34} - \left(a_{R_m}\right)_{32}\left(A_{R_{m-1}}\right)_{24} - \left(a_{R_m}\right)_{31}\left(A_{R_{m-1}}\right)_{14}$$

$$= -\left(A_{R_m}\right)_{34}$$

$$\left(A^{-1}_{R_m}\right)_{13} = \left(A^{-1}_{R_{m-1}}\right)_{11}\left(a^{-1}_{R_m}\right)_{13} + \left(A^{-1}_{R_{m-1}}\right)_{12}\left(a^{-1}_{R_m}\right)_{23} + \left(A^{-1}_{R_{m-1}}\right)_{13}\left(a^{-1}_{R_m}\right)_{33} + \left(A^{-1}_{R_{m-1}}\right)_{14}\left(a^{-1}_{R_m}\right)_{43}$$

$$= \left(a_{R_m}\right)_{24}\left(A_{R_{m-1}}\right)_{44} + \left(a_{R_m}\right)_{23}\left(A_{R_{m-1}}\right)_{34} + \left(a_{R_m}\right)_{22}\left(A_{R_{m-1}}\right)_{24} + \left(a_{R_m}\right)_{21}\left(A_{R_{m-1}}\right)_{14}$$

$$= \left(A_{R_m}\right)_{24}$$

$$\left(A^{-1}_{R_m}\right)_{14} = \left(A^{-1}_{R_{m-1}}\right)_{11}\left(a^{-1}_{R_m}\right)_{14} + \left(A^{-1}_{R_{m-1}}\right)_{12}\left(a^{-1}_{R_m}\right)_{24} + \left(A^{-1}_{R_{m-1}}\right)_{13}\left(a^{-1}_{R_m}\right)_{34} + \left(A^{-1}_{R_{m-1}}\right)_{14}\left(a^{-1}_{R_m}\right)_{44}$$

$$= -\left(a_{R_m}\right)_{14}\left(A_{R_{m-1}}\right)_{44} - \left(a_{R_m}\right)_{13}\left(A_{R_{m-1}}\right)_{34} - \left(a_{R_m}\right)_{12}\left(A_{R_{m-1}}\right)_{24} - \left(a_{R_m}\right)_{11}\left(A_{R_{m-1}}\right)_{14}$$

$$= -\left(A_{R_m}\right)_{14}$$

$$\left(A^{-1}_{R_m}\right)_{21} = \left(A^{-1}_{R_{m-1}}\right)_{21}\left(a^{-1}_{R_m}\right)_{11} + \left(A^{-1}_{R_{m-1}}\right)_{22}\left(a^{-1}_{R_m}\right)_{21} + \left(A^{-1}_{R_{m-1}}\right)_{23}\left(a^{-1}_{R_m}\right)_{31}$$
$$+ \left(A^{-1}_{R_{m-1}}\right)_{24}\left(a^{-1}_{R_m}\right)_{41}$$
$$= -\left(a_{R_m}\right)_{44}\left(A_{R_{m-1}}\right)_{43} - \left(a_{R_m}\right)_{43}\left(A_{R_{m-1}}\right)_{33} - \left(a_{R_m}\right)_{42}\left(A_{R_{m-1}}\right)_{23}$$
$$- \left(a_{R_m}\right)_{41}\left(A_{R_{m-1}}\right)_{12}$$
$$= -\left(A_{R_m}\right)_{43}$$

$$\left(A^{-1}_{R_m}\right)_{22} = \left(A^{-1}_{R_{m-1}}\right)_{21}\left(a^{-1}_{R_m}\right)_{12} + \left(A^{-1}_{R_{m-1}}\right)_{22}\left(a^{-1}_{R_m}\right)_{22} + \left(A^{-1}_{R_{m-1}}\right)_{23}\left(a^{-1}_{R_m}\right)_{32}$$
$$+ \left(A^{-1}_{R_{m-1}}\right)_{24}\left(a^{-1}_{R_m}\right)_{42}$$
$$= \left(a_{R_m}\right)_{34}\left(A_{R_{m-1}}\right)_{43} + \left(a_{R_m}\right)_{33}\left(A_{R_{m-1}}\right)_{33} + \left(a_{R_m}\right)_{32}\left(A_{R_{m-1}}\right)_{23}$$
$$+ \left(a_{R_m}\right)_{31}\left(A_{R_{m-1}}\right)_{13}$$
$$= \left(A_{R_m}\right)_{33}$$

$$\left(A^{-1}_{R_m}\right)_{23} = \left(A^{-1}_{R_{m-1}}\right)_{21}\left(a^{-1}_{R_m}\right)_{13} + \left(A^{-1}_{R_{m-1}}\right)_{22}\left(a^{-1}_{R_m}\right)_{23} + \left(A^{-1}_{R_{m-1}}\right)_{23}\left(a^{-1}_{R_m}\right)_{33}$$
$$+ \left(A^{-1}_{R_{m-1}}\right)_{24}\left(a^{-1}_{R_m}\right)_{43}$$
$$= -\left(a_{R_m}\right)_{24}\left(A_{R_{m-1}}\right)_{43} - \left(a_{R_m}\right)_{23}\left(A_{R_{m-1}}\right)_{33} - \left(a_{R_m}\right)_{22}\left(A_{R_{m-1}}\right)_{23}$$
$$- \left(a_{R_m}\right)_{21}\left(A_{R_{m-1}}\right)_{13}$$
$$= -\left(A_{R_m}\right)_{23}$$

$$\left(A^{-1}_{R_m}\right)_{24} = \left(A^{-1}_{R_{m-1}}\right)_{21}\left(a^{-1}_{R_m}\right)_{14} + \left(A^{-1}_{R_{m-1}}\right)_{22}\left(a^{-1}_{R_m}\right)_{24} + \left(A^{-1}_{R_{m-1}}\right)_{23}\left(a^{-1}_{R_m}\right)_{34} + \left(A^{-1}_{R_{m-1}}\right)_{24}\left(a^{-1}_{R_m}\right)_{44}$$

$$= \left(a_{R_m}\right)_{24}\left(A_{R_{m-1}}\right)_{43} + \left(a_{R_m}\right)_{13}\left(A_{R_{m-1}}\right)_{33} + \left(a_{R_m}\right)_{12}\left(A_{R_{m-1}}\right)_{23} + \left(a_{R_m}\right)_{11}\left(A_{R_{m-1}}\right)_{13}$$

$$= \left(A_{R_m}\right)_{13}$$

$$\left(A^{-1}_{R_m}\right)_{31} = \left(A^{-1}_{R_{m-1}}\right)_{31}\left(a^{-1}_{R_m}\right)_{11} + \left(A^{-1}_{R_{m-1}}\right)_{32}\left(a^{-1}_{R_m}\right)_{21} + \left(A^{-1}_{R_{m-1}}\right)_{33}\left(a^{-1}_{R_m}\right)_{31} + \left(A^{-1}_{R_{m-1}}\right)_{34}\left(a^{-1}_{R_m}\right)_{41}$$

$$= \left(a_{R_m}\right)_{44}\left(A_{R_{m-1}}\right)_{42} + \left(a_{R_m}\right)_{43}\left(A_{R_{m-1}}\right)_{32} + \left(a_{R_m}\right)_{42}\left(A_{R_{m-1}}\right)_{22} + \left(a_{R_m}\right)_{41}\left(A_{R_{m-1}}\right)_{12}$$

$$= \left(A_{R_m}\right)_{42}$$

$$\left(A^{-1}_{R_m}\right)_{32} = \left(A^{-1}_{R_{m-1}}\right)_{31}\left(a^{-1}_{R_m}\right)_{12} + \left(A^{-1}_{R_{m-1}}\right)_{32}\left(a^{-1}_{R_m}\right)_{22} + \left(A^{-1}_{R_{m-1}}\right)_{33}\left(a^{-1}_{R_m}\right)_{32} + \left(A^{-1}_{R_{m-1}}\right)_{34}\left(a^{-1}_{R_m}\right)_{42}$$

$$= -\left(a_{R_m}\right)_{34}\left(A_{R_{m-1}}\right)_{42} - \left(a_{R_m}\right)_{33}\left(A_{R_{m-1}}\right)_{32} - \left(a_{R_m}\right)_{32}\left(A_{R_{m-1}}\right)_{22} - \left(a_{R_m}\right)_{31}\left(A_{R_{m-1}}\right)_{12}$$

$$= -\left(A_{R_m}\right)_{32}$$

$$\left(A^{-1}_{R_m}\right)_{33} = \left(A^{-1}_{R_{m-1}}\right)_{31}\left(a^{-1}_{R_m}\right)_{13} + \left(A^{-1}_{R_{m-1}}\right)_{32}\left(a^{-1}_{R_m}\right)_{23} + \left(A^{-1}_{R_{m-1}}\right)_{33}\left(a^{-1}_{R_m}\right)_{33}$$
$$+ \left(A^{-1}_{R_{m-1}}\right)_{34}\left(a^{-1}_{R_m}\right)_{43}$$
$$= \left(a_{R_m}\right)_{24}\left(A_{R_{m-1}}\right)_{42} + \left(a_{R_m}\right)_{23}\left(A_{R_{m-1}}\right)_{32} + \left(a_{R_m}\right)_{22}\left(A_{R_{m-1}}\right)_{22}$$
$$+ \left(a_{R_m}\right)_{21}\left(A_{R_m}\right)_{12}$$
$$= \left(A_{R_m}\right)_{22}$$

$$\left(A^{-1}_{R_m}\right)_{34} = \left(A^{-1}_{R_{m-1}}\right)_{31}\left(a^{-1}_{R_m}\right)_{14} + \left(A^{-1}_{R_{m-1}}\right)_{32}\left(a^{-1}_{R_m}\right)_{24} + \left(A^{-1}_{R_{m-1}}\right)_{33}\left(a^{-1}_{R_m}\right)_{34}$$
$$+ \left(A^{-1}_{R_{m-1}}\right)_{34}\left(a^{-1}_{R_m}\right)_{44}$$
$$= -\left(a_{R_m}\right)_{14}\left(A_{R_{m-1}}\right)_{42} - \left(a_{R_m}\right)_{13}\left(A_{R_{m-1}}\right)_{32} - \left(a_{R_m}\right)_{12}\left(A_{R_{m-1}}\right)_{22}$$
$$- \left(a_{R_m}\right)_{11}\left(A_{R_{m-1}}\right)_{12}$$
$$= -\left(A_{R_m}\right)_{12}$$

$$\left(A^{-1}_{R_m}\right)_{41} = \left(A^{-1}_{R_{m-1}}\right)_{41}\left(a^{-1}_{R_m}\right)_{11} + \left(A^{-1}_{R_{m-1}}\right)_{42}\left(a^{-1}_{R_m}\right)_{21} + \left(A^{-1}_{R_{m-1}}\right)_{43}\left(a^{-1}_{R_m}\right)_{31}$$
$$+ \left(A^{-1}_{R_{m-1}}\right)_{44}\left(a^{-1}_{R_m}\right)_{41}$$
$$= -\left(a_{R_m}\right)_{44}\left(A_{R_{m-1}}\right)_{41} - \left(a_{R_m}\right)_{43}\left(A_{R_{m-1}}\right)_{31} - \left(a_{R_m}\right)_{42}\left(A_{R_{m-1}}\right)_{21}$$
$$- \left(a_{R_m}\right)_{41}\left(A_{R_{m-1}}\right)_{11}$$
$$= -\left(A_{R_m}\right)_{41}$$

$$\left(A^{-1}_{R_m}\right)_{42} = \left(A^{-1}_{R_{m-1}}\right)_{41}\left(a^{-1}_{R_m}\right)_{12} + \left(A^{-1}_{R_{m-1}}\right)_{42}\left(a^{-1}_{R_m}\right)_{22} + \left(A^{-1}_{R_{m-1}}\right)_{43}\left(a^{-1}_{R_m}\right)_{32} + \left(A^{-1}_{R_{m-1}}\right)_{44}\left(a^{-1}_{R_m}\right)_{42}$$

$$= \left(a_{R_m}\right)_{34}\left(A_{R_{m-1}}\right)_{41} + \left(a_{R_m}\right)_{33}\left(A_{R_{m-1}}\right)_{31} + \left(a_{R_m}\right)_{32}\left(A_{R_{m-1}}\right)_{21} + \left(a_{R_m}\right)_{31}\left(A_{R_{m-1}}\right)_{11}$$

$$= \left(A_{R_m}\right)_{31}$$

$$\left(A^{-1}_{R_m}\right)_{43} = \left(A^{-1}_{R_{m-1}}\right)_{41}\left(a^{-1}_{R_m}\right)_{13} + \left(A^{-1}_{R_{m-1}}\right)_{43}\left(a^{-1}_{R_m}\right)_{23} + \left(A^{-1}_{R_{m-1}}\right)_{43}\left(a^{-1}_{R_m}\right)_{33} + \left(A^{-1}_{R_{m-1}}\right)_{44}\left(a^{-1}_{R_m}\right)_{43}$$

$$= -\left(a_{R_m}\right)_{24}\left(A_{R_{m-1}}\right)_{41} - \left(a_{R_m}\right)_{23}\left(A_{R_{m-1}}\right)_{31} - \left(a_{R_m}\right)_{22}\left(A_{R_{m-1}}\right)_{21} - \left(a_{R_m}\right)_{21}\left(A_{R_{m-1}}\right)_{11}$$

$$= -\left(A_{R_m}\right)_{21}$$

$$\left(A^{-1}_{R_m}\right)_{44} = \left(A^{-1}_{R_{m-1}}\right)_{41}\left(a^{-1}_{R_m}\right)_{14} + \left(A^{-1}_{R_{m-1}}\right)_{42}\left(a^{-1}_{R_m}\right)_{24} + \left(A^{-1}_{R_{m-1}}\right)_{43}\left(a^{-1}_{R_m}\right)_{34} + \left(A^{-1}_{R_{m-1}}\right)_{44}\left(a^{-1}_{R_m}\right)_{44}$$

$$= \left(a_{R_m}\right)_{14}\left(A_{R_{m-1}}\right)_{41} + \left(a_{R_m}\right)_{13}\left(A_{R_{m-1}}\right)_{31} + \left(a_{R_m}\right)_{12}\left(A_{R_{m-1}}\right)_{21} + \left(a_{R_m}\right)_{11}\left(A_{R_m}\right)_{11}$$

$$= \left(A_{R_m}\right)_{11}$$

From the above we see that if the assumption is true for $A^{-1}_{R_{m-1}}$ it is also true for $A^{-1}_{R_m}$. Now $A^{-1}_{R_1} = a^{-1}_{R_1}$ and by equation 11, the inverse matrix assumption is true for m = 1. Therefore, by induction, the product matrix inversion is true for all m.

APPENDIX E

RELATION BETWEEN (GN - HL) AND (RN - SL) WITH F = 0

This appendix proves the important relation that

$$\frac{RN - SL}{GN - HL} = \frac{K}{L} \tag{1}$$

when

$$F \equiv NK - LM = 0 \tag{2}$$

The proof is as follows. Rewriting equations 1 and 2 we obtain

$$\frac{\frac{R}{L} - \frac{S}{N}}{\frac{G}{L} - \frac{H}{N}} = \frac{K}{L} \tag{3}$$

and

$$\frac{K}{L} = \frac{M}{N} \tag{4}$$

From the following definitions

$$\frac{G}{L} = \frac{J_{13} - J_{23}}{J_{11} - J_{21}}, \quad \frac{H}{N} = \frac{J_{33} - J_{43}}{J_{31} - J_{41}}, \quad \frac{R}{L} = \frac{J_{14} - J_{24}}{J_{11} - J_{21}}$$

$$\frac{S}{N} = \frac{J_{34} - J_{44}}{J_{31} - J_{41}}, \quad \frac{K}{L} = \frac{J_{12} - J_{22}}{J_{11} - J_{21}} \text{ and } \frac{M}{N} = \frac{J_{32} - J_{42}}{J_{31} - J_{41}}$$

equations 3 and 4 can be written as

$$\frac{(J_{14} - J_{24})(J_{31} - J_{41}) - (J_{34} - J_{44})(J_{11} - J_{21})}{(J_{13} - J_{23})(J_{31} - J_{41}) - (J_{33} - J_{43})(J_{11} - J_{21})} = \frac{J_{12} - J_{22}}{J_{11} - J_{21}} \tag{5}$$

and

$$\frac{J_{12}- J_{22}}{J_{11} - J_{21}} = \frac{J_{32}- J_{42}}{J_{31}- J_{41}} \tag{6}$$

Then rearranging the L HS of equation 5 using equation 6 yields

$$\frac{(J_{14}-J_{24})(J_{31}-J_{41}) - (J_{34}- J_{44})(J_{11}-J_{21})}{(J_{13}-J_{23})(J_{32}-J_{42}) - (J_{33}-J_{43})(J_{12}-J_{22})} \cdot \frac{J_{12}- J_{22}}{J_{11} - J_{21}} = \frac{J_{12}- J_{22}}{J_{11}- J_{21}} \tag{7}$$

Therefore if we can show that

$$(J_{19}- J_{24})(J_{31}- J_{41}) - (J_{34}- J_{44})(J_{11}- J_{21})$$
$$= (J_{13}- J_{23})(J_{32}- J_{42}) - (J_{33}- J_{43})(J_{12}- J_{22}) \tag{8}$$

or

$$(J_{33}- J_{43})(J_{22}- J_{12}) - (J_{14}- J_{24})(J_{31}- J_{41})$$
$$= (J_{13}- J_{23})(J_{42}- J_{32}) - (J_{34}- J_{44})(J_{11}- J_{21}) \tag{9}$$

we will have proved that equation 1 is true when equation 2 is satisfied.

By definition $J = E_m^{-1} A$ where $A = A_{m-1}$ and since $(E_m^{-1})_{jk} \equiv 0$ for $j + k$ = odd integer, we have

$$(J_{33}-J_{43})(J_{22}-J_{12}) = J_{33}J_{22}- J_{33}J_{12}- J_{43}J_{22}+ J_{43}J_{12}$$

$$= E_{31}^{-1}E_{22}^{-1}(A_{13}A_{22}) + E_{31}^{-1}E_{24}^{-1}(A_{13}A_{42}) + E_{33}^{-1}E_{22}^{-1}(A_{33}A_{22})$$

$$+ E_{33}^{-1}E_{24}^{-1}(A_{33}A_{42}) - E_{31}^{-1}E_{11}^{-1}(A_{13}A_{12}) - E_{31}^{-1}E_{13}^{-1}(A_{13}A_{32})$$

$$- E_{31}^{-1}E_{13}^{-1}(A_{13}A_{32}) - E_{33}^{-1}E_{11}^{-1}(A_{33}A_{12}) - E_{33}^{-1}E_{13}^{-1}(A_{33}A_{32})$$

$$- E_{42}^{-1}E_{22}^{-1}(A_{23}A_{22}) - E_{42}^{-1}E_{24}^{-1}(A_{23}A_{42}) - E_{44}^{-1}E_{22}^{-1}(A_{43}A_{22})$$

$$+ E_{42}^{-1}E_{11}^{-1}(A_{23}A_{12}) + E_{42}^{-1}E_{13}^{-1}(A_{23}A_{32}) + E_{44}^{-1}E_{11}^{-1}(A_{43}A_{12})$$

$$+ E_{44}^{-1}E_{13}^{-1}(A_{43}A_{32}) \tag{10}$$

and

$$(J_{14} - J_{24})(J_{31} - J_{41}) = J_{14}J_{31} - J_{14}J_{41} - J_{24}J_{31} + J_{24}J_{41}$$

$$= E_{11}^{-1}E_{31}^{-1}(A_{14}A_{11}) + E_{11}^{-1}E_{33}^{-1}(A_{14}A_{31}) + E_{13}^{-1}E_{31}^{-1}(A_{34}A_{11})$$

$$+ E_{13}^{-1}E_{33}^{-1}(A_{34}A_{31}) - E_{11}^{-1}E_{42}^{-1}(A_{14}A_{21}) - E_{11}^{-1}E_{44}^{-1}(A_{14}A_{41})$$

$$- E_{13}^{-1}E_{42}^{-1}(A_{34}A_{21}) - E_{13}^{-1}E_{44}^{-1}(A_{34}A_{41}) - E_{22}^{-1}E_{31}^{-1}(A_{24}A_{11})$$

$$- E_{22}^{-1}E_{33}^{-1}(A_{24}A_{31}) - E_{24}^{-1}E_{31}^{-1}(A_{44}A_{11}) - E_{24}^{-1}E_{33}^{-1}(A_{44}A_{31})$$

$$+ E_{22}^{-1}E_{42}^{-1}(A_{24}A_{21}) + E_{22}^{-1}E_{44}^{-1}(A_{24}A_{41}) + E_{24}^{-1}E_{42}^{-1}(A_{44}A_{21})$$

$$+ E_{24}^{-1}E_{44}^{-1}(A_{44}A_{41})$$

where we have dropped the n subscript on E_n^{-1} elements to simplify the notation.

From the elements of E_n^{-1} we have in addition the following relations

$$E_{33}^{-1}E_{22}^{-1} = - E_{24}^{-1}E_{31}^{-1}$$

$$E_{44}^{-1}E_{11}^{-1} = - E_{13}^{-1}E_{42}^{-1} \tag{12}$$

Regrouping, making use of equations 12, we obtain

$$(J_{33}-J_{43})(J_{22}-J_{12}) - (J_{14}-J_{24})(J_{31}-J_{41})$$

$$= E_{31}^{-1}E_{22}^{-1}(A_{13}A_{22}+A_{24}A_{11}) + E_{33}^{-1}E_{22}^{-1}(A_{33}A_{22}-A_{13}A_{42}+A_{24}A_{31}-A_{44}A_{11})$$

$$+ E_{33}^{-1}E_{24}^{-1}(A_{33}A_{42}+A_{44}A_{31}) - E_{31}^{-1}E_{11}^{-1}(A_{13}A_{12}+A_{14}A_{11})$$

$$- E_{31}^{-1}E_{13}^{-1}(A_{13}A_{32}+A_{34}A_{11}) - E_{33}^{-1}E_{11}^{-1}(A_{33}A_{12}+A_{14}A_{31})$$

$$- E_{33}^{-1}E_{13}^{-1}(A_{33}A_{32}+A_{34}A_{31}) - E_{42}^{-1}E_{24}^{-1}(A_{23}A_{22}+A_{24}A_{21}) \qquad (13)$$

$$- E_{42}^{-1}E_{24}^{-1}(A_{23}A_{42}+A_{44}A_{21}) - E_{44}^{-1}E_{22}^{-1}(A_{43}A_{22}+A_{24}A_{41})$$

$$- E_{44}^{-1}E_{24}^{-1}(A_{43}A_{42}+A_{44}A_{41}) + E_{42}^{-1}E_{11}^{-1}(A_{23}A_{12}+A_{14}A_{21})$$

$$+ E_{44}^{-1}E_{13}^{-1}(A_{43}A_{32}+A_{34}A_{41}) + E_{44}^{-1}E_{11}^{-1}(A_{43}A_{12}-A_{22}A_{32}+A_{14}A_{41}-A_{34}A_{21})$$

Similarly for the RHS of equation 9, we have

$$(J_{13}-J_{23})(J_{42}-J_{32}) = J_{13}J_{42} - J_{13}J_{32} - J_{23}J_{42} + J_{23}J_{32}$$

$$= E_{11}^{-1}E_{42}^{-1}(A_{13}A_{22}) + E_{11}^{-1}E_{44}^{-1}(A_{13}A_{42}) + E_{13}^{-1}E_{42}^{-1}(A_{33}A_{22})$$

$$+ E_{13}^{-1}E_{44}^{-1}(A_{33}A_{42}) - E_{11}^{-1}E_{31}^{-1}(A_{13}A_{12}) - E_{11}^{-1}E_{33}^{-1}(A_{13}A_{32})$$

$$- E_{13}^{-1}E_{31}^{-1}(A_{33}A_{12}) - E_{13}^{-1}E_{33}^{-1}(A_{33}A_{32}) - E_{22}^{-1}E_{42}^{-1}(A_{23}A_{22})$$

$$- E_{22}^{-1}E_{44}^{-1}(A_{23}A_{42}) - E_{24}^{-1}E_{42}^{-1}(A_{43}A_{22}) - E_{24}^{-1}E_{44}^{-1}(A_{43}A_{42}) \qquad (14)$$

$$+ E_{22}^{-1}E_{31}^{-1}(A_{23}A_{12}) + E_{22}^{-1}E_{33}^{-1}(A_{23}A_{32}) + E_{24}^{-1}E_{31}^{-1}(A_{43}A_{12})$$

$$+ E_{24}^{-1}E_{33}^{-1}(A_{43}A_{32})$$

and

$$(J_{34} - J_{44})(J_{11} - J_{21}) = J_{34}J_{11} - J_{34}J_{21} - J_{44}J_{11} + J_{44}J_{21}$$

$$= E_{31}^{-1}E_{11}^{-1}(A_{14}A_{11}) + E_{31}^{-1}E_{13}^{-1}(A_{14}A_{31}) + E_{33}^{-1}E_{11}^{-1}(A_{34}A_{11})$$

$$+ E_{33}^{-1}E_{13}^{-1}(A_{34}A_{31}) - E_{31}^{-1}E_{22}^{-1}(A_{14}A_{21}) - E_{31}^{-1}E_{24}^{-1}(A_{14}A_{41})$$

$$- E_{33}^{-1}E_{22}^{-1}(A_{34}A_{21}) - E_{33}^{-1}E_{24}^{-1}(A_{34}A_{41}) - E_{42}^{-1}E_{11}^{-1}(A_{24}A_{11}) \qquad (15)$$

$$- E_{42}^{-1}E_{13}^{-1}(A_{24}A_{31}) - E_{44}^{-1}E_{11}^{-1}(A_{44}A_{11}) + E_{44}^{-1}E_{13}^{-1}(A_{44}A_{31})$$

$$+ E_{42}^{-1}E_{22}^{-1}(A_{24}A_{21}) + E_{42}^{-1}E_{24}^{-1}(A_{24}A_{41}) + E_{44}^{-1}E_{22}^{-1}(A_{44}A_{21})$$

$$+ E_{44}^{-1}E_{24}^{-1}(A_{44}A_{41})$$

Regrouping, again using equations 12, yields

$$(J_{13} - J_{23})(J_{42} - J_{32}) - J_{34} - J_{44})(J_{11} - J_{21})$$

$$= E_{31}^{-1}E_{22}^{-1}(A_{23}A_{12} + A_{14}A_{21}) + E_{33}^{-1}E_{22}^{-1}(A_{23}A_{32} - A_{43}A_{12} - A_{34}A_{21} - A_{14}A_{41})$$

$$+ E_{33}^{-1}E_{24}^{-1}(A_{43}A_{32} + A_{34}A_{41}) - E_{31}^{-1}E_{11}^{-1}(A_{13}A_{12} + A_{14}A_{11})$$

$$- E_{31}^{-1}E_{13}^{-1}(A_{33}A_{12} + A_{14}A_{31}) - E_{33}^{-1}E_{11}^{-1}(A_{13}A_{32} + A_{34}A_{11})$$

$$- E_{33}^{-1}E_{13}^{-1}(A_{33}A_{32} + A_{34}A_{31}) - E_{42}^{-1}E_{22}^{-1}(A_{23}A_{22} + A_{24}A_{21}) \qquad (16)$$

$$- E^{-1} \quad - E_{42}^{-1}E_{24}^{-1}(A_{43}A_{22} + A_{24}A_{41}) - E_{44}^{-1}E_{22}^{-1}(A_{23}A_{42} + A_{44}A_{21})$$

$$- E_{44}^{-1}E_{24}^{-1}(A_{43}A_{42} + A_{44}A_{41}) + E_{42}^{-1}E_{11}^{-1}(A_{13}A_{22} + A_{24}A_{11})$$

$$+ E_{44}^{-1}E_{13}^{-1}(A_{33}A_{42} + A_{44}A_{31}) + E_{11}^{-1}E_{44}^{-1}(A_{13}A_{42} - A_{33}A_{22} + A_{44}A_{11} - A_{24}A_{31})$$

From the inverse of A given in Appendix D, we see that

$$A_{13}A_{22} + A_{24}A_{11} = A_{22}A_{24}^{-1} + A_{24}A_{44}^{-1} = -A_{21}A_{14}^{-1} - A_{23}A_{34}^{-1}$$
$$= A_{14}A_{21} + A_{23}A_{12} \quad \text{since } (AA^{-1})_{24} \equiv 0 \tag{17}$$

$$A_{33}A_{42} + A_{44}A_{31} = A_{33}A_{31}^{-1} + A_{31}A_{11}^{-1} = -A_{32}A_{21}^{-1} - A_{34}A_{41}^{-1}$$
$$= A_{43}A_{32} + A_{34}A_{41} \quad \text{since } (AA^{-1})_{31} \equiv 0 \tag{18}$$

$$A_{13}A_{32} + A_{34}A_{11} = -A_{13}A_{32}^{-1} - A_{11}A_{12}^{-1} = A_{12}A_{22}^{-1} + A_{14}A_{42}^{-1}$$
$$= A_{12}A_{33} + A_{14}A_{31} \quad \text{since } (AA^{-1})_{12} \equiv 0 \tag{19}$$

$$A_{23}A_{42} + A_{44}A_{21} = -A_{42}A_{23}^{-1} - A_{44}A_{43}^{-1} = A_{41}A_{13}^{-1} + A_{43}A_{33}^{-1}$$
$$= A_{43}A_{22} + A_{41}A_{24} \quad \text{since } (AA^{-1})_{43} \equiv 0 \tag{20}$$

In addition

$$A_{33}A_{22} + A_{24}A_{31} = A_{22}A_{22}^{-1} + A_{24}A_{42}^{-1} = 1 - A_{23}A_{32}^{-1} - A_{21}A_{12}^{-1}$$
$$= 1 + A_{23}A_{32} + A_{21}A_{34} \quad \text{since } (AA^{-1})_{22} \equiv 1 \tag{21}$$

$$A_{13}A_{42} + A_{44}A_{11} = A_{13}A_{31}^{-1} + A_{11}A_{11}^{-1} = 1 - A_{12}A_{21}^{-1} - A_{14}A_{41}^{-1}$$
$$= 1 + A_{12}A_{43} + A_{14}A_{41} \quad \text{since } (AA^{-1})_{11} \equiv 1 \tag{22}$$

and thus

$$A_{33}A_{22} + A_{24}A_{31} - A_{13}A_{42} - A_{44}A_{11} = A_{23}A_{32} + A_{21}A_{34} - A_{12}A_{43} - A_{14}A_{41} \tag{23}$$

Now comparing equation 13, the LHS of equation 9, with equation 16, the RHS of equation 9, using equations 17, 18, 19, 20, and 23 we see that equation 9 is indeed true. Therefore we have proved that

$$\frac{RN - SL}{GN - HL} = \frac{K}{L} \tag{1}$$

when

$$F \equiv NK - LM = 0 \tag{2}$$

APPENDIX F

LIST OF SYMBOLS DEFINED IN TEXT

Symbol		Definition
Type	Script	
m	m	subscript indicating m^{th} layer
		constants
a	α	layer compressional velocity
β	β	layer shear velocity
ω	ω	angular frequency
k	k	horizontal wave number
c	c	$= \omega/k$: horizontal phase velocity
kr_a	$k\eta_\alpha$	vertical compressional wave
		number
kr_β	$k\eta_\beta$	vertical shear wave number
q	q	radial displacement
v	v	azimuthal displacement
w	w	vertical displacement
$\dot{u}$	$\dot{u}$	horizontal plane wave velocity
σ	σ	normal plane wave stress
R	R	spherical coordinate

Symbol		Definition
R	R	subscript denoting quantities associated with Rayleigh waves
L	L	subscript denoting quantities associated with Love waves
L	L	force
L'	L'	couple
s	s	subscript denoting the layer containing the source
a_s	a_s	cavity radius for explosive source
λ	λ	Lamé's constant
μ	μ	Lamé's constant of elastic rigidity
ρ	ρ	density
k_α	k_α	$= \frac{\omega}{\alpha}$: spherical compressional wave number
k_β	k_β	$= \frac{\omega}{\beta}$: spherical shear wave number
z_m	z_m	depth to bottom of layer m
d_m	d_m	$z_m - z_{m-1}$: layer thickness

Symbol		Definition
$-$	$-$	superscript denoting Fourier time transformed quantity
o	o	subscript denoting evaluation at free surface
$\{\ \}_{R_j}$	$\{\ \}_{R_j}$	residue contribution for Rayleigh waves, j^{th} mode
$\{\ \}_{L_j}$	$\{\ \}_{L_j}$	residue contribution for Love waves, j^{th} mode
$[\ ]_{H_j}$	$[\ ]_{H_j}$	homogeneous plane wave ratios, j^{th} mode
$\cdot$	$\cdot$	superscript denoting first derivative with respect to time
t_{as}	t_{o_s}	source origin time
A	$\mathcal{A}$	spectral amplitude
O_{Rs}	O_{Rs}	vertical finite fault factor for Rayleigh waves
O_{Ls}	O_{Ls}	vertical finite fault factor for Love waves
τ	$\mathcal{T}$	tangential plane wave stress
T	$\mathcal{T}$	$= \frac{2\pi}{kc}$: period

Symbol		Definition
r	$\mathcal{r}$	radial cylindrical coordinate
z	$\mathcal{z}$	vertical cylindrical coordinate

REFERENCES

Ben-Menahem, A., Radiation of seismic surface-waves from finite moving sources, Bull. Seism. Soc. Am., 51, 401-435, 1961.

Blake, F. G., Jr., Spherical wave propagation in solid media, Journ. Acoust. Soc. Amer., 24, 211-215, 1952.

Dorman, J., M. Ewing, and J. Oliver, Study of shear velocity distribution by mantle Rayleigh waves, Bull. Seism. Soc. Am., 50, 87-115, 1960.

Dorman, J., Period equation for waves of Rayleigh type on a layered, liquid-solid half space, Bull. Seism. Soc. Am., 52, 389-397, 1962.

Ewing, J., W. Jardetzky, and F. Press, Elastic Waves in Layered Media, McGraw-Hill Book Company, New York, 1957.

Fu, C. Y., On the origin and energy of oscillatory earthquake waves, Bull. Seism. Soc. Am., 35, 37-42, 1945.

Gilbert, F., Jr., Seismic wave propagation in a two-layer half-space, Thesis, Massachusetts Institute of Technology, 1956.

Gilbert, F., Jr., and G. J. F. MacDonald, Free oscillations of the earth, 1, Toroidal oscillations, J. Geophys. Research, 65, 675-693, 1960.

Harkrider, D. G., and D. L. Anderson, Computation of surface wave dispersion for multilayered anisotropic media, Bull. Seism. Soc. Am., 52, 321-332, 1962.

Haskell, N. A., The dispersion of surface waves on multilayered media, Bull. Seism. Soc. Am., 43, 17-34, 1953.

Jardetzky, W. S., Period equation for an n-layered half space and some related questions, Columbia Univ. Lamont Geol. Obs. Tech. Rept. Seismology, 29, 1953.

Kawasumi, H., and R. Yosiyama, On an elastic wave animated by the potential energy of initial strain, Bull. Earthquake Res. Inst., Tokyo, 13, 496-503, 1935.

Kellis-Borok, V. I., Interference seismic waves in a layered median, Thesis, Inst. of Physics of the Earth, Acad. Sci., U.S.S.R., 1953.

Kellis-Borok, V. I., and T. B. Yanovskaya, Dependence of the spectrum of surface waves on the depth of the focus within the earth's crust, Izv. Akad. Nauk SSSR, Geophys. Ser., 1532-1539, 1962.

Knopoff., L., and A. F. Gangi, Seismic Reciprocity, Geophysics, 24, 681-691, 1959.

Menzel, H., Uber das spektrum seismischer Wellen, die durch Sprengungen erzeugt werden, Annali di Geofisica, 4, 301-321, 1951.

Press, F., D. Harkrider, and C. A. Seafeldt, A fast, convenient program for computation of surface-wave dispersion curves on multilayered media, Bull. Seism. Soc. Am., 51, 495-502, 1961.

Rayleigh, Lord, The Theory of Sound, 1, Dover Publications, New York, 1877.

Sharpe, J. A., The production of elastic waves by explosive pressures, Geophysics, 7, 144-154, 1942.

Sherwood, J. W. C., and T. W. Spencer, Signal-to-noise ratio and spectra of explosion-generated Rayleigh waves, Bull. Seism. Soc. Am., 52, 573-594, 1962.

Sneddon, J., Fourier Transforms, McGraw-Hill Book Company, New York, 1950.

Thomson, W. T., Transmission of elastic waves through a stratified solid medium, Jour. Appl. Phys., 21, 89, 1950.

Yanovskaya, T. B., On the determination of the dynamic parameters of the focus hypocenter of an earthquake from records of surface waves, 1, Isv. Akad. Nauk, SSSR, Geophys. Ser., 289-201, 1958.

FIGURE CAPTIONS

Figure 1. Direction of axes, numbering of layers, and the depth of interfaces and source.

Figure 2. Realization of vertical fault-plane.

Figure 3. Geometry of free surface.

Figure 4. Horizontal force geometry

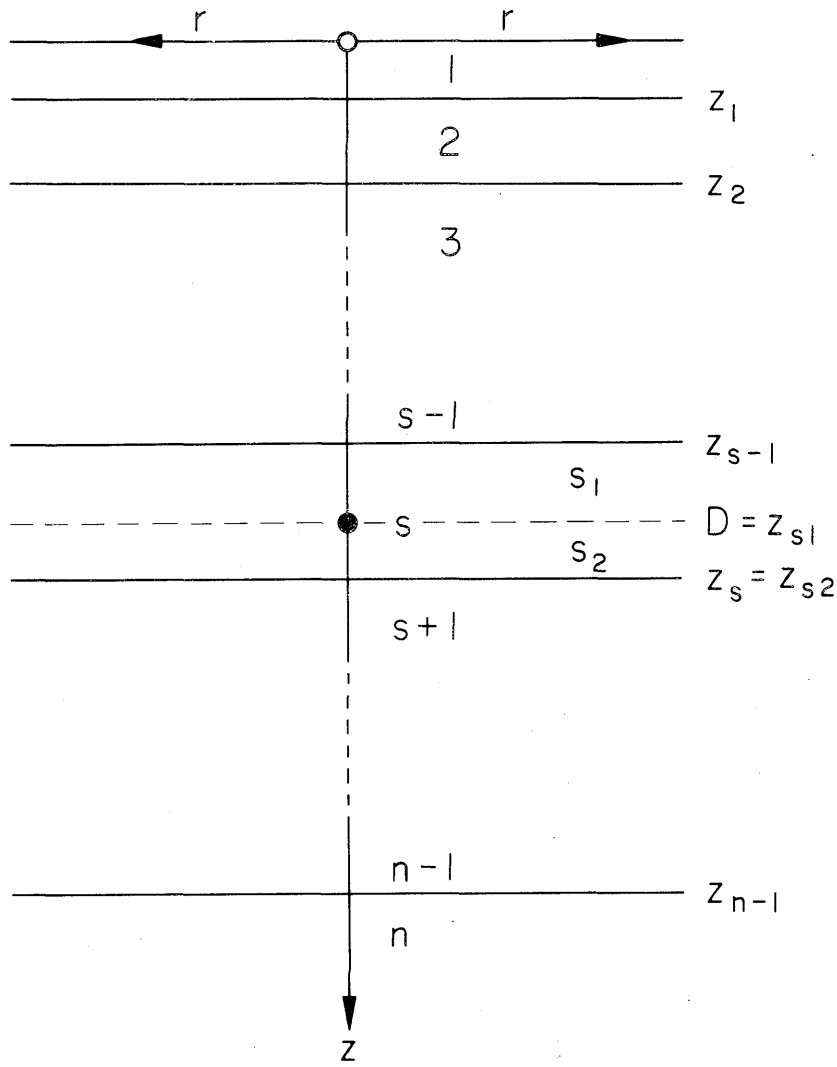

Fig. 1

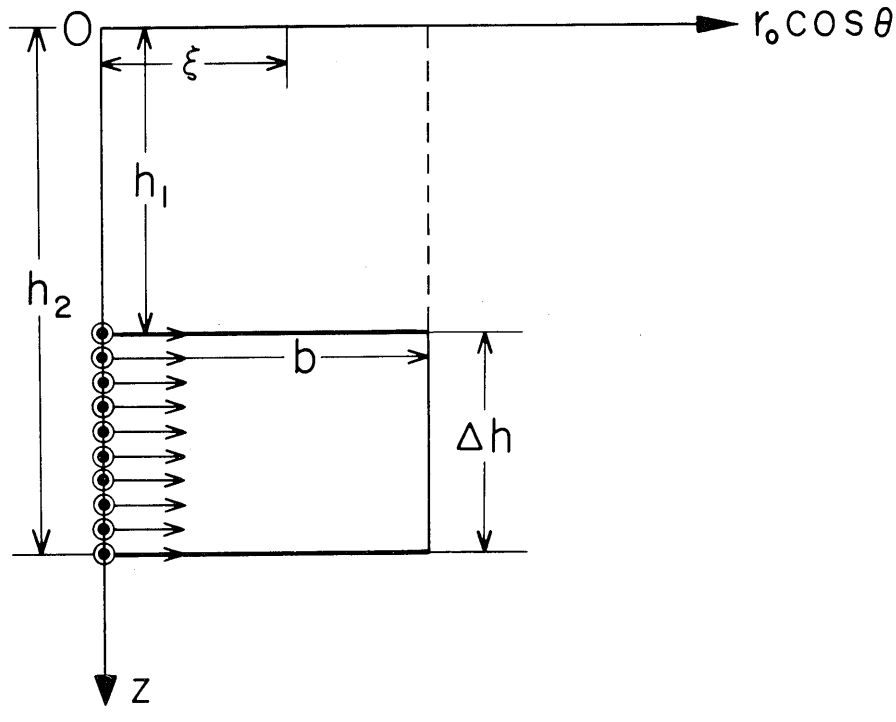

Fig. 2

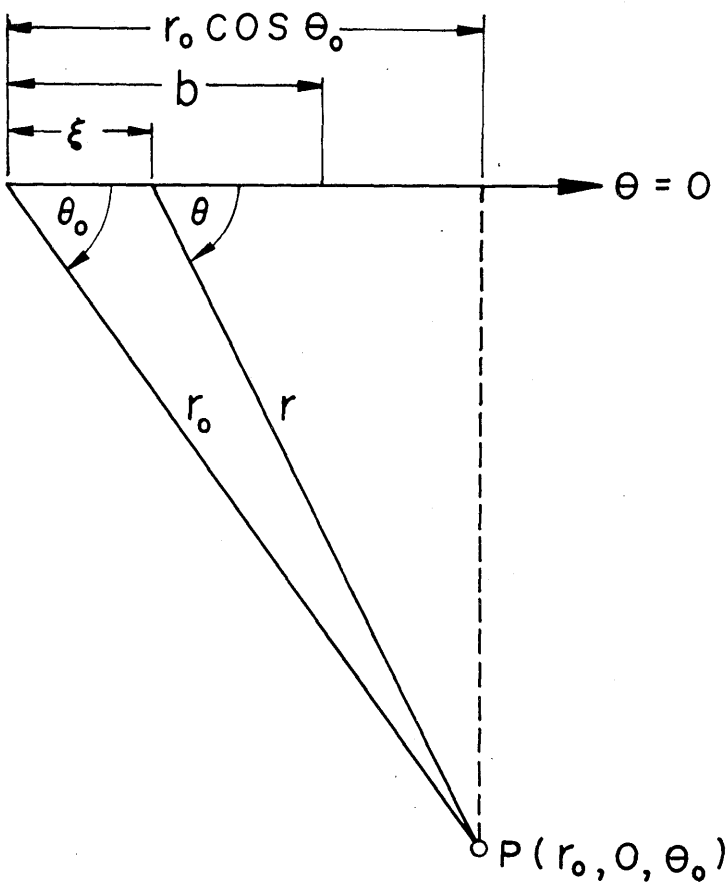

Fig. 3

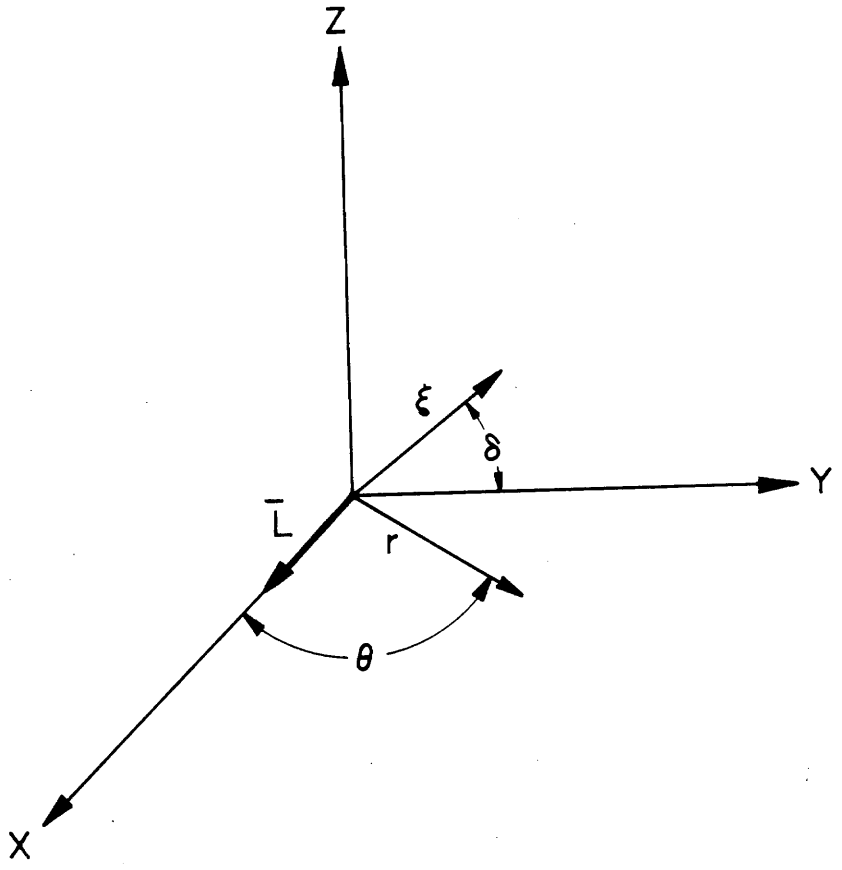

Fig. 4